Angeliki Karatza

Investigating the role of Atypical Chemokine Receptor 3 in cancer development

MARCH 2020

Submitted in fulfilment of the requirements for the degree of Doctor of Philosophy College of Medical, Veterinary and Life Sciences Institute of Molecular, Cell and Systems Biology

Abstract

Atypical Chemokine Receptor 3 (ACKR3) is a seven-transmembrane spanning receptor with pleiotropic functions in development, homeostasis and pathophysiology. The spatiotemporal expression of ACKR3 is tightly regulated, a fact that highlights its importance in several biological processes. ACKR3, similar to the other atypical chemokine receptors, does not signal through G proteins. ACKR3 exerts its functions by a) recruiting the β arrestins and b) scavenging its ligands thus shaping their concentration in the extracellular milieu.

ACKR3 expression is often dysregulated in pathophysiological conditions, including cancer. There is a growing body of evidence that implicates ACKR3 in certain types of human cancers.

In the present study, we interrogated publicly available databases of cancer patients in order to assess ACKR3 expression in different types of human cancers. These analyses revealed that ACKR3 is upregulated in several types of human cancers, including lung cancer. To this end, we investigated the role of ACKR3 in cancer progression with a particular focus on lung cancer.

In order to overcome the lack of specific ACKR3 antibodies, we used a GFP fluorescent reporter mouse to assess ACKR3 expression in the different stromal cell populations in the lung. Our approach revealed that ACKR3 is expressed in the fibroblasts, blood and lymphatic endothelial cells in the resting lung. Furthermore, in this study, we tried to address the discrepancies in the literature about ACKR3 expression that is a result of the nonspecific nature of commercially available antibodies. More specifically, we tested commercially available flow cytometry anti-ACKR3 antibodies in the GFP/ACKR3 reporter mouse. Our approach revealed that both of the ACKR3 antibodies that were tested were inefficient in staining but also nonspecific in all the cell populations that were tested.

Subsequently, we employed the CRISPR/Cas9 genome editing technologies to generate ACKR3 null cancer cell lines that we used subsequently *in vivo* in different mouse models. Our study identified ACKR3 as a positive regulator in lung cancer progression. Furthermore, ACKR3 was also identified as a crucial player at the early steps of metastasis and colonisation of metastatic circulating tumour cells in the lung.

Collectively our data suggest that ACKR3 is a promising candidate for drug targeting in certain types of human lung cancer.

Author's Declaration

I declare that the work described in this thesis is original and was generated as a result of my own work. No part of this thesis has been submitted for any other degree, either at the University of Glasgow, or at any other institution.

Signature: .....

Printed name: Angeliki Karatza

Table of contents

List of abbreviations

7TM seven- transmembrane

A

ACKR atypical chemokine receptor

ADM adrenomedullin

AIDS acquired immunodeficiency syndrome

AMP adenosine monophosphate

ApoE apolipoprotein E

B

BAM22 bovine adrenal medulla 22

BEC blood endothelial cell

BLCA urothelial bladder carcinoma

BM bone marrow

BRET bioluminescence resonance energy transfer

BSA bovine serum albumin

C

CAD coronary artery disease

CAFs cancer- associated fibroblasts

CD31 cluster of differentiation 31

CD74 cluster of differentiation 74

CESC cervical squamous cell carcinoma and endocervical adenocarcinoma

CHOL cholangiocarcinoma

CIA collagen-induced arthritis

CNS central nervous system

CLR calcitonin receptor- like

CRISPR clustered regularly interspaced short palindromic repeats

CRC colorectal cancer

D

DAG diacylglycerol

DC dendritic cell

DSB double-strand break

E

ECM extracellular matrix

EGFP enhanced green fluorescent protein

EGFR epidermal growth factor receptor

ELR Glu-Leu-Arg

EMT epithelial to mesenchymal transition

ERKs extracellular signal-regulated kinases

EpCAM epithelial cell adhesion molecule

EPCs endothelial progenitor cells

ES embryonic stem

ESCA esophageal Carcinoma

EAE experimental autoimmune encephalomyelitis model

F

FACs fluorescence activated cell sorting

FBS fetal bovine serum

FSC forward scatter

FMO fluorescence minus one

FPR formyl peptide receptors

G

GAG glycosaminoglycans

GBM glioblastoma

GBMLGG glioma

GDP guanosine diphosphate

GEMMs genetically engineered mouse models

GFP green fluorescence protein

GLI1 glioma-associated oncogene 1

GPCR G protein-coupled receptors

GTP guanosine triphosphate

GSK-3 glycogen synthase kinase 3

H

HBEGF heparin-binding EGF-like growth factor

HCC hepatocellular carcinoma

HDR homology directed repair

HIC1 hypermethylated in cancer 1

HIV human immunodeficiency virus

HIF-1 α hypoxia-inducible factor -1 alpha

HLA-DR human leukocyte antigen – DR isotype

HMVECs human microvascular endothelial cells

HNSC head-neck squamous cell carcinoma

HS heparan sulphate

HSC hematopoietic stem cell

HUVECs human umbilical vein endothelial cells

I

ID-1 inhibitor of DNA binding 1

INDELS insertions/deletions

IMIDs immune-mediated inflammatory diseases

IP3 inositol triphosphate

J

JAG1 jagged1

K

KICH kidney chromophobe

KIPAN pan-kidney

KIRP kidney renal papillary cell carcinoma

KO knock out

L

LB Luria-Bertani

LDL low-density lipoprotein

LDLR low-density lipoprotein receptor

LEC lymphatic endothelial cell

LIHC liver hepatocellular carcinoma

LLC Lewis lung carcinoma

LPS lipopolysaccharides

LT leukotriene receptors

LUAD lung adenocarcinoma

LUSC lung squamous carcinoma

M

MAPKs mitogen-activated protein kinases

MHCII major histocompatibility complex class II molecules

MIF macrophage migration inhibitory factor

MMP matrix metalloproteinases

N

NCI National Cancer Institute

NET neutrophil extracellular trap

NHGRI National Human Genome Research Institute

NF-κB nuclear factor kappa-light-chain-enhancer of activated B cells

NHEJ non-homologous end-joining

NK natural killer

NRF2 nuclear factor (erythroid-derived 2)-like 2

NSCC non-small cell lung cancer

P

PAAD pancreatic adenocarcinoma

PAMPs pathogen-associated molecular patterns

PBMCs peripheral blood cells

PBS phosphate-buffered saline

PCPG pheochromocytoma and Paraganglioma

PCR polymerase chain reaction

PDPN podoplanin

PDGFRα platelet-derived growth factor receptor alpha

PECAM-1 platelet endothelial cell adhesion molecule 1

PGC primordial germ cells

PIP2 phosphatidylinositol (4,5)-bisphosphate

PKC protein kinase C

PLC phospholipase C

PNX pneumonectomy

RAD prostate Adenocarcinoma

PRRs pattern recognition receptors

R

RA rheumatoid arthritis

RAMP receptor activity modifying protein

READ rectum adenocarcinoma

RNA ISH RNA *in situ* hybridisation

RMS rhabdomyosarcoma

RSEM RNA-Seq by Expectation Maximisation

RT room temperature

S

SCLC small cell lung cancer

SD standard deviation

SDF-1 stromal derived factor -1

SNPs single nucleotide polymorphisms

SSC side scatter

STAD stomach adenocarcinoma

STES esophageal carcinoma

T

TAMs tumour-associated macrophages

TANS tumour-associated neutrophils

TCGA the cancer genome atlas program

TEM transendothelial migration

Th2 T helper cells

THYCA thyroid cancer

Tregs T regulatory cells

U

UCEC uterine corpus endometrial carcinoma

V

VCAM-1 vascular cell-adhesion molecule-1

VEGF vascular endothelial growth factor

VSMCs vascular smooth muscle cells

W

WT wild type

List of Figures

CHAPTER 1

Introduction

1.1 Inflammation and cancer

Inflammation is a complex biological response and one of the essential mechanisms of the immune response of our body against microbial and viral infections but also against specific injuries. Inflammation can be classified as acute or chronic.

Acute inflammation is a rapid response that occurs within minutes or hours after injury or infection. It is a non-specific first line of defence and includes processes such as the recruitment of white blood cells at the inflamed site. Some of the common symptoms of acute inflammation include redness, swelling, increased temperature and pain, which are the result of increased blood flow in the inflamed tissue. Acute inflammation is characterised by two phases: initiation and resolution. Initially, the first cells attracted to a site of injury or infection are neutrophils, followed by eosinophils, monocytes and macrophages. These cells belong to the white blood cells, commonly named as leukocytes and are recruited to the inflamed site following chemotactic gradients in a process that is called chemotaxis[1,2].

During the initiation phase, “patrolling” polymorphonuclear neutrophils which are abundant in the blood circulation, migrate to the area of infection or injury, attracted by pro-inflammatory mediators such as leukotrienes and chemokines. Neutrophils leave the blood circulation and enter the inflamed tissues in a multistep process that involves rolling activation, firm adhesion, and extravasation to the inflamed tissue. Neutrophils are phagocytes, and they can engulf and digest harmful foreign particles, bacteria, and dead cells.

Subsequently, during the resolution phase, circulating blood monocytes are attracted to the site of inflammation and infiltrate the inflamed tissue. There, they differentiate into macrophages or dendritic cells that act as phagocytes engulfing pathogens but also apoptotic cells, thus signalling the resolution phase of inflammation[3].

Acute inflammation resolution is a prerequisite for tissue repair and homeostasis restoration, and is achieved through apoptosis and clearance of the cell debris and

immune cells. Acute inflammation is a short-term process that lasts a few days, and it is usually self-resolving. However, in some cases, it can progress to unresolved chronic inflammation contributing to a variety of chronic inflammatory diseases. Chronic inflammation, unlike acute inflammation, is the aberrant and persistent inflammation. Chronic inflammation is also characterised by the simultaneous destruction and repair of the tissue due to the prolonged inflammatory microenvironment[4,5].

The first observation that linked inflammation and cancer is placed back in the 19th century when Rudolf Virchow noticed the presence of leukocytes within tumours. He introduced the hypothesis that the sites of chronic inflammation are the sites of origin for cancer. Despite this, only over the last two decades, cancer inflammation and tumour immune microenvironment have become the intense subject of study. The tumour immune microenvironment includes macrophages, neutrophils, mast cells, myeloid-derived suppressor cells, dendritic cells, natural killer cells, T and B lymphocytes. Besides the inflammatory cells, the tumour microenvironment is rich in pro-inflammatory cytokines and chemokines that can be secreted by tumour cells themselves but also from tumour- associated leukocytes, fibroblasts and other stromal cells. This network of inflammatory cells and pro-inflammatory mediators can contribute to the tumour progression[6].

It is now generally accepted that prolonged inflammation is linked with DNA damage, which can lead to the development of cancer. Inflammatory cells such as leukocytes can induce DNA damage in cells, through the production and release of reactive oxygen and nitrogen species that are typically produced by these cells to fight infections. In chronic inflammatory conditions, repeated tissue damage and regeneration of tissue lead to a highly proliferative epithelium. In these proliferative epithelial cells, the highly reactive nitrogen and oxygen species can oxidise the DNA, resulting in permanent genomic alterations such as point mutations, deletions, or genomic rearrangements[7]. One observation that supports the positive correlation between chronic inflammation and cancer is the fact that the frequency of mutations in the p53 tumour suppressor gene (*TP53*) in tumours, is observed at similar rates in

chronic inflammatory diseases such as rheumatoid arthritis and inflammatory bowel disease[8].

The study of particular subsets of human inflammatory diseases has brought an invaluable insight into the correlation between inflammation and cancer. Epidemiological and clinical studies have revealed that chronic inflammation that can be caused by infections, autoimmune diseases or irritants is associated with 15%-20% of human cancers. Some examples of chronic inflammation-associated cancers include *Helicobacter pylori* infections in the gastric mucosa that are linked with lymphoid tissue lymphoma, *Hepatitis* B or C infections that can lead to hepatocellular carcinoma (HCC) and inflammatory bowel disease that is associated with colorectal cancer (CRC)[9].

1.1.1 Inflammatory cells

One of the most crucial and well-organised mechanisms of inflammation includes the recruitment of white blood cells to the inflamed site. The essential subsets of white blood cells (also known as leukocytes) that play a crucial role in cancer inflammatory responses are briefly introduced below.

Neutrophils

Neutrophils are the most abundant leukocyte population in the circulation and are considered to be the first line of defence mechanism after infection or injury. Neutrophils exhibit high mobility; they have a short life span and are densely packed with secretory granules. Neutrophils are produced in the bone marrow and differentiate from hematopoietic stem cells to common myeloid progenitor cells to lineage-committed progenitors that subsequently mature into neutrophils[10].

Neutrophils have three mechanisms to kill microbes: phagocytosis, degranulation and neutrophil extracellular trap (NET) formation. Neutrophils are considered phagocytes because of their ability to engulf and digest harmful foreign particles, bacteria, and dead cells. Neutrophils are also referred to as granulocytes because

they have characteristic granules in their cytoplasm. Molecules that are stored in certain types of these intracellular granules have antimicrobial properties and can regulate the rapid and accurate response to infections. Other granule proteins regulate adhesion, transendothelial migration, phagocytosis, and neutrophil extracellular trap (NET) formation. Neutrophils can modify their chromatin to trap and kill microbes. These structures are called NETs. NETs are large, extracellular, structures composed of cytosolic and granule proteins that are assembled on a skeleton of chromatin. The use of modified chromatin as a host defence mechanism is evolutionarily conserved and appears in many organisms, including plants[11].

Neutrophils are ‘’patrolling’’ leukocytes in the blood circulation, and they are recruited to sites of inflammation responding to chemokine gradients. The most critical chemokine responsible for their recruitment is CXCL8, as neutrophils express the CXCL8-binding receptors CXCR1 and CXCR2[12].

Dendritic cells

Dendritic cells (DCs) are central players of the immune system, and they hold a key role linking innate and adaptive immunity. Dendritic cells are phagocytes and their role is to “screen” for pathogen at the tissues in which they reside. DCs utilise pattern recognition receptors (PRRs) to engage pathogen-associated molecular patterns (PAMPs). PAMPS can be nucleic acids of viral or bacterial pathogens or elements of the viral envelope or the bacterial cell wall. Upon recognition of a pathogen, DCs sequester the encountered pathogen through endocytosis or micropinocytosis, and the pathogen is processed and presented in the form of peptides on MHC class I and MHC class II complexes on their surfaces to activate naïve T cells. The antigen presentation and T cell activation take place in the lymph nodes. To present antigens to naive T cells, dendritic cells migrate from inflamed or injured peripheral tissues to the closest draining lymph nodes through lymphatic vessels. More specifically, antigens that are presented on the MHC class I complex activate CD8+ cytotoxic T cells, while antigens presented on the MHC class II complex activate CD4+ helper T cells. Antigen presentation process is the bridge between innate and adaptive immunity[13].

Dendritic cell migration to lymph nodes

During embryonic development, DC progenitors (pre-DCs) reside in the skin, the inner lining of the nose, lungs, stomach, intestines and other organs and give rise to immature DCs that act as sentinels of the immune system. DCs get activated and mature when they interact with pathogens. This activation leads to an increase in the expression of the CCR7 that is accompanied by increased mobility. CCR7 that is expressed on the surface of migrating DCs interacts with its ligand CCL21, which is constitutively produced by lymphatic vessels in peripheral tissues and directs the DCs into the lumen of afferent lymphatic vessels. Experiments with CCR7 knockout mouse models confirmed that CCR7 is essential for the migration of dendritic cells through the lymphatics to the lymph nodes. Following their entry to the afferent lymphatic vessels, DCs follow gradients of both CCL21/CCL19 to migrate into the lymph nodes although it has been shown that CCL21 alone is sufficient to drive their migration. When they reach the subcapsular sinus of lymph nodes, DCs following again a CCL21 gradient that leads to the lymph node paracortex (an area that is T- cell-rich), migrate and meet the naïve T cells to present the antigens and initiate the adaptative immune responses. ACKR4 is expressed by the lymphatic endothelial cells in the ceiling of the subcapsular sinus and shapes the CCL21 chemokine gradient guiding the DCs towards T cell-rich areas in the lymph node (also discussed in 1.10.3 section)[14,15,16].

Macrophages

Macrophages comprise a very heterogeneous cell population that plays a vital role in almost every biological function of an organism including development, homeostasis, tissue repair and immune responses to pathogens. Macrophages are specialised phagocytic cells and are characterised by high plasticity. Macrophages have distinct origins such as yolk sac, foetal liver and bone marrow. Inflammatory macrophages originate from bone marrow-derived monocytes. Tissue-resident macrophages can derive from yolk sac macrophages, foetal liver monocytes, or adult bone-marrow monocytes. Depending on the tissue in which they reside, macrophages can be categorised as alveolar macrophages (lung resident), Kupffer cells (liver resident), microglia (central nervous system resident), splenic macrophages (spleen resident),

peritoneal macrophages (peritoneal cavity resident) and osteoclasts (bone resident)[17,18].

Macrophages, as a response to extracellular signals, can be activated and adopt different functions in a process that is known as macrophage polarisation. Polarised macrophages can be classified as M1 (classically activated macrophages) and M2 (alternatively activated macrophages). The classically activated M1 macrophages are aggressive against bacteria and produce high amounts of proinflammatory cytokines. The alternatively activated, anti-inflammatory M2 macrophages are involved in parasite control, tissue remodelling, immune regulation and also have tumour-promoting properties[19,20].

T cells

T cells are major components of the adaptive immune system. T lymphocytes originate from the bone marrow and they migrate to the thymus where, after maturation and selection, they enter the circulation. Peripheral T cells consist of different subsets, including naive T cells, memory T cells and regulatory T (Treg) cells. Memory T cells are essential for the maintenance of long-term immunity and regulatory T (Treg) cells for regulating immune responses. Regulatory T cells are critical immune suppressor cells. They play vital roles in the maintenance of peripheral immunological tolerance and preventing autoimmunity. Naive T cells circulate through the lymph nodes and peripheral tissues until they recognise antigens presented by antigen-presenting cells in the lymph nodes. Naïve T cells can be subdivided into helper T cells and cytotoxic T cells. Helper T cells express the CD4 protein on their surface. As indicated by their name, their main roles after they get activated, are to help B cells to secrete antibodies, to activate cytotoxic T cells, to kill target cells, but also to assist macrophages in destroying pathogens. There are different subsets of T helper cells, including Th1,Th2,Th9,Th17 and Th22. Helper T cells become activated when antigen-presenting cells present them with peptide antigens by MHC class II molecules. Cytotoxic T cells express CD8 protein on their surface and their primary role is to kill virus-infected cells and malignant cells but they are also implicated in transplant rejection. Cytotoxic T cells become activated

when antigen-presenting cells present them with peptide antigens associated with MHC class I molecules[21,22].

T cell activation is a process that requires several signals. The first recognition signal includes antigen presentation where the T cell receptor (TCR) that is expressed on both CD4+ helper T cells and CD8+ cytotoxic T cells binds to the antigen-peptide that is presented on the MHC complex, on the surface of the antigen presenting cells. Subsequently the CD4 and CD8 molecules bind to the MHC II and I molecules, stabilising the structure. The second signal for T cell activation occurs when the co-stimulatory molecules CD80 and CD86, that are expressed on the surface of the antigen-presenting cells, bind to CD28 that is present on the T cell surface. This binding event induces the release of different cytokines from the T cell and promotes the proliferation and clonal expansion of T cells. The T cell subsets are distinguished by the cytokines that they release upon activation. CD8 cytotoxic T cells require a third cytokine signal produced by macrophages or dendritic cells, to get activated and elicit immune responses. CD8+ T cells that do not receive a third signal in addition to signal 1 and signal 2 fail to develop the cytotoxic function and become unresponsive. Recent studies identified IL-12, type I IFN (IFNα/β) and possibly IL-21 as the major sources of signal 3 in a variety of responses, and are now considered to be the signal 3 in T cell activation[23,24].

Natural Killer cells

Natural Killers (NK) cells are large lymphocytes, derived from bone marrow. NK cells are mostly in the blood circulation, and they comprise of about 10% of human circulating lymphocytes. Apart from the blood circulation, NK cells can reside in organs such as the spleen, lung, lymph nodes, liver, and thymus. The role of NK cells is to recognise and kill virally infected cells, but also, they are responsible for tumour surveillance as they can recognise and kill malignant cells. The NK cells in the blood circulation, are usually inactive and they get activated by cytokines. In contrast to T cells, NK cells do not express clonotypic receptors. However, they initiate strong anti-tumour cytotoxicity and generate significant quantities of pro-inflammatory cytokines. The absence of clonotypic receptors is substituted by multiple NK cell activation

receptors such as NKG2D, NCR1, NCR2, NCR3, NKG2C, CD244, Ly49D, and Ly49H. The expression of a combination of these activation receptors that recognize self or pathogen-derived ligands provides NK cells with inherent, innate abilities to initiate effector immune responses[25].

After activation, NK cells infiltrate to pathogen-infected or malignant tissues, to kill the infected cells or tumour cells depending on the pathophysiological context. Furthermore, during inflammation, NK cells enter the lymph nodes and can regulate the T cell immune response. NK cells can be activated by DCs in the lymph nodes and the spleen, and after activation, they secrete interferon γ, increasing the T cell - mediated killing response. For instance, they can promote Th1 cells polarisation by releasing IFNγ. NK cells can also regulate T cells indirectly via modulation of antigen-presenting cells. For example, the NK- dendritic cell crosstalk can stimulate the production of IFNγ from NK cells, which further promotes dendritic cells activation. However, NK cells can, in some instances, restrict the expansion of activated T cell populations by directly killing them[26].

1.2 Cell migration

Cell migration is a fundamental process in the development and maintenance of multicellular organisms. The main types of cellular migration are introduced below.

Chemotaxis is the directed movement of cells in response to an extracellular chemical gradient[27]. Cell chemotaxis is a fundamental process in several physiological events such as leukocyte recruitment in inflamed tissues during immune responses and stem cells and specialised cell migration during development[28]. Although most of the chemotactic factors have dual roles in cell growth and survival, they can also mediate cytoskeletal rearrangements that result in chemotaxis[29,30]. Chemotaxis is also involved in pathophysiological conditions including autoimmune diseases and cancer, where metastatic tumour cells migrate through the blood circulation, and ‘’colonise’’ distant secondary metastatic sites.

Eukaryotic cells can sense the presence of chemotactic stimuli in their microenvironment through seven-transmembrane spanning heterotrimeric G-protein-coupled receptors (GPCRs), a class representing a significant portion of the genome[31]. The main classes of chemoattractants / chemotactic receptors are the following:

- formyl peptides - formyl peptide receptors (FPR)
- chemokines - chemokine receptors (CCR / CXCR)
- leukotrienes - leukotriene receptors (LT)

Haptotaxis is another type of cellular movement in which the cells move in a directional way in response to adhesive substrates such as the extracellular matrix (ECM). In haptotaxis, the gradient of the chemoattractant is expressed or is bound on a surface mostly commonly in the ECM. Haptotaxis is different from chemotaxis in which the chemoattractant gradient is in a soluble form. Finally, chemokinesis is the random, non-directional cellular movement in response to an external chemical stimulus[32].

1.3 Chemokine family

The chemokine superfamily comprises of small (6-16 kDa) secreted proteins which play a fundamental role in a broad range of physiological processes including embryogenesis, haematopoiesis and immune system development. Initially, chemokines were mostly appreciated for their ability to orchestrate immune responses and maintain immune system homeostasis. Subsequently, chemokines were also linked to pathophysiological conditions like HIV infection, atherosclerosis, autoimmune diseases, cancer development and metastasis. Chemokines act as chemoattractants leading to directed migration of target cells towards increasing chemokine gradients[33,34].

1.3.1 Evolution

Chemokines and chemokine receptors arose in vertebrates. Chemokines and their receptors evolved rapidly through species-specific gene duplications that lead to the differences in chemokines between species. In the human genome, the majority of the CC and CXC chemokine genes are located in two chromosomal regions, thus forming two large gene clusters, the CXC chemokines cluster (chromosome 4) and the CC chemokine cluster (chromosome 17). Apart from these two mega clusters, there are also mini clusters that consist of 2-3 chemokine genes and some chemokines genes that are not located in any gene cluster. This genomic organization of the chemokine genes is the result of evolutionary pressures and is linked to their functions (orchestrating the immune response, homeostatic regulation)[35].

Phylogenetic analyses indicate that only CXCL12 and CXCL14 have orthologues in fish. The remaining mammalian CXC chemokines do not have orthologues in any other vertebrate class. This supports the hypothesis that CXCL12 and CXCL14 phylogenetically represent the most ancestral CXC chemokines. Furthermore, phylogenetic analyses revealed that one of the most evolutionarily conserved chemokine signalling axes is the CXCL12/CXCR4 axis, which has orthologs in vertebrate species ranging from fish to humans. Studies in zebrafish revealed that CXCL12 and CXCR4 are also crucial to the migration of primordial germ cells to the gonads. More specifically, it was shown that in *Odysseus*, a zebrafish homologue, CXCR4, is required for the chemotaxis of the germ cells and their proper spatial distribution. CXCR4 mutant germ cells were still able to migrate, but this migration lacked directionality towards the target tissue, resulting in randomly positioned germ cells. It was also shown that CXCL12, a ligand for CXCR4, was responsible for the germ cells proper migration and positioning in the tissue as CXCL12 mutant embryos phenocopied the CXCR4 null phenotype[36].

1.3.2 Nomenclature

Previously, chemokines have been named arbitrarily, without following a defined system. Some chemokines were named according to their function (e.g. macrophage

chemotactic protein), others according to the cell type that produces the chemokine, (e.g. platelet factor 4), some were included in the interleukins (e. g. IL-8), and some were named using abbreviations (e.g. RANTES). To this end, there was an immediate need to agree on a universal and straightforward nomenclature system for chemokines. The systematic chemokine nomenclature system, names the chemokines according to the position of the cysteines in their structure, followed by a number that indicates the order in which the chemokine was discovered (e.g. CCL1). Chemokines exhibit a highly conserved primary structure regarding the position of their cysteine residues. Based on this primary characteristic, chemokines can be classified into four distinct subfamilies: CXC, CC, CX3C and XC (Figure 1.1). So far, in humans, there are more than 45 chemokines identified, that bind to 19 chemokine receptors, triggering signalling cascades that generate various cellular responses such as chemotaxis, Ca+ influx, proliferation, cell adhesion and endocytosis (Figure 1.2). Although each receptor subtype typically binds multiple chemokines (redundancy), the specificity is restricted by chemokine subfamily in the inflammatory chemokine receptors[37].

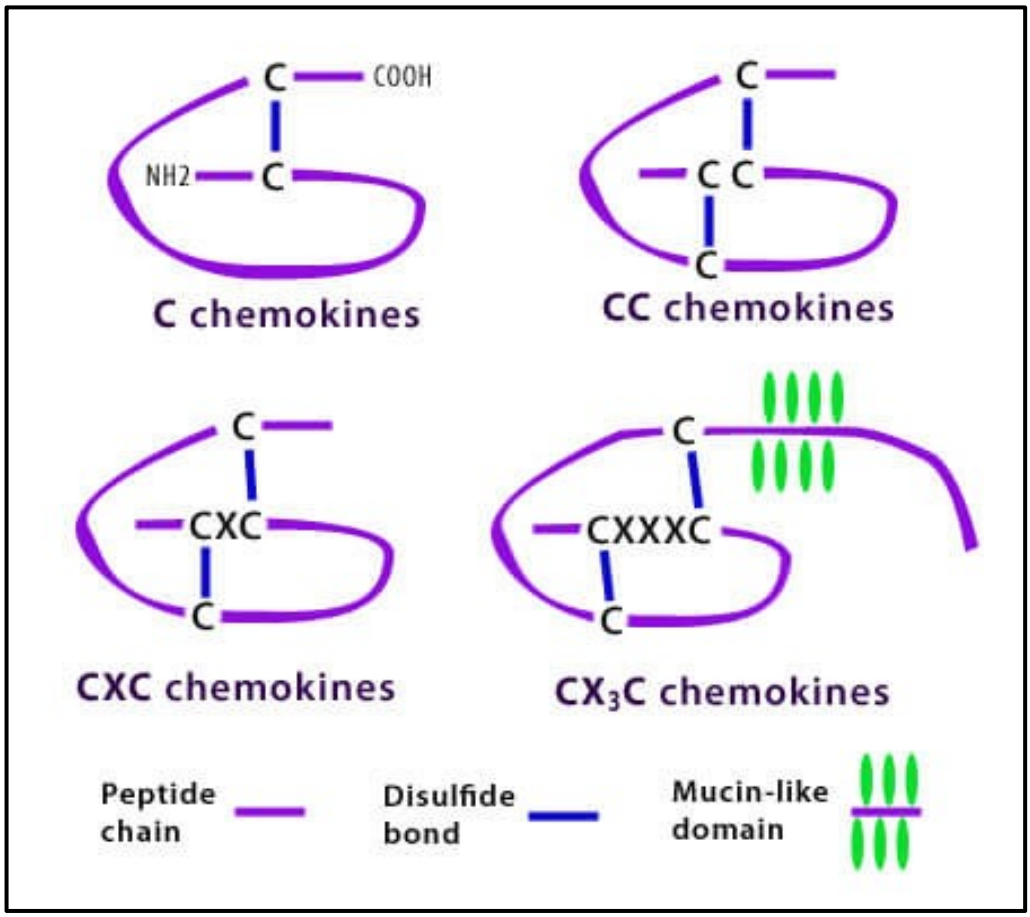

Figure 1.1 Chemokine subfamilies according to their cysteines' residues position. Cysteine residues are linked by intramolecular disulfide bonds. The CX_3C family members possess a transmembrane mucin-like domain.

Functionally, chemokines can be classified into two distinct groups: homeostatic and inflammatory chemokines. Homeostatic chemokines such as CCL19, CCL20, CCL21, CCL25, CCL27, CXCL12 and CXCL13, are constitutively expressed and are responsible for the development and maintenance of the immune system. Inflammatory chemokines are inducible, in response to tissue damage or infection and play a crucial role in the inflammatory response, attracting immune cells to the site of inflammation[38,39]. Some examples of inflammatory chemokines are CXCL8, CCL2, CCL3, CCL4, CCL5, CCL11 and CXCL10.

1.3.3 Structure

NMR and crystallography studies have revealed that chemokines (monomeric form) adopt the same folding architecture. Their generic structural pattern consists of a flexible disordered N-terminus, the ‘’signalling domain’’, followed by a structured core that consists of three-stranded antiparallel β-sheets, on which is folded a C-terminal α-helix. In chemokines, the highly conserved cysteine residues, form disulfide bridges that are crucial for maintaining the proper protein folding and structural integrity, which is essential for chemokine–receptor binding[40].

Chemokine monomers usually self-interact and usually form homodimers, but in some cases can also form tetramers and higher-order aggregates. CC chemokines dimerise through their N-terminal regions and they form a new antiparallel β-sheet. Instead CXC chemokines dimerise through their β-sheet regions. It has been reported that CXC chemokine dimers are active whereas CC chemokine dimers are not. This difference can be explained based on their different dimer structures. CXC chemokine dimerisation leaves the receptor-binding and activation regions exposed, whereas CC chemokine dimerisation involves the N-terminal region, which is crucial for receptor activation. Chemokine oligomerisation can be facilitated by interactions with glycosaminoglycans and can alter the chemokine functions. Chemokines bind to GAGs through high-order oligomer formation while chemokines bind and activate their respective receptors as monomers[41].

1.3.4 Interaction with GAGs

Glycosaminoglycans (GAGs) are sulphated carbohydrates and their interactions with chemokines localise chemokines on and near cell surfaces and the extracellular matrix to provide direction to the cell movement. GAGs are present on endothelial cells and in the extracellular matrix. The interactions with GAGs can be crucial in many cases, for modulating chemokine functions such as leukocyte recruitment, chemokine oligomerisation, receptor binding and enhancement of stability [42,43].

The interactions between GAGs and chemokines can be predicted based on their structure since GAGs are acidic polysaccharides, and most chemokines are rich in basic amino acids like Lys, Arg and His. As a consequence, the acidic GAGs bind to basic residues within chemokines through electrostatic and H-bonding interactions[44,45].

One example of chemokine- GAGs interactions functions is Heparan Sulphate (HS). Heparan Sulphate is one of the most common GAGs and is present on the surface of endothelial cells. HS is an anionic GAG and part of the glycocalyx on the surface of the endothelial cells[46]. Experimental evidence of the importance of the interactions between chemokines and GAGs was provided when chemokine mutants that were able to bind the chemokine receptors but failed to bind GAGs *in vitro*, failed to activate cell migration *in vivo*. This paradigm highlights the importance of chemokine/GAG interactions for creating a chemokine gradient and modulating leukocyte migration and inflammatory responses[47].

1.4 Chemokine subfamilies

1.4.1 CC chemokine subfamily

The CC chemokines have as a common structural feature the presence of two adjacent cysteine residues located close to the N terminus. The CC chemokine subfamily contains at least 28 members, including CCL1- CCL28 chemokines. CC chemokines usually possess four cysteines, but a few of them possess six cysteine residues. CC chemokines bind to CCRs but also to members of the Atypical Chemokine Receptor (ACKR) family and more specifically to ACKR1, ACKR2 and ACKR4. Depending on their functions, CC chemokines can be characterised as allergenic, pro-inflammatory, developmental and homeostatic, but this characterisation is not exclusive as a chemokine can belong to more than one subgroup. The chemokines that belong to the allergenic and pro-inflammatory group are considered inducible, while the developmental and homeostatic are generally constitutively expressed[48].

The allergenic subgroup includes the CCL1, CCL2, CCL7, CCL8, CCL11 and CCL13 chemokines. They are potent eosinophil or basophil attractants and can lead to histamine release. CCL8-deficient mice exhibit markedly less eosinophilic inflammation than wildtype mice[49]. Members of the pro-inflammatory subgroup include CCL3, CCL4, CCL5, CCL6 and CCL18. CCL3, previously known as macrophage inflammatory protein (MIP) 1-α, is responsible for the recruitment of monocytes, macrophages, dendritic cells and both CD4+and CD8+ T cells during the acute immune response. Mice that are null for CC inflammatory chemokine receptors also exhibit defects in monocyte migration. For example the CCR5 and CCR2 knockout mice appear to have a partial defect in macrophage function and exhibited a decreased Th1 immune response, as measured by a reduced production of Th1 cytokines, such as IFN-γ[50].

CCL2, CCL7, CCL8 and CCL13 play a crucial role in the recruitment of monocytes to inflammatory sites. Finally, the subgroup of developmental and homeostatic CC chemokines includes the CCL17,CCL19,CCL20,CCL21,CCL22 and CCL25. CCL17 is highly expressed in the thymus and shares similar roles with CCL22 as they both attract Th2 cells. CCL20 has been shown to recruit TH17 cells[51]. CCL19 and CCL21 are produced constitutively by lymphoid tissues and organs and are responsible for the recruitment of mature dendritic cells and T cells in the lymph nodes for the antigen presentation process[52].

1.4.2 CX3C chemokine subfamily

The CX3C subfamily consists of only one member: the CX3CL1 chemokine that has three amino acids between its first two cysteines. CX3CL1 binds specifically to its receptor CX3CR1. CX3CL1 is usually associated with cell membranes, via a mucin stalk linked to transmembrane and cytoplasmic domains. CX3CL1 is mostly present as a membrane-bound cytokine, but a soluble form (95 kDa) has also been detected. The soluble form acts as a potent chemoattractant for T cells and monocyte subsets. On the other hand, the membrane-bound form, that is detected in primary endothelial cells, promotes strong adhesion of leukocytes[53,54] .

1.4.3 C chemokine subfamily

The C chemokine subfamily members have only two cysteine residues, one N-terminal cysteine and one cysteine downstream. This subfamily has only two members: XCL1 (lymphotactin-α) and XCL2 (lymphotactin-β), that are different from each other in two adjacent amino acids. XCL1 can induce the chemotaxis of lymphocytes but not monocytes or neutrophils, by binding to the receptor XCR1[55,56].

1.4.4 CXC chemokine subfamily

CXC chemokines display a plethora of effects regulating immunity, angiogenesis, and organ-specific metastasis in the context of cancer. The CXC chemokine subfamily consists of 17 members (CXCL1-CXCL17) which belong to the inflammatory chemokines, with the only exceptions being CXCL16, CXCL12 and CXCL13 that are homeostatic chemokines. The common characteristic of the CXC chemokines is that they have an amino acid between the first two cysteines. CXC chemokines are key players that can activate or inhibit angiogenesis through their interaction with cognate receptors that are expressed by endothelial cells. Regarding this, the CXC subfamily can be further divided into ELR+ and ELR- chemokines depending on the presence of an ELR (Glu-Leu-Arg) motif. ELR+ chemokines are considered angiogenic and mediate their angiogenic activity through binding and activating CXCR2 on the endothelium. ELR+ chemokines include the following members: CXCL1, CXCL2, CXCL3, CXCL5, CXCL6, CXCL7 and CXCL8. ELR- chemokines include CXCL4, CXCL9, CXCL10, CXCL11 and CXCL17. ELR- chemokines in general, are inducible by interferon γ, are potent inhibitors of angiogenesis and (except CXCL17) bind to CXCR3 on the endothelium[57].

In wounding, CXC chemokines coordinate the interplay between angiogenesis and inflammation, leading to tissue repair. At the wound site, platelets that are attracted, release vasoactive mediators that regulate the formation of the fibrin clot. Subsequently activated platelets release CXCL1, CXCL5 and CXCL7 chemokines that initiate the recruitment of neutrophils. The cooperative expression of CXCL1 and CXCL8 in the superficial wound bed supports additional neutrophil recruitment to the

wound site. Neutrophils provide defence against contaminating microorganisms and they are involved in the phagocytosis of cell debris. CXCL8 secreted by wounded epithelial cells induces massive angiogenesis, leading to the formation of new blood vessels that exhibit high CXCR2 expression. When the tissue repair is achieved, upregulation of the angiostatic chemokines CXCL9, CXCL10 and CXCL11 prevents unlimited vessel growth, arresting migration and growth of CXCR3+ proliferating endothelial cells[58].

CXCL12 is one of the most extensively studied chemokines. CXCL12 is a homeostatic chemokine and binds to CXCR4 and ACKR3. CXCL12 is constitutively expressed by stromal cells in the bone marrow, but during inflammation, CXCL12 can be secreted by most stromal cells, which leads to chemotaxis of lymphocytes towards the affected area. CXCL12 is also involved in the promotion of angiogenesis and the maintenance of tissues[59].

1.5 Chemokine Receptor Family

Chemokine receptors belong to the superfamily of 7-transmembrane spanning G protein-coupled receptor (GPCRs). They are usually around 350 amino acids long. They consist of a flexible extracellular N terminus that can be sulfated on tyrosine residues and contains N-linked glycosylation sites. The N terminus is essential for ligand binding. The N terminus is followed by a seven α-helical transmembrane region separated by three intracellular and three extracellular loops. Finally, there is a cytoplasmic C terminus responsible for G protein association and signalling cascade initiation. A disulfide bond links the highly conserved cysteines in extracellular loops one and two[60]. Chemokine receptors are GPCRs that belong to the family of rhodopsin-like receptors, γ subgroup, chemokine receptor cluster. Genetically, these receptors are located in clusters on different chromosomes. This suggests a common ancestral origin which may have evolved through genome duplications[61]. Chemokine receptors are divided into “typical” and “atypical” chemokine receptors, based on their ability to elicit G protein-mediated responses. Furthermore, typical chemokine

receptors can be subcategorized based on the class of chemokines they bind: CCR bind CC chemokines, CXCR bind CXC chemokines, XCR1 binds XC chemokines, and CX3CR1 binds CX3CL1 chemokine. Chemokine receptors follow the chemokine nomenclature and are named after the chemokines that they bind to. This has led to a logical chemokine receptor nomenclature system in which each receptor is designated by the chemokine subfamily name (C, CC, CXC, CX3C), followed by the letter R (stands for a receptor), and a number based on the chronological order in which the receptor was identified. So far, 45 chemokines and 19 chemokine receptors have been identified in humans. The numerical mismatch between chemokines and receptors makes it apparent that ligand-receptor relationships are not always exclusive (more than one chemokine can bind to one receptor and a single chemokine can bind to different receptors) and in some cases responses can be elicited by as many as 10 individual ligands[62].

Chemokine receptors can be functionally characterised as either inflammatory or homeostatic. Constitutively expressed homeostatic chemokine receptors play a crucial role in developmental processes and basal leukocyte trafficking. Inflammatory chemokine receptors are characterised by inducible expression and their role is to orchestrate and fine-tune the immune response in acute but also chronic inflammatory conditions. Regarding this classification, the CXC chemokine receptors can be inflammatory (CXCR1-3) or homeostatic (CXCR4-6). CC chemokine receptors include ten members (CCR1-10). CCR1-5 are all associated with inflammation, although CCR1,CCR2 and CCR5 are considered to be the classical inflammatory receptors. The CC chemokine receptors are expressed on immune cells including eosinophils, basophils, lymphocytes, macrophages, and dendritic cells, whereas the CXC receptors are expressed mainly on neutrophils and lymphocytes. CXCR1 and CXCR2 are expressed on neutrophils and are crucial as they regulate their migration of during inflammation[63].

CCR2 is expressed on a subset of inflammatory monocytes and plays an important role in their recruitment into the tissue. CCR6 is constitutively expressed on immature dendritic cells and in Th17 cells. CCR8 is constitutively expressed in the thymus and

is upregulated during T-cell activation and is a marker of TH2 cells. CCR7 is expressed in mature dendritic cells and T cells. Apart from leukocytes some chemokine receptors are upregulated in malignant cells. For example, CXCR4 is upregulated in tumour cells and drives metastasis to secondary sites that are rich in its ligand CXCL12[64].

The importance of the chemokine receptors in immune system regulation and development is highlighted by *in vivo* studies in which chemokine receptors or their respective ligands were ablated in animal models. For example, the deletion of CXCR4 or its ligand CXCL12 both result in a lethal embryonic phenotype[65]. Deletion of CCR7 or its ligand CCL21 results in mice that, although they are viable, lack the correct architecture of secondary lymphoid tissues[66,67]. Similarly, in mice deficient in CXCR5 the organization of primary splenic follicles is severely impaired[68].

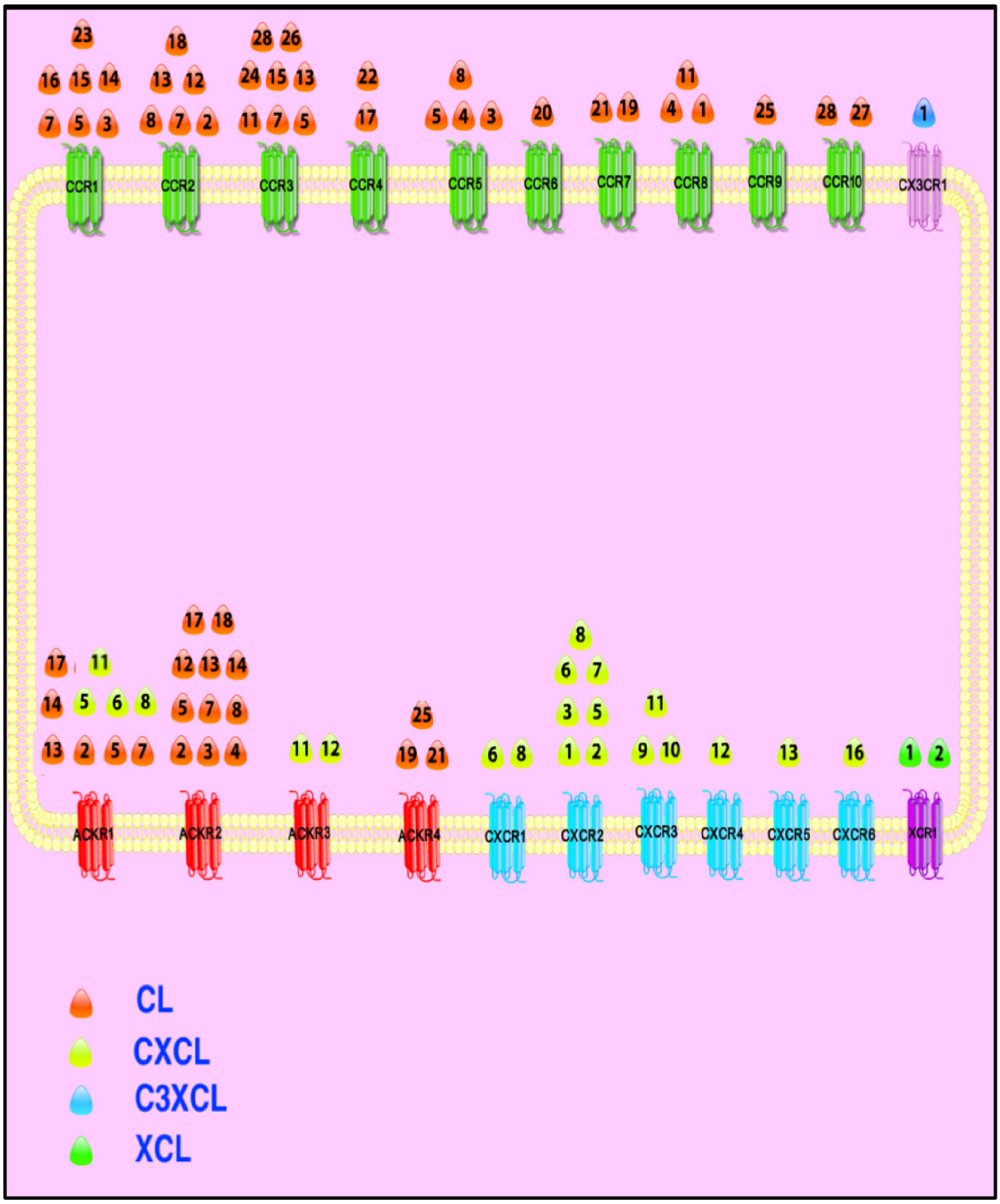

Figure 1.2 Schematic representation of the chemokine receptors and their respective chemokine ligands. *Chemokines of the four subclasses (CCL, CXCL, CX 3 CL, and XCL) bind to more than one chemokine receptors(redundancy).*

1.6 Chemokine receptor signalling

The typical chemokine receptors signal (but not exclusively) through G- proteins. In the cytoplasm, G proteins are protein complexes, that exist in trimeric form and consist of three different subunits Gα, Gβ and Gγ. They act as molecular switches and transmit signals from the surface of the cell downstream.

G-proteins' ability to transmit signals, lies in their ability to bind and hydrolyse guanosine triphosphate (GTP) to guanosine diphosphate (GDP). In their inactive state, G- proteins have GDP bound in their subunits. Upon binding of the chemokine, chemokine receptors associate with G-proteins, allowing the exchange of GDP for GTP. These events are followed by the dissociation of the three G protein subunits. The Gα subunit is responsible for the activation of an enzyme known as Phospholipase C (PLC) that is bound to the cell membrane. PLC cleaves Phosphatidylinositol (4,5)-bisphosphate (PIP2) to form two secondary messenger molecules called inositol triphosphate (IP3) and diacylglycerol (DAG). Subsequently, DAG activates another enzyme called protein kinase C (PKC), and inositol 1,4,5-triphosphate (IP3) that triggers the release of calcium from intracellular stores. Calcium influx initiates many signalling cascades in the cell as a response to the original external stimuli[69].

1.7 Chemokines and receptors in diseases

Chemokines and their respective receptors play a fundamental role in orchestrating the immune response in several inflammatory conditions that can be acute or chronic. The chemokine/ chemokine receptor involvement in some of the more significant inflammatory disorders is described below.

1.7.1 Atherosclerosis

Several studies have shown that CCL2 is highly expressed in atherosclerotic plaques, suggesting a role for monocyte extravasation in the formation of atherosclerotic plaques[70]. New evidence from studies using transgenic mice support this hypothesis. More specifically, CCL2/LDLR (low-density lipoprotein (LDL) receptor) double knock

out mice have significantly less lipid deposition than WT/LDLR mice in arteries following a high-fat diet[71].

Furthermore, CCR2 deficient mice that are also deficient in apolipoprotein E (double knock out mice) exhibited reduced atherosclerotic lesions compared to the control group after a high-fat diet[72]. These data strongly suggested that CCL2 is an essential player in the development of atherosclerotic plaques. Furthermore, monocyte subsets expressing CCR2 were increased in atherosclerotic lesions. This finding is consistent with the observation that hypercholesteraemic patients have elevated numbers of CCR2 positive monocytes[73]. Histological studies have also shown that activated T cells are present in atherosclerotic lesion development[74].

In the literature, several studies highlight the critical role of the CX3CL1/CX3CR1 axis in atherosclerosis. Two different mouse models of atherosclerosis support this role. More specifically, it has been shown that CX3CL1−/− ApoE−/− (Apolipoprotein E) mice exhibited decreased atherosclerotic lesion formation in the brachiocephalic artery but not the aortic root. In the second CX3CL1−/−LDLR−/− (low-density lipoprotein receptor) mouse model, atherosclerotic lesions were reduced both in the brachiocephalic artery and the aortic root[75].

In humans, it was found that two CX3CR1 polymorphisms and, more specifically, the V249I and T280M, were linked with coronary artery disease (CAD). The V249I polymorphism in CX3CR1, was associated with a lower risk of CAD. Another study revealed the cardioprotective effects of the T280M polymorphism in acute coronary syndromes[76,77].

1.7.2 Human immunodeficiency virus (HIV)

HIV can infect a variety of cells such as CD4+ helper T cells and macrophages that express the CD4 molecule on their surface. HIV-1 enters macrophages(M-tropic) and helper T cells(T-tropic) not only through the interaction of the viral envelope glycoproteins with the CD4 molecule but also with its chemokine co-receptors expressed on the surface of the target cells[78].

Maybe the most well-known paradigm and exciting discovery in the chemokine involvement in pathophysiology, is the involvement of CCR5 in HIV-1 infection. It was shown that M-tropic HIV-1 strains use both CD4 and CCR5 to infect the target cells. The HIV-1 envelope glycoprotein structure assists HIV-1 entry into the target cell. The HIV-1 envelope glycoprotein structure consists of two protein subunits: the gp120 external subunit and the gp41 transmembrane subunit. CCR5 is the primary co-receptor used by gp120 together with CD4 during HIV-1 infection. During HIV-1 infection, gp120 binds both CD4 and CCR5 co-receptor in order for the viral/target cell membrane fusion to proceed. The tyrosine-sulphated amino terminus of CCR5 is crucial for binding to gp120[79].

In 1996, different research groups identified a 32-bp deletion(Δ32) of the CCR5 gene. This CCR5 deletion leads to a non-functional CCR5 receptor that degrades fast and does not support membrane fusion or infection by macrophage and dual tropic HIV-1 strains. It is estimated that around one per cent of the population of northern Europe are homozygous for the CCR5Δ32 mutation and have no functional CCR5 receptor activity[80]. This deletion provides an advantage in certain diseases. Individuals that are homozygous for this mutation are resistant to infections by these HIV-1 strains. Furthermore, it has also been reported that CCR5Δ32 heterozygous HIV-positive individuals, take longer to develop acquired immunodeficiency syndrome (AIDS) symptoms[81]. Furthermore, this mutation provides protective effects in many inflammatory disorders. For example, CCR5Δ32 mutation seems to be protective against rheumatoid arthritis (RA), including extra-articular symptoms and joint erosions[82].

However, in some cases, CCR5Δ32 is non-protective. More specifically, CCR5Δ32 carrier individuals are more susceptible to developing lethal encephalopathy after West Nile virus infection than patients with wild-type CCR5[83].

The knowledge of the mechanisms that HIV-1 uses to exploit CCR5 co-receptor to infect immune cells led to the development of CCR5 inhibitors. These CCR5 specific inhibitors can block HIV entry into the target cells. So far one CCR5 antagonist, Maraviroc, has been clinically approved in 2007 as an drug against HIV infections[84].

1.7.3 Psoriasis

Immune-mediated inflammatory diseases (IMIDs), are a group of clinically unrelated disorders that are characterized by immune dysregulation and chronic non-resolving inflammation. IMIDs have been associated with cytokine dysregulation that is crucial for the pathophysiology of these diseases. There is evidence that leukocyte trafficking into peripherally inflamed tissues is altered in patients with IMIDs. Furthermore, genes associated with IMIDs are linked with leukocyte recruitment and migration[85]. Chemokines regulate the leukocyte migration into and out of tissues and play a vital role in the positioning of leukocytes within the inflamed site.

High expression of members of the CC and CXC chemokine subfamilies has been associated with many inflammatory diseases including arthritis, psoriasis, multiple sclerosis and lung disorders. High expression of CXCL8 was detected in the epidermis of psoriatic patients[86]. A high number of neutrophils and T cells were also present in the epidermis of these patients. It was also shown, that CXCR1 and CXCR2 expression, was almost ten times higher in psoriatic epidermis compared to epidermis from healthy individuals[87]. These observations lead to the assumption that CXCL8 is responsible for the inflammatory phenotype observed in psoriatic epidermis. This inflammatory phenotype includes leukocyte infiltration, increased HLA-DR (Human Leukocyte Antigen – DR isotype) expression in keratinocytes and epidermal hyperplasia[88]. Furthermore, psoriasis has been linked with T cell recruitment to the skin. CCR6 and CCL20 are highly expressed in psoriasis. In

psoriatic lesions, keratinocytes express CCL20 and recruit CCR6 expressing Th17 cells[89]. Keratinocytes in psoriasis also express CCL27 and attract T cells that express CCR10[90]. These paradigms indicate the vital role of chemokines and their receptors in the pathophysiology of this disease.

1.7.4 Rheumatoid arthritis (RA)

Rheumatoid arthritis (RA) is a chronic inflammatory disease characterized by massive infiltration of synovial tissue and synovial fluid with immune cells, mediated by chemokines and adhesion molecules. It is well accepted that monocyte/macrophage numbers are increased in clinically affected joints and these numbers correlate with the clinical signs and symptoms. In RA, leukocytes extravasate through the vascular endothelium into the synovial tissue. Several chemokines and chemokines receptors are linked with this process. In rheumatoid arthritis, pro-inflammatory chemokines are present at high levels in the synovial tissue, resulting in accelerated inflammation. Chemokines are also involved in endothelial activation and angiogenesis, synovial fibroblast migration and proliferation[91].

Many CXCRs have been associated with the pathophysiology of rheumatoid arthritis. CXCR1 and CXCR2 are highly expressed by the neutrophils in the RA synovium and are associated with neutrophil recruitment to the inflamed joints. CXCR3 may be the most crucial receptor in leukocyte homing into the RA synovium and is associated with Th17 cell recruitment[92]. Among CC chemokine receptors, CCR1, CCR2, CCR3, CCR4, CCR5, CCR6, CCR7 and CCR10 are highly expressed in the synovium in RA. CCR6 is linked with Th1 cells infiltration. CCR1, CCR2 and CCR5 each bind multiple CC chemokines that have essential roles in the pathogenesis of RA[93].

Numerous antagonists to these receptors have been developed and tested in animal models. Data from *in vivo* studies have provided evidence about the role of chemokines in RA. In collagen-induced arthritis (CIA) mouse model study, CCR2 knockout mice developed severe, aggressive CIA compared with wild-type mice.

Furthermore, it was shown that when lethally irradiated wildtype mice received bone marrow transplants from CCR2 null mice, the transplanted mice developed CIA. In contrast, wildtype mice transplanted with wild-type bone marrow did not develop CIA. This supports the hypothesis that CCR2 expression in the hematopoietic compartment is a crucial element of CIA development[94]. In contrast, another study showed that CCR5 null mice developed CIA to the same level as wild-type mice[95]. Despite this,CCR5 is a promising candidate for drug targeting in RA. Pharmacological targeting of these receptors in clinical trials did not improve the clinical outcome in these diseases. There are several challenges in therapeutic targeting of chemokine receptors (discussed in section 1.9).

1.8 Chemokines and cancer

For a long time, chemokines, have been associated with cancer since they orchestrate the recruitment and spatial positioning of leukocyte subsets in tumours. It is also increasingly recognised that chemokines play an essential role in facilitating communication between cancer cells and non-malignant cells in the tumour microenvironment, including endothelial cells and fibroblasts, promoting the infiltration and activation of tumour-associated neutrophils (TANs) and tumour-associated macrophages (TAMs). In the tumour microenvironment, chemokines are expressed and secreted from different cell types, including tumour cells, cancer-associated fibroblasts (CAFs) endothelial cells, but also tumour-infiltrating leukocytes. Chemokines signal, through binding their respective chemokine receptors, and mediate tumour proliferation, invasion, angiogenesis and immune evasion. Most tumours secrete chemokines that belong to the CXC or CC subfamilies. Usually, CXC chemokines are active on neutrophils and lymphocytes whereas CC chemokines act on several leukocyte subsets including monocytes, eosinophils, dendritic cells but also on lymphocytes and natural killer cells. The following synopsis summarises the most crucial processes that are regulated by chemokines within the tumour microenvironment[96].

Leukocyte Recruitment

Inflammation is one of the critical characteristics of the tumour microenvironment and one of the hallmarks of cancer[97]. Chemokines regulate immune cell attraction and infiltration within the tumour. It has been shown in several studies that inflammatory CC (CCL2, CCL5) and CXC (CXCL1, CXCL2, CXCL5, CXCL6, and CXCL8) chemokines are responsible for attracting to the tumour CCR2+ and CXCR2+ leukocytes. More specifically, it has been shown, that CC inflammatory chemokines that are secreted from the tumour, attract CCR2+ monocytes to the tumour. Those CCR2+ monocytes, after recruitment, infiltrate into the tumour and differentiate into tumour-associated macrophages (TAMs). Correspondingly, CXC chemokines attract CXCR2+ neutrophils in the tumour that then subsequently transform into tumour-associated neutrophils (TANs)[98,99].

Furthermore, other studies have shown that CCL21 and CCL19 attract CCR7+ dendritic cells but also regulatory T cells into tumours[100]. Also, CCL17 and CCL22 attract CCR4+ Tregs and Th2 lymphocytes, that promote tumour growth[101].CXCL9 and CXCL10 can recruit NK cells, CD4+, Th1 and CD8+ cytotoxic lymphocytes, which can attack the tumour cells[102,103].

Metastasis

Several studies have shown that cancer cells express chemokine receptors that can promote their metastasis and colonisation to secondary metastatic sites where there is a high concentration of their respective chemokine ligands[104].

One appropriate paradigm of these receptors is CXCR4. CXCR4 is expressed in a variety of cancers. CXCR4 drives the metastasis of the cancer cells on which it is expressed, to secondary organs that produce and retain high concentrations of CXCL12[105]. In breast cancer metastasis, CXCL12 triggers recruitment of breast cancer cells to secondary sites (bone marrow, liver, lung and lymph nodes) and this metastatic process can be inhibited by anti-CXCR4 antibodies.

One other paradigm of chemokine receptor involved in metastasis of cancer cells is CCR7, that drives cancer cells to lymph nodes where there are high concentrations of its ligands CCL19 and CCL21[106]. Furthermore, the CCR7 – CCL21 axis, regulates metastasis of tumour cells to the lymph nodes in many types of cancer including breast cancer, murine B16 melanoma, non-small cell lung cancer (NSCLC) and colorectal cancer[107,108,109]. In melanoma CCR10, and its ligand CCL27, are essential during metastasis as they increase the adhesion and survival of metastatic cancer cells[110].

Angiogenesis

Angiogenesis is an essential process for the growth of tumours. Chemokines play a role in tumour-associated angiogenesis, and members of the CC and the CXC chemokine families have been shown to induce angiogenesis and tumour growth in the tumour microenvironment[111].

Members of the CXC chemokine family has been shown to play an essential role in different types of cancer, including lung, stomach, pancreas, prostate, colon and brain, among others. CXC chemokines that possess the three amino acids motif (Glu-Leu-Arg) are ERL+ and are pro-angiogenic, whereas ELR− CXC chemokines are angiostatic. In human melanoma, the angiogenic chemokines, CXCL1, CXCL2, and CXCL3 are overexpressed. The chemokine receptor, CXCR2, is expressed in melanoma and is the receptor for these chemokines that mediates the angiogeneic response[112]. In lung cancer, the angiogenic CXC chemokines CXCL5 and CXCL8, play an essential role in cancer angiogenesis[113]. In pancreatic cancer, one study has shown that the CXC chemokines/CXCR2 axis promotes tumour angiogenesis both *in vivo* and *in vitro*[114].

Tumour growth and proliferation

Chemokines, through binding to their receptors expressed in cancer cells, can activate signalling cascades that directly promote cancer cell proliferation such as

PI3K/Akt/NF-κB and MAPK/ERK pathways[116,117]. Furthermore, they can promote the survival of cancer cells by preventing their apoptosis and regulating the equilibrium between apoptotic and antiapoptotic molecules[118]. In pancreatic carcinoma cells, CCL20 enhances the tumour growth of malignant cells and migration of TAMs that infiltrate the tumour[119]. In melanoma, inhibition of CXCL1 or the CXCR2 receptor inhibits cell proliferation *in vitro*[120].

1.9 Pharmacological targeting of chemokine receptors

Chemokine receptors belong to the G-protein-coupled receptor (GPCRs) superfamily. In the pharmaceutical industry, G-protein coupled receptors are the most frequently targeted of cell-membrane receptors, as they play a significant role in human pathophysiology. Even though they constitute only twelve percent of all human druggable targets, one-third of the small-molecule drugs on the market are designed to target them.

Since 2007, two drugs targeting chemokine receptors have been clinically approved. More specifically, Maraviroc- a CCR5 inhibitor for preventing HIV infection and Mozobil (commercial name for Plerixafor) a CXCR4 inhibitor. Mozobil is used in the clinic to stimulate the release of hematopoietic stem cells from the bone marrow into the blood to stimulate the immune system in patients with non-Hodgkin lymphoma and multiple myeloma[121].

In the past, several pharmaceutical companies performed clinical trials for antagonists of chemokine receptors as antiretroviral agents and autoimmune and anti-inflammatory agents. Some clinical trial examples include CCR1 targeting for rheumatoid arthritis (Pfizer, CCR1 antagonist CP-481,715)[122]. Although this trial initially demonstrated promising results and entered the clinical phase II, eventually the antagonist failed to demonstrate any signs of efficacy after six weeks of treatment. CCR1 targeting in multiple sclerosis had a similar outcome in the clinic

(Berlex Laboratories, CCR1 antagonist BX471)[123] . This clinical trial also entered phase II but was terminated after failing to provide any improvement in the clinical outcome of the patients.

CCR2 was also a promising target for treating rheumatoid arthritis and multiple sclerosis (Merck, CCR2 antagonist MK-0812). The rheumatoid arthritis trial involved a 12-week protocol with 149 patients randomized to receive placebo treatment or MK-0812. MK-0812 failed to provide any significant improvement for any of the end points studied and the trial was terminated early. Regarding the multiple sclerosis trial Merck removed the drug from its pipeline probably due to negative results, although they were never made publicly available[124].

Furthermore, CXCR3 was also a target for psoriasis treatment (ChemoCentryx/Amgen CXCR3 antagonist AMG-487). Although the CXCR3 antagonist showed positive results during clinical phase I and entered phase II, subsequently the trial was terminated due to lack of efficacy[125].

Despite all these efforts, all the clinical trials failed to provide a therapeutic benefit for the patients, and none of these antagonists were approved for clinical use. Several reasons could explain the clinical failures when targeting chemokine receptors. One reason is the fact that it is challenging to retain sufficient levels of drug/inhibitor in the plasma to efficiently inhibit the receptor target. Furthermore, clinical failure could be due to the differences between the immune system of humans versus animal models. Finally, several receptors may be involved in the pathophysiology of the disease, so pharmacological targeting one or two receptors is not sufficient to improve the clinical outcome of the disease.

1.10 Atypical Chemokine Receptors

Atypical Chemokine Receptors belong to the chemokine receptor family, and they present many structural similarities. This chemokine receptor subfamily consists of at least four members: ACKR1, ACKR2, ACKR3 and ACKR4. These receptors, (except for ACKR1), although they exhibit high homology with several conventional chemokine receptors, are unable to initiate the classical signalling pathways upon ligand binding. These receptors, mostly serve as scavenger receptors that bind their respective chemokine ligands (Table 1) leading to their degradation, thus regulating the chemokine concentration in the local microenvironment[126,127].

RECEPTOR	LIGANDS	EXPRESSION
ACKR1	CCL2, 5, 7, 11, 13, 14, 17, CXCL5 ,6, 8 ,11	Erythrocytes, vascular endothelial cells, Purkinje cells
ACKR2	CCL2, 3, 4, 5, 7, 8, 11, 12, 13,14, 17, 18	Lymphatic endothelial cells, leukocytes, keratinocytes, trophoblasts
ACKR3	CXCL11, CXCL12, ADM, BAM22, MIF	Hematopoietic cells, lymphatic endothelial cells, blood endothelial cells, mesenchymal cells and. neuronal cells
ACKR4	CCL19, 21, 25	Lymphatic endothelial cells and epithelial cells

Table 1. Summary of ACKR ligands and their expression pattern in different cell types

Regarding the aforementioned characteristics, in 2012, a committee of experts was formed in order to develop a new nomenclature/ classification for these receptors. They collectively agreed on the name Atypical Chemokine Receptors (ACKRs) that

is now approved by most of the scientific organisations and is used almost exclusively in the scientific literature[128].

All the ACKRs have alterations in the highly conserved DRYLAIV motif. This motif is located between the third transmembrane domain and the second intracellular loop and is the binding site of G proteins. Since the ACKRs exhibit altered DRYLAIV motifs, they fail to recruit and activate G proteins and subsequently trigger G protein-dependent signalling pathways[129].

Although ACKRs were initially considered as non-signalling receptors, recently, evidence has emerged that members of the ACKR family can signal through noncanonical pathways like β arrestins, mitogen-activated protein kinases (MAPKs) and heterodimerization with other signalling receptors[130,131].

1.10.1 ACKR1

ACKR1 (previously named DARC), binds more than 20 inflammatory chemokines members of the CC and CXC subfamilies. It is expressed on endothelial cells and erythrocytes. During inflammation, ACKR1 binds chemokines with high affinity, thus regulating the concentration of bioavailable circulating chemokines[132,133,134]. In endothelial cells, ACKR1 has been linked with chemokine transcytosis by mediating the transportation of chemokine from the basal to the apical side of the endothelium. Furthermore, ACKR1 expression in endothelial cells has been linked to negative regulation of angiogenesis by scavenging the angiogenic ELR+ chemokines[135,136,137].

ACKR1 serves as a receptor for two human malarial parasites: *Plasmodium vivax* and *Plasmodium knowlesi*. These parasites use this receptor to invade erythrocytes. Some individuals belonging to certain ethnic groups (African, Yemenite Jews) exhibit resistance to malaria infections. These individuals carry natural polymorphisms that result in erythrocytes null for ACKR1[138,139,140].

Like all other ACKRs, ACKR1 lacks the typical DRYLAIV motif, so does not signal through G proteins. In contrast to other ACKRs, ACKR1 is not a constitutively internalising receptor, but it internalises only upon ligand binding. Another difference in this context, is that ACKR1, upon ligand binding and internalisation does not lead the ligand to degradation[141].

ACKR1 knock out mice, in acute and chronic inflammation models show reduced neutrophil recruitment. In atherogenesis models, ACKR1 KO mice exhibit a protective phenotype that is associated with reduced levels of inflammatory monocytes in the aorta[142].

1.10.2 ACKR2

ACKR2 is one of the most well characterised of the atypical chemokine receptors (previously named D6). It is a scavenging receptor for a broad number of inflammatory CC chemokines such as CCL2, CCL3,CC4,CCL5 CCL7, CCL8, CCL11, CCL12, CCL13, CCL14 and CCL17 and CCL18. ACKR2 plays a pivotal role in orchestrating the inflammatory response and does not bind to any of the homeostatic chemokines[143].

ACKR2 is present in many organs tissues and cells. More specifically, in the immune cells, ACKR2 is expressed on B cells and some subsets of human dendritic cells and monocytes. In the non-immune compartment ACKR2 is expressed in hepatocytes in the liver, in the skin by keratinocytes and by trophoblasts in the placenta. ACKR2 is also expressed in lymphatic endothelial cells but not in blood endothelial cells [144,145].

In the immune system, ACKR2 expression has been detected in some leukocyte subsets including T cells, B cells, neutrophils mast cells and macrophages[146,147]. ACKR2 has been shown to regulate lymphatic vessel density and function[148]. In the placenta, ACKR2 is expressed on trophoblasts. ACKR2 null mice exhibit abnormal embryo phenotypes like reduced foetal weight and increased neonatal death

rate[149,150]. In the skin, ACKR2 null mice exhibit a severe skin inflammatory phenotype that resembles psoriasis. ACKR2 also regulates the inflammatory response in the lung and the gut[151,152,153,154]. It has also shown to be important in infectious diseases like *Mycobacterium tuberculosis*. More specifically, ACKR2 null mice infected by *Mycobacterium tuberculosis* exhibited reduced survival, compared to WT mice. This lethal phenotype was attributed to an increased number of lung and lymph node-infiltrating mononuclear cells and an increase in pro-inflammatory cytokines and CC chemokines. ACKR2 is also involved in liver inflammation in chronic *Hepatitis* C. More specifically, genetic *in silico* and statistical analyses, proposed a correlation between ACKR2 genetic variants with the grade of liver inflammation in chronic *Hepatitis C* patients[155] .

In the context of cancer, ACKR2 in two different studies is involved in the early steps of metastasis by regulating the recruitment and infiltration of subsets of natural killer cells or neutrophils to the tumour[156]. Finally, ACKR2 is involved in skin cancer[157] and colorectal cancer by regulating the inflammatory environment and thus the progress of the disease[158].

1.10.3 ACKR4

ACKR4 (previously named CCRL1) is a scavenger receptor for CCL19, CCL21 and CCL25 homeostatic chemokines. It is expressed in a wide variety of tissues and cells like lymphatic endothelial cells, blood endothelial cells, thymic epithelial cells, skin keratinocytes and brain. ACKR4 has a DRYWAVT motif, instead of the typical DRYLAIV, so it does not induce Ca^{2+} influx. ACKR4 functions as a chemokine scavenger receptor, causing ligand internalisation and subsequent lysosomal degradation[159] .

ACKR4 KO mice have increased levels of CCL21 in the plasma and increased levels of both CCL19 and CCL21 in lymph nodes but not in the spleen[160]. ACKR4 null mice have shown reduced dendritic cell (DC) lymph node homing. This phenotype might

be due to desensitisation of CCR7 (also binds CCL19 and CCL21) that is present on dendritic cells[161]. A recent study by Ulvmar et al. highlights the importance of ACKR4 for shaping the CCL21 gradients in lymph nodes. The authors in this study have shown that the lymphatic endothelial cells lining the ceiling of the subscapular sinus, express ACKR4, which is responsible for scavenging CCL21. ACKR4 scavenges CCL21, thus creating a local gradient that guides the CCR7-expressing dendritic cells in the lymph node cortex[162].

1.11 Atypical Chemokine Receptor 3 (ACKR3)

Atypical Chemokine Receptor 3 (formerly named CXCR7) is a seven transmembrane spanning receptor that like the other members of the ACKR family, cannot activate and signal through G proteins upon ligand binding.

ACKR3 has two ligands that belong to the chemokine family: CXCL11 and CXCL12 (Figure 1.4). Apart from these chemokine ligands, ACKR3 has been shown to interact with the following ligands: adrenomedullin (ADM), bovine adrenal medulla 22 (BAM22) and macrophage inhibitory factor (MIF).

The human ACKR3 gene is on chromosome 2 in genomic location 2q37.3. The human ACKR3 gene has two transcripts that encode two proteins 362 and 210 amino acids long (Ensembl genome database). However, there is no scientific literature regarding the expression of the different ACKR3 isoforms in different tissues or different pathophysiological conditions. The ACKR3 protein sequence is evolutionarily conserved, a fact that highlights the importance of this receptor in fundamental biological processes. The high level of ACKR3 protein conservation among different species can be observed in protein sequence alignments obtained from UNIPROT protein database and compared using Clustal algorithm as presented in Figure 1.3.

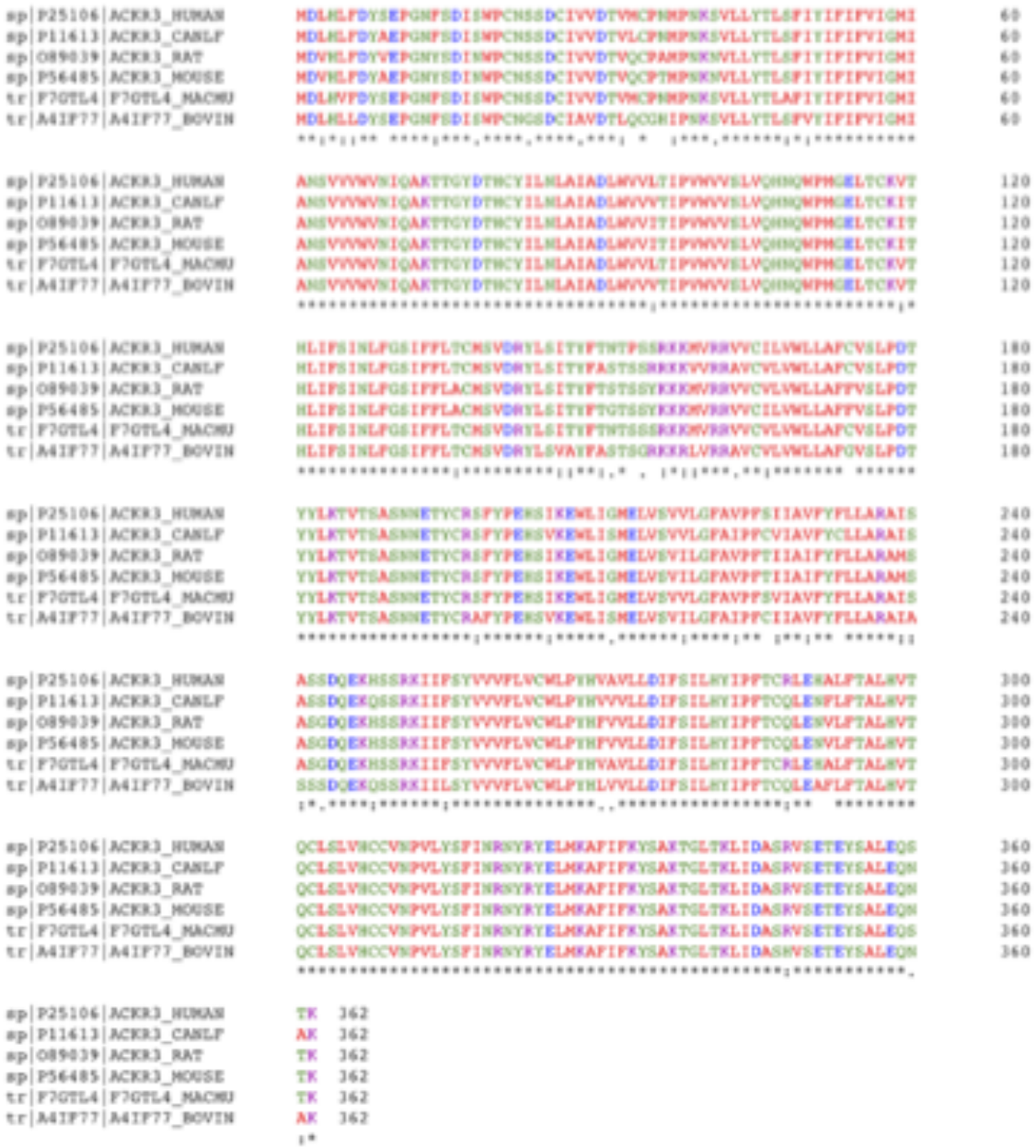

Figure 1.3 Multiple sequence alignment of ACKR3 protein sequences of different species were obtained from UNIPROT and generated with Clustal algorithm reveals the high level of conservation. The symbols are used to indicate amino acids aligned at the sites marked with the symbol. "*" indicates perfect alignment. ":" indicates a site belonging to group exhibiting strong similarity. "." indicates a site belonging to a group exhibiting weak similarity. The species' symbols that were used indicated the following: HUMAN(human), CANFL(canine), RAT(rat), MOUSE(mouse), MACMU(Rhesus macaque), BOVIN(bovine).

1.11.1 ACKR3 signalling and cellular properties

Initially, ACKR3 was considered to be a scavenging receptor due to its inability to initiate G protein-mediated responses. This inability to signal through G proteins had initially been attributed to the fact that ACKR3 has a DRYLSIT motif instead of the classical DRYLAIV motif in the second intracellular loop that is essential for G protein interaction in other chemokine receptors. However, it has been shown in some studies that the replacement of DRYLSIT of ACKR3 with the DRYLAIV failed to induce G protein signalling cascades such as Ca2+ mobilisation, extracellular signal-regulated kinase (ERK) phosphorylation or chemotaxis. This experiment suggests that the lack of the DRYLAIV motif in ACKR3 is not solely responsible for the ACKR3 inability to signal through G proteins[163,164].

The interaction of ACKR3 with G proteins remains controversial, as there are studies that have reported ACKR3 and G protein interaction. In one study, the ACKR3 and G protein interactions were reported using bioluminescence resonance energy transfer (BRET) in the absence of an agonist, but no G protein activation was reported in this case. In a subsequent study, it was reported that CXLC12 was able to initiate Gi/o activation upon binding to ACKR3 in primary rodent astrocytes. More specifically, the authors performed [35S]-GTPγS binding assays using membranes extracts of rodent astrocytes from CXCR4-/- mice. They noticed an increase in GTPγS binding after incubation of these membranes with CXCL12, an effect that was abrogated after silencing ACKR3 expression using siRNA. These observations contradict the general view that ACKR3 does not signal through G proteins and suggest that ACKR3 signalling responses upon ligand binding are context-dependent[165].

Recent studies have shown that ACKR3 can initiate signalling cascades through β arrestins. It has been shown that ACKR3, upon CXCL12 binding, can recruit β-arrestins that lead to Akt and ERK phosphorylation/activation, together with JAK2/STAT3 activation[166]. Furthermore, CXCL11 treatment in HEK293 cells overexpressing ACKR3 induces β-arrestin recruitment and ERK phosphorylation/ activation. However, stimulation with CXCL11 of rat vascular smooth muscle cells

expressing endogenous ACKR3 failed to show phosphorylation of ERKs. This highlights the importance of the cellular context in dictating signalling responses[167].

ACKR3 acts as a scavenger receptor for its ligands. When the ligands bind to ACKR3, then the complex of ligand-receptor is efficiently internalised, and the ligand gets degraded in the lysosomes. In the resting state, ACKR3 is mostly present on the membrane of endocytic vesicles. Truncations of the receptor's C terminal tail resulted in a significant increase in the plasma membrane localisation. ACKR3 internalisation is β-arrestin-, clathrin- and dynamin-dependent, thus in the presence of a dominant-negative dynamin mutant (K44A dynamin null), all ACKR3 is localised at the plasma membrane. This does not alter constitutive β-arrestin recruitment. In this case, upon CXCL12 stimulation of ACKR3, β-arrestin recruitment is significantly increased, and ERK phosphorylation is significantly prolonged. These observations suggest that ACKR3 can signal when it is located exclusively at the plasma membrane[168].

Several studies in zebrafish revealed the role of ACKR3 in cell migration during development. In zebrafish, the collective migration of cells during development, is CXCL12-CXCR4 axis-driven. The zebrafish lateral-line primordium is a cohesive cohort of over 100 cells that is guided through CXCR4-CXCL12 signals. In zebrafish, knock out of CXCL12 resulted in a phenotype that is stronger than the CXCR4 KD in the same model. This suggests that other CXCL12 receptors play a role in the collective cell migration in zebrafish. Indeed, morpholino-mediated knockdown of both CXCR4 and ACKR3, results in a lateral-line- cell migration phenotype that is similar to the one observed in CXCL12 KO. In this study, it was shown that CXCL12, controls the cell migration during zebrafish development through two independent receptors, CXCR4 and ACKR3[169].

1.11.2 ACKR3 expression

ACKR3 spatial and temporal expression in tissue is tightly regulated, supporting the fundamental role of ACKR3 in developmental processes and immune surveillance. Human ACKR3 under homeostatic conditions has been detected in several tissues including heart, brain, spleen, kidney, lungs, thyroid and placenta as verified by RT-PCR and immunoistochemistry[170,171,172]. ACKR3 is also expressed in immune cells in homeostatic and pathophysiological conditions.

ACKR3 expression in the immune system

ACKR3 expression in lymphocyte and leukocyte subsets is controversial, partly because of differences in the techniques that were applied, but mostly due to the lack of specific antibodies for this receptor. ACKR3 has been detected in lymphocytes, granulocytes and some peripheral blood cells subsets in the bone marrow[173]. Several studies have reported ACKR3 expression in subsets of T cells, monocytes, B cells[174] and natural killer (NK) cells[175,176,177]. In most of these studies, ACKR3 was mostly detected intracellularly using flow cytometry (after permeabilisation), and only a small amount was detected in the cell membrane fraction. It is proposed that ACKR3 internalises constitutively and this constitutive internalisation is independent of chemokine ligand binding. After ligand binding, the receptor-ligand complex internalises and goes to lysosomes for ligand degradation. After the chemokine - ligand degradation, the receptor recycles back to the plasma membrane, available for the next round of chemokine binding and scavenging[178].

ACKR3 is implicated in B cell development[179]. ACKR3 is proposed to be essential for B cell function and differentiation into plasma cells. This is based on the observation that during B cell development and differentiation, only the ACKR3+ subset of B cells, identified by flow cytometry analyses, is viable and can produce antibodies.

ACKR3 expression in non-immune cells

ACKR3 has been detected during embryogenesis in foetal liver and is believed to be essential in vasculogenesis but not in haematopoiesis. ACKR3 is expressed in cardiac endothelial cells (as verified by immunofluorescence and RT-RCR analyses) and plays a role in angiogenesis[180]. The fact that ACKR3 is also expressed in endothelial and trophoblast cells in the placenta (verified by RT-PCR and immunohistochemistry) suggests additional functions during pregnancy and embryo development[181,182]. In neurobiology, several studies have shown ACKR3 expression (verified by immunofluorescence and RT-PCR) in neurons and astrocytes, and it is important for proper migration and spatial distribution of cortical interneurons[183,184,185]. Furthermore, in astrocytes and Schwann cells, CXCL12 binds to ACKR3 and activates Akt and ERK-mediated signalling responses[186,187].
In the kidneys, ACKR3 is expressed in renal blood and lymphatic vessels. It regulates the blood flow and contributes to vascular development through shaping the concentration of its ligands CXCL11, CXCL12 and ADM[188,189].

ACKR3 is also involved in reproductive processes through its ligands, CXCL12 and ADM. CXCL12 regulates the chemotaxis of immune cells to the uterus, the trophoblast invasion process and the synthesis of angiogenic factors during pregnancy[190,191]. During the first weeks of pregnancy, trophoblast-derived
CXCL12 leads to the recruitment of natural killer (NK) cells from peripheral blood to the uterus. These cells (peripheral blood NK), together with the NK cells that reside in the uterus, contribute to processes like spiral artery remodelling and development of immune tolerance of the foetus[192,193,194]. Apart from CXCL12, it is also proposed that ADM regulation through ACKR3 scavenging, contributes to efficient embryo attachment to the maternal decidua.

In addition to ACKR3 involvement in the regulation of reproductive processes in females, ACKR3 is also reported to be a player in male reproduction. ACKR3 during testis development is expressed in undifferentiated spermatogonia and contributes to

the fine-tuning of the CXCL12: CXCR4 signalling in this context[195,196]. However, the exact role of ACKR3 during spermatogenesis remains unclear.

1.12 ACKR3 ligands

Major ligands

1.12.1 CXCL12

CXCL12 (previously named SDF-1) is a chemokine that has a fundamental role in several developmental processes and regulates immune surveillance. It is highly expressed in the lung, liver, lymph nodes, brain and bone marrow[197,198]. It is also expressed at lower levels in the skin, kidney and small intestine. CXCL12 expression in the aforementioned tissues defines secondary metastatic niches in several types of cancer[199]. CXCL12 has also been shown to be chemotactic for leukocytes, mesenchymal stem cells, endothelial progenitor cells and neural progenitor cells[200,201,202]. In pathophysiology, CXCL12 upregulation is associated with several conditions including ischemia, autoimmune diseases, inflammation and cancer[203,204]. CXCL12 binding to ACKR3 is not able to induce calcium mobilization or G protein activation but signals through β arrestin recruitment and ERK / AKT activation[205,206]. CXCL12 binding to CXCR4 is able to induce G protein recruitment. G proteins are heterotrimeric and they consist of the Gα subunit and the tightly associated Gβγ subunits. There are many classes of Gα subunits such as Gsα (G stimulatory), Giα (G inhibitory), Goα (G other), Gq/11α, and G12/13α. CXCL12 binding promotes a CXCR4 conformation that favours mainly Giα subunit protein complexes. However, CXCR4 can also couple to other G proteins such as G12/13α and Gqα[207].

1.12.2 CXCL11

CXCL11 (named I-TAC in the past), is expressed in peripheral blood cells (PBMCs), in the liver, thymus lung, spleen and pancreas[208]. CXCL11 binds to ACKR3 and the two isoforms of CXCR3 A and B. CXCL11 binding to ACKR3 or CXCR3–A is

associated with a more proliferative phenotype while binding to CXCR3-B has the opposite effect[209]. CXCL11 signals through Gi protein following the binding to CXCR3-A and Gs upon binding to CXCR3-B. CXCL11 interaction with ACKR3 results in β arrestin-2 recruitment but is unable to promote ERK or AKT mediated signalling cascades [210,211].

Minor ligands

1.12.3 Adrenomedullin (ADM)

Adrenomedullin is a 52 amino acid hormone peptide with vasodilatory properties[212]. Adrenomedullin plays a key role in cardiac development and lymphangiogenesis[213,214,215.] Adrenomedullin binds and signals through a receptor complex that consists of a GPCR protein called CLR (calcitonin receptor like receptor) and a RAMP protein (receptor activity modifying protein). The interaction of adrenomedullin with its classical receptor complex can lead to cyclic AMP and nitric oxide production[216,217]. Recently it was shown that adrenomedullin binds ACKR3 that acts as a scavenger receptor but cannot initiate G protein-mediated signalling. The signalling properties of adrenomedullin and ACKR3 remain uninvestigated, and further studies need to be done to fully understand the importance of this interaction in different biological contexts.

1.12.4 Bovine Adrenal Medulla 22 (BAM 22)

BAM22 was initially isolated from the adrenal medulla[218,219] and acted like an opioid but also has other functions[220]. BAM22 is expressed in the central nervous system and acts through binding the opioid receptors μ-, δ- and κ[221,222,223,224].

A recent study revealed that BAM22 is a ligand for ACKR3 and binds with high affinity. This interaction leads to glucocorticoid secretion. It was also shown that binding to ACKR3 recruits β arrestin 1 and 2 but did not increase cAMP or lead to calcium mobilization[225].

1.12.5 Macrophage Inhibitory Factor (MIF)

Macrophage Inhibitory Factor is a cytokine that regulates the innate immune system and is expressed by a variety of cell types like endothelial cells, epithelial cells, eosinophils and macrophages[226,227,228]. Its main role is to inhibit macrophage migration[229]. MIF has been shown to bind to several receptors like the cluster of differentiation 74 (CD74)[230], CXCR2 and CXCR4[231]. MIF has been recently linked to ACKR3 in pathological conditions such as Rhabdomyosarcoma, where it regulates tumour cell migration and in platelets where it prevents apoptosis via AKT dependent survival cascades[232,233].

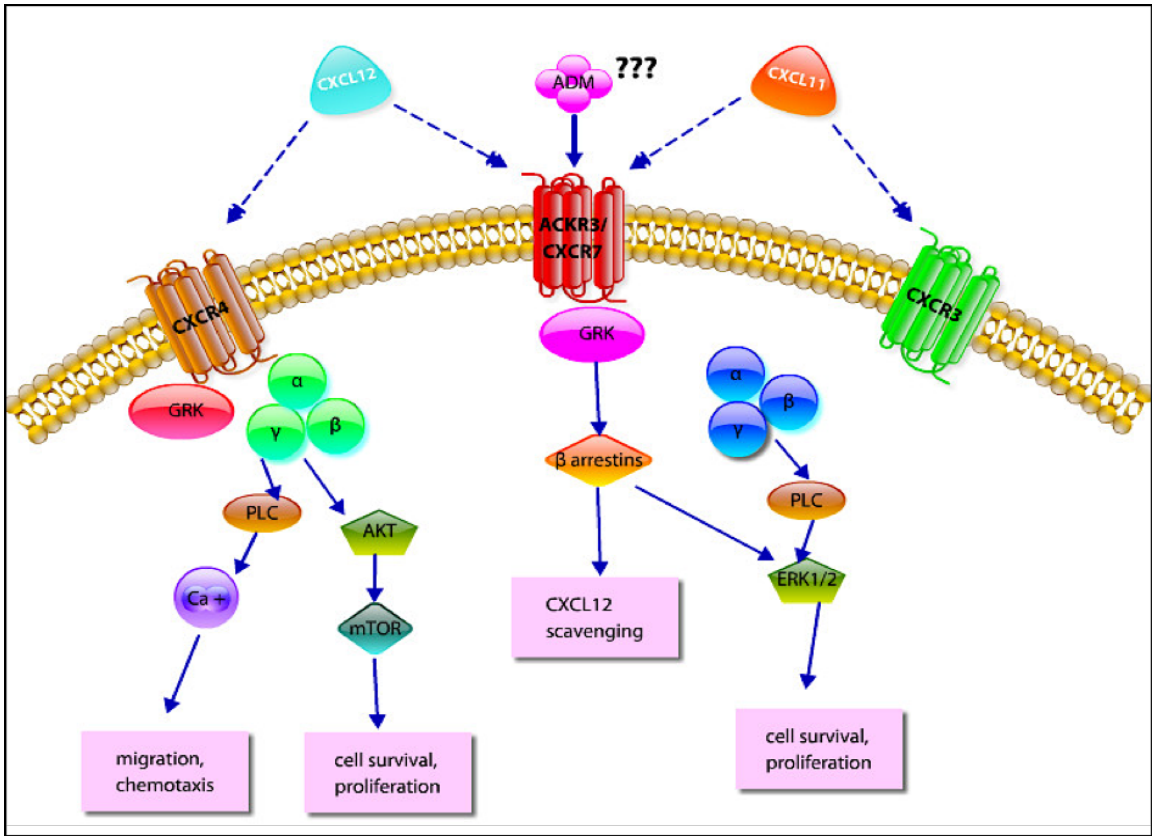

Figure 1.4 Schematic representation of ACKR3 and its chemokine ligands.
ACKR3 shares CXCL12 and CXCL11 with CXCR4 and CXCR3 chemokine receptors. ACKR3, in contrast with CXCR4, cannot elicit G protein-dependent signalling responses. Instead, ACKR3 can recruit and activate β arrestins- dependent signaling cascades.

1.13 The role of ACKR3 in physiology

The spatiotemporal distribution of chemokines during embryonic development has been shown to play a fundamental role in lineage commitment, organogenesis and chemotaxis. After the discovery that ACKR3 is another receptor for CXCL12 and due to the high importance of CXCL12 in various developmental processes and immune responses, the role of ACKR3 was also interrogated in this context.

In one of the initial developmental studies on ACKR3, it was revealed that it is essential for primordial germ cell (PGCs) migration in zebrafish. The authors demonstrated that morpholino-mediated knockdown of ACKR3 resulted in aberrant PGC migration that impaired gonad development. To explain this phenotype, they proposed a mechanism in which ACKR3 is expressed in the somatic microenvironment of PGCs and scavenges CXCL12, thus creating a gradient for this chemokine. Migrating PGCs do not express ACKR3 but express CXCR4b chemokine receptor that binds to CXCL12 and leads their migration from areas with low CXCL12 concentration to higher ones[234].

In 2007 Sierro et al. generated ACKR3 null mice that showed rapid postnatal death within 24 hours of birth. The few embryos that survived exhibited severe cardiac abnormalities and aortic valve defects, a phenotype that was also present in the ACKR3 +/- mice. *In situ* hybridization experiments revealed expression of ACKR3 in the brain and the endothelium of the embryonic heart. Specific ACKR3 depletion from the endothelium phenocopied the ACKR3 knockout cardiac abnormalities. Subsequently, gene expression analysis on ACKR3-/- embryonic valve leaflets revealed significant downregulation of Adrenomedullin and Heparin-binding EGF-like growth factor (HBEGF) genes, among others. Adrenomedullin expression in ACKR3 null mice was also validated in other tissues with no apparent differences noticed[235].

In a subsequent study, Klein et al., using ADM overexpressing knock-in mice (ADM hi/hi), showed that these mice exhibit the ACKR3 null lethal phenotype. This observation supports the idea of ACKR3- ADM interaction being crucial in

angiogenesis and lymphangiogenesis during embryonic development. Furthermore, genetic reduction of ADM by crossing ACKR3 -/- and ADM +/- mice could reverse the ACKR3 null phenotype verifying that ACKR3 acts as a homeostatic regulator of ADM levels in the heart and dermal lymphatic system during development[236].

Besides these findings in the endothelial system, other studies have highlighted the importance of ACKR3 in mouse brain development. In the embryonic brain, ACKR3 is expressed in the protrusions of cortical interneurons and seems to play a CXCR4-independent role in migration and spatial distribution of these cells. This phenotype is β arrestin/ MAPK mediated and does not follow the typical G protein recruitment signalling pathways[237].

Several studies highlight the involvement of ACKR3 in tissue regeneration after injury. Ding and et al. using an acute and a chronic liver injury model demonstrated the importance of ACKR3 and CXCR4 in liver regeneration. They demonstrated that after liver injury, accumulated CXCL12 on the site of injury leads to ACKR3 overexpression in liver endothelial cells. ACKR3, together with CXCR4, coordinates the start of the regeneration process through the activation of the transcription cofactor, inhibitor of DNA binding 1 (ID-1)[238].

In another study, the same research team revealed that the CXCL12 - CXCR4/ACKR3 axis is necessary for lung alveolar regeneration. They demonstrated that after surgical removal of the left lobe by pneumonectomy (PNX), accumulated platelets deposit CXCL12 in the pulmonary capillary endothelial cells. Using CXCR4 and ACKR3 endothelial-specific knockouts, they proposed that platelet-derived CXCL12 triggers a CXCR4/ACKR3 signalling cascade that is fundamental for the initiation of the alveolar regeneration process[239].

In the lung, ACKR3 involvement in lung alveolar repair and fibrosis after chronic injury was demonstrated. The authors proposed that a Notch ligand, Jagged1 (JAG1), is secreted by activated pulmonary capillary endothelial cells and induces the activation

of Notch signalling to the fibroblasts in the alveolar microenvironment after chronic bleomycin injury, promoting a fibrotic phenotype. In this model, they also observed that ACKR3 that is normally expressed in the capillary endothelial cells was significantly downregulated in the fibrotic environment. Administration of an ACKR3 agonist reduced the levels of Jag1 and reversed the fibrotic phenotype suggesting a protective role of ACKR3 in alveolar epithelial damage[240].

1.14 ACKR3 in pathophysiology

There is a substantial body of evidence that highlights the role of ACKR3 in the development and progression of several pathological conditions, including cancer. The implication of ACKR3 in several types of malignancies has been extensively reviewed in the recent past. ACKR3 is expressed in the tumour cells in the lung, in the brain, in the pancreas, in the prostate and the tumour vascular cells.

In cardiovascular biology, ACKR3 is upregulated in arteries after injury and promotes ischemia-induced angiogenesis and endothelial cell proliferation after myocardial infarction. These findings highlight the role of ACKR3 as a homeostatic regulator of cardiac remodelling and repair after injury[241]. In diabetes *mellitus* ACKR3, expressed in endothelial progenitor cells, provides survival advantage and enhances the angiogenic capacity of these cells. The authors proposed a mechanism whereby CXCL12 binds ACKR3 and blocks GSK-3β that inhibits the nuclear factor (erythroid-derived 2)-like 2 (NRF2), transcription factor, thus allowing NRF2 activation. Subsequently activated NRF2 target genes promote cell survival, angiogenesis and provide antioxidative protection against oxidative stress, a characteristic of the disease[242].

In atherosclerosis, ACKR3 is expressed in macrophage populations in atherosclerotic plaques. ACKR3 expression in these cells increases their phagocytic activity via MAP kinase mediated signalling. In another study, the authors propose the involvement of ACKR3 in thrombosis and inflammation. They showed that macrophage migration

inhibitory factor (MIF) interacts with ACKR3 expressing platelets, mediates antiapoptotic effects in these cells and also promotes antithrombotic effects after arterial injury both *in vitro* and *in vivo*[243].

1.15 ACKR3 role in cancer biology

CXCR4 is one of the most studied chemokine receptors in the context of cancer because it is upregulated in more than 23 types of human cancers of epithelial, mesenchymal and haematopoietic origin. CXCL12 is the only ligand for CXCR4, and this interaction is extensively studied since CXCL12 has been detected in primary tumour sites in lymphomas, gliomas, ovarian and pancreatic cancer and at secondary metastatic sites in breast and thyroid cancer[244,245,246].

CXCL11 was believed to be the only binding partner of ACKR3. Recently, it was discovered that CXCL12 could also bind ACKR3 with higher affinity than CXCR4. The affinity of the CXCL12 – ACKR3 interaction is also higher than the affinity of CXCL11 – ACKR3 interaction but failed as well to induce Ca+ influx, chemotaxis or integrin activation, leaving the biological relevance of this interaction unclear[247].

There is a growing body of evidence that suggests the involvement of ACKR3 in cancer progression and metastasis, but our understanding of the exact mechanisms that ACKR3 uses to regulate these processes remains elusive. ACKR3 expression is elevated in several solid tumours and the tumour-associated vasculature. ACKR3 is overexpressed in a variety of cancers like astrocytoma and glioblastoma[248], prostate[249,250], breast[251], pancreas[252], lung[253,254], colorectal[255], bladder[256,257] and kidney[258,259]. These observations suggest that ACKR3, like CXCR4, plays a crucial role in cancer biology by regulating tumour immune microenvironment, tumour angiogenesis, stem cell trafficking, and metastasis (Figure 1.5) .

ACKR3 is often reported to be co-expressed with CXCR4. Usually, these two receptors are clearly expressed in cancers such as glioma and breast cancer. Instead, in some other cancers, for example in pancreatic cancer, ACKR3 and

CXCR4 are co-expressed. The co-expression of these two receptors on the same cells may suggest heterodimerization between them and the initiation of distinctive signalling pathways. Another hypothesis is that this co-expression is maybe crucial for tumour growth regulation in an autocrine manner. Apart from CXCR4, ACKR3 may also functionally interact with crucial other signalling receptors, such as estrogen and epidermal growth factor receptors (EGFRs) in breast cancer[260].

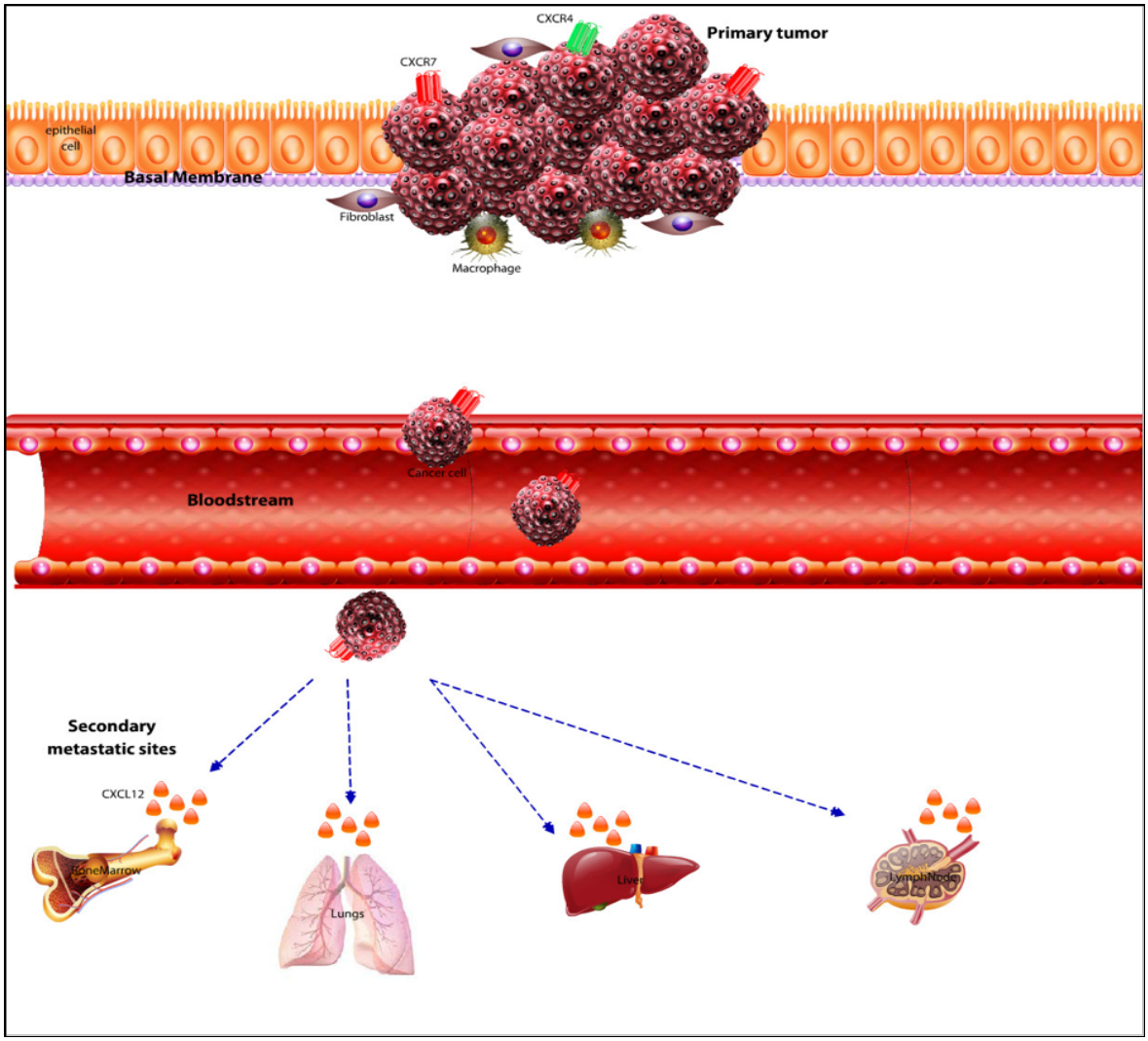

Figure 1.5 CXCR4 and ACKR3 (CXCR7) are expressed in primary solid tumours and are involved in metastasis in organs that CXCL12 is highly expressed such as the bone marrow, the lung, the liver and the lymph nodes.

1.15.1 ACKR3 role in tumour-associated angiogenesis

Apart from the expression of ACKR3 in tumour cells, it is also extensively reported that ACKR3 is highly expressed in tumour-associated vasculature. Hypoxia is a common characteristic in solid tumours. In this hypoxic microenvironment, VEGF and CXCL8 that are present in high concentrations, lead to the higher expression of ACKR3, creating a positive feedback loop[261,262].

ACKR3 is expressed in endothelial progenitor cells (EPCs) and is implicated in transendothelial migration, proliferation and tube formation of EPCs, that are essential steps in the angiogenic process[263]. Although ACKR3 can enhance the transendothelial migration of EPCs, its role in the migration of tumour cells is less clear, as it may either synergize with or impair CXCR4 action.

In a study in human meningiomas, ACKR3 was detected in tumour endothelial cells. More specifically, the authors assessed the ACKR3 expression at both mRNA and protein level in human post-surgical human meningioma specimens. Using RT PCR, the authors observed an increase in the ACKR3 mRNA levels when comparing benign and aggressive meningioma specimens. Furthermore, immunohistochemistry and immunofluorescence analyses in these specimens revealed ACKR3 expression in tumour endothelial cells, but these observations are debatable due to the use of a new polyclonal anti ACKR3 antibody(Abcam) that has not used extensively in the literature or validated for its specificity[264].

In hepatocellular carcinoma(HCC), ACKR3 expression in human HCC tissues and cell lines was associated with tumour angiogenesis, verified by transwell co-cultures with primary human endothelial cells and tumour growth, assessed by xenografts *in vivo*[265] .

In colon cancer, transwell co-culture of human colorectal cell lines that overexpress ACKR3, with primary endothelial cells, enhanced angiogenesis via AKT/ERK pathway activation. This effect was abrogated when using cell lines that express

shRNAs against ACKR3. The angiogenic contribution of ACKR3 in colon cancer was also validated in vivo in subcutaneous mouse models. In these models, ACKR3 expressing cell lines exhibited increased expression of vascular endothelial growth factor (VEGF) as was revealed after immunohistochemistry analyses of the tumours[266]. Also, in patients with glioblastoma, ACKR3 expression by endothelial cells correlated with a better prognosis[267].

1.15.2 ACKR3 role in metastasis

In the literature, there are contrasting conclusions about the role of ACKR3 in the metastatic process. In some cases, ACKR3 can reduce CXCR4 mediated effects. For example, in a breast cancer model ACKR3 inhibited tumour invasion by downregulating metalloproteinase-12, impaired CXCL12-stimulated matrix degradation and invasion, and decreased spontaneous lung metastasis[268].

In contrast with this study, another breast cancer study revealed a positive correlation between ACKR3 overexpression and lymph node metastasis. More specifically, immunohistochemical analyses of human breast cancer tissues and tissue microarrays revealed that ACKR3 was upregulated in the cancerous tissues and associated with higher tumour aggressiveness and metastasis to the lymph nodes. Furthermore, using subcutaneous models of murine breast cancer cells, but also allograft experiments, the authors proposed that ACKR3 controls tumour growth but also lung metastasis in these models[254,269]. Another breast cancer study in mouse models proposes that glioma-associated oncogene 1 (GLI1) transcription factor enhances breast cancer cell lung metastasis by upregulating transcription from the CXCR4 and ACKR3 genes[271]. ACKR3 may also regulate CXCR4-mediated transendothelial migration (TEM) in a CXCL12-dependent manner. More specifically, human Burkitt's lymphoma cell line NC-37, which expresses CXCR4, CXCR5, ACKR3 and CCR7, was used as a model in TEM assays. These cells failed to migrate through HUVECs monolayers in increasing concentrations of CXCL13 (CXCR5 ligand) or CCL19 (CCR7 ligand). Surprisingly the same cells could able to migrate towards CXCL13 or CCL19 after stimulation with CXCL12. The later phenotype was

abrogated after using the ACKR3 inhibitor CCX771 suggesting that ACKR3 mediates TEM in this system. However it is important to note that CCX771 inhibitor is not very specific for ACKR3 and can act as an agonist for CXCR4 (data not presented in this thesis). This *in vitro* setting may recapitulate the *in vivo* cancer cell migration towards the lymph nodes[272].

Finally, in rhabdomyosarcoma (RMS), ACKR3 is expressed in human rhabdomyosarcoma cell lines. Using an intravenous injection model of human RMS cells that overexpressed ACKR3 in SCID mice, the authors assessed the effect of ACKR3 in metastasis to the bone marrow. They observed an increased seeding efficiency of tumour cells that overexpress ACKR3 to the bone marrow [273]. This suggests a positive correlation between ACKR3 expression and the seeding efficiency of tumour cells to secondary metastatic sites in this model.

1.15.3 ACKR3 role in cell proliferation, adhesion and tumour growth

In breast cancer, ACKR3 has been shown to enhance vascular cell-adhesion molecule-1 (VCAM-1) expression. This suggests a role for ACKR3 in tumour invasion to surrounding tissues as cell adhesion to the basement membrane is a crucial step in this process[270].

In the human glioblastoma cell line U373, ACKR3 induced proliferation upon CXCL12 treatment, a phenotype that was abrogated after treatment with the ACKR3-specific inhibitor CCX733[274]. In bladder cancer, recent studies have identified ACKR3 as one of the chemokine receptors that is upregulated in several bladder cancer tissues and cell lines. In human bladder cancer cell lines, ACKR3 mediated proliferation through activation of AKT, ERK and STAT3 pathways. Furthermore, in allograft subcutaneous mouse models, J82 cancer cells that stably overexpressed ACKR3, showed enhanced tumour growth[275].

In an endometrial carcinoma study, ACKR3 mRNA was detected in patient specimens but also cell lines. These observations were also verified at a protein level using immunohistochemical analyses. ACKR3 expression was associated with a proliferative phenotype in AN3CA cell line after treatment with CXCL12 ligand. The proliferation in these cells was inhibited after ACKR3 knockdown[276].

In lung cancer, ACKR3 expression was associated with tumour growth and a more aggressive phenotype. In subcutaneous murine models, ACKR3 knockdown inhibited tumour growth. The use of ACKR3- specific inhibitors, phenocopied the ACKR3 silencing experiments. ACKR3 was detected using immunohistochemistry in lung cancer patient specimens using the 11G8 antibody[253].

In contrast with the previous studies, in oral lingual squamous cell carcinoma, ACKR3 inhibited growth in *in vitro* invasion assays. ACKR3 expression in Tca8113 cells inhibited epithelial to mesenchymal transition (EMT) by downregulating crucial extracellular matrix proteins that are involved in cell migration[277].

Some viruses appear to be associated with ACKR3 receptor dysfunction. The role of ACKR3 in virus-related cancers has not been extensively studied; existing evidence suggests that these viruses commonly induce ACKR3 upregulation through the expression of viral oncogenes. In these cancers, ACKR3 expression seems to be associated with cell growth, transformation and survival[278].

1.15.4 Factors that regulate the ACKR3 expression in cancer

Several factors have been linked with ACKR3 expression in tumours. In glioma cells, it has been shown that hypoxic conditions control the ACKR3 upregulation in the tumour-associated endothelial cells. More specifically, hypoxia inducible factor -1 alpha (HIF-1 α) is associated with ACKR3 increase in the tumour microenvironment. Furthermore, hypermethylated in cancer 1 (HIC1) tumour suppressor has been proposed to regulate ACKR3 expression in the context of cancer[279,280].

Several miRNAs have been linked to ACKR3 gene expression. For example, miRNA -430 is significantly downregulated in bladder cancer cells that exhibit high levels of ACKR3 expression. In another study, overexpression of miRNA -101, that is considered a tumour suppressive miRNA, in hepatocellular carcinoma cells and xenograft mice models has led to reduced expression of ACKR3[281].

1.15.5 The role of ACKR3 in lung cancer

ACKR3 expression is reported in different types of lung cancer. In a study using lung adenocarcinoma cell lines it was demonstrated that TGFβ1 overexpression induced the upregulation of ACKR3 gene as verified by qPCR analyses. Furthermore ACKR3 knockdown constrained the TGFβ1-mediated cell motility and epithelial to mesenchymal transition. Subsequently, the authors proposed that ACKR3 is involved in TGFβ1-promoted cancer stem cells' (CSC) formation. The aforementioned observations were shown to be CXCR4- independent, since CXCR4 knockdown in the same lung cancer cell lines did not phenocopy the ACKR3-mediated phenotypes[318].

In another study, is was proposed that ACKR3 regulates tumour growth in lung adenocarcinoma among other types of cancer. More specifically, stable ACKR3 knockdown Lewis lung carcinoma cells were transplanted subcutaneously in immunocompetent mice and tumour growth was measured overtime. In this model, ACKR3 ablation reduced significantly the tumour growth although the exact mechanism responsible for this phenotypes was not investigated in this study. Furthermore, ACKR3 expression was detected using immunohistochemistry in the tumour associated vasculature in human lung adenocarcinoma resections[253]. The antI- ACKR3 antibody that was used for the immunohistochemical analyses in this study, was clone 11G8 that we validated for specificity in Chapter 4.

Furthermore, in another lung cancer study, the authors assessed the gene expression of CXCR3 , CXCR4 and ACKR3 in surgical specimens of 127 non-small cell lung cancer (NSCLC) patients who underwent complete tumour resection. They observed a higher CXCR4 and ACKR3 expression in patients with recurrence of secondary tumours, compared to the non- recurrence group. These results suggest that ACKR3 and CXCR4 may be involved in a more aggressive post-surgical tumour

phenotype. In the same study, it was revealed a positive correlation between ACKR3 mRNA expression and the presence of EGFR mutations, suggesting a positive involvement of ACKR3 in this subset of lung cancer patients[254].

Aims of the study

ACKR3 is a seven-transmembrane spanning receptor that can fine-tune several physiological processes including development, tissue repair and homeostatic regulation. ACKR3 is also linked to a number of pathological conditions, including diabetes and atherosclerosis. ACKR3 was discovered to be a binding receptor for CXCL12. Because of the involvement of the CXCR4/CXCL12 axis in cancer progression and metastasis, ACKR3 was also interrogated in the cancer context. ACKR3 is upregulated in several types of human cancers but also in the tumour-associated vasculature.

Because of the lack of specific ACKR3 antibodies and due to technical limitations and differences in experimental approaches, there are a lot of discrepancies in the scientific literature regarding ACKR3 expression and role in cancer development and progression.

To this end, the aims of the present study where:

- to shed more light on the expression of ACKR3 in particular organs in which ACKR3 expression is linked with cancer development with a particular focus on the lung
- To validate commercially available ACKR3 antibodies
- to understand the contribution of ACKR3 to cancer development with the help of genome editing technologies
- to model ACKR3 role in cancer using *in silico* analyses and *in vivo* murine models

To accomplish these aims, we employed a combination of genome editing approaches, fluorescent reporter mice analyses, bioinformatic analyses and established *in vivo* cancer murine models.

CHAPTER 2

Materials and Methods

2.1 Microbiological techniques and reagents

2.1.1 *E. coli* bacteria culture reagents

LB (Luria-Bertani) liquid medium composition and preparation

Initially, 10 g tryptone, 5 g yeast extract and 10 g NaCl were added to 500 ml of water. Subsequently, the ingredients were mixed by shaking or stirring until the solutes were dissolved and the final volume of the solution was adjusted to 1 litre by adding water. Finally, the solution was sterilised by autoclaving for 20 minutes.

Ampicillin antibiotic 1000x stock preparation

Ampicillin powder (Sigma) was dissolved in distilled water (or 70 % ethanol) to a concentration of 100 mg/mL and filtered using a .22 µm filter before storing at -20°C. Final working concentration after addition to the media was determined at 100 µg/ml.

LB (Luria-Bertani) solid medium (agar) preparation

Initially, 3 g of tryptone, 1.5 g of yeast extract, 3 g NaCl and 4.5 g of agar were weighed. Subsequently, distilled water was added to the tryptone, yeast extract and NaCl mixture, until it was dissolved. Then, the pH of the solution was adjusted to 7.0, agar powder was added, and the mixture was autoclaved. After autoclaving, the LB agar was allowed to cool down to 55°C, and ampicillin was added. Finally, the LB-agar ampicillin was poured into Petri dishes (approximately 10 ml per dish), and the agar dishes were left to solidify at room temperature.

Solution I for preparation of competent cells

For solution I preparation, the following ingredients were added in distilled water and stirred until the ingredients were dissolved.

Solutes	Final concentration in solution
KAc	30 mM
KCl	100 mM
$CaCl_2$	10 mM
$MnCl_2$	50 mM
Glycerol	15% (v/v)

Subsequently, pH was adjusted to 5.8 with addition of acetic acid. Finally, the solution was filtered using a .22 µm filter and stored at 4°C.

Solution II for preparation of competent cells

For solution II preparation, the following ingredients were added in distilled water and stirred until the ingredients were dissolved.

Solutes	Final concentration in solution
KCl	10 mM
$CaCl_2$	75 mM
Glycerol	15% (v/v)

Subsequently, pH was adjusted to 6.5 with addition of KOH. Finally, the solution was filtered using a .22 µm filter and stored at 4°C.

2.1.2 Preparation of competent bacteria

The *E. coli* strain XL-1 blue (Agilent) was chosen to propagate plasmid DNA. An LB-agar plate with no antibiotics was spread with non-transformed XL-1 blue cells and colonies were allowed to grow overnight at 37°C. The next day, one of the colonies was picked and inoculated in 5 ml of LB medium with no antibiotics for the following night at 37°C. The following day, 5 ml of the bacterial culture were sub-cultured in 100 ml of LB broth with no antibiotics and grown at 37°C until the optical density at 600 nm reached a value of 0.3-0.4. After chilling 5 minutes on ice, cells were spun at 3000 rpm for 10 min at 4°C in 50 ml sterile Falcon tubes. Each pellet was resuspended in 20 ml of solution I by gentle pipetting, chilled for 5 minutes and spun as previously. Each pellet was then resuspended in 2.2 ml of solution II, by gently pipetting up and down and chilled for a further 15 minutes. Finally, cells were aliquoted by placing 200 µl per Eppendorf tube, then were snap-frozen in dry ice and stored at -80°C for future use.

2.2 Tissue culture

2.2.1 LLC murine cell line

The Lewis Lung Carcinoma cell line was first isolated from a spontaneous epidermoid carcinoma of the lung in C57BL/6 mice in 1954 by Dr Margaret Lewis. It has been an important tumour model for cancer therapy, as it has helped in the study of metastasis and angiogenesis and has been involved in developing anti-tumour chemotherapeutic drugs. LLCs hold an advantage because they were isolated from a spontaneous tumour in C57BL/6 mice; thus they are immunologically compatible with this strain of mice, so they can be engrafted into immunocompetent C57BL/6 (both sexes are suitable hosts for engraftment) mice and not be rejected by their immune system. Together with the lack of immune-dependent obstacles, being syngeneic allowed the study of every aspect of the tumour microenvironment, including the role of the resident and recruited immune cells[282].

2.2.1.1 Maintenance

LLC cell line was cultured in DMEM medium (Invitrogen) supplemented with 10% FBS (Invitrogen), 1% L Glutamine (Invitrogen) and 1% penicillin/ streptomycin (Invitrogen), at 37°C in 5% CO_2. Cells were passaged by incubating for 5 minutes at 37°C in trypsin-EDTA 0.5 % when they reached 80% confluency, which usually occurred every second or third day due to their extremely high rate of proliferation. During passaging, 10^6 cells were placed in a new T75 cell culture flask.

2.2.2 B16F10 murine cell line

B16 cells were first isolated and maintained from a tumour that developed spontaneously behind the ear of a C57BL/6 mouse. The tumour was then resected, transplanted, and maintained *in vivo*. During the 1970's Dr Isaiah J. Fidler, established protocols for the use of the B16 model. Dr Fidler stained B16 cells, with 125I-5-iodo-2′-deoxyuridine for tracking and implanted the cells into C57BL/6J mice. Subsequently, he sacrificed the mice at different time points and measured the B16 cells in the blood and in different organs. He observed that 99% of the original cell population had died within the first day and that only a small population of about 400 cells had colonised the lung. This study was pioneering because it established a metastasis model that was simple, reliable and gave consistent results. It also demonstrated that metastasis is regulated by various factors and does not rely only on the presence or the number of tumour cells. Only a few cells from the original population could enter the circulation, colonise the lung and begin to form a tumour[283].This cell line was used in female C57BL/6 mice in our studies.

2.2.2.1 Maintenance

B16-F10 murine melanoma cell line (ATCC) was cultured in DMEM medium (Invitrogen) supplement with 10% FBS (Invitrogen), 1% L Glutamine (Invitrogen) and 1% penicillin/streptomycin (Invitrogen), at 37°C under 5% CO_2. Cells were passaged by incubating for 5 minutes at 37°C in trypsin-EDTA 0.5 % when they reached 80% confluency, which usually occurred every four days after placing 10^6 cells in a T75 cell culture flask.

2.2.3 Freezing procedures

The freezing medium that was used during the freezing process was FBS containing 10 % DMSO. Usually, an 80% confluent T75 cell culture flask yielded 8-10 x10^6 cells. Usually, 10^6 cells were resuspended in 1 ml of freezing medium, and stored in cryovials at -80°C for 24 hours and then stored in Liquid Nitrogen (−195.79°C) for an indefinite period.

2.3 Cell biology

2.3.1 Lipofectamine 2000 transfection

Lipofectamine (Invitrogen) is a cationic liposome formulation, which can form complexes with negatively charged nucleic acids such as DNA or RNA. The resulting complexes can easily fuse with the negatively charged plasma membrane of living cells, allowing the liposome- nucleic acids complexes to cross into the cytoplasm so the nucleic acids can be expressed. To be efficiently expressed the transfected product should enter the nucleus; therefore, transfection is recommended on subconfluent cells, which are more proliferative and can undergo mitosis.

2.3.1.1 Transfection of B16F10/ LLC cells in six- well plates

The day before transfection, 3x10^5 cells per well were seeded in a 6-well plate. The following day, in an Eppendorf tube, 2 µg of DNA per transfection reaction was diluted in 150 µl of Opti-MEM medium (Invitrogen). In another Eppendorf tube, 8 µl of Lipofectamine 2000 was diluted in 150 µl of Opti-MEM medium. Subsequently, the contents of the two Eppendorf tubes were combined, mixed for 5 seconds by vortexing and incubated for 5 minutes at room temperature to allow the formation of complexes. Then, the DNA/ lipofectamine mix was dispensed dropwise into each well. After 24 hours, the cells were assessed for the efficiency of the transfection.

2.4 Molecular biology

2.4.1 Guide RNA cloning protocol to PX461 vector

At first, a digestion reaction was set up in an Eppendorf tube. More specifically, 1 μg of PX461 plasmid DNA (Addgene), 1 μl of Fast Digest BbsI enzyme (Thermo scientific), 2 μl 10X FastDigest Buffer (Thermo scientific), 1 μl Fast AP (Thermo scientific) were mixed, and distilled water was added to a final volume of 20 μl. Then, the digestion mixture was incubated for 30 min at 37°C. After the incubation, the digested plasmid was gel purified using the QIAquick Gel Extraction Kit (Qiagen), according to the manufacturers' protocol. At the next step, each pair of guide RNA oligos was phosphorylated and annealed. For this, a reaction was set by adding 1 μl of oligo 1 (100mM), 1 μl of oligo 2 (100mM), 1 μl of 10X T4 Ligation Buffer (NEB), 6.5 μl distilled water and 0.5 μl T4 PNK (NEB) in a PCR tube. The oligos were annealed, by placing the reaction in a thermocycler using the following parameters: 37°C for 30 min 95°C for 5 min and then ramp down to 25°C at 5°C /min. Then ligation reaction was set and incubated at room temperature for 10 min. The ligation reaction mix contained 1 μl of BbsI digested plasmid from the digestion reaction (50ng), 1 μl of phosphorylated and annealed oligo duplex (1:200 dilution), 5 μl of 2X Quickligation Buffer (NEB) and X μl of distilled water to a final volume of 11 μl. Finally, the ligation reaction was incubated at 37°C for 30 min. At the last step, DH5a bacteria were transformed with the ligation reaction.

The sequences of the guide RNAs used in this study are listed below:

	Guide RNAs sequence ('5-3' direction)
Mouse ACKR3 Forward	TACATTTTCATCTTCGTGAT
Mouse ACKR3 Reverse	ATCACGAAGATGAAAATGTA
Mouse ACKR3 Forward 2	AACAAGAACGTGCTTCTGTA
Mouse ACKR3 Reverse 2	TACAGAAGCACGTTCTTGTT
Mouse CXCR4 Forward	GGAGCATGACGGACAAGTAC
Mouse CXCR4 Reverse	GTACTTGTCCGTCATGCTCC
Mouse CXCR4 Forward 2	TCTTCTGGTAACCCATGACC
Mouse CXCR4 Reverse 2	GGTCATGGGTTACCAGAAGA

The following primer was used for Sanger sequencing to verify successful cloning of the guide RNAs: U6 Forward :GAGGGCCTATTTCCCATGATTCC.

2.4.2 Bacteria DH5a transformation protocol

Competent *E. coli* bacteria (strain DH5a) cells were allowed to thaw on ice. Then the cells were gently mixed with a pipet tip and aliquoted by putting 50 µl of cells for each transformation into 1.5 ml tubes that have been pre-chilled on ice. Then 1-5 µl DNA (1-100ng) was added to the cells, and they were mixed gently by pipetting. Then the cells/ DNA mixture was placed on ice for 30 minutes. Afterwards, the bacteria were heat-shocked at 42°C for 30- 45 seconds without shaking. Then the tubes were placed on ice for 2 minutes. After this, 500 µl of pre-warmed (37°C) LB medium were added, and the bacteria were placed in a rocking incubator at 37°C for 1 hour.

Finally, 100 µl of each transformation was plated on LB plates with the appropriate antibiotic for selection, and bacterial colonies were allowed to grow overnight at 37°C.

2.4.3 FACS cell sorting and data analysis

Cas9-EGFP transiently transfected B16F10 and LLC1 cells were trypsinised, resuspended in FACS buffer [DPBS 1X without Calcium (Invitrogen) +2% FBS (Invitrogen 10270106) +2mM EDTA)] and sorted using a BD FACS Aria TM III sorter.

2.4.4 CRISPR validation

B16F10 and LLC cells have undergone genome editing processes. After transfection with the Cas9/GFP plasmid, cells were subjected to single-cell sorting in 96 well plates, and single-cell clones were allowed to grow for 3-4 weeks. When clones reached 80% confluency, the genomic DNA was extracted, followed by PCR amplification of the gene of interest. Genomic DNA PCR products were analysed and pre-screened for their size on an agarose gel. The selected PCR products were TA cloned inside pGEM T-Easy vector and sequenced to verify biallelic knockouts.

2.4.5 Genomic DNA extraction

Genomic DNA was extracted using the QuickExtract Solution (Lucigen). Cells were placed in a 0.2 mL PCR tube and 100 µl of QuickExtract Solution was added to each tube. Then cells were vortexed at 300g for 15 seconds and incubated at 65°C for 10-15 minutes. Subsequently, cells were vortexed for 15 seconds and incubated at 98°C for 2 minutes. After this, the extracted genomic DNA was ready to use for PCR amplification or for storage at -20◦C for later use. For CRISPR validation, the genomic DNA from different single-cell expanded clones, was PCR amplified using specific genomic primers (that span the area of the expected double-strand break).

The genomic PCR product was run in a 2% w/v agarose gel and the clones of interest were interrogated by comparing the size of the PCR band with the PCR band from the WT clone that served as a control. Selected PCR products, from the clones of interest, were then gel purified and prepared for the subsequent TA cloning step.

2.4.6 Genomic PCR

The genomic DNA extracted from the cells was amplified using the Q5 High-Fidelity 2X Master Mix (New England Biolabs). More specifically 2 µl (50- 100 ng) of genomic DNA was added to 25 µl of 2X PCR Master Mix, 2,5 µl of forward and 2,5 µl of reverse

primer (final concentration 10 µM) and 18 µl of distilled water. Reactions were run with the following programme:

Initial Denaturation	98°C	30 seconds
35 Cycles	98°C	5–10 seconds
	68 °C	10–30 seconds
	72°C	20–30 seconds/kb
Final Extension	72°C	2 minutes
Hold	4°C	

The primers used for the genomic PCR were the following:

Forward ACKR3	CACTCTTCACCTCTGGCCTAA
Reverse ACKR3	GCTACTGTGCTTCTCCTGGT
Forward CXCR4.	TTGGTTCCACTAAAGAGGGCA
Reverse CXCR4	CCCTTGGAGTGTGACAGCTT

2.4.7 Gel electrophoresis

PCR products were run on a 2% agarose gel to determine the size. The gel was made by dissolving 3g of agarose (Sigma-Aldrich) to 150ml of tris acetate ethylenediaminetetraacetic acid (TAE) buffer. Subsequently, 7.5 ml of ethidium bromide were added and the solution was poured into a gel electrophoresis tank and left to solidify. Samples were loaded and run for 60 min at 100 volts. The gel was imaged by UV illumination using an Alpha 2200 Digital UV- Visphoto (Alpha Innotech, Santa Clara, California).

2.4.8 TA cloning

Genomic PCR amplification products were blunt-ended dsDNA oligonucleotides because a high-fidelity DNA polymerase was used. TA cloning protocol required single nucleotide 3' overhang at each strand. At the first step, blunt-ended genomic PCR products were incubated with dATP (Ambion), Taq polymerase (New England Biolabs) and Taq polymerase buffer at 70°C for 30 min. The pGEM T-Easy (Promega) is a linearized vector with a single dTTP 5' overhang. Subsequently, the pGEM T-Easy, the genomic PCR products with overhangs added, and DNA ligase (Promega) were incubated together for 1 hour at room temperature. After one-hour, competent bacteria were transformed with the ligation product.

2.4.9 Genome editing using the D10A Cas9 (nickase) strategy

Mutant D10A Cas9 encoded in PX461 vector (Addgene) was used for the genome editing approaches (Figure 2.1). Mutation of D10A impairs the DSB (double-strand break) formation ability of WT Cas9, giving it the ability to generate a single nick on the complementary strand. Therefore, to generate a DSB, a pair of nickases, with two different guide RNAs is required, reducing the possibility of off-target effects greatly. The efficiency of the genome editing is reduced if the distance between the two gRNAs is greater than 20 nucleotides.

One disadvantage of the nickase method is the fact that it is more challenging to find a target region in which the two guide RNAs are closely spaced and at the same time are located close to the beginning of the gene, to achieve efficient gene disruption. The main advantage of the nickase approach is that the genome targeting is extremely precise, with a reduced number of off-target effects occurring.

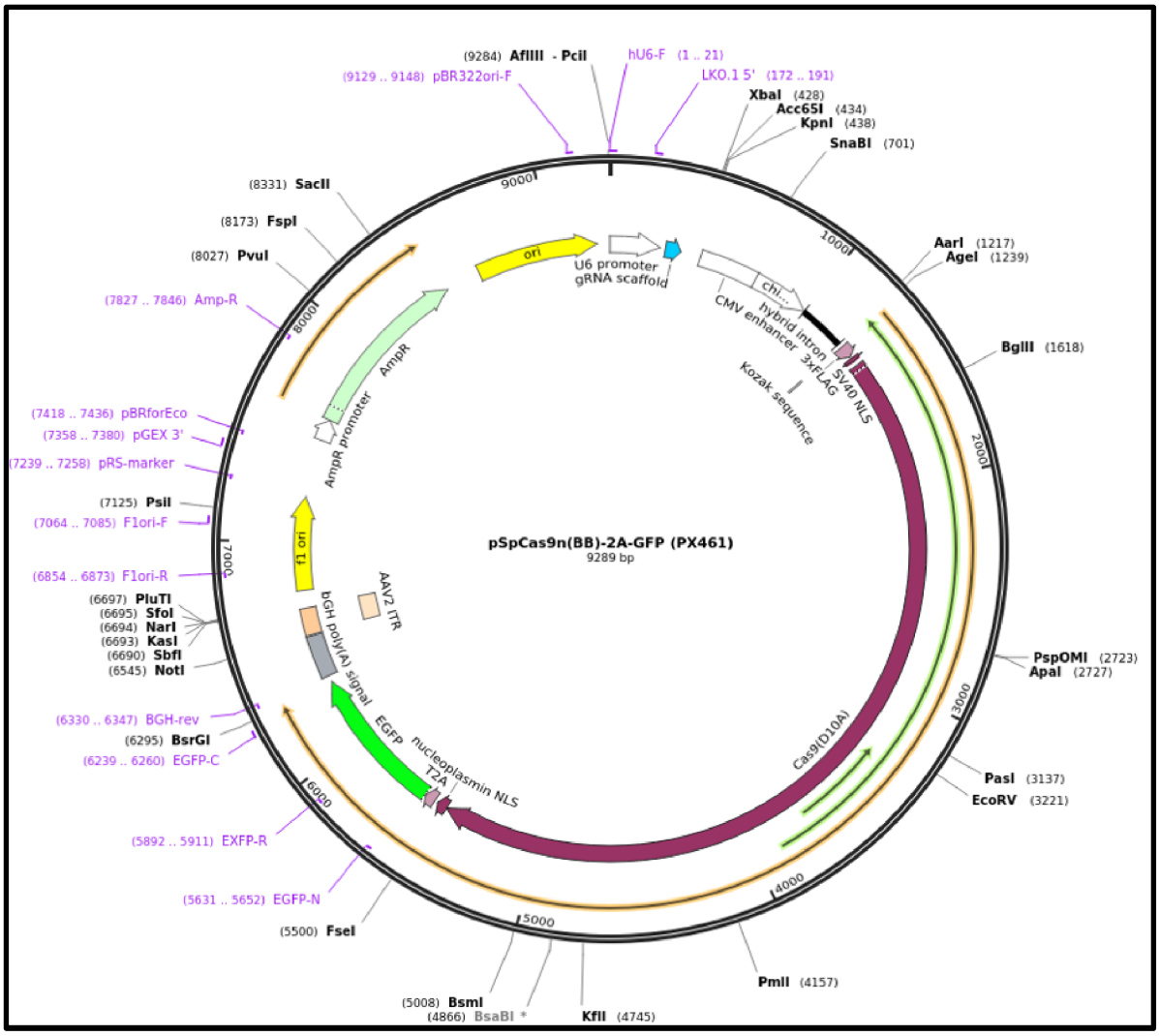

Figure 2.1 Diagram of the in PX461 vector that encodes for mutant D10A Cas9 protein (source Snapgene software)

2.5 Flow cytometry

Flow cytometry is an analytical laser-based cell biology technique, that exploits the refracted or emitted light from cells, to count and identify different cell types in a heterogeneous fluid mixture. Cells are usually stained with fluorescent antibodies against cell markers, that allow the cell type identification so that light is first absorbed and then emitted at different wavelengths. Then cells are suspended in a fluid and injected into the flow cytometer instrument. The flow cytometer applies fluidics pressure to regulate flow rate, ideally allowing one cell at a time through a laser beam and the light scattered is characteristic to the cell type. Flow cytometry is a powerful method because it allows the rapid and accurate collection of data related to many parameters from a heterogeneous fluid mixture containing live cells.

2.5.1 Forward Scatter (FSC)

Forward Scatter light is refracted by a cell in the flow channel and continues along in the light path. The forward scattered light is detected by a sensor in the light path and is typically used to identify particle size. The forward scattered light is most commonly used to detect the size of the cell. Larger cells will produce more forward scattered light than smaller cells, and larger cells will have a stronger forward scatter signal.

2.5.2 Side Scatter (SSC)

Side-scattered light is usually used to determine the granularity and complexity of the cell. Cells with high granularity and a large amount of internal complexity, like neutrophils, will produce more side-scattered light, and a higher side-scatter signal than cells with a low-granularity and complexity.

2.5.3 Flow cytometry analysis

When acquiring samples in the flow cytometer, FSC and SSC voltages were set to a suitable value to make sure that all the cell events were ‘’on scale’’ and included for analysis. When analysing flow cytometry data, cells of interest were gated using FSC and SSC, cell doublets were discriminated using SSC-A (Side Scatter- Area) and SSC-H (Side Scatter- Height) or FSC-A and FSC-H, and live cells were selected based on negativity of dead cell dye staining. This gating strategy was applied to all the flow cytometry data before proceeding to further gating analyses.

2.5.4 Fluorescent minus one controls (FMO)

Fluorescence minus one (FMO) controls were used to assess and gate on positive staining accuracy. In every antibody panel, an FMO was made for each fluorophore of the panel. FMO for an antibody involves staining the cells with a cocktail of antibodies that includes all the colours of the panel apart from one. The missing fluorophore in each FMO sample would be used to assess any spill-over of fluorescence from other channels, while also serving as a negative control, allowing clear visualisation of the positive staining.

2.5.5 Doublet discrimination

Doublet exclusion is a critical step in flow cytometry to ensure we include single cells and exclude doublets from the subsequent analysis. This can be critical in cell sorting, cell cycle analysis. If a doublet containing a fluorescence positive and negative cell passes through the laser it will produce a positive signal leading to false positives. Doublet exclusion is performed by plotting the height or width against the area for forward scatter or side scatter. Doublets will have double the area and width values of single cells while the height is roughly the same.

2.5.6 Flow cytometry antibodies and viability dyes

Cell marker	**Antibody clone**	**Final antibody dilution**	**Fluorophore**
CD45	30F11 (Biolegend)	1:200	APC Cy7
EpCAM	G8.8 (Biolegend)	1:200	PERCP 5,5
CD31	MEC13.3 (Biolegend)	1:200	PE, BV650
Gp38	8.1.1 (Biolegend)	1:200	PE Cy7
CD140A	APA5 (Biolegend)	1:200	APC
ACKR3	11G8(RnD Systems)	1:100	PE
ACKR3	10D1(BD Biosciences)	1:100	BV421
Viability dye	Viability Dye eFluor 506 ThermoFisher	1:5000	BV510

2.5.7 Live dead viability staining for flow cytometry

After digestion, cells were isolated and stained with a viability dye. These dyes are commonly used in cellular staining for flow cytometry analysis and are based on the reaction of a fluorescent reactive dye with cellular proteins (amines). The viability dyes cannot penetrate cell membranes of live cells, so only a few cell surface proteins are available to react with the dye, resulting in dim staining. The viability dyes can permeate the interrupted membranes of dead cells and stain both the surface and interior protein amines, resulting in brighter staining.

The viability staining step is essential for the flow cytometry data analysis since it is a common practice to exclude dead cells from the data analysis. This is because dead cells have higher autofluorescence and exhibit increased non-specific antibody binding, which can lead to false positives[284].

2.5.8 ACKR3 antibody intracellular staining for flow cytometry

Lung cell suspensions after the viability staining step were stained for extracellular markers. More specifically, cells were stained with an antibody cocktail (detailed in 2.5.6 section) for 20 minutes on ice in the dark in the presence of FcR blocking reagent (Miltenyi) according to the manufacturers' instructions. Subsequently, the cells were fixed and permeabilised in 200µl of BD Cytofix/Cytoperm buffer per sample. Cells were incubated in this buffer for 20-30 minutes on ice. The fixation step before intracellular staining is essential to ensure stability of the antigens. Subsequently, the cells were washed in 1ml 1x Perm Wash Buffer per sample (10x solution buffer was diluted to 1x using distilled). Cells were centrifuged at 400xg for 5 minutes.

At the next step, ACKR3 intracellular staining was performed by diluting the ACKR3 antibody in 1x Perm Wash Buffer. ACKR3 antibody staining was performed in permeabilization buffer to ensure the cells remain permeable. The cells were incubated for 20-30 minutes on ice in the dark. After this, the cells were washed in 1ml 1x Perm Wash Buffer per sample as previously and collected by centrifugation at 400xg for 5 minutes.

2.5.9 Chemokine uptake assay

Synthetic chemokines directly labelled with a fluorophore provide a useful tool for studying chemokine and chemokine receptor interactions[285]. It has been shown that chemical attachment of a fluorophore at the C terminus of a chemokine does not alter its biological function. The chemokine uptake assay takes advantage of the use of a C-terminally fluorescently-labelled chemokine. The internalization of the labelled chemokine is proportional to the presence of the chemokine receptor in question. The uptake medium consists of RPMI 1640 + 0.5% BSA. For the chemokines uptake assay we used the mouse CXCL12 C terminus-tagged Alexa Fluorophore 647 (Almac).

Briefly, 90 µl of cells were suspended in uptake medium at a concentration of 10^6 cells /ml (90,000 cells per well) in a round bottom 96 well plate. Subsequently,10 µl of 10x concentrated fluorescent chemokine (final concentration 25nM) were diluted in uptake medium and the final diluent was added dropwise to the cells. Then cells were incubated at 37 °C for 1 hour. Subsequently, the cells were washed twice with uptake medium and were centrifuged at 300g for 5 min at RT. Cells were resuspended in 150-200 µl of uptake medium and were analysed using a flow cytometer.

2.5.10 Ki-67 proliferation assay

Ki-67 is a protein which is located in the nucleus of eukaryotic cells. Fluorescent antibodies against Ki-67 are regularly used in order to assess the proliferative capability of cells, making it a commonly used biomarker. In our study, the proliferation rate of the cells was assessed by flow cytometry. Briefly, the staining protocol is the following: 70% ethanol was prepared and chilled overnight at -20°C. Cells were trypsinised and centrifuged at 300g for 5 min at 4°C. The cells were then washed with FACS buffer and centrifuged at 300g for 5 min at 4°C. Then, if desirable, cells were stained for other cell markers. Cells were rewashed with FACS buffer and centrifuged at 300g for 5 min at 4°C. Supernatant was discarded, and the cell pellet was loosened by vortexing. One drop of ice-cold 70% ethanol was added to the pellet,

and the pellet was vortexed. Then, 500 µl of ice-cold ethanol was added to the pellet and vortexed. After this, the cells were incubated for 1 hour at -20°C.
Then the cells were washed and centrifuged at 300g for 5 min at 4°C and resuspended in FACS buffer. Then, the anti-Ki-67 antibody was added to the samples at 1:220 dilution. Samples were incubated in the dark at RT (room temperature) for 30 min. After this, the samples were washed and centrifuged at 300g for 5 min at 4°C and resuspended in FACS buffer before reading in the flow cytometer.

2.5.11 Murine lung and trachea tissue dissociation and cell isolation for flow cytometry

Digestion solution
RPMI (Invitrogen) containing:
Dispase II (800 µg /ml, Roche)
Collagenase P (200 µg/ml, Roche)
DNAse I (100 µg/ml, Roche)

Mice were euthanised by a Schedule 1 procedure. Lungs were perfused by flushing the heart through the right ventricle with 20 ml of ice-cold PBS (using a 20 ml syringe and an 18G needle) until lungs were cleared of blood. Subsequently, lungs/tracheas were removed and placed in a petri dish containing PBS on ice. Afterwards, lungs/tracheas were moved to a clean petri dish, other tissues were trimmed off, and the lungs were minced using scissors. Then 2.5 ml of digestion solution was added per lung/trachea and incubated for 20-30 min at 37°C on a rocking platform. Afterwards, lungs were passed through a cell strainer (100 µm), and the separated cells were collected in 50 ml Falcon tubes. Then, the cells were centrifuged at 300g for 5 minutes. At the next step, red blood cell lysis using ACK lysis solution (Invitrogen) was performed for 5 minutes at room temperature, and the reaction was stopped by adding DMEM + 5% FBS serum. Cells were centrifuged at 300g for 5 minutes. If the pellet was not white, the red blood lysis step was repeated one more time. After this step, cells were ready for antibody staining.

2.6 *In vivo* techniques

2.6.1 Mice strains

C57BL/6 mice

C57BL/6, often called" C57" or" black 6", refers to an inbred strain of mice widely used in labs all over the world. Some of the reasons for the success and the widespread use of this mouse strain, are the fact that they are easy to breed, they are robust, and a lot of congenic strains are available for crossings. The strain C57BL/6 was created in 1921 at the Bussey Institute, and its genome was the second whole genome ever sequenced[286].

C57BL/6-Ackr3tm1Litt /J reporter mice

The entire exon 2 that encodes for the *ACKR3* gene was replaced by the EGFP sequence. A 5′ homology arm containing a 5.4-kb genomic fragment containing part of intron 1 and 26 bp of exon 2 immediately upstream of the ATG start codon was PCR amplified using C57BL/6 genomic DNA as a template, and then cloned in front of EGFP coding sequence. A 3′ homology arm containing a 5.2-kb genomic fragment including DNA sequence immediately downstream of the stop codon of *ACKR3* gene was PCR amplified using C57BL/6 genomic DNA and cloned after a neomycin-resistant gene cassette flanked by Lox P sites. The targeting construct was electroporated into albino C57BL/6 embryonic stem (ES) cells.

The colonies doubly resistant for the aminoglycoside G418 and ganciclovir were screened by Southern blot analyses with BsrgI, BamHI, and HindIII digestions for homologous recombination. Positive clones were injected into mouse blastocysts. Mice were subsequently crossed with EIIa-cre mice to remove the neomycin-resistant cassette[287].

2.6.2 Animal Welfare

All the mice that were used in the present study were housed in the Biological Services Central Research Facility at the University of Glasgow and maintained in specific pathogen-free conditions with unrestricted access to food and water. All experiments were approved by the University of Glasgow Ethical Review Committee and performed under the auspices of a licence from the United Kingdom Home Office.

2.6.3 Subcutaneous tumour cell injections

Wild type female C57BL/6 mice aged 8-9 weeks; back skin was shaved the day before injections. Before injection, mice were anaesthetised with isoflurane, then $2x10^5$ LLCs per mouse were injected directly beneath their dorsal skin. Tumours were measured every day from the day the tumour became visible below the skin until their largest radius reached the length of 12 mm in compliance with the Home Office Procedure Project License (PLL number 70//8377) and with a Procedure Individual Licence (PIL number ID34B8D13). At the end of the growth period, mice were subjected to a Schedule 1 procedure and pictures of the tumour were taken, and tumours were weighed.

2.6.4 Intravenous tumour cells injections

$2x10^5$ B16F10 cells were injected into the tail vein of female C57BL/6 mice aged 8-9 weeks. Mice were weighed daily (in compliance with the Home Office project animal license) after the day of injection. After two weeks from the day of injection, mice were subjected to Schedule 1 procedures; lungs were removed and assessed macroscopically (counting individual tumour nodules) regarding the tumour burden.

More specifically, lungs from different groups were blinded before counting and subsequently were counted by two different individuals and measurements were compared to assure an unbiased measurement .

2.7 Software

2.7.1 Flow cytometry data analysis

All data obtained from flow cytometry were analysed using FlowJo software. Samples were gated initially on forward and side-scatter parameters to exclude debris, forward scatter average against height to exclude doublets and cells negative for viability dye to exclude dead cells. Individual stains were gated based on FMO, if available. For individual tissues and cell types, standard gating strategies were applied as detailed in the results section.

2.7.2 Statistical Analysis

For statistical analysis, Prism (GraphPad) software was used. For all statistical analyses in this study, the following methods were used : When two groups were compared, an un paired t-test was applied. For comparison of more than two groups, one-way analysis of variance (ANOVA) was applied with Tukey's or Bonferroni's correction for multiple comparisons. For comparison of groups with data that did not follow the normal distribution assumption, the Kruskal-Wallis test was applied. Statistical significance was indicated as: *P≤0.05, **P≤0.01, ***P≤0.001, ****P≤0.0001, ns = P>0.05. Error bars represented the standard deviation of the mean.

Box-and-whisker plot: Whiskers indicate 10th and 90th percentile boxes indicate 25th to 75th percentile, and the horizontal solid line indicates the median. Circles indicate the minimum and maximum values.

CHAPTER 3

Characterisation of ACKR3 expression in the adult lung

3.1 Introduction and aims of the chapter

One of the most critical obstacles when studying GPCRs is the lack of specific antibodies due to the high number of GPCRs and the high structural homology among GPCR members of the same subfamily. Antibodies against ACKR3 are not an exception to this general rule. There are several discrepancies reported in the literature regarding ACKR3 expression in different tissues, that are mostly attributed to the non- specific nature of the anti ACKR3 antibodies. For example, in lung cancer, ACKR3 expression in patients' biopsies is mostly assessed by immunohistochemistry using antibodies that were not validated in ACKR3 KO cell lines or ACKR3 KO mice. In murine lung cancer models cells are examined for ACKR3 expression using immunohistochemistry and flow cytometry using anti -ACKR3 antibodies.
To this end, it is very important to validate some of the most commonly used ACKR3 antibodies in order to be able to critically evaluate the ACKR3 expression in lung cancer and other cancers.

To circumvent this problem, other complementary methods are used to assess the expression of ACKR3. For *in vitro* studies, competition binding assays of labelled chemokines among others, are usually performed as supplementary methods of identification. For *in vivo* studies, the use of ACKR3 fluorescent reporter animals is a reliable approach to characterize ACKR3 expression in different tissues.

To this end, for this study, we used the C57BL/6-Ackr3tm1Litt /J reporter mouse to interrogate ACKR3 expression in the resting lung. The Ackr3*tm1Litt/J* mouse strain was generated in the laboratory of Dr Dan Littman in New York University. More specifically, the EGFP (enhanced green fluorescent protein) cDNA was knocked into the second exon of the gene immediately after the endogenous start codon. This mouse strain is maintained in the heterozygous state since the homozygous GFP (ACKR3 knockout) mice die postnatally (Figure 3.1)[288].

The aforementioned reporter mouse provides a powerful tool to assess ACKR3 expression in stromal cell subsets, in the resting lung. The main reason for the

selection of this particular tissue for analysis is that ACKR3 is overexpressed in lung cancer (described in chapter 5). Lung cancer can originate from cell populations that reside in the lung. Furthermore, the ACKR3 reporter mouse provides a valuable tool to validate commercially available anti-ACKR3 antibodies.

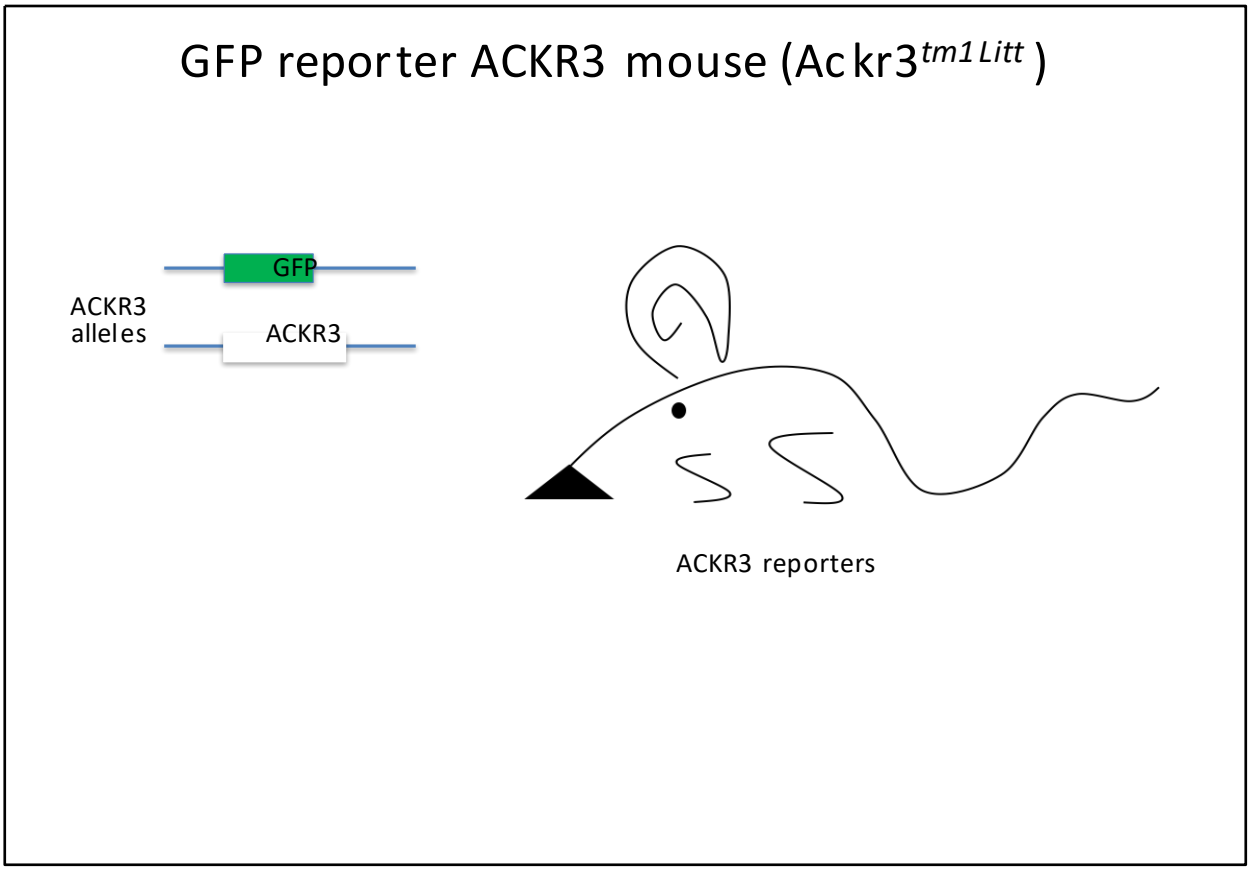

Figure 3.1 Schematic representation of C57BL/6-Ackr3tm1Litt /J reporter mouse strain. *This mouse strain is maintained in the heterozygous state since the homozygous GFP (ACKR3 knockout) mice die postnatally. The EGFP (enhanced green fluorescent protein) cDNA was knocked into the second exon of the gene immediately after the endogenous start codon.*

3.2 Interrogation of ACKR3 expression in the resting lung stroma using flow cytometry

For this study, both female and male ACKR3 GFP reporter animals aged 10-12 weeks were used to assess expression of ACKR3 in resting lung. More specifically, we isolated cells from the lung and stained them with a cocktail of antibodies against cell markers that would allow us to discriminate between major stromal cell types, using flow cytometry. Four major stromal cell types were interrogated for ACKR3 (GFP) expression: lymphatic endothelial cells (LECs), blood endothelial cells (BECs), epithelial cells and fibroblasts. An overview of the general gating strategy we applied to analyse the flow cytometry data from the lung is presented in Figure 3.2.

Cell type	***Gating strategy***
Epithelial cells	***Live, CD45-,CD31-,EpCam+***
Lymphatic endothelial cells	***Live, CD45-,CD31+,Gp38+***
Blood endothelial cells	***Live, CD45-,CD31+,Gp38-***
Fibroblasts	***Live, CD45-,CD31-,CD140a+***

Figure 3.2 Stromal cell markers used for flow cytometry gating of the lung stromal cell populations.

At first, lungs were dissected from the animals, and tissues were minced with a pair of scissors and subsequently digested (described in detail in the Materials and

Methods, section 2.5.11). After the live/dead staining (described in detail in the Materials and Methods, section 2.5.7), we stained the cell isolates with a fluorescent-tagged antibody cocktail against cell markers characteristic of distinct cell subsets. We included appropriate FMO (Fluorescence Minus One) controls for every fluorophore that was present in our antibody panel.
After staining, cells were fixed, and the following day were analysed using a BD LSR Fortessa cytometer analyser. Single fluorophore stained beads were used to calibrate the cytometer lasers before running the cell samples.

3.3 Interrogation of ACKR3 expression in the resting lung

The first population we interrogated for ACKR3 (GFP) expression in the resting lung was epithelial cells. For this purpose, we used the general pan- epithelial marker, epithelial cell adhesion molecule (EpCAM). More specifically, in the flow cytometry data analysis, at first dead cells were excluded because dead cells often have higher autofluorescence and also bind antibodies non-specifically, thus generating artefacts in the downstream analyses (detailed in Materials and Methods section 2.5.7).
To this end, we selected only the live cell population for further analyses, as presented in the Figure 3.3 A. Subsequently, we gated the single cells (doublet discrimination) as presented in Figure 3.3 B.
Then we used the CD45 (lymphocyte common antigen) cell marker that is a general pan-leukocyte marker. CD45 is a transmembrane protein, a receptor-linked protein tyrosine phosphatase that is expressed on all leukocytes and plays a crucial role in the function of these cells[289].
We selected the CD45- (non-leukocyte) cell population (Figure 3.3 C) and then enriched for the CD31- negative population (Figure 3.3 D). CD31 is a general pan - endothelial marker. This step is essential since a significant portion of epithelial cells is also positive for CD31, possibly due to the highly vascularized nature of the lung epithelium and the tight association of endothelial and epithelial cells in the lung[290].
After the CD31 depletion step, we enriched for the EpCAM positive population (Figure 3.3 E). This population was subsequently interrogated for GFP (ACKR3) expression (Figure 3.4).

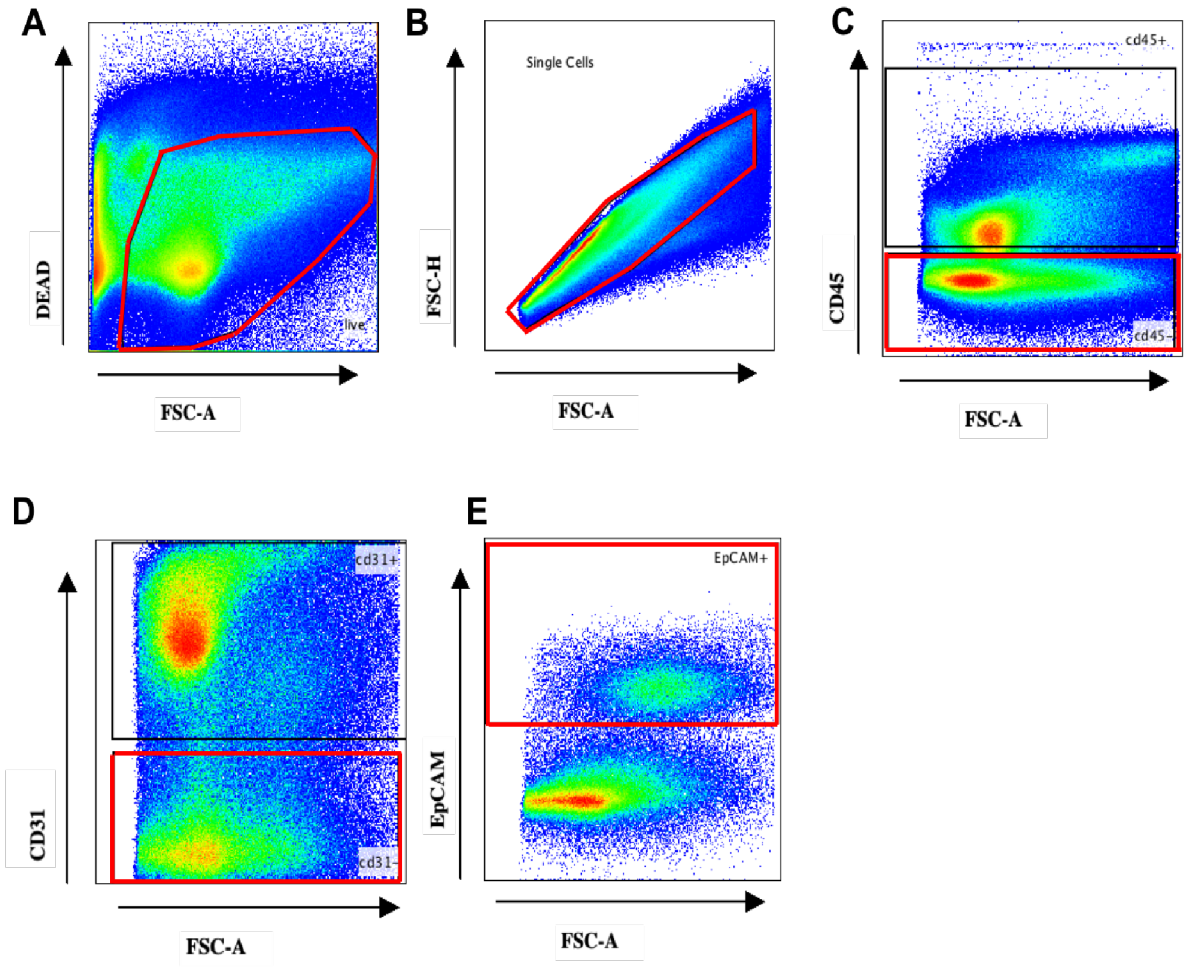

Figure 3.3 Flow cytometry gating strategy to identify epithelial cells in the resting lung of the ACKR3 (GFP) reporter mouse.

Flow cytometry data plots of fibroblasts in the resting lung of the ACKR3(GFP) reporter mouse. The gated populations selected for analysis are depicted in red. A) Dead cells and cell debris were excluded, then B) single cells were gated (doublet discrimination) C) CD45- cells were selected to exclude white blood cells D) CD31- cells for endothelial cell exclusion and E) EpCAM+ cells were selected.

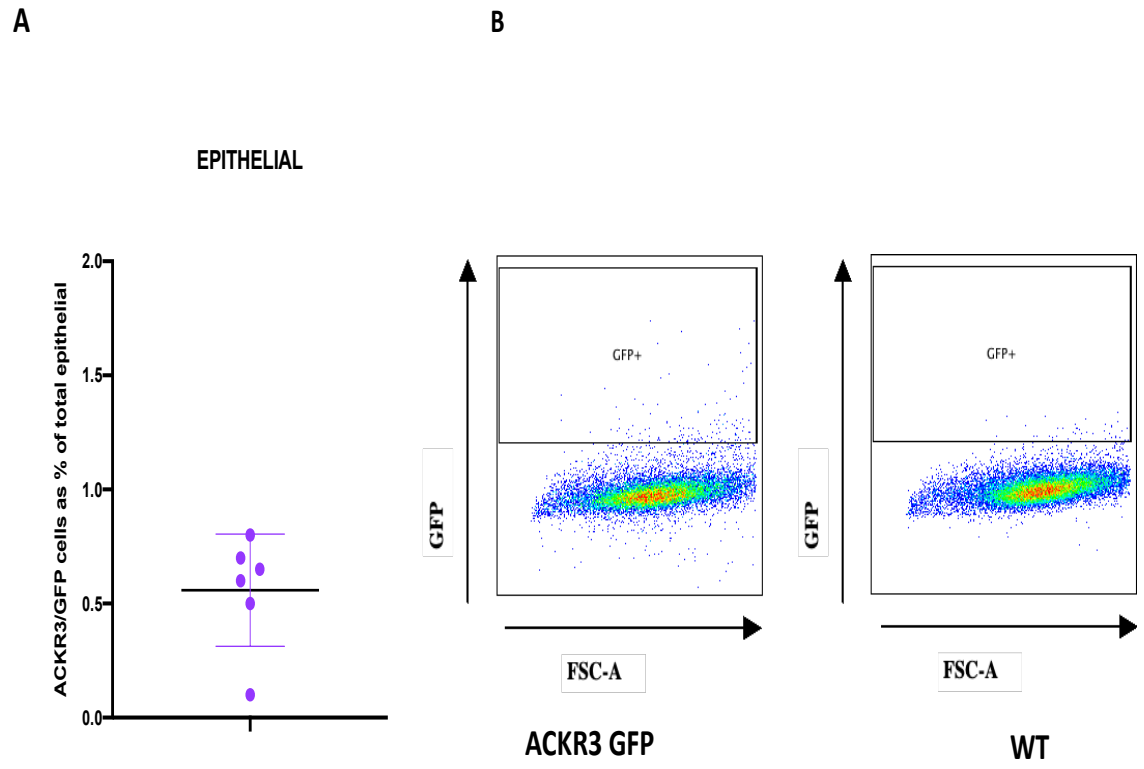

Figure 3.4 ACKR3 is not expressed in the epithelial cells in the resting lung. *A) Graph representing the ACKR3/ GFP expressing epithelial cells from six ACKR3/GFP reporter mice. The GFP/ACKR3 expression is presented as % percentage of GFP expressing epithelial to total epithelial in the resting lung. Error bars represent the SD of the mean. B) Representative flow cytometry data plots of epithelial from ACKR3 (GFP) and WT mice. One WT mouse served as a negative control for the FITCH(GFP) fluorescence.*

.

As observed in figure 3.4, the GFP/ ACKR3 expression in the reporter mice (left plot) is almost identical to the GFP expression in the WT control mouse (right plot). This observation was consistent among all six GFP/ACKR3 mice examined and compared with the wt control mouse and suggests that ACKR3 is not expressed in resting lung epithelium.

Subsequently, we interrogated the fibroblastic cell population in the lung. Fibroblasts are a very heterogeneous cell population and different cell markers, dependent on the tissue, are used for the identification of this cell population. In this study, for the resting lung analysis, we used the CD140A cell marker. This marker is also known as Platelet-Derived Growth Factor Receptor Alpha (PDGFRα).

For the fibroblasts flow cytometry gating strategy, similar to the epithelial cell gating, we enriched for live single cells, CD45- and CD31- (Figure 3.5. A, B, C and D). Subsequently, the CD31- population was enriched for CD140A positive cells (Figure 3.5 E). The fibroblastic CD140A population was examined for GFP (ACKR3) expression.

After our analysis, we interrogated the flow cytometric data from six ACKR3 GFP mice, and we observed that on average, a portion of fibroblasts in the resting lung, express ACKR3 (Figure 3.6). More specifically, it was observed that around 13-18 % of the total fibroblasts expressed GFP/ACKR3 in the resting lung (Figure 3.6A).

As mentioned previously, CD140a is a general marker for fibroblasts in the lung and fibroblasts are a very heterogeneous population. To this end, more cell markers should be used to further characterise the fibroblastic subpopulations that express ACKR3 and to gain a better understanding about the possible biological roles of ACKR3 in these cell populations.

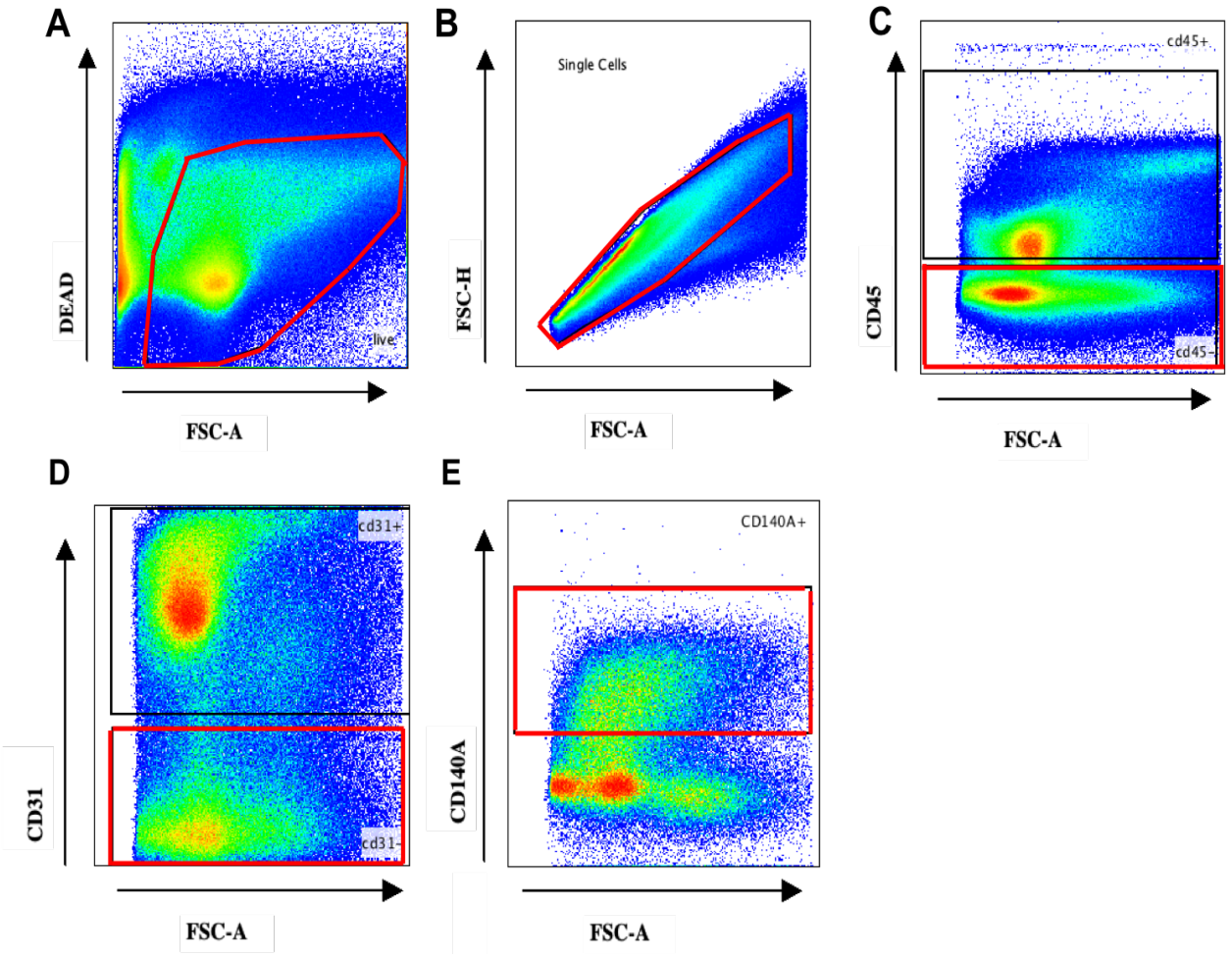

Figure 3.5 Fibroblasts gating strategy in the resting lung.

Flow cytometry data plots of fibroblasts in the resting lung of the ACKR3(GFP) reporter mouse. The gated populations for analysis are depicted in red colour. A) Live (B) single cells were selected, then C) CD45- cells were gated for immune cells exclusion. Subsequently D) CD31- were gated to exclude endothelial cells and E) CD140A+ cells were selected.

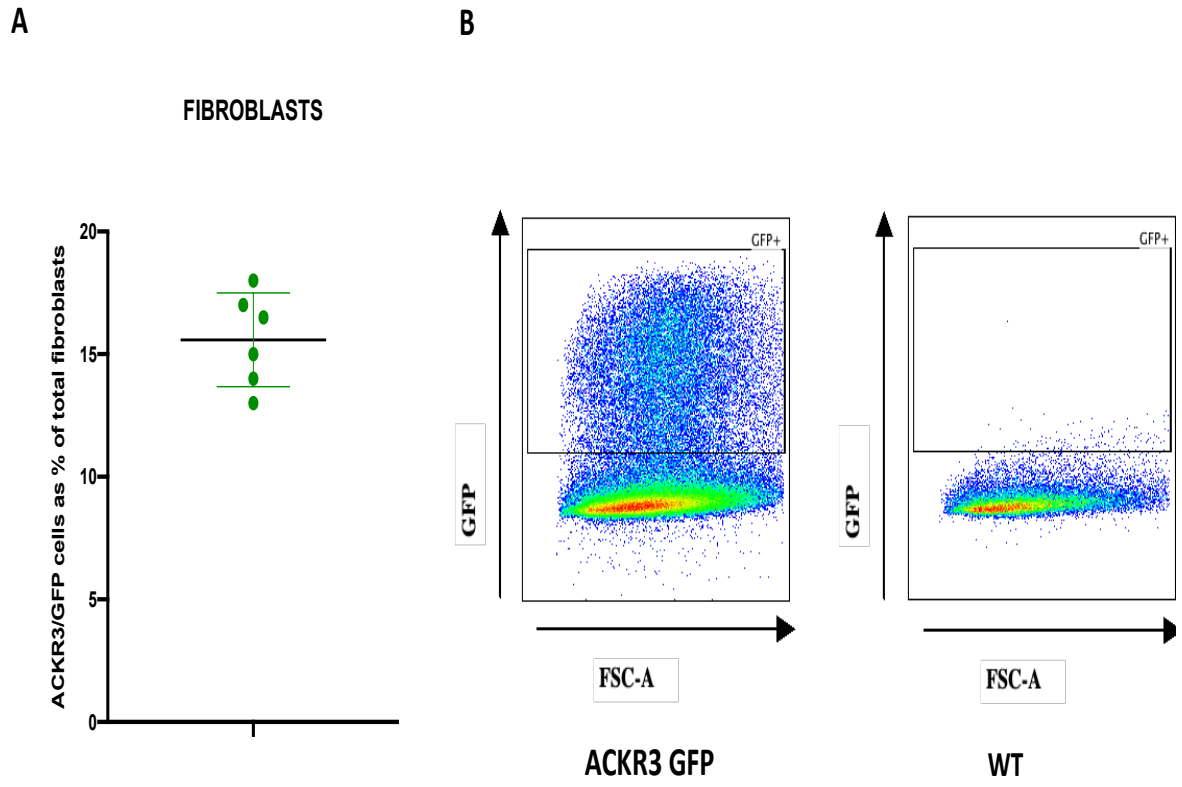

Figure 3.6 ACKR3 is expressed in fibroblasts in the resting lung.

A) Graph representing the ACKR3/ GFP expressing fibroblasts from six ACKR3/GFP reporter mice. The GFP/ACKR3 expression is presented as % percentage of GFP expressing fibroblasts to total fibroblasts in the resting lung. Error bars represent the SD of the mean. B) Representative flow cytometry data plots of fibroblasts from ACKR3 (GFP) and WT mice. One WT mouse served as a negative control for the FITCH(GFP) fluorescence.

The next lung stromal population we analysed was blood endothelial cells (BECs). For this subset of cells, we used the general pan- endothelial marker CD31(cluster of differentiation 31). CD31 is also known as platelet endothelial cell adhesion molecule (PECAM-1) and is expressed in a variety of endothelial cells, including lymphatic endothelial cells.

The gating strategy we followed for the identification of the blood endothelial cells, included live single cells and CD45- selection (Figure 3.7 A, B,C) and then CD31 positive cells (Figure 3.7D). At this step of the analysis, in order to exclude lymphatic endothelial cells that also express CD31, we used the Gp38 cell marker. Gp38 protein, also known as podoplanin (PDPN), is a specific lymphatic vessel marker[291]. Regarding this, we selected from the CD31+ cells, the Gp38 negative cells to exclude LECs (Figure 3.7E). Finally, the Gp38- cells that consist of the BECs, were interrogated for GFP (ACKR3) expression (Figure 3.8). Also, in this case, analysis of flow cytometry data from GFP/ACKR3 reporter mice revealed that a significant number of BECs in the lung express ACKR3. Data from six GFP reporter mice that were compared with one WT control mouse, verified the ACKR3 expression in the BECs in the resting lung. More specifically, around 35-45% of BECs express GFP in the resting adult lung.

This observation is in accordance with several studies that highlight the expression of ACKR3 in blood endothelial cells in several tissues and organs. ACKR3 expression has been associated with endothelial cell homeostasis, CD31 redistribution, loss of endothelial cell contacts and inhibition of endothelial barrier function. Some studies propose that ACKR3 expression in endothelial cells can regulate angiogenesis under certain conditions[292].

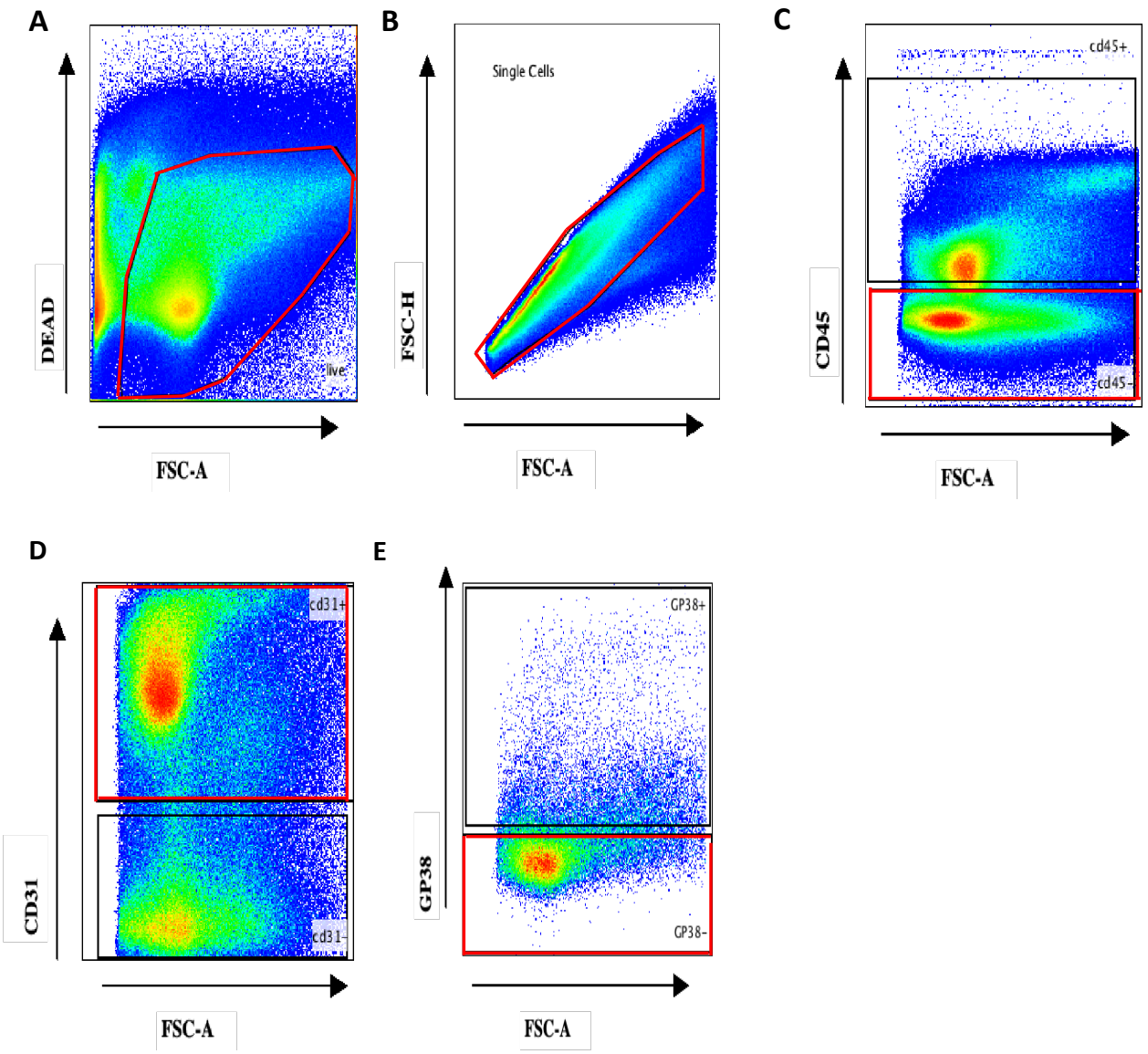

Figure 3.7 Blood endothelial cell gating strategy in the resting lung. *Representative flow cytometry data plots of blood endothelial cells in the resting lung of the ACKR3(GFP) reporter mouse. The gated populations for analysis are depicted in red colour. A) Live cells were selected, then B) single cells C) CD45- cells were gated for immune cells exclusion, D) then CD31+ and E) GP38- cells were selected.*

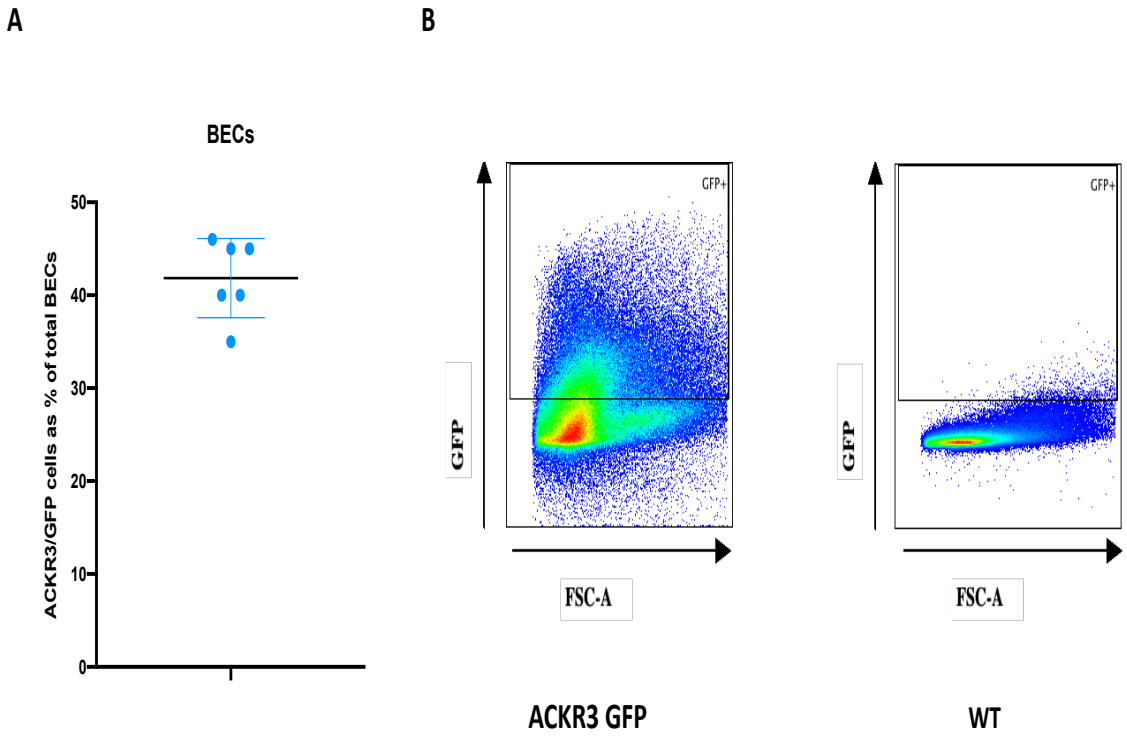

Figure 3.8 ACKR3 is expressed in blood endothelial cells in the resting lung.
A) Graph showing GFP/ACKR3 expressing blood endothelial cells, as the percentage of the total blood endothelial cells. Error bars represent the SD of the mean. B) Representative flow cytometry data plots of lymphatic endothelial cells from ACKR3 (GFP) and WT mice. One WT mouse served as a negative control for the GFP fluorescence.

The last stromal population we assessed for ACKR3 expression in the lung was lymphatic endothelial cells (LECs). As in the previous stromal cell populations, we selected live single and CD45- cells (Figure 3.9 A, B, C). Then we enriched for CD31+ and Gp38+ cells (Figure 3.9 D, E) that is a specific marker for LECs. A significant

portion of this population was ACKR3 positive LECs (Figure 3.10). More specifically, after analysing flow cytometry data from 6 GFP / ACKR3 reporter mice, we observed that 24-31 % of the total lymphatic endothelial cells express GFP/ACKR3 (Figure 3.10 A). This observation is reported in the literature, and the critical role of ACKR3 in lymphatic vessel development has been highlighted in past studies[236].

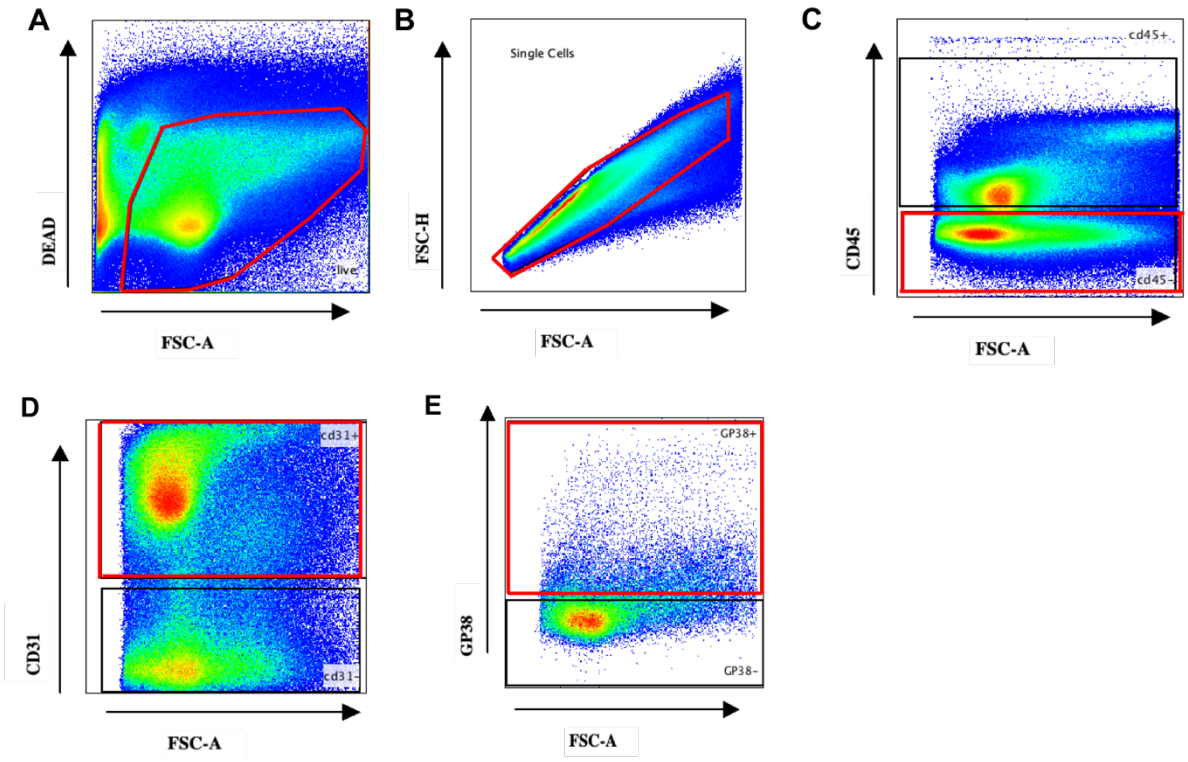

Figure 3.9 ACKR3 gating strategy in lymphatic endothelial cells in the resting lung. *Representative flow cytometry data plots of lymphatic endothelial cells in the resting lung of the ACKR3(GFP) reporter mouse. The gated populations for analysis are depicted in red colour. A) Live cells were selected, then B) single C) CD45- cells were gated for immune cell exclusion, then D) CD31+ and E) GP38+ cells were selected.*

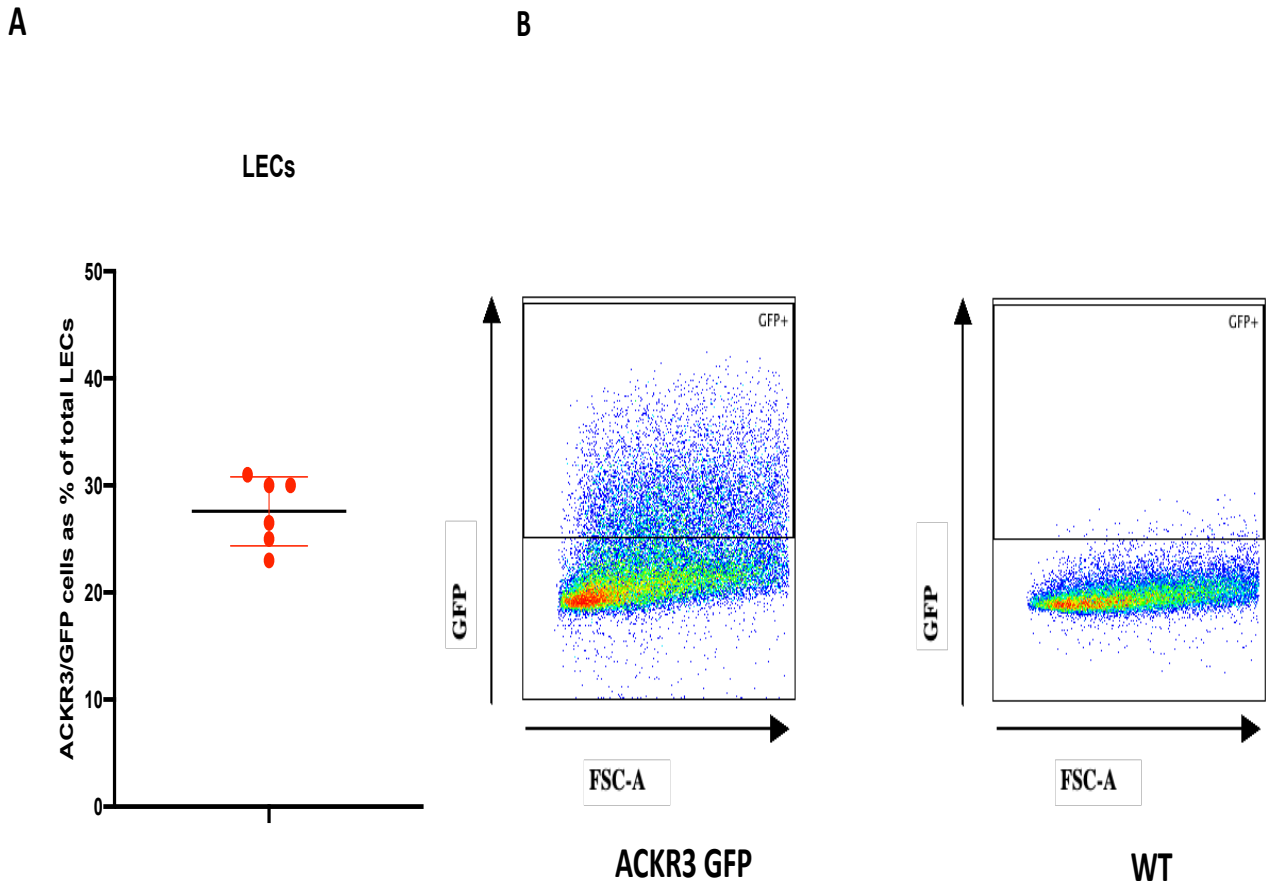

Figure 3.10 Lymphatic endothelial cells in resting lung, express ACKR3 *A) Graph showing comparative GFP/ACKR3 as a percentage of total lymphatic endothelial cells. Error bars represent the SD of the mean B) Representative flow cytometry data plots of lymphatic endothelial cells from ACKR3 (GFP) and WT mice. One WT mouse served as a negative control for the GFP fluorescence.*

Finally, we assessed GFP/ACKR3 expression in CD45- non-immune cells (Figure 3.11) and CD45+ immune cells (Figure 3.12). Data from six reporter mice revealed that ACKR3/GFP positive cells were around 14% (mean value) of the total CD45- cells (Figure 3.11A). The same analysis revealed that ACKR3/GFP positive cells were around 3.9 % (mean value) of the total CD45+ immune cells (Figure 3.12A).

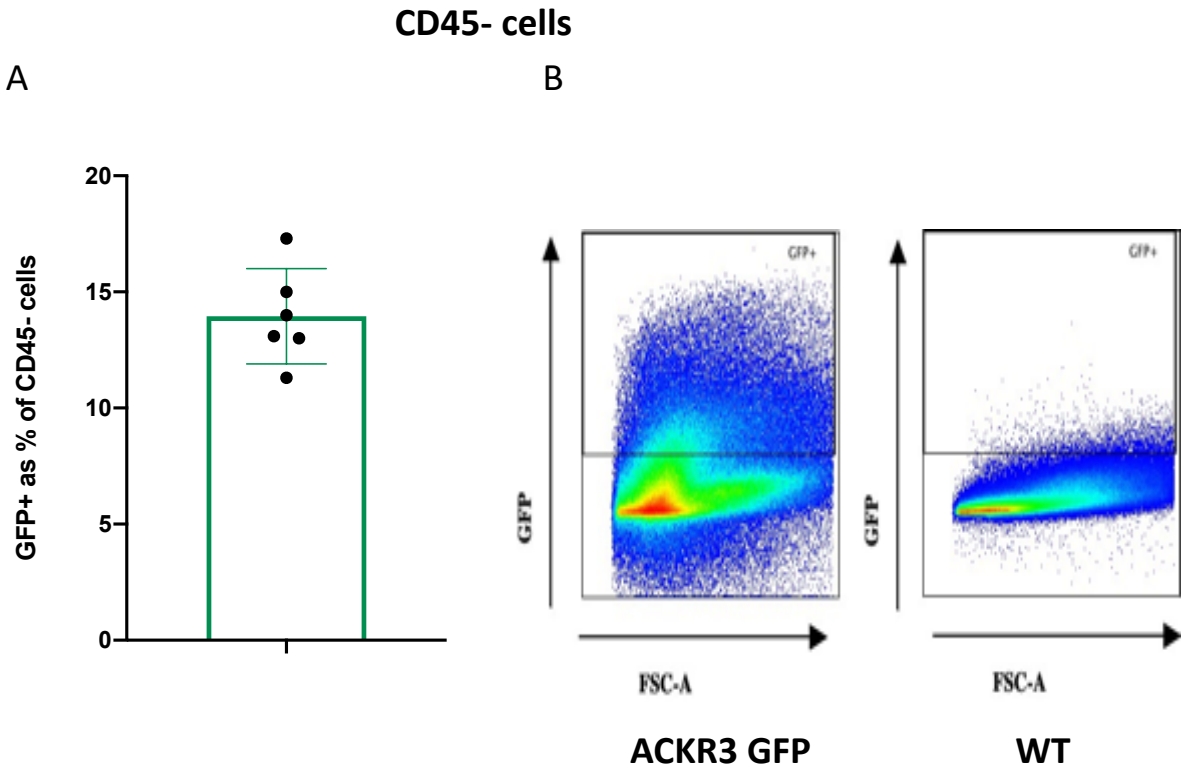

Figure 3.11 ACKR3 expression in the non-immune cells in the resting lung. *A)Graph representing the ACKR3/ GFP expressing CD45- cells from six ACKR3/GFP reporter mice. The GFP/ACKR3 expression is presented as the percentage of GFP expressing CD45- cells of the total CD45- cells in the resting lung. Error bars represent the SD of the mean. B) Representative flow cytometry data plots of CD45- cells derived from ACKR3 (GFP) and WT mice .*

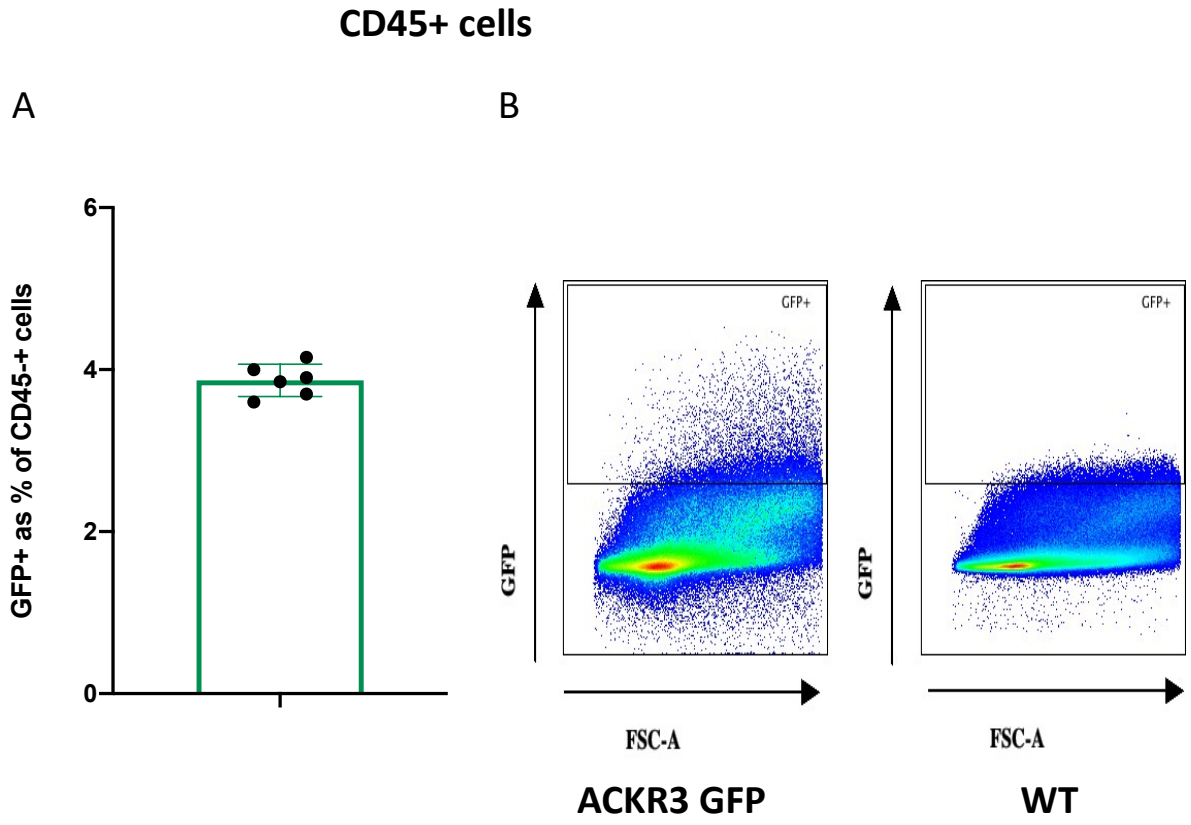

Figure 3.12 ACKR3 expression in leukocytes in the resting lung.

A) Graph representing the ACKR3/ GFP expressing leukocytes from six ACKR3/GFP reporter mice. The GFP/ACKR3 expression is presented as percentage of GFP expressing leukocytes of the total leukocytes in the resting lung. Error bars represent the SD of the mean. B) Representative flow cytometry data plots of leukocytes derived from ACKR3 (GFP) and WT mice .

3.4 Antibody validation using the ACKR3 GFP reporter mouse

As mentioned previously, one of the major challenges in ACKR3 studies, is the lack of specific anti-ACKR3 antibodies. After verifying ACKR3 expression in the stromal cell subsets in the resting lung, we attempted to assess the specificity and the efficiency of commercially available flow cytometry anti-ACKR3 antibodies. More specifically, we used two anti-ACKR3 antibodies and stained the same stromal cell populations in the lung of the ACKR3/GFP reporter mice. This approach allowed us to compare the ACKR3 antibody-stained cell populations with ACKR3/GFP fluorescent cells.

3.4.1 ACKR3 (10D1) antibody validation

First, we attempted to validate the anti ACKR3 antibody clone 10D1(BD). For this purpose, murine lung tissues from the ACKR3/GFP mice were processed as described previously (described in details in Materials and Methods, section 2.5.11) and cell isolates were permeabilised and fixed (detailed in Materials and Methods 2.5.8) before the antibody staining step. The permeabilisation/ fixation step is essential for ACKR3 detection in flow cytometry experiments since ACKR3 is known to be a constitutively internalising receptor, with only a small portion being present on the plasma membrane.

The flow cytometric comparative analyses between ACKR3 stained cells and ACKR3/GFP fluorescent cells revealed the following:

Epithelial cells: We observed that anti-ACKR3 antibody stained a small population of around 7,8% of the total epithelial cells (Figures 3.13 B and 3.14A). This observation is in contrast to what we observed with the ACKR3/ GFP expression that is negative in epithelial cells (Figures 3.13 D and 3.14 A). Furthermore, when we interrogated the ACKR3 antibody- stained cell population for GFP expression, we noticed that the ACKR3 positively -stained cells were mostly negative for GPF expression with only around 7% (median value) of these cells shown to be GFP/ACKR3 positive (Figures 3.13 C and 3.14 B). Collectively these data indicate that ACKR3 staining with the 10D1 antibody in epithelial cells was non-specific.

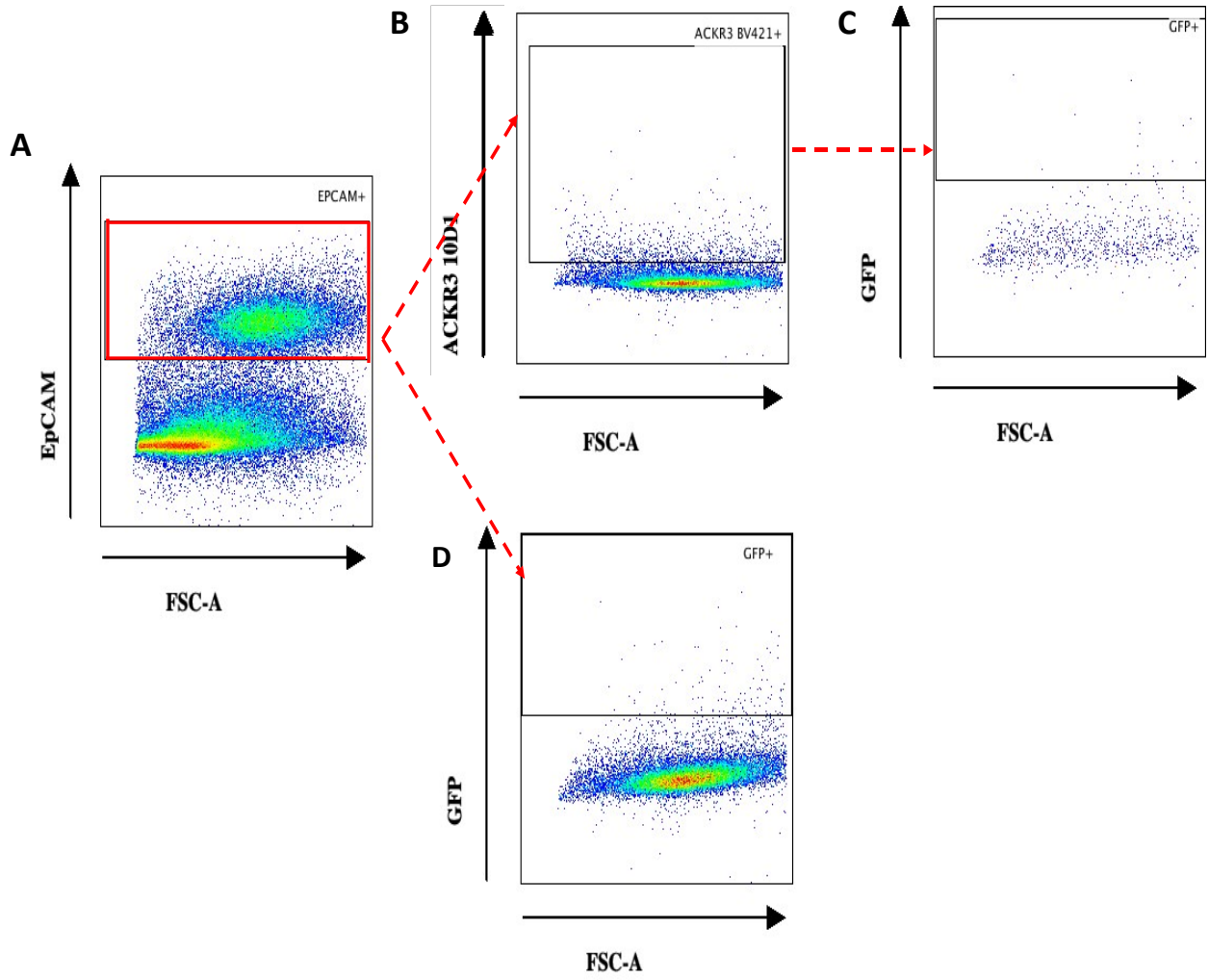

Figure 3.13 ACKR3 (10D1) antibody validation in lung epithelial cells of the ACKR3/GFP reporter mice.

Representative flow cytometry data plots of epithelial cells in the resting lung. A) Epithelial cells were positive for B) ACKR3 staining but this population was negative for C) ACKR3/GFP fluorescence. D) total epithelial cells were mostly negative for ACKR3/GFP fluorescence.

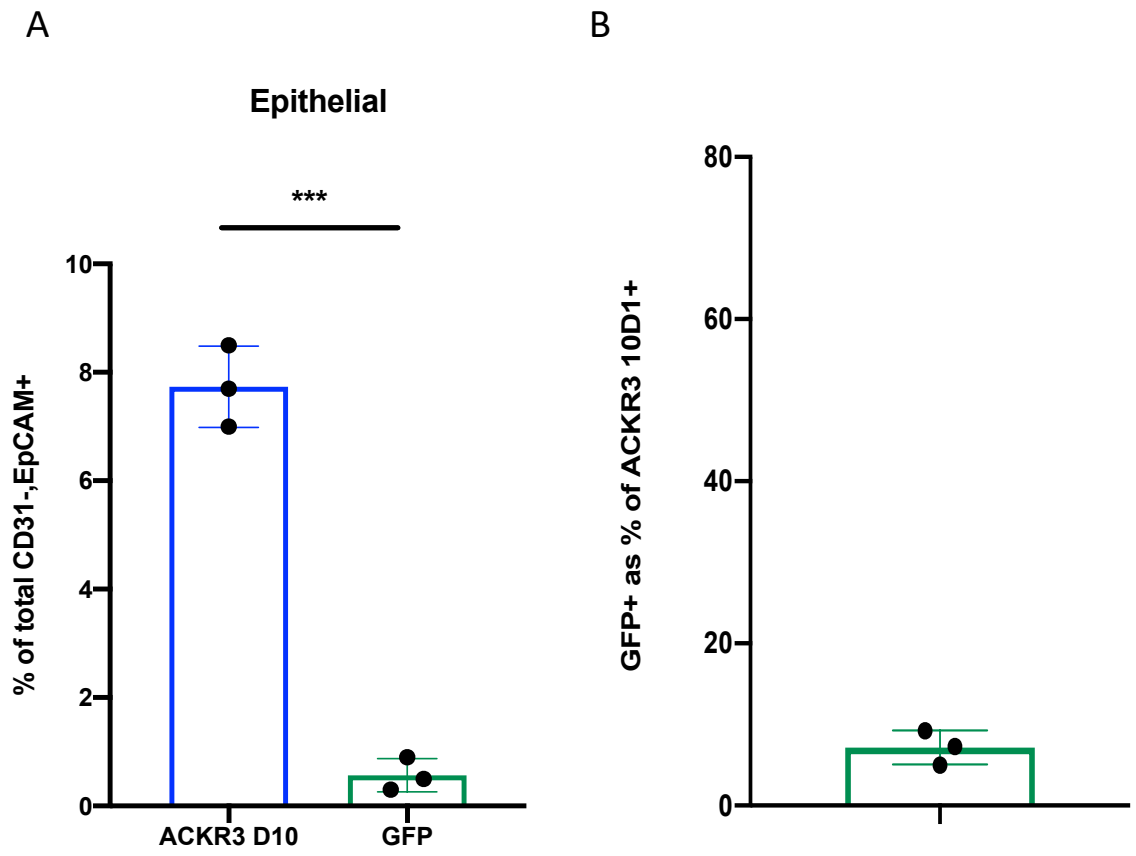

Figure 3.14 ACKR3 (10D1) antibody validation in epithelial cells of the ACKR3/GFP reporter mice.

*A) Comparison between the percentages of total epithelial cells that were positive after ACKR3 (10D1) antibody staining and ACKR3/GFP fluorescence. B) Graph representing the percentage of ACKR3(10D1) positively stained cells that were expressing GFP. An unpaired t-test was applied to the groups of ACKR3 (10D1) vs GFP samples. Statistical significance is indicated as *P≤0.05, **P≤0.01,***P≤0.001, ****P≤0.0001, ns = P>0.05.All error bars represent the SD of the mean.*

Blood endothelial cells: After staining with anti ACKR3 antibody, we observed that only a small population of the total blood endothelial cells around 10% were stained with this antibody (Figure 3.15 C). When we interrogated this population for ACKR3/GFP expression, we noticed that around 57% of these cells were expressing GFP, but there were still many GFP negative cells (Figures 3.15 D and 3.16 B). These observations are significantly different from our previous data that indicate that almost

40% of blood endothelial cells in the resting lung are GFP/ACKR3 positive (Figures 3.8 and 3.15E and 3.16A). These data suggest that ACKR3 antibody staining is significantly less efficient but also nonspecific in this cell subset.

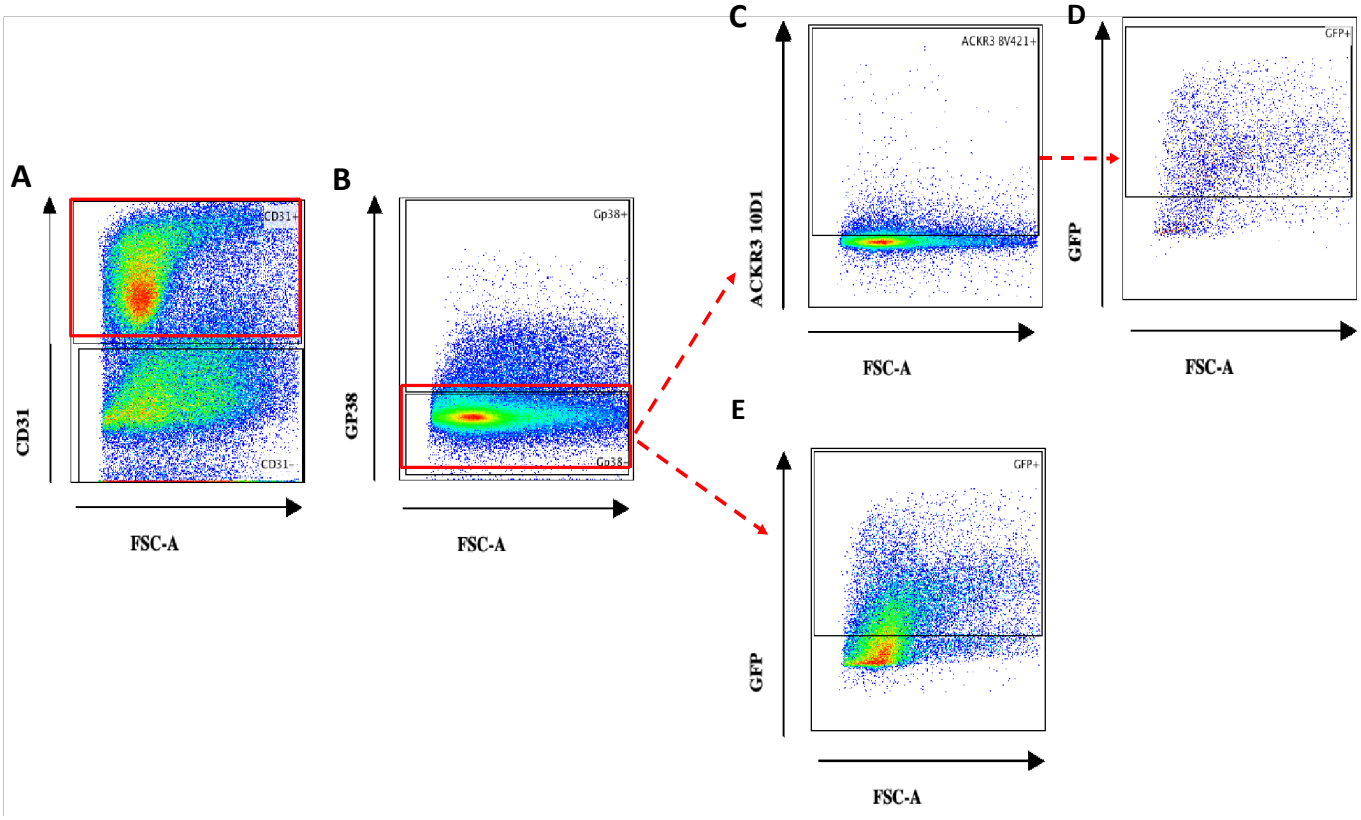

Figure 3.15 ACKR3 (10D1) antibody validation in the blood endothelial cells of the ACKR3/GFP reporter mice.

Representative flow cytometry data from blood endothelial cells in the resting lung. A,B) CD31+,Gp38- blood endothelial cells were C) positive for a small subset of cells after ACKR3 staining and this population was partially positive for D) ACKR3/GFP fluorescence. E) The total blood endothelial cell population was strongly positive for ACKR3/GFP fluorescence.

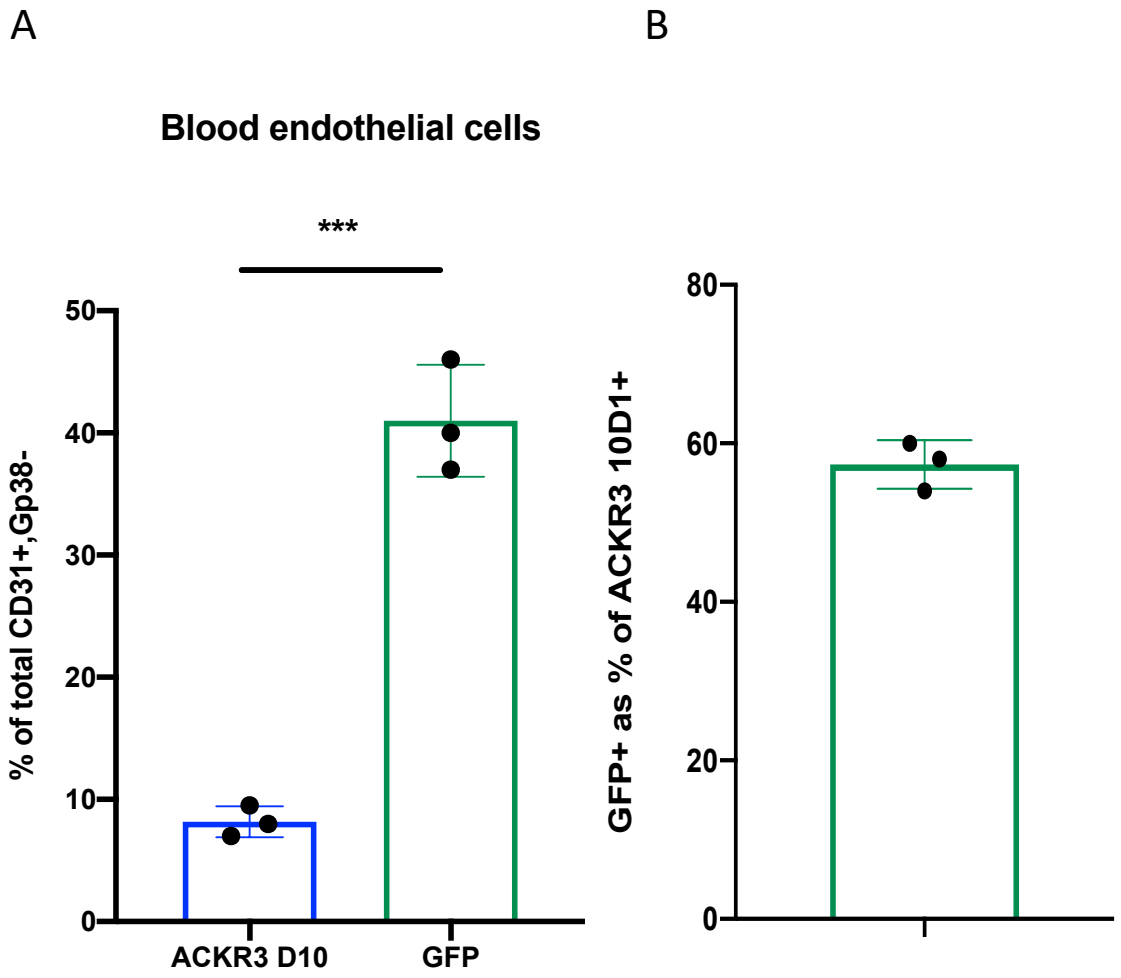

Figure 3.16 ACKR3 (10D1) antibody validation in blood endothelial cells of the ACKR3/GFP reporter mice. *A) Comparison between the percentages of total blood endothelial cells that were positive after ACKR3 (10D1) antibody staining and ACKR3/GFP fluorescence. B) Graph representing the percentage of ACKR3 (10D1) positively stained cells that were expressing GFP. An unpaired t-test was applied to the groups of ACKR3 (10D1) vs GFP cell populations. Statistical significance is indicated as: *P≤0.05, **P≤0.01,***P≤0.001, ****P≤0.0001, ns = P>0.05. All error bars represent the SD of the mean.*

Lymphatic endothelial cells: The last stromal cell population we interrogated for ACKR3 antibody staining was lymphatic endothelial cells. In this cell population, we observed that the ACKR3 antibody staining was very inefficient (Figure 3.17 C) as only around 8% of the total lymphatic endothelial cell population was positively stained. This is in contrast with the almost 30% of ACKR3/GFP expression we observed previously (Figures 3.10, 3.17E and 3.18A). Furthermore, the ACKR3 antibody positively stained population is mostly negative for GFP/ACKR3 expression since only 27% is GFP positive (Figures 3.17 D and 3.18B), a fact that indicates the antibody's non-specific binding nature.

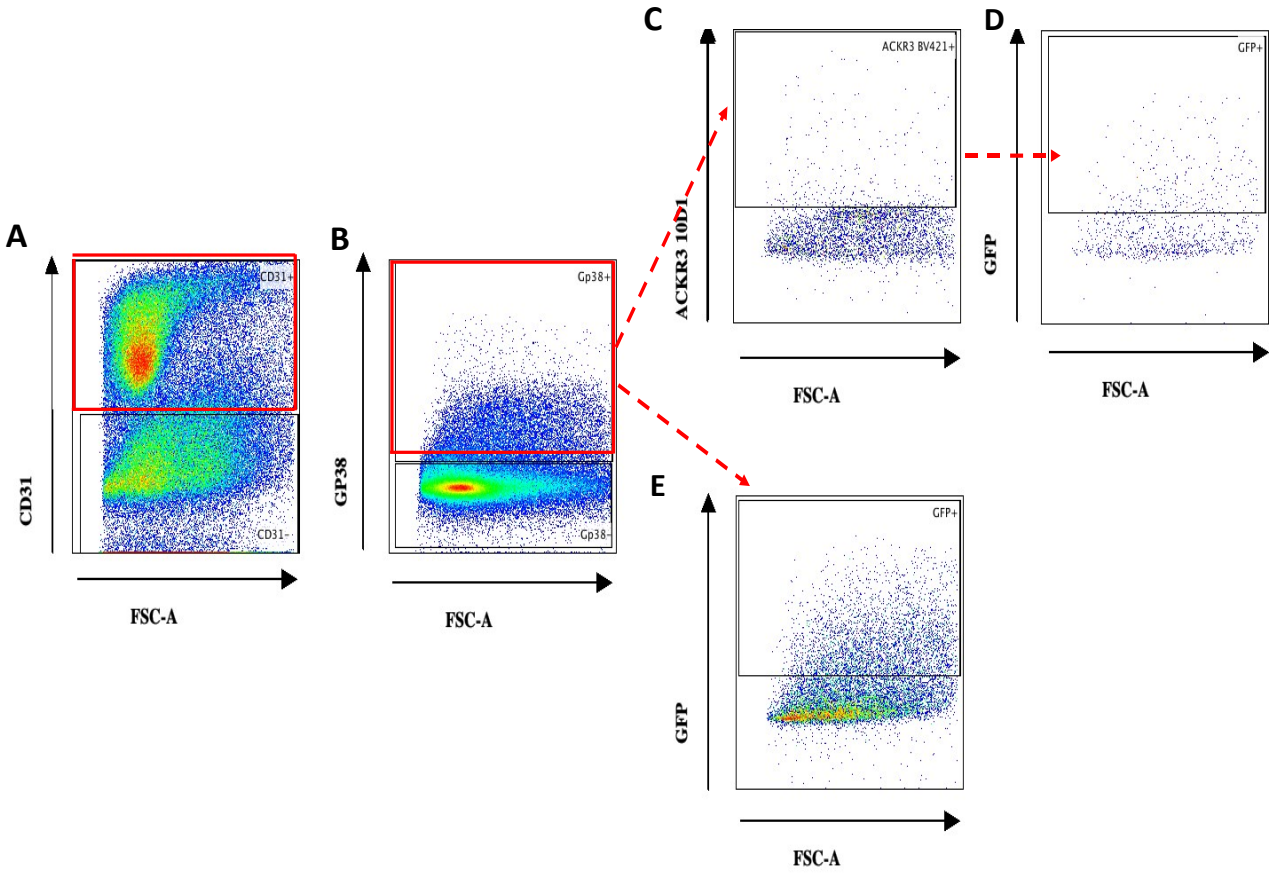

Figure 3.17 ACKR3 (10D1) antibody validation in lymphatic endothelial cells of the ACKR3/GFP reporter mice. *Representative flow cytometry data from lymphatic endothelial cells in the resting lung. A,B) CD31+,Gp38+ lymphatic endothelial cells were C) positive for a small subset of cells after ACKR3 staining and this population was partially positive for D) ACKR3/GFP fluorescence. E) The total lymphatic endothelial cell population was greatly positive for ACKR3/GFP fluorescence.*

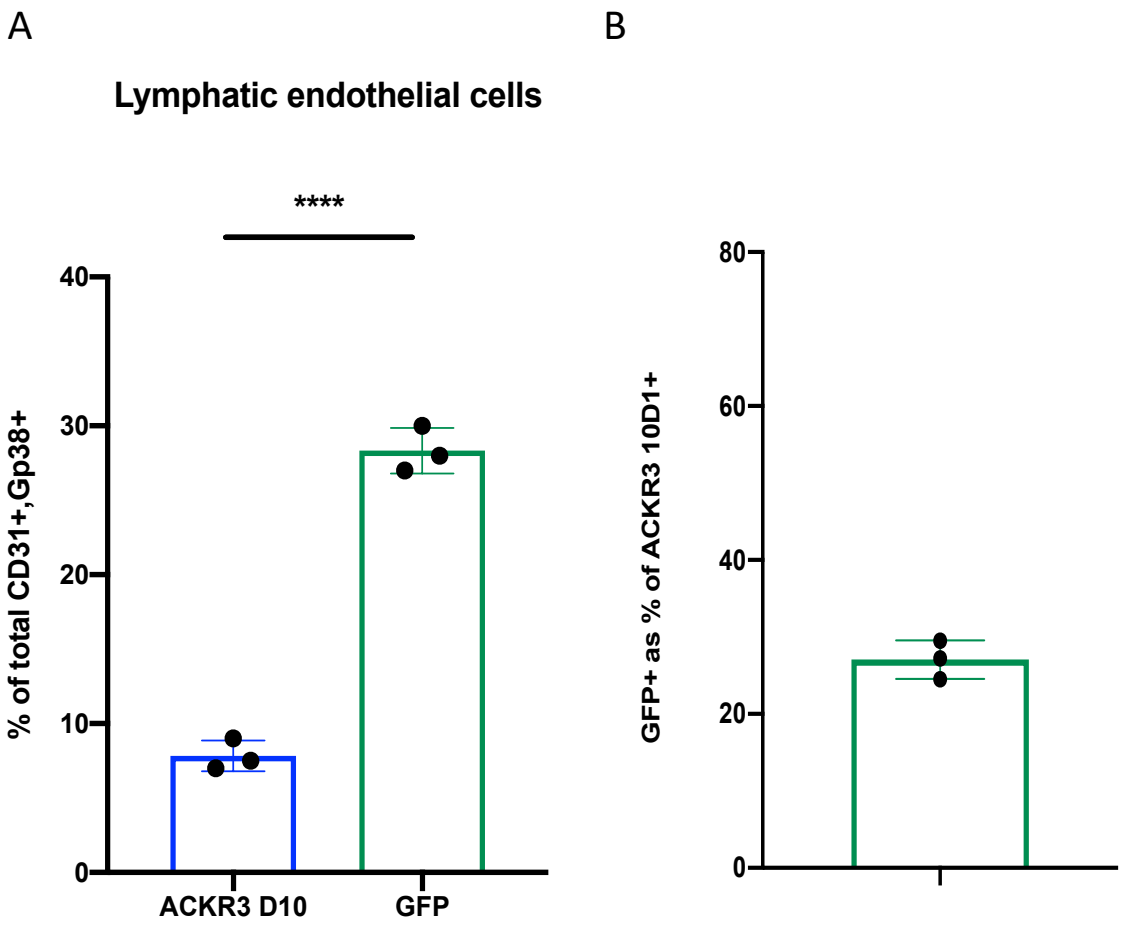

Figure 3.18 ACKR3 (10D1) antibody validation in lymphatic endothelial cells of the ACKR3/GFP reporter mice. *A) Comparison between the percentages of total epithelial cells that were positive after ACKR3 (10D1) antibody staining and ACKR3/GFP fluorescence. B) Graph representing the percentage of ACKR3 (10D1) positively stained cells that were expressing GFP. An unpaired t-test was applied to the groups of ACKR3 (10D1) vs GFP samples. Statistical significance is indicated as *P≤0.05, **P≤0.01,***P≤0.001, ****P≤0.0001, ns = P>0.05. All error bars represent the SD of the mean.*

3.4.2 ACKR3 (11G8) antibody validation

Subsequently, we followed the same approach to validate the ACKR3 antibody clone 11G8 (R&D Systems). The comparison between the ACKR3 11G8 antibody staining and GFP fluorescence in different lung stromal cell types revealed the following:
In epithelial cells (Figure 3.19) this ACKR3 antibody did not exhibit positive staining, consistent with the negative GFP fluorescence.

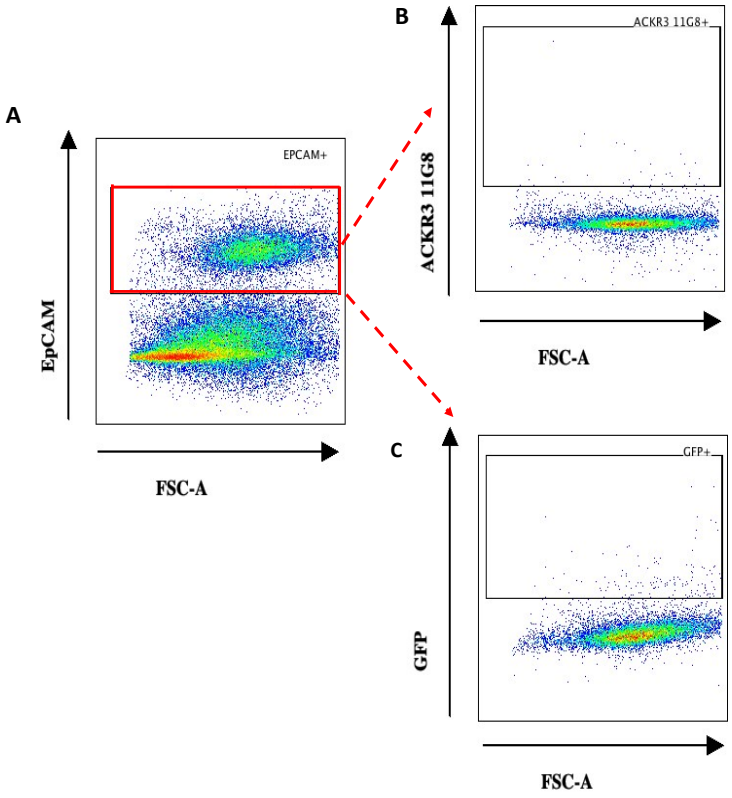

Figure 3.19 ACKR3 (11G8) antibody validation in lung epithelial cells of the ACKR3/GFP reporter mice. *Representative flow cytometry data from epithelial cells in the resting lung. A) Epithelial cells were negative for B) ACKR3 staining and total epithelial cell population was also negative for C) ACKR3/GFP fluorescence.*

In lymphatic endothelial cells (Figure 3.20), the ACKR3 11G8 antibody stained around 10% of the total lymphatic endothelial cells which is significantly lower than the 30% GFP/ACKR3 expressing lymphatic endothelial cells (Figures 3.20C and 3.21 A). Furthermore, the ACKR3 staining in this population appeared to be unspecific as only around 44% of the antibody-stained positive population was also GFP positive (Figures 3.20 D and 3.21 B). These observations suggest that ACKR3 11G8 antibody stained less efficiently, but also non-specifically, this cell population.

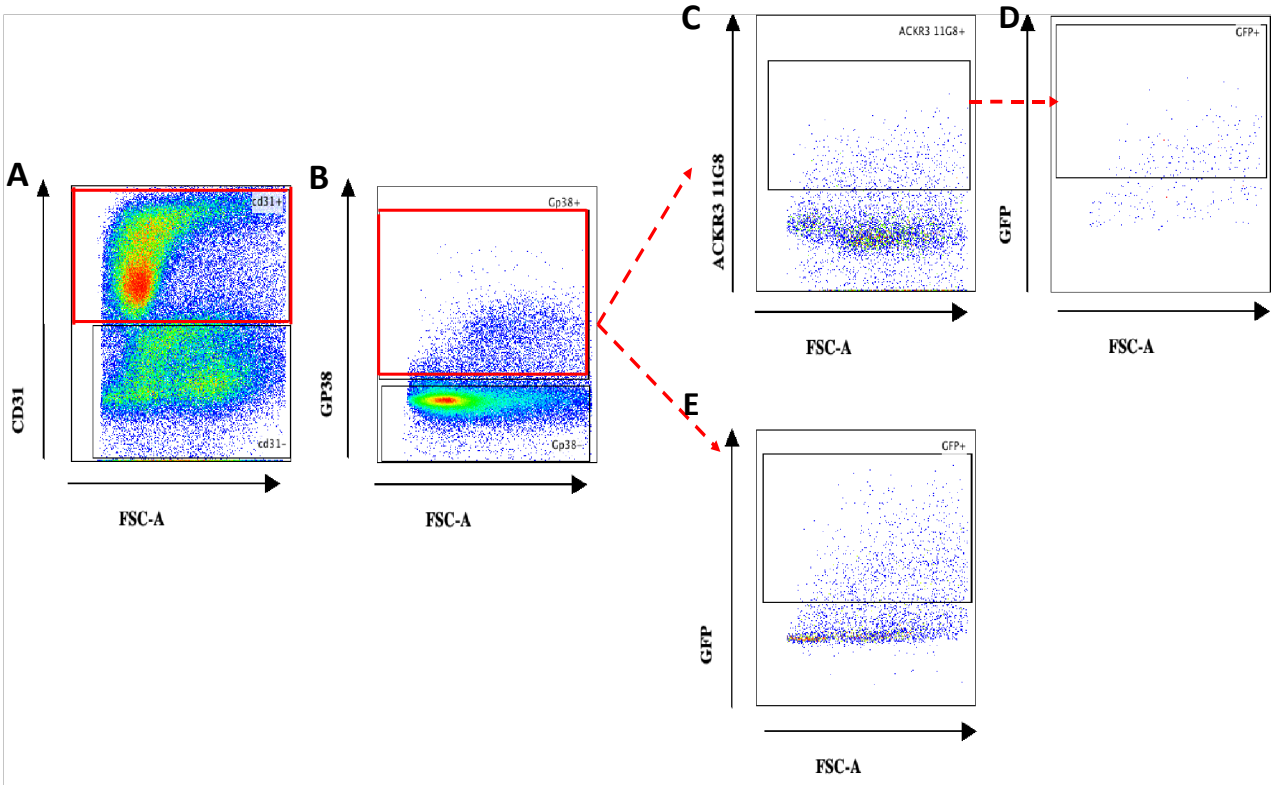

Figure 3.20 ACKR3 (11G8) antibody validation in lymphatic endothelial cells of the ACKR3/GFP reporter mice. *Representative flow cytometry data from lymphatic endothelial cells in the resting lung.*

A, B) CD31+,Gp38+ lymphatic endothelial cells were C) positive for a subset of cells after ACKR3 staining and this population was partially positive for D) ACKR3/GFP fluorescence. E) The total lymphatic endothelial cell population was greatly positive for ACKR3/GFP fluorescence.

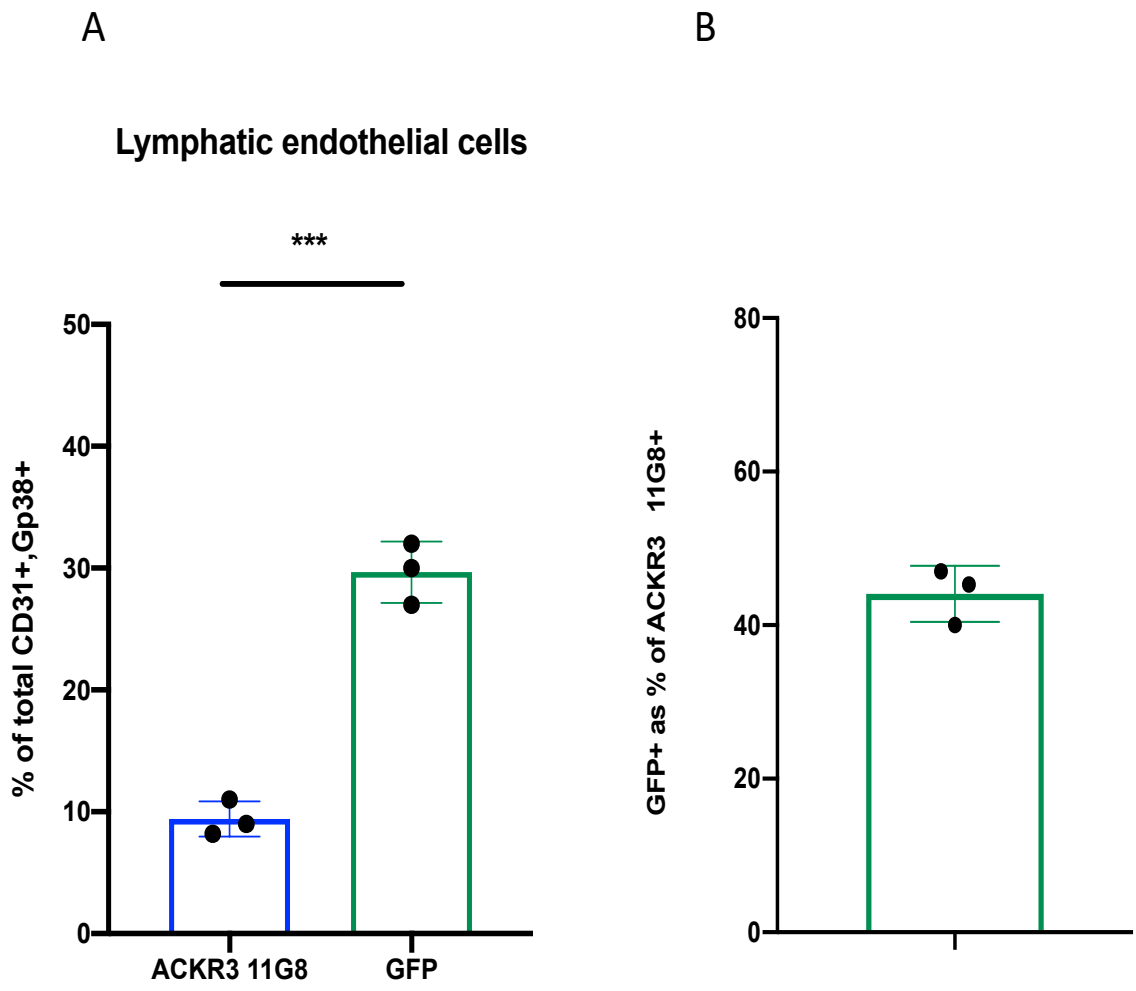

Figure 3.21 ACKR3 (11G8) antibody validation in lymphatic endothelial cells of the ACKR3/GFP reporter mice.

*A) Comparison between the percentages of total lymphatic endothelial cells that were positive after ACKR3(11G8) antibody staining and ACKR3/GFP fluorescence. B) Graph representing the percentage of ACKR3(11G8) positively stained cells that were expressing GFP. An unpaired t-test was applied to the groups of ACKR3 (11G8) vs GFP samples. Statistical significance is indicated as: *P≤0.05, **P≤0.01, ***P≤0.001, ****P≤0.0001, ns = P>0.05. All error bars represent the SD of the mean.*

In blood endothelial cells ACKR3 11G8 antibody stained only a small percentage of this cell population (Figures 3.22 C and 3.23 A) but the ACKR3 staining was also non-specific in this cell population as indicated in Figures 3.22 D and 3.23 B. More specifically, anti- ACKR3 antibody clone 11G8, stained only around 13 % of the total

blood endothelial cells compared to around 40% that was GFP/ACKR3 positive as indicated by the reporter mice (Figure 3.23 A). Furthermore, when we interrogated the anti-ACKR3 11G8 antibody-stained cell population for GFP/ACKR3 expression, we observed that around 56 % expressed GFP/ACKR3, that suggests that this antibody staining is non-specific (Figure 3.23 B).

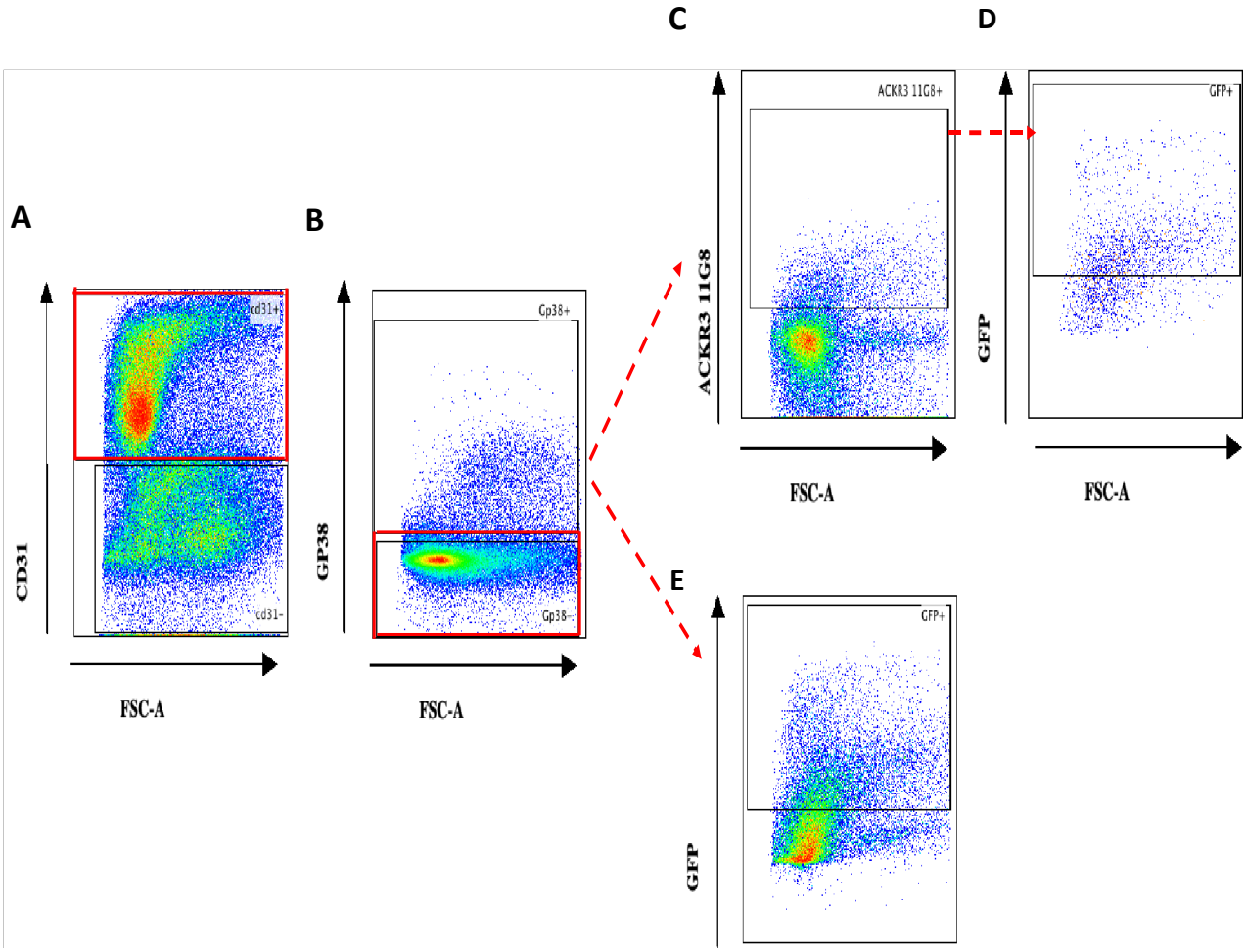

Figure 3.22 ACKR3 (11G8) antibody validation in blood endothelial cells of the ACKR3/GFP reporter mice. *Representative flow cytometry data from blood endothelial cells in the resting lung. A,B) CD31+,Gp38- lymphatic endothelial cells were C) positive for a small subset of cells after ACKR3 staining and this population was partially positive for D) ACKR3/GFP fluorescence. E) The total blood endothelial cell population was greatly positive for ACKR3/GFP fluorescence.*

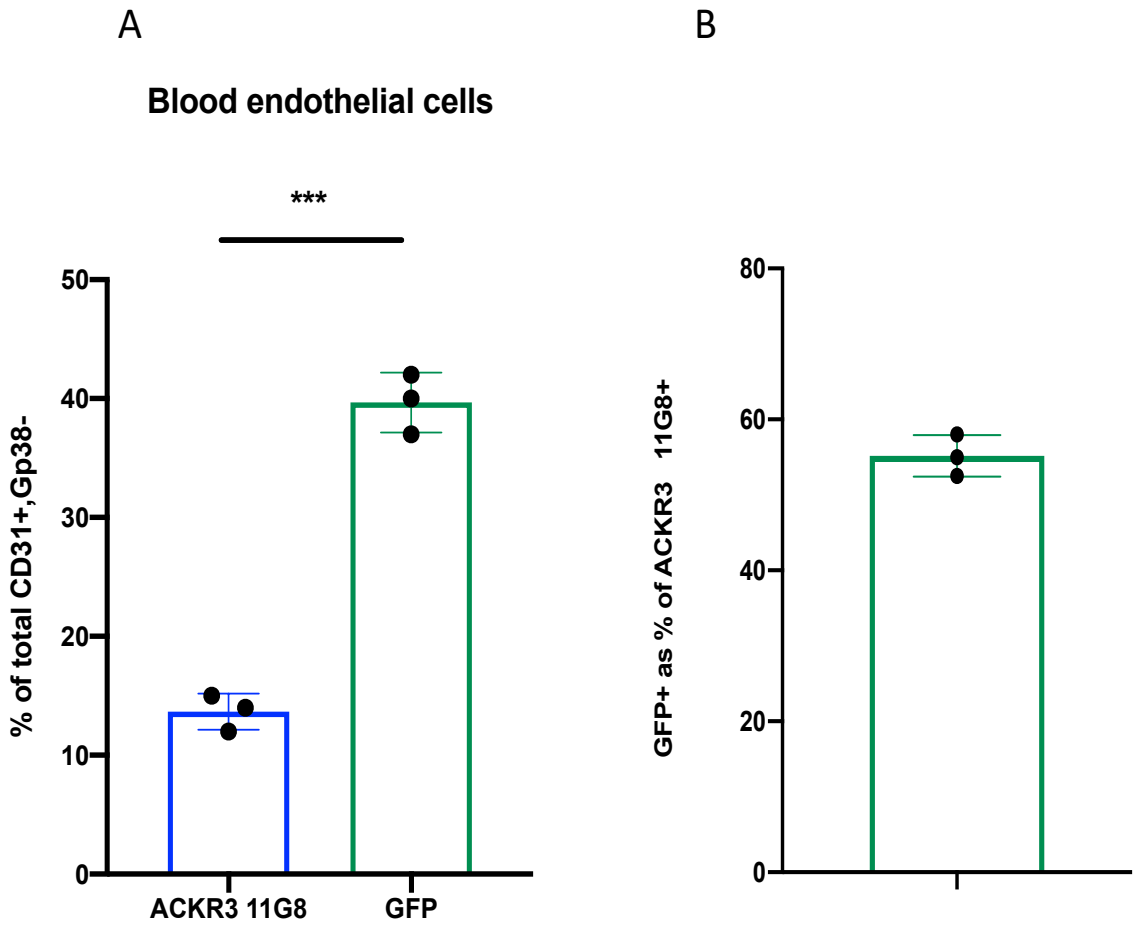

Figure 3.23 ACKR3 (11G8) antibody validation in the blood endothelial cells of the ACKR3/GFP reporter mice. *A) Comparison between the percentages of total blood endothelial cells that were positive after ACKR3(11G8) antibody staining and ACKR3/GFP fluorescence. B) Graph representing the percentage of ACKR3(11G8) positively stained cells that were expressing GFP. An unpaired t-test was applied to the groups of ACKR3(11G8) vs GFP samples. Statistical significance is indicated as: *P≤0.05, **P≤0.01,***P≤0.001, ****P≤0.0001, ns = P>0.05.All error bars represent the SD of the mean.*

3.5 Interrogation of ACKR3 expression in the resting trachea

In our next step, we tried to assess ACKR3 expression in the trachea in the same stromal cell populations that we interrogated in the resting lung. More specifically, our cell populations of interest were epithelial cells, blood endothelial cells, lymphatic endothelial cells and fibroblasts. We applied the same cell markers gating strategy (live, single cells, CD45-, CD31-, EpCAM+) in the flow cytometry data to distinguish these cell populations. The first population we analysed was the trachea epithelial cells. We observed the existence of a small population of epithelial cells in the trachea that express ACKR3. The significance of this finding needs further investigation as ACKR3 expression in the resting epithelial tissues has not been reported in the literature (Figure 3.24).

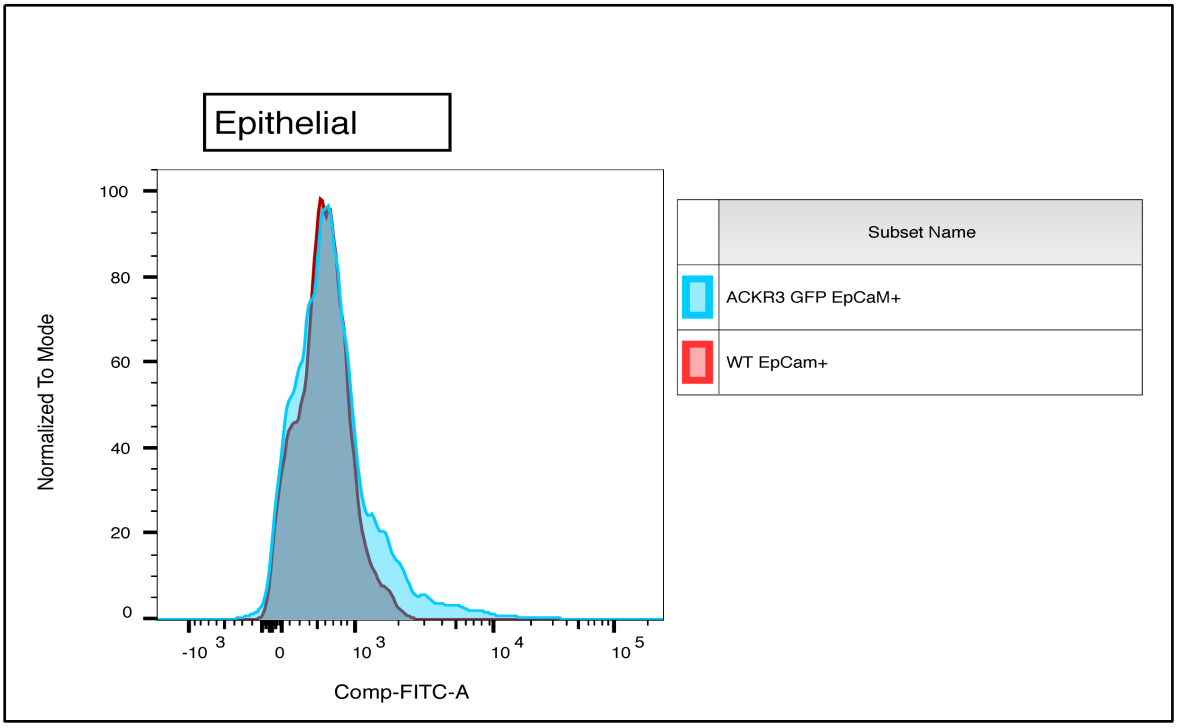

Figure 3.24 ACKR3 is expressed in epithelial cells in the resting trachea. *Single parameter histograms of flow cytometric analysis of resting trachea epithelial cells. Histogram overlay of flow cytometry data of resting trachea blood endothelial cells from WT (depicted in red colour) and ACKR3 (GFP) reporter mouse (depicted in blue colour). WT mouse served as negative control for the GFP fluorescence.*

Subsequently, we analysed the blood endothelial cell population and observed that a significant number of cells belonging to this population express ACKR3 (Figure 3.25). Although there are no previous reports about ACKR3 expression in the trachea, ACKR3 has been described to be expressed in endothelial cells in several organs and endothelial cell lines and plays an important role in endothelial cells homeostasis and angiogenic processes.

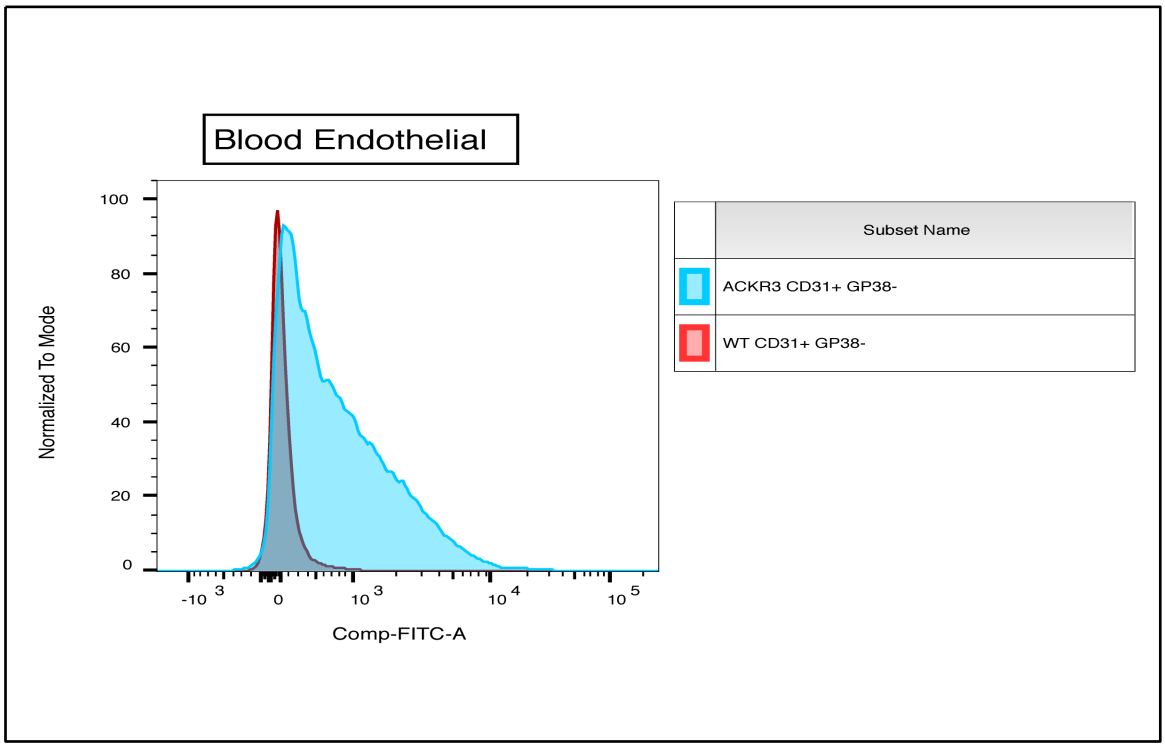

Figure 3.25 Blood endothelial cells express ACKR3 in the resting trachea*. Single parameter histograms of flow cytometric analysis of the resting trachea blood endothelial cells. Histogram of the overlay of flow cytometry data of resting tracheal blood endothelial cells from WT (depicted in red colour) and ACKR3 (GFP) reporter mouse (depicted in blue colour). WT mouse served as a negative control for the GFP fluorescence.*

The next population we analysed was lymphatic endothelial cells and we observed that a significant number of cells belonging to this population express ACKR3 (Figure 3.26). This finding is in accordance with the observation that ACKR3 is present in lymphatic endothelial cells in several tissues and primary cell isolates. The role of ACKR3 in lymphangiogenesis during embryonic development is highlighted in a recent study[236].

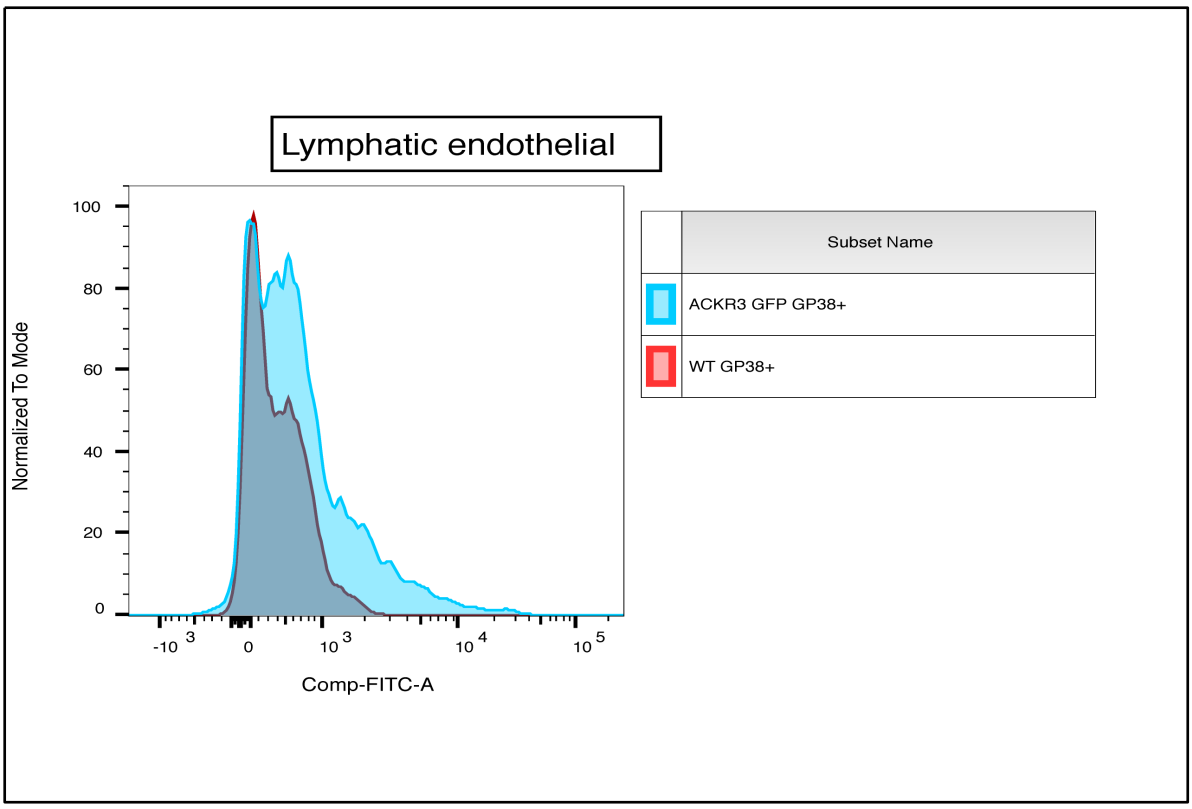

Figure 3.26 Lymphatic endothelial cells express ACKR3 in the resting trachea. *Single parameter histograms of flow cytometric analysis of the resting trachea lymphatic endothelial cells. Overlay of the ACKR3 negative cell population from WT mice (depicted in red colour) and ACKR3 (GFP) positive population from the GFP reporter mouse (depicted in blue colour). WT mouse served as a negative control for the GFP fluorescence.*

Finally, we assessed ACKR3 expression in resting tracheal fibroblasts and we also verified ACKR3 expression in this cell population (Figure 3.27). Fibroblasts are a very heterogeneous cell population and further characterisation is needed to specify the fibroblastic subpopulations that express ACKR3.

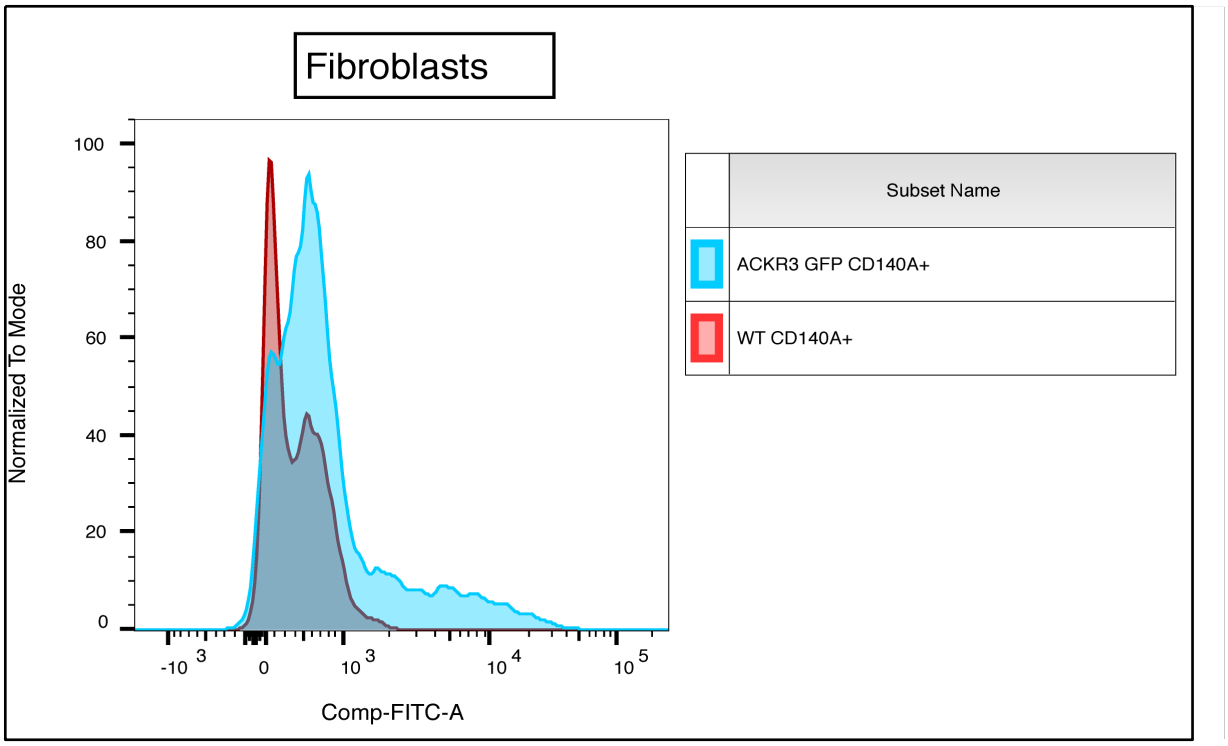

Figure 3.27 Fibroblasts express ACKR3 in resting trachea. *Single parameter histograms of flow cytometric analysis of the resting trachea fibroblasts. Overlay of the ACKR3 negative cell population from WT mice (depicted in red colour) and ACKR3 (GFP) positive population from the GFP reporter mouse (depicted in blue colour). WT mouse served as a negative control for the GFP fluorescence.*

Some of the most important caveats when working with trachea murine tissues are the limited amount of starting material and the limited viability after tissues digestion and processing for flow cytometry. More specifically, we were able to obtain live cells for flow cytometry analyses only from one mouse out of the six ACKR3/ GFP mice we processed. This suggests that our tissue digestion protocol needs further optimisation and other complimentary methods (such us immunofluorescence) should be used to assess the ACKR3 expression in murine trachea tissues.

3.6 Summary and discussion of the chapter

In this chapter, we took advantage of an ACKR3 GFP reporter mouse to interrogate ACKR3 expression in the adult resting lung and trachea. For this purpose, we employed flow cytometry to assess ACKR3 expression in four stromal cell populations: LECs, BECs, epithelial cells and fibroblasts. Our analyses revealed that a significant portion of LECs, BECs and fibroblasts in the adult resting lung and trachea, express ACKR3. According to our study, epithelial cells in the adult resting lung do not express ACKR3. Our findings in the context of previously published studies are the following:

ACKR3 expression in lymphatic endothelial cells: The role of AKCR3 in lymphatic system development has been recently described. More specifically, Klein et al. proposed that ACKR3 binds and scavenges ADM hormone and modulates ADM mediated lymphangiogenesis. In the same study, ACKR3 KO mice exhibited enhanced cardiac lymphangiogenesis. This phenotype is due to increased levels of ADM in the plasma and increased ADM-dependent lymphatic endothelial cell migration[236]. Regarding this, a similar developmental role is possible for ACKR3 in lymphatics in the lung. It is possible that ACKR3 regulates ADM signalling and lymphangiogenesis also in the lung, but this has not been investigated so far in the literature or the aforementioned study. In another study, ACKR3 has also been shown to be expressed in lymphatic endothelial cells in renal allografts. ACKR3 in lymphatic endothelial cells was increased during allograft rejection. It is possible that ACKR3 through its ligand CXCL12 is involved in lymphatic trafficking of inflammatory leukocytes in the area of rejection[293,294].

These studies suggest a similar role for ACKR3 in the lymphatic vessels in the lung. Possibly in lung inflammatory conditions, ACKR3 scavenges CXCL11, and CXCL12 thus regulating the trafficking of leukocytes expressing CXCR4, ACKR3 or CXCR3 to the sites of inflammation.

ACKR3 expression in blood endothelial cells. Regarding the expression of ACKR3 in blood endothelial cells in the lung and trachea, several studies highlight the role of ACKR3 in these cells. ACKR3 is expressed by human endothelial cells, including HUVECs (human umbilical vein endothelial cells)[295] HMVECs[296] (human microvascular endothelial cells), pulmonary microvascular endothelial cells[297], and endothelial cells within the central nervous system[298]. ACKR3 expression in blood endothelial cells has been associated with angiogenesis, proliferation and migration of endothelial progenitor cells. It has been shown that CXCL12 can induce angiogenesis through ACKR3 in primary HUVECs, and this process is Akt dependent. Similar angiogenic properties were observed after treating HUVECs with TC14012, a synthetic ACKR3 agonist[292]. In another study, it was shown that ACKR3 is expressed in human brain microvascular endothelial cells (HBMECs) and regulates endothelial cell functions such as proliferation, tube formation, migration and adhesion. Transient knockdown of ACKR3 in these cells inhibited the cells' responses after exogenous treatment with CXCL12, despite the presence of CXCR4. In a different context, using an experimental autoimmune encephalomyelitis model (EAE), for multiple sclerosis, it has been shown that ACKR3, which scavenges CXCL12, regulates leukocyte entry via endothelial barriers into the central nervous system (CNS). ACKR3 was upregulated in endothelial barriers during EAE at sites of inflammation[299].

ACKR3 expression in fibroblasts. During our analyses in chapter 3, we also observed ACKR3 expression in fibroblastic cell populations in the lung and trachea tissues. Fibroblasts are a very heterogeneous cell population. The use of more specific cell markers is necessary for the identification of the different fibroblastic subsets that express ACKR3. This characterisation will also allow us to gain a better understanding of the possible biological function of ACKR3 in these cell populations. In the literature, it has been reported that ACKR3 is endogenously expressed in Vascular Smooth Muscle Cells (VSMCs). Furthermore, stimulation of these cells with the ACKR3 ligands CXCL11 and CXCL12 led to β-arrestin recruitment but no G protein-mediated responses were detected[131].

Regarding the epithelium, we observed no expression of ACKR3 in epithelial cells in the resting lung. There are no previous reports that suggest the presence of ACKR3 in resting epithelial tissues. In one study, ACKR3 expression is upregulated in lung tissue upon LPS stimulation, a fact that implicates ACKR3 expression with inflammatory conditions is the lung epithelium. Although the authors presented gene expression real-time PCR data to assess the ACKR3 upregulation after lipopolysaccharide (LPS) treatment, they used immunofluorescence to assess ACKR3 localisation in the lung tissue. More specifically, they used a polyclonal anti ACKR3 antibody (sc-107515; Santa Cruz Biotechnology) that has not been validated for its specificity. Furthermore, taking into account the anti ACKR3 antibody validation data presented in this chapter, and general concerns about the specificity of anti ACKR3 antibodies, the findings of this study about ACKR3 expression in the lung epithelium should be considered carefully[300].

One of the major obstacles in ACKR3 studies is the lack of specific anti ACKR3 antibodies. Regarding this, we used the ACKR3/GFP reporter mouse to validate the anti ACKR3 antibody clones 10D1 and 11G8. Comparison of the ACKR3 antibody stained cell populations with the GFP fluorescence revealed that both antibodies were less efficient at staining the GFP/ACKR3 positive cells, and they also stained non-specifically in certain cell types. Our data are in agreement with the previous reports[301] about the non-specific nature of ACKR3 antibodies and explained several discrepancies in the literature about AKCR3 expression in different tissues.

CHAPTER 4

Generation of ACKR3 knock out cell lines using CRISPR/Cas technology

4. 1 Introduction and aim of the chapter

4.1.1 The CRISPR/Cas system

CRISPR stands for clustered regularly interspaced short palindromic repeat DNA sequences. CRISPR had been noticed initially as an unusual DNA repeat element in prokaryotic organisms before it was recognised as part of the bacterial immune system and subsequently it has been exploited as a genome-editing tool. The CRISPR repeats are separated by non-repeating DNA sequences in the prokaryotic genome that are called spacers. The CRISPR gene-editing technology is based on the Cas9 protein with endonuclease activity, that forms complexes with short guide RNAs that can ‘’guide’’ the Cas9 with high specificity to the DNA target region of the genome.

Cas9 nuclease is a powerful tool for genome editing, which works by inducing double-strand breaks (DSBs) at its target site, in turn stimulating two endogenous DNA damage repair pathways. The high fidelity homology-directed repair (HDR) pathway, needs a homologous template for recombination to repair DSBs. The non-homologous end-joining (NHEJ) pathway, does not require a template and frequently produces insertions or deletions (indels) as a consequence of repair. Exogenous HDR templates can be designed and introduced along with Cas9 and sgRNA to promote exact sequence alteration at a target locus; however, this process typically occurs only in dividing cells and at low efficiency[302,303].

The wild-type Cas9 enzyme makes use of two conserved nuclease domains, HNH and RuvC, to cleave DNA. A “nickase” mutant (Cas9n) can be generated by alanine substitution at crucial catalytic residues. More specifically D10A substitution inactivates the RuvC domain while N863A substitution inactivates HNH domain. A pair of nickases, appropriately spaced and oriented at the same locus, can effectively generate DSBs with high specificity and low off-target activity[304].

The main aim of this chapter was the generation of ACKR3 and CXCR4 knock out (KO) cancer cell lines to define ACKR3 involvement in cancer progression and metastatic potential. The KO cell lines generated in this chapter were used in two well-characterised and established mouse cancer models in chapter 5 to interrogate ACKR3 contribution in cancer in an in vivo setting. Regarding this, we took advantage of CRISPR/Cas9 genome editing technology to generate ACKR3 and CXCR4 knock out cell lines. For our studies, we generated two ACKR3 and CXCR4 KO B16F10 cell lines and an ACKR3 KO Lewis Lung Carcinoma (LLC) cell line. The workflow of the generation of the KO cell lines included: a) transfection of Cas9 GFP plasmid in B16F10/LLC cells, b) single-cell sorting of GFP positive cells in 96 well plates, c) clonal expansion and genomic PCR of the gene of target and d) KO validation by Sanger sequencing of the genomic PCR products (Figure 4.1).

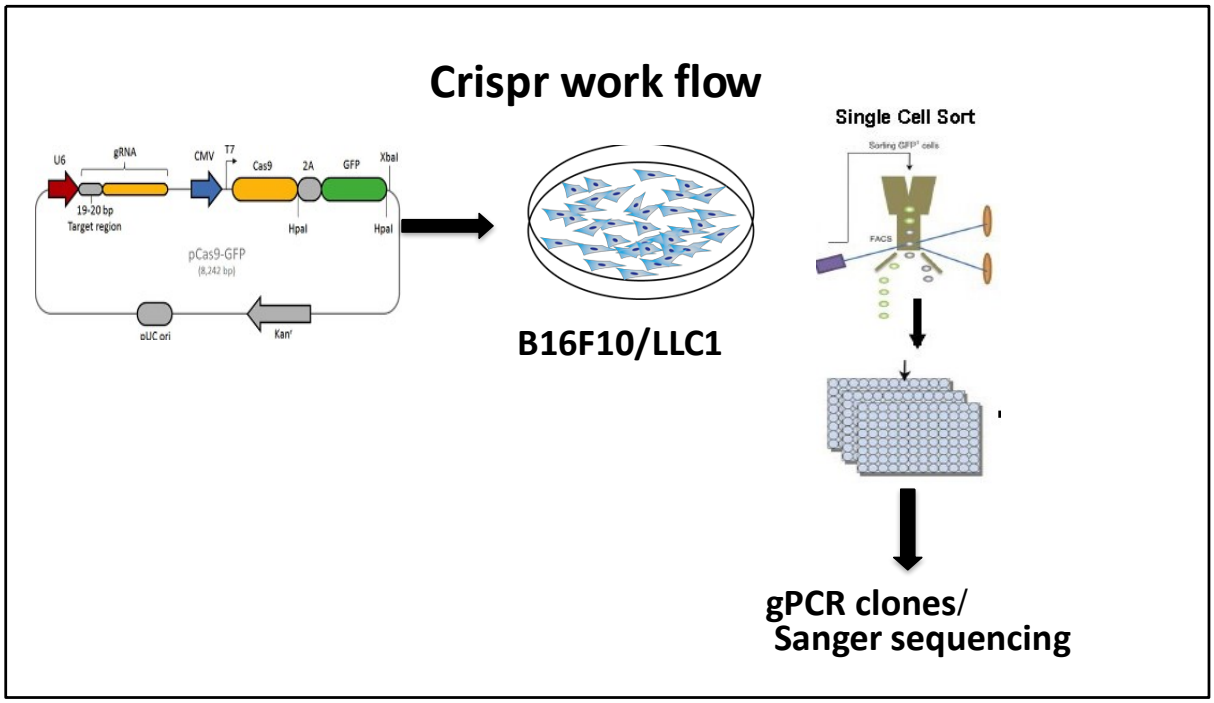

Figure 4.1 Schematic depiction of CRISPR/Cas9 workflow for the generation of KO cell lines. *The strategy included transfection of Cas9 – GFP plasmid in B16F10/ LLC cells, single-cell sorting of the GFP positive cells in 96 well plates, clonal expansion and genomic PCR/ Sanger sequencing validation of the clones.*

4.2 Generation of B16F10 ACKR3 and CXCR4 KO cell lines

For the generation on the gene KO cell lines, we employed the CRISPR/Cas9 nickase approach. This approach has the advantage that it almost eliminates the possibility of off-target effects that is one of the main disadvantages associated with the wild type Cas9 nuclease. CRISPR/Cas9 nickase mutants introduce single-strand breaks in DNA (nicks) instead of the double-strand breaks created by wild type Cas enzymes. In order for the nickase endonucleases to create a double-strand break, the two pairs of gRNAs that target opposite strands of the DNA need to be in close proximity (less than 20 base pairs). These double nicks create a double-strand break (DSB) that is repaired using the error-prone non-homologous end joining (NHEJ) DNA repair pathway (Figure 4.2). One of the main disadvantages of using the Cas9 nickases approach is the reduced efficiency in generating DSB.

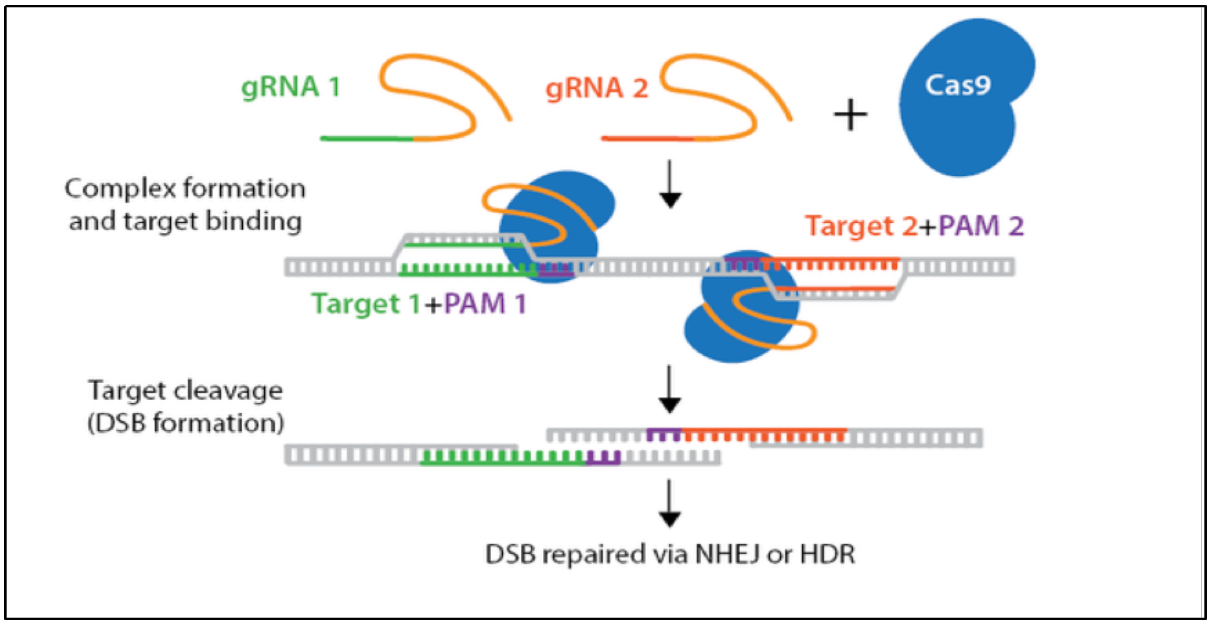

Figure 4.2 Schematic depiction of the CRISPR/ Cas9 nickase mechanism of action *Cas9 nickase proteins forms different complexes with two gRNAS (gRNA1 and gRNA2) that can bind to adjacent genomic target regions (Target 1 and 2) preceding the Cas9 recognition sequences PAM1 and 2. The nickase/gRNA complexes after binding the DNA create double-strand breaks (DBS) that can be repaired using the error-prone non-homologous end joining (NHEJ) or the high fidelity homology-directed repair (HDR) mechanism (source Addgene).*

To design the guide RNAs, we used the crispr.mit.edu web tool designer (the sequences of mouse ACKR3 and mouse CXCR4 guides and plasmids generated for this study are presented in Appendices section). For every KO, a pair of nickases are needed, so a pair of guide RNAs were designed for each gene KO (Figures 4.3 and 4.4). These 20 bp long guide RNAs were cloned into the pSpCas9n(BB)-2A- GFP plasmid vector (PX461 Addgene) that includes as a selection marker the GFP protein that is attached to the C terminal of the Cas9 nickase protein. The GFP tag allows the selection of GFP positive cells by flow cytometry.

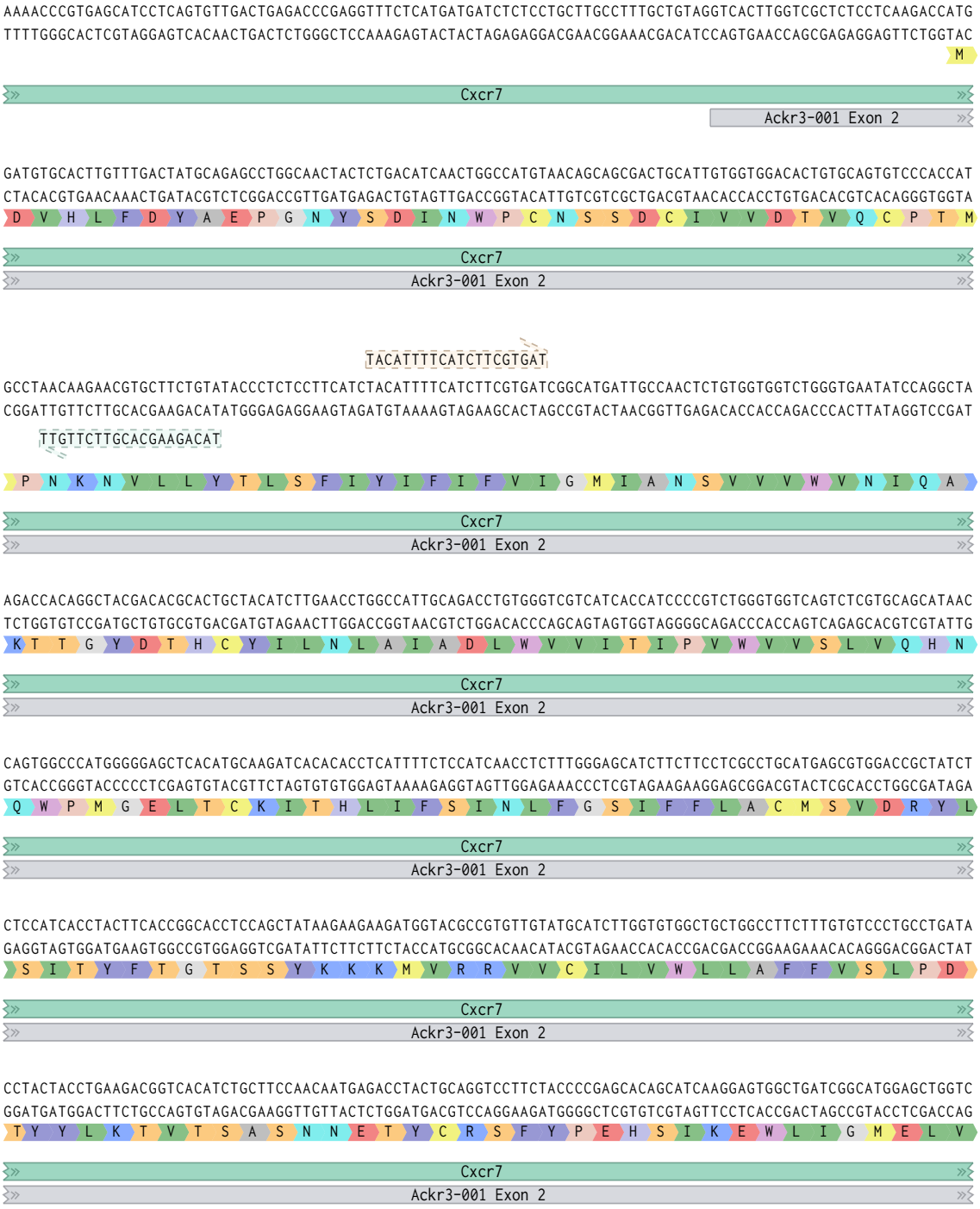

Figure 4.3 Representative image that illustrates the location that the pair of guides RNAs aligns to the exon 2 of the mouse ACKR3 gene. *The pair of guide RNAs bind in close proximity to each other and guide the Cas9 nickase protein to generate a double-strand break that can lead to gene disruption. ACKR3 protein amino acids that are encoded by their respective codons are depicted in different colours.*

Figure 4.4 Representative image that illustrates the location that the pair of guide RNAs aligns to the exon 2 of the mouse CXCR4 gene. *The pair of guide RNAs bind in close proximity to each other and guide the Cas9 nickase protein to generate a double-strand break that can lead to gene disruption. CXCR4 protein amino acids that are encoded by their respective codons are depicted in different colours.*

After verifying the successful cloning of gRNAs through Sanger sequencing, we tried to optimise the best transfection conditions for efficient delivery and expression of the CAS9 GFP plasmid into our cell of interest. To this end, we transfected B16F10 cells when they reached 60-70% confluency, using Lipofectamine 2000 since it has been described in the literature as effective in transfection of these cells. We harvested the cells at two different time points: six hours and overnight (16 hours) but also using different Lipofectamine/plasmid DNA ratios.

Subsequently, to assess the transfection efficiency, cells were analysed for GFP fluorescence using flow cytometry. Briefly, live cells were selected (Figure 4.5 A), we enriched for single cells (doublet cell discrimination) (Figure 4.5 B), and the different transfection conditions were evaluated according to GFP fluorescence (Figure 4.5 C). We noticed that there was not a significant difference in the transfection efficiencies under different conditions, with the only exception being the 3:1 ratio after 6 hours which exhibited the lowest efficiency (Figure 4.5 C, D). More specifically, after 6 hours the 3:1 ratio lead to transfection efficiency of 26.90%, the 4:1 lead to 37.60%, the 5:1 to 38.80% and the 6:1 to 45.30% respectively. The transfection efficiencies after overnight incubation for the same DNA/ Lipofectamine ratios were 37.60%, 38.90%, 40.70% and 41.60% (Figure 4.5 D).

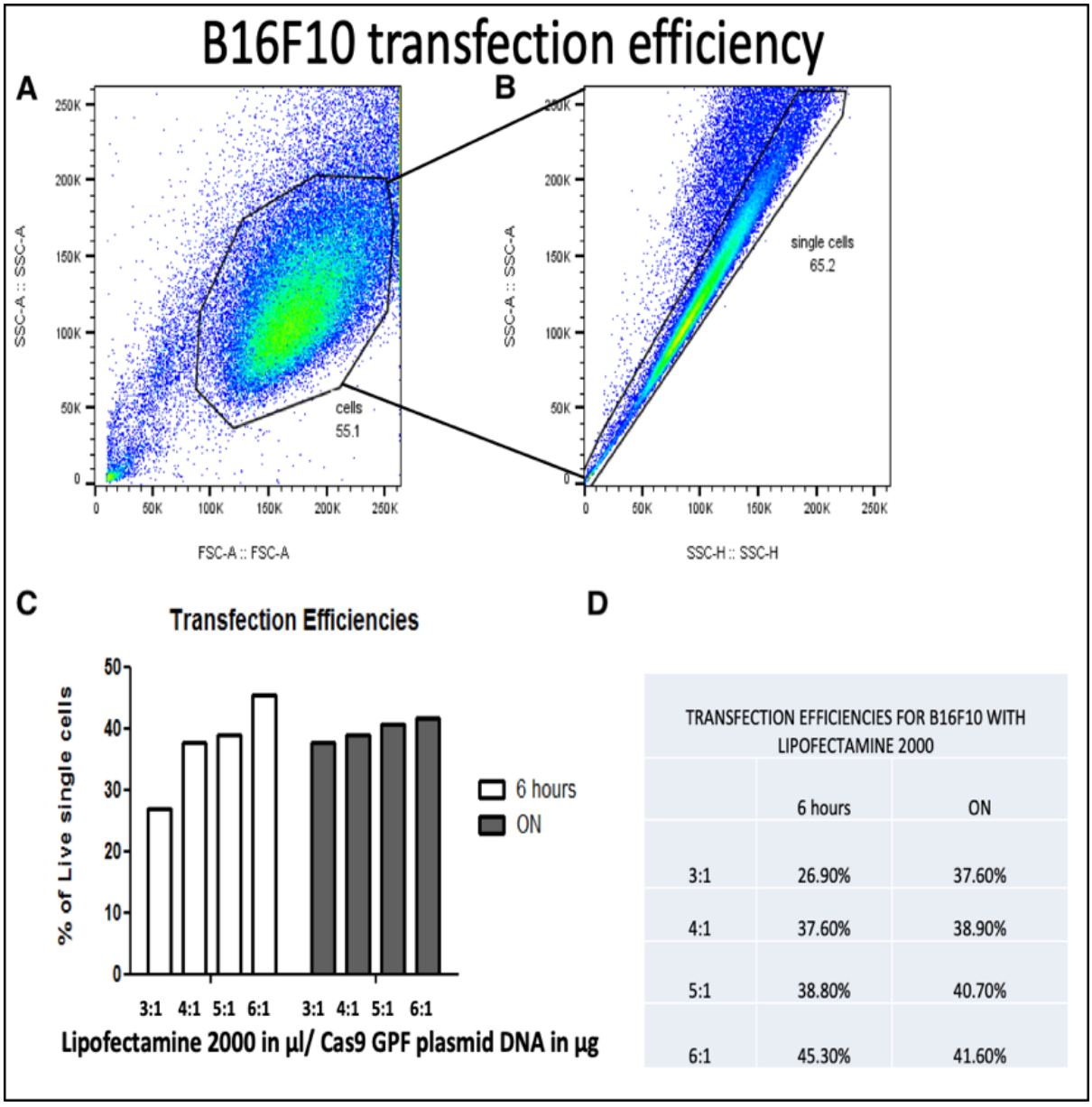

TRANSFECTION EFFICIENCIES FOR B16F10 WITH LIPOFECTAMINE 2000

	6 hours	ON
3:1	26.90%	37.60%
4:1	37.60%	38.90%
5:1	38.80%	40.70%
6:1	45.30%	41.60%

Figure 4.5 Flow cytometry-based assessment of transfection efficiency in B16F10 cells. *A) B16F10 live B) single cells were selected for the analysis. C,D) Different ratios of Lipofectamine 2000 / Cas9 GFP plasmid DNA were evaluated for transfection efficiency (GFP positivity) after 6 hours and overnight incubation(16 hours).*

4.3 B16F10 single-cell sorting of KO cells lines

Regarding the aforementioned, we decided to use the 4:1 Lipofectamine/ DNA ratio and incubate the cells overnight with the transfection mixture. The next day we single-cell sorted the cells in a 96-flat bottom well plate. Appropriate controls were included for setting the GFP positivity during sorting. More specifically, we included two control conditions for the B16F10 cells: untransfected and mock-transfected to assess the GFP autofluorescence.

Subsequently, we set the GFP positive gates during sorting. Then we single-cell sorted cells that belonged to the GFP positive population, excluding the top 10% of the brightest population, as this cell population usually exhibits lower survival rates after sorting. Cells were sorted in flat bottom 96 well plates containing DMEM + 20% FBS without antibiotics (the presence of antibiotics usually decrease cell survival after single-cell sorting) (Figure 4.6). We noticed that almost 54% of the transfected cells were GFP positive (Figure 4.6C).

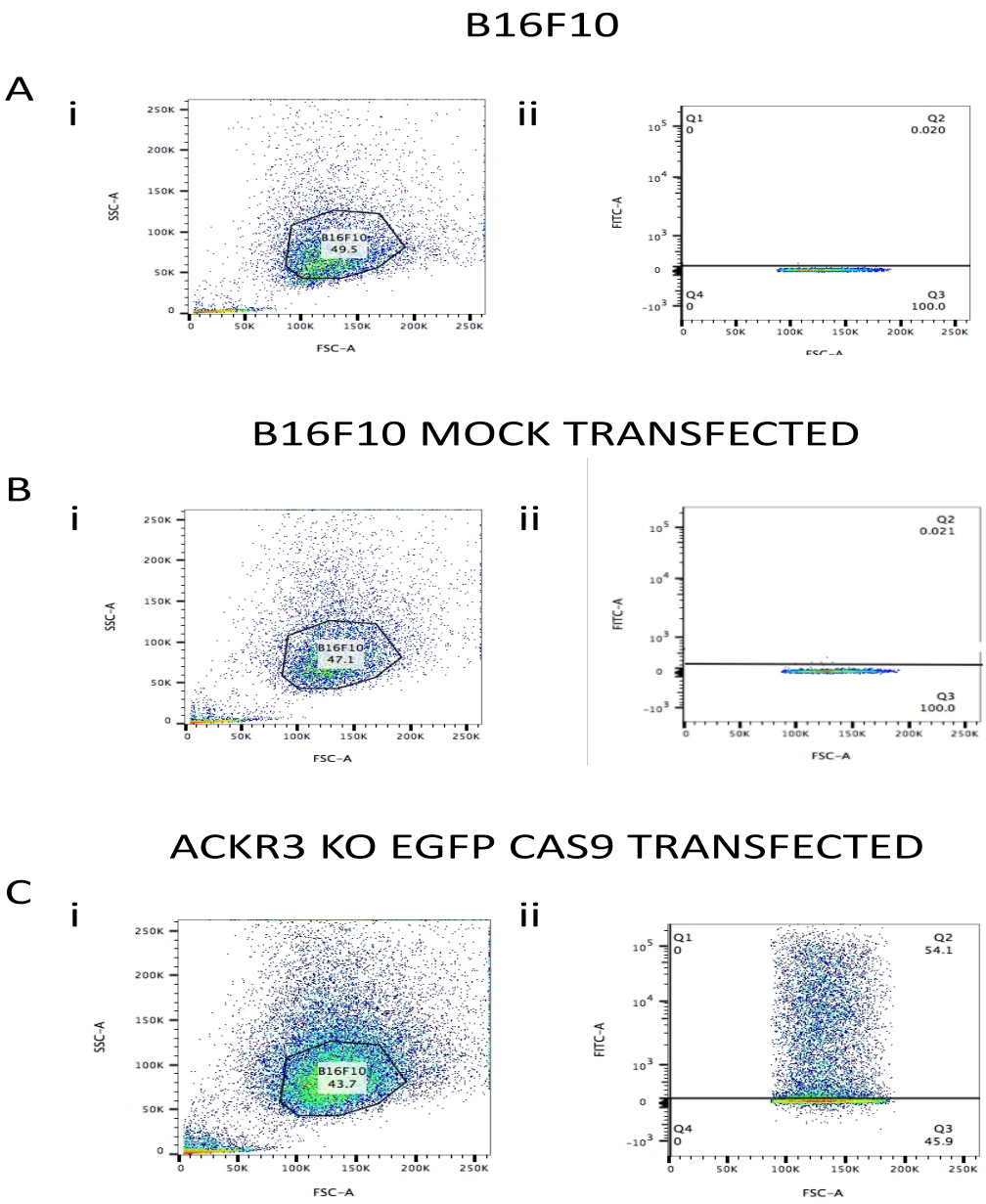

Figure 4.6 Flow cytometry plots from single-cell sorting of B16F10 ACKR3/CXCR7 KO cells. *Cells were sorted 24 hours post-transfection. A) untransfected control i) B16F10 live cells were selected ii) gates were set to determine FITCH/GFP positivity B) mock-transfected control i) B16F10 live cells were selected and ii) gates were set to determine FITCH/GFP positivity. C) ACKR3 EGFP CAS9 transfected cells i) live cells were selected ii) FITCH/GFP positive cells were selected.*

4.4 Clonal expansion and evaluation of the clones

After single-cell sorting, the clones were incubated and allowed to expand until they reached 80-90% confluency. For the B16F10 cell line, this occurred after two weeks. During the expansion period, the medium was replaced every 3-4 days. When the cells reached the desired confluency, one third of the cells from each well was passaged to retain the clones until KO verification and the remaining two-thirds were used for genomic DNA extraction (detailed in Materials and Methods, section 2.4.5) and genomic PCR products were analysed in a 2% agarose gel electrophoresis (Figures 4.7 and 4.8). The analysis of the genomic PCR products was essential in order be able to identify possible KO clones by observing the band pattern and comparing it with the wt control PCR bands. This is an efficient alternative approach in cases in which there are not good antibodies available to allow for the identification of the gene KO clones at the protein level.

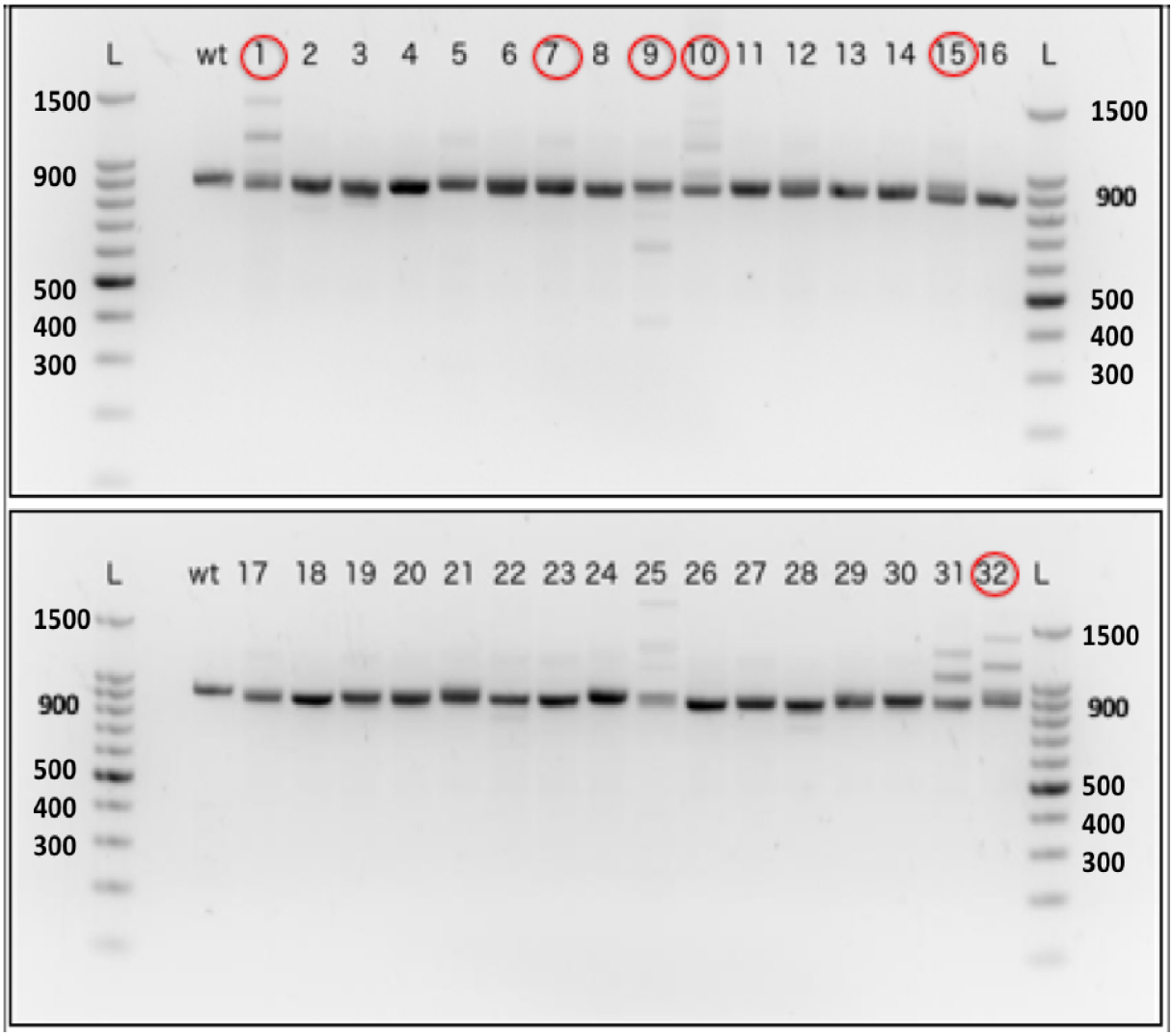

Figure 4.7 Representative images of genomic PCR products of B16F10 CXCR4 KO clones. *The first and the last lanes were loaded with DNA ladder 100bp(L). Clones in which the genomic PCR products were different in size than the wt were selected for further analyses. These differences in PCR products size are an indication of INDELs (insertions/ deletions) that occurred after Cas9 cut the genomic DNA. Circled in red are some of the clones that were chosen for further analyses. Control PCR product from Wild type (wt) B16F10 cells was also included to allow comparison.*

We compared the size of the DNA band with the DNA band from the wild type PCR product, but also, selected for further analyses clones that had a different number of bands than the wt. The differences in the size of the PCR products are a good indication that Cas9 cut the genomic DNA, and random insertions/deletions (INDELs) occurred. The existence of more than one band in the same clone is a strong indication of heterozygosity. For example, in the same clone, maybe one allele has a deletion while the other has an insertion or is wt. Furthermore, in biallelic KO clones we mostly observed that the gene alleles exhibited different alterations, for example, ACKR3 KO clones 14 and 15, maybe one allele had one small deletion and the other a large insertion. Despite these observations, we expect that KO clones will exhibit the same phenotype in our *in vivo* models in chapter 5. Heterozygous KO clones (1 KO allele and 1 wt) were not tested *in vivo*.

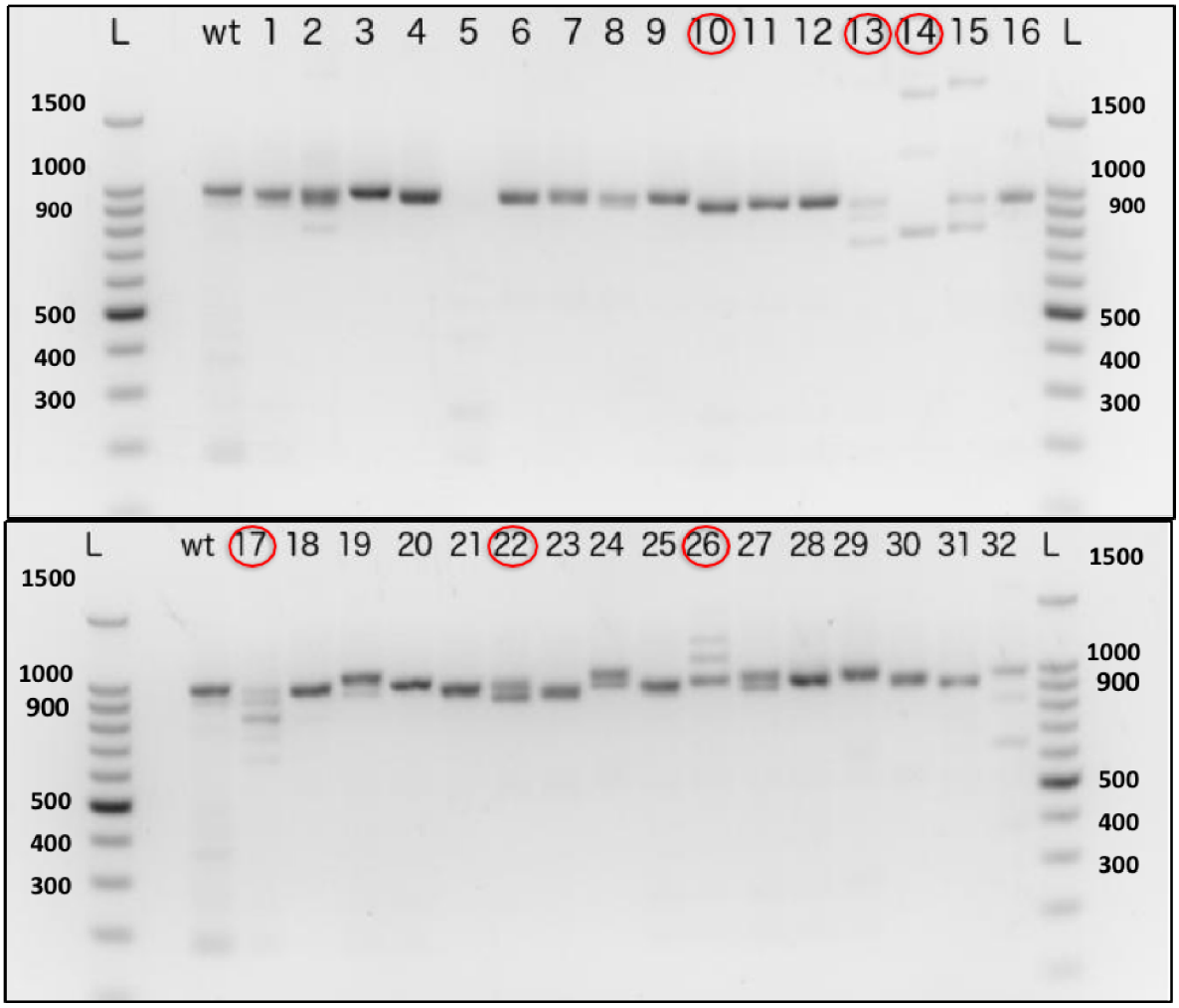

Figure 4.8 Representative images of genomic PCR products of B16F10 ACKR3 KO clones. *The first and the last lanes were loaded with DNA ladder 100 base pair(L). Wild type (wt) control PCR product was also included to allow comparison. Clones in which the genomic PCR products were different in size than the wt PCR were selected for further analyses. These differences in PCR products size are an indication of INDELs (insertions/ deletions) that occurred after Cas9 cut the genomic DNA. The existence of more than one band in the same clone is a strong indication of heterozygosity. Circled in red are some of the clones that were chosen for further analyses.*

4.5 Generation of LLC ACKR3 KO cell lines

Following the same approach, we generated LLC ACKR3 KO cells. We used the already validated in the literature, 4:1 lipofectamine/DNA ratio for the GFP Cas9 transfection and incubated the cells overnight. The following day the cells were single cell sorted in flat bottom 96 well plates. Untransfected and mock-transfected cells were included as controls to determine background fluorescence (Figure 4.9). Almost 17% of the cells were Fitch/ GFP positive (Figure 4.9 D).

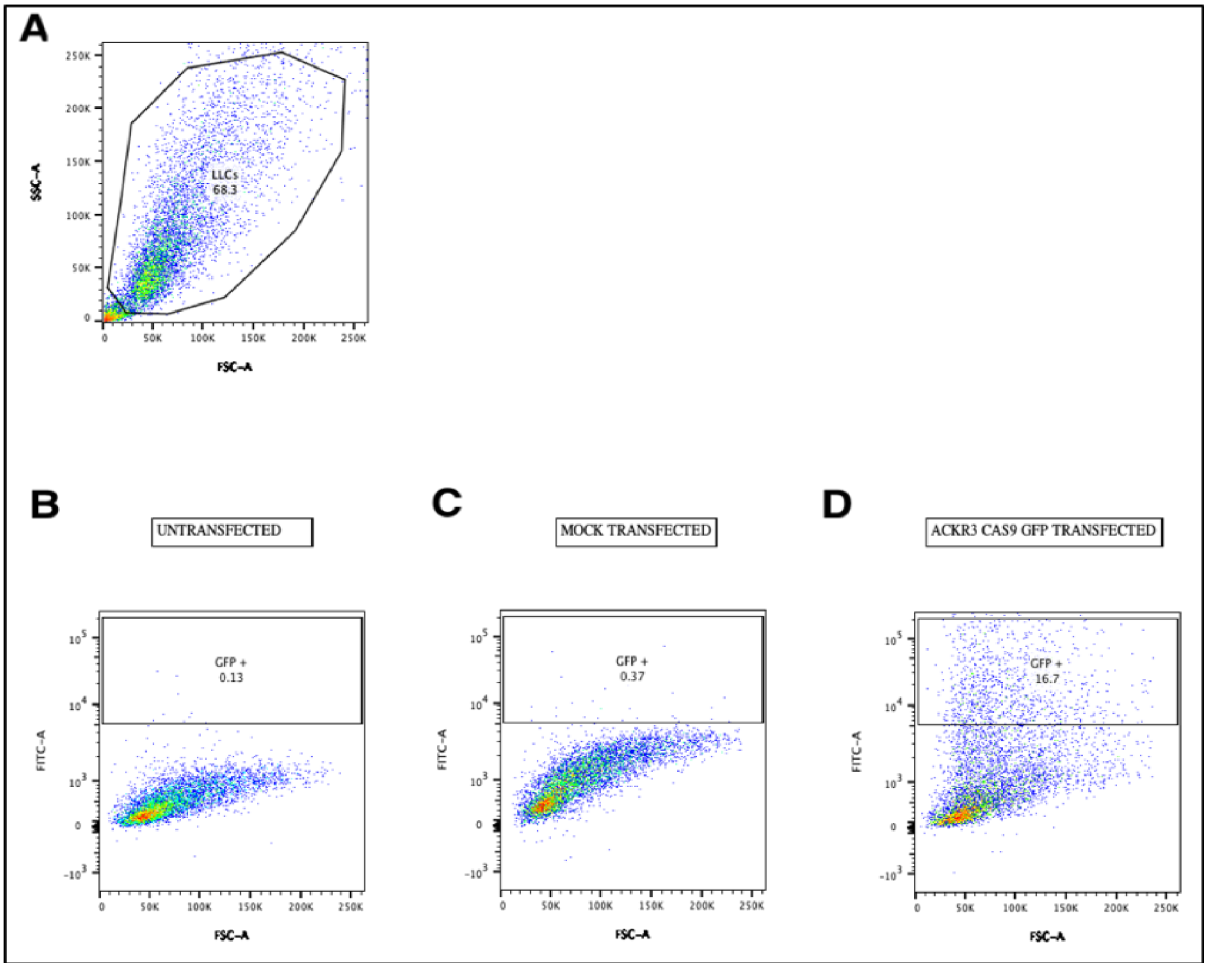

Figure 4.9 Flow cytometry plots from single-cell sorting of LLC cells for ACKR3 KO cell line generation. *A) Live LLCs (68,3% of the total cell population) were selected. B) Untransfected LLC served as a negative GFP control C) Mock transfected served as a negative GFP control for gating setting D) LLCs GFP positive cells were selected for single-cell sorting.*

GFP positive single-cell clones were allowed to grow for three weeks until they reached 80% confluency. At this point, following the same strategy we had for the B16F10 knockouts generation, we harvested the clones and used some of the cells for genomic PCR analysis (Figure 4.10). Clones that exhibited different band size than the wt product were selected for the next step of validation. For example, clones 8,13, 25, 31 among others, exhibited smaller size bands the wt and this was a strong indication of the occurrence of a deletion in the genomic region that we targeted.

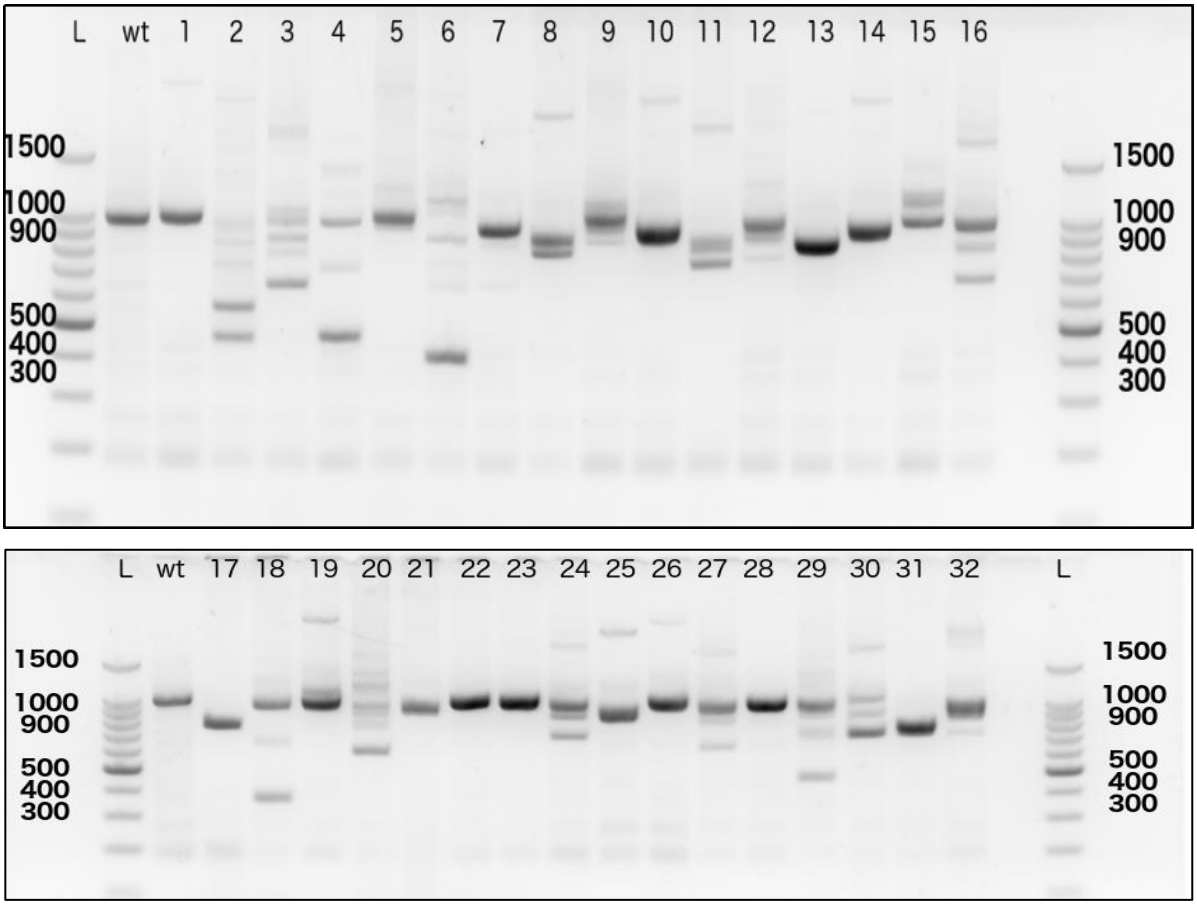

Figure 4.10 Representative images of genomic PCR products of LLC ACKR3 KO clones. *The first and the last lanes were loaded with DNA ladder 100 base pair(L). Wild type (wt) control PCR product was also included to allow comparison. Clones that exhibited different size than the wt were selected for further analyses. These differences in PCR products size are an indication of INDELs (insertions/ deletions) that occurred after Cas9 cut the genomic DNA. The existence of multiple bands in the same clone is a strong indication of heterozygosity.*

Subsequently, the clones we selected from the genomic PCR validation step were further validated using an Alexa 647 -CXCL12 uptake assay (detailed described in Materials and Methods, section 2.5.9). From the literature, we know that LLCs do not express CXCR4, a fact that allows us to use this functional assay as a readout to identify ACKR3 null clones[253]. Cas9 wt clones were also used as controls. After the uptake assay, the clones were analysed in a flow cytometer to measure fluorescence..All the mean fluorescence intensities of the clones were normalised against the control clone Cas10 (Figure 4.11). The clones that showed the lowest fluorescence – lowest uptake of CXCL12- were further validated by Sanger sequencing to confirm the biallelic knockout (Figure 4.12).

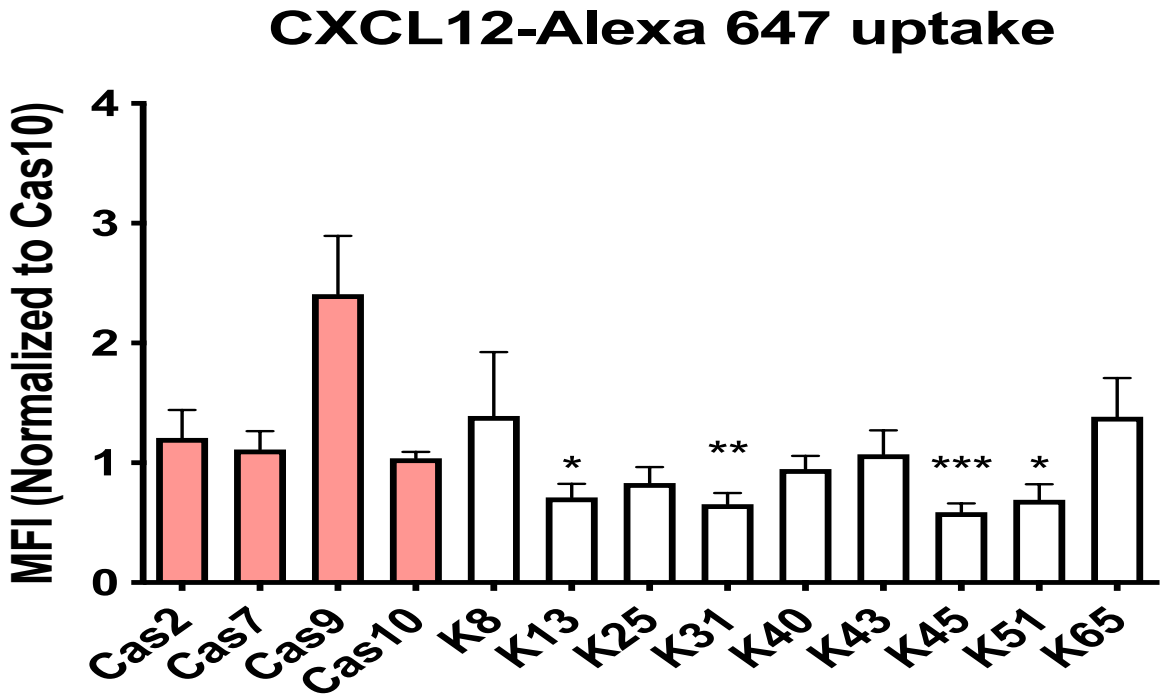

Figure 4.11 Chemokine uptake assay of Alexa 647 CXCL12 in LLC ACKR3 KO clones. *The median fluorescence intensity (MFI) of every clone was compared to Cas10 clone. The data were obtained from three independent experiments. An one-way ANOVA test with multiple comparisons and a Bonferroni corrections was applied between every ACKR3 KO clone and Cas10 WT clone. Statistical significance is indicated as: *P≤0.05, **P≤0.01,*

****P≤0.001, ****P≤0.0001, ns = P>0.05. All error bars represent the SD of the mean.*

Chemokines are considered to be ‘’sticky’’ proteins and they can stick to plastic surfaces and bind non-specifically to the plasma membrane of the cells. Regarding this, the chemokine uptake assay has a high background that make the interpretation of the results challenging. In this case, complementary methods should be used to verify the results of this assay.

The genomic DNA PCR products of the selected clones were cloned into the pGEM easy vector and verified by Sanger sequencing for the existence of a biallelic knockout. Protein sequences of the KO clones were aligned with the wt sequence using the Clustal online algorithm to verify efficient disruption of the protein product. (Figures 4.12, 4.13 and 4.14).

```
CLONE31A2       MDVHLFDYAEPGNYSDINWPCNSSDCIVVDTVQCPTMPNKNVLLYTLSFIYIFIFVIGMI     60
ACKR3WT         MDVHLFDYAEPGNYSDINWPCNSSDCIVVDTVQCPTMPNKNVLLYTLSFIYIFIFVIGMI     60
CLONE31A1       MDVHLFDYAEPGNYSDINWPCNSSDCIVVDTVQCPTMPNKNVLLYTLSFIYIFIFVIGMI     60
                ************************************************************

CLONE31A2       A-----------------------------------------------------------     61
ACKR3WT         ANSVVVWVNIQAKTTGYDTHCYILNLAIADLWVVITIPVWVVSLVQHNQWPMGELTCKIT     120
CLONE31A1       ANSVVA*-----------------------------------------------------     66
                *

CLONE31A2       -------------------------TYVTGTSSYKKKMVRRVVCILVWLLAFFVSLPDT     95
ACKR3WT         HLIFSINLFGSIFFLACMSVDRYLSITYFTGTSSYKKKMVRRVVCILVWLLAFFVSLPDT     180
CLONE31A1       -----------------------------------------------------------     66


CLONE31A2       YYLKTVTSASNNETYCRSFYPEHSIKEWLIGM----------------------------     127
ACKR3WT         YYLKTVTSASNNETYCRSFYPEHSIKEWLIGMELVSVILGFAVPFTIIAIFYFLLARAMS     240
CLONE31A1       -----------------------------------------------------------     66


CLONE31A2       -----------------------------------------------------------     127
ACKR3WT         ASGDQEKHSSRKIIFSYVVVFLVCWLPYHFVVLLDIFSILHYIPFTCQLENVLFTALHVT     300
CLONE31A1       -----------------------------------------------------------     66


CLONE31A2       -----------------------------------------------------------     127
ACKR3WT         QCLSLVHCCVNPVLYSFINRNYRYELMKAFIFKYSAKTGLTKLIDASRVSETEYSALEQN     360
CLONE31A1       -----------------------------------------------------------     66


CLONE31A2       --       127
ACKR3WT         TK       362
CLONE31A1       --       66
```

Figure 4.12 Representative Clustal protein alignment sequence of the LLC murine ACKR3 31 KO clone generated by CRISPR/Cas genome editing technology. *The protein sequence of the KO clone was aligned with the wt sequence using the Clustal online algorithm to verify efficient disruption of the protein product. The ACKR3 wt was aligned with the sequences of the two alleles (A1 and A2) of the ACKR3 31 KO clone that verified the biallelic KO of the ACKR3 gene.*

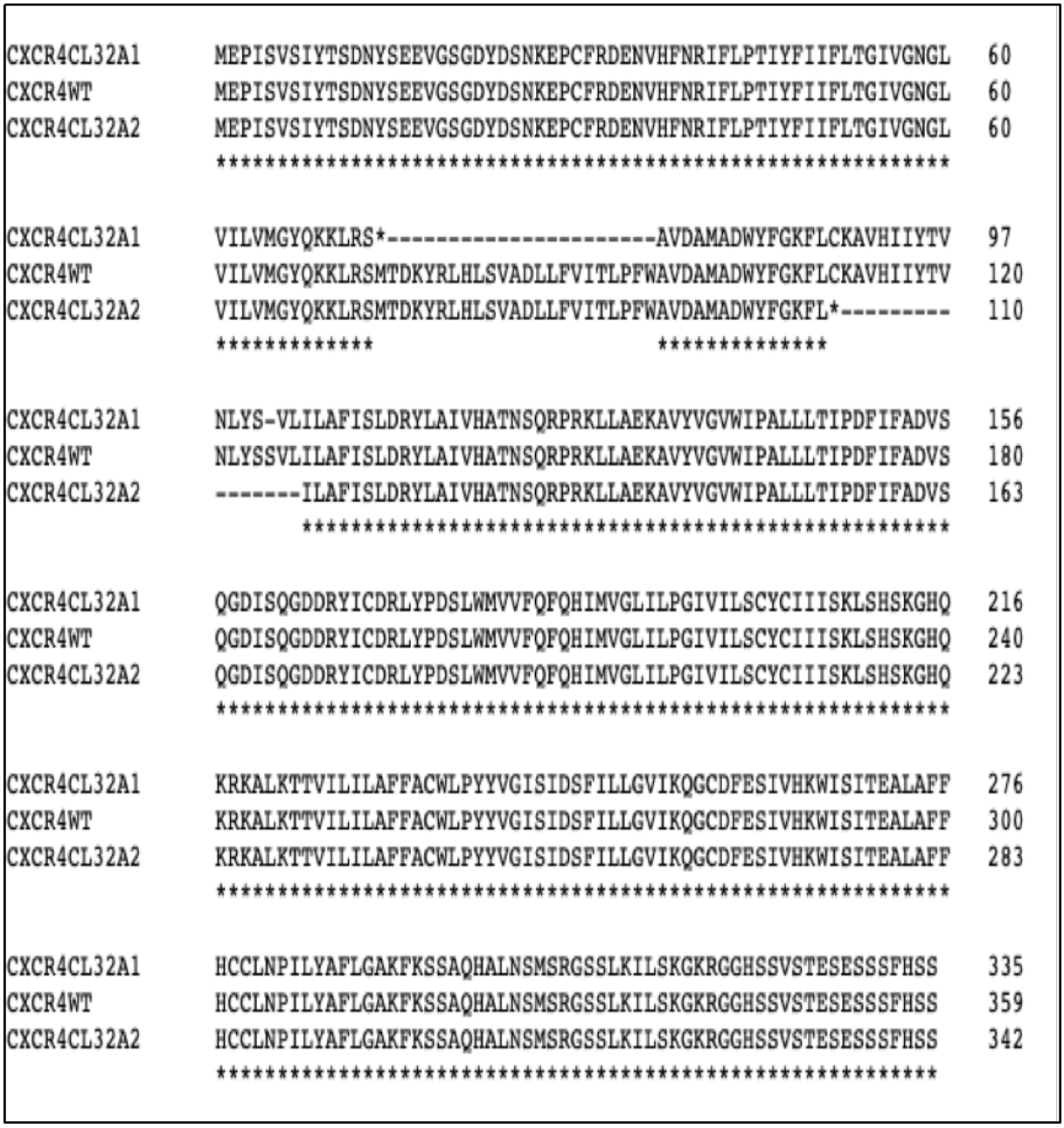

Figure 4.13 Representative Clustal protein alignment sequence of the B16F10 CXCR4 32 KO clone generated by CRISPR/Cas genome editing technology. *Protein sequences of the 32 CXCR4 KO clone were aligned with the wt sequence using the Clustal online algorithm to verify efficient disruption of the protein product. In the second row, the CXCR4 wt sequence is depicted and in the first and third row the sequences of the two alleles (A1 and A2) of the 32 CXCR4 KO clone that verified the biallelic KO.*

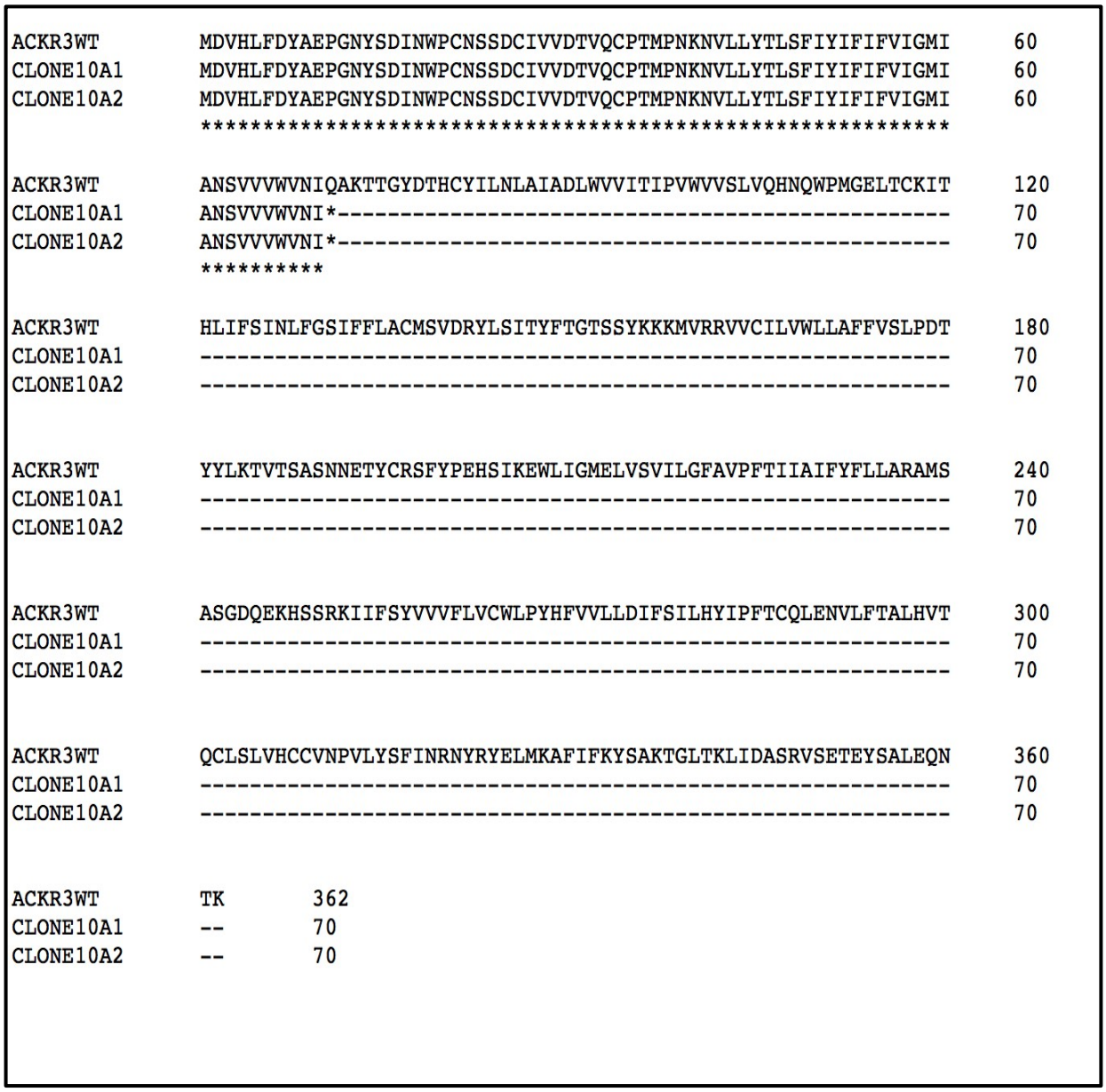

Figure 4.14 Representative Clustal protein alignment sequence of the B16F10 ACKR3 10 KO clone generated by CRISPR/Cas genome editing technology. *Protein sequences of the ACKR3 KO clone 10 were aligned with the ACKR3 WT sequence using the Clustal online algorithm to verify efficient disruption of the protein product. In the first row, the ACKR3 WT sequence is depicted and in the second and third row the sequences of the two alleles (A1 and A2) of the ACKR3 KO clone 10 that verified the biallelic KO.*

Subsequently, we evaluated if the cells derived from single-cell clones were proliferating equally *in vitro*. This step is essential to understand if the ACKR3 KO clones had a proliferation defect or advantage compared to Cas9 controls. It is also useful to understand if the clones belonging to the same group proliferate at the same rate. Clones that could show serious defects in proliferation and if this phenotype is not consistent within the same group had to be eliminated from downstream application since the phenotype is probably a problem related to damage during sorting or single-cell expansion and not an ACKR3-dependent phenotype. To characterise the clones regarding their proliferation rate, we used a flow cytometry-based assay KI67 staining (described in detail in Materials and Methods, section 2.5.10). The cells, after staining with the KI67 antibody, were analysed using a flow cytometer to measure fluorescence intensity. Cas9 control clones (cells deriving from transfection with Cas9 with no guides RNAs) were included to compare the proliferation rate. The fluorescence intensity was normalised against the control clone Cas10. Most of the clones exhibited the same proliferation rate, equal to the Cas9 control clones (Figure 4.15).

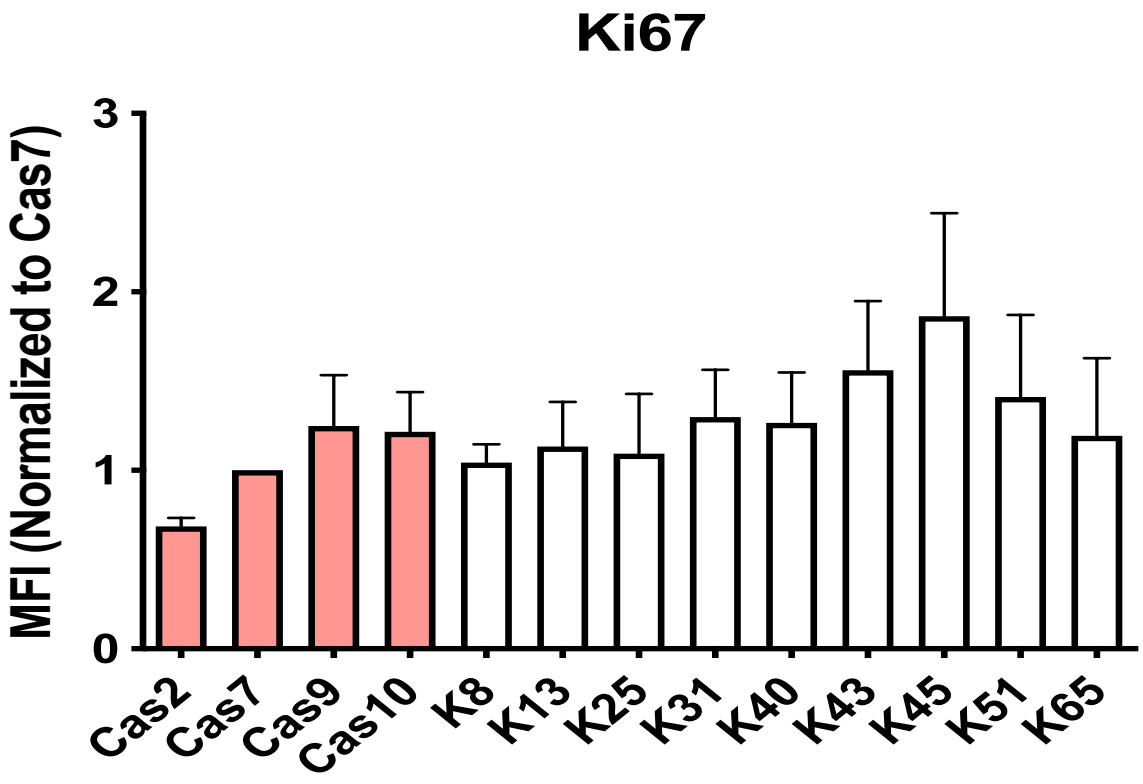

Figure 4.15 Ki67 flow cytometry-based proliferation assay in LLC ACKR3 KO clones. *The median fluorescence intensity (MFI) of every clone was normalized to Cas7 control clone. All ACKR3 KO clones exhibited comparable proliferation rates with the Cas9 controls. The data were obtained from three independent experiments. An one-way ANOVA test with multiple comparisons and a Bonferroni correction was applied between every ACKR3 KO clone and Cas10 WT clone. *P≤0.05, **P≤0.01,***P≤0.001, ****P≤0.0001, ns = P>0.05. All error bars represent the SD of the mean.*

4.6 Summary and discussion of the chapter

In chapter 4, we employed CRISPR/Cas genome editing technology, to generate single gene knock out cell lines, null for ACKR3 or CXCR4. The purpose of this approach was to use these KO cell lines in chapter 5 *in vivo* to model ACKR3 and CXCR4 involvement in cancer. Our strategy included the use of the double nickase approach that significantly reduces off-target effects.

We chose B16F10 murine melanoma cells, a very well established and characterised cell line, to study the contribution of ACKR3 to the early events of metastasis (seeding) in the lung. For this purpose, we generated two different B16F10 knock out cell lines. More specifically, we generated B16F10 CXCR4 null cells and B16F10 ACKR3 null cells.

Subsequently, we generated Lewis Lung Carcinoma (LLC) ACKR3 null cells. We chose this cell line because it is commonly used in research for tumour development studies, but also because ACKR3 is significantly upregulated in human lung cancer. Even though it is widely used in cancer studies, the LLC cell line is not fully characterised regarding the mutation burden in crucial oncogenes. To this end, it is challenging to classify this cell line as Lung Adenocarcinoma, the Lung Squamous Carcinoma or the mixed (Adenosquamous) lung cancer subtype. Despite this, this cell line is a useful tool in tumour development and tumour growth studies.

During the process of generating ACKR3 and CXCR4 knockout cell lines, one obstacle we needed to overcome was the lack of specific antibodies for ACKR3 but also for CXCR4. Usually, the validation of knockout cell lines requires verification at the protein level that the targeted gene of interest does not lead to the expression of any protein product. The use of unspecific antibodies while validating knockout cells, can lead to false results as knockout cells can appear to still be expressing the targeted protein.

To overcome this issue, other complementary assays were used when it is possible and finally verify the knockout cell clones using Sanger sequencing. In our case, we used Alexa 647 labelled CXCL12 chemokine uptake assay[286] and Sanger sequencing to validate the ACKR3 knockout in LLCs. In the B16F10 cell line, the validation of both ACKR3 and CXCR4 knock out cell lines was carried out using only Sanger sequencing of the genomic DNA of a single cell-derived clone. In B16F10 cells, labelled CXCL12 chemokine uptake assay could not be applied for the validation of ACKR3 and CXCR4 knockout cells since this cell line expresses both ACKR3 and CXCR4 and both receptors can bind and internalise CXCL12[305,306].

Collectively our experimental approach in this chapter provides a useful guideline for generating and validating a CRISPR/Cas-mediated gene KO when antibodies against the gene of interest are not available.

CHAPTER 5

The role of ACKR3 in cancer

5.1 Introduction and aims of the chapter

The aims of this chapter were: A) to use the information deposited in publicly available cancer databases to get information about ACKR3 expression in different types of human cancers. Furthermore, in these databases we can get information about the mutational burden (if any) of ACKR3 in different types of cancer B) to assess the role ACKR3 in cancer development using in vivo mouse models. Two well established and characterised mouse models where used. First, the B16F10 melanoma model was used to understand the early steps of metastasis. Subsequently we used the LLC subcutaneous model to determine any involvement of ACKR3 in tumour growth. For both models, we used the knockout cell lines that were generated in chapter 4.

5.2 Analysis of publicly available datasets for ACKR3 expression in cancer

In the era of “Big Data”, it is vital for the research community and the general public to be able to access data of high interest like patient data, data from clinical trials and genomic data. Data collection and curation can originate from different sources such as individual researchers/ research groups, charities/philanthropies, organisations and national projects. Data can range from a limited number of sample datasets to fully integrated data produced by high throughput technology platforms and thousands of samples.

In any case, there is a need to be general agreement on the way that data are collected, curated and stored before they are made available to the scientific community and the public.

To date, there are several publicly available databases with data related to major human diseases like cancer, diabetes and autoimmune diseases.

For the purpose of this study, we exploited the publicly available information deposited in these databases to query the expression of ACKR3 gene in different types of human cancer.

5.2.1 Oncomine platform

Oncomine platform is an RNA sequencing and DNA microarray web-based database that contains a significant amount of data regarding gene expression analyses from several studies in the context of cancer. Oncomine database contains gene expression datasets from individual cancer studies but also the Cancer Genome Atlas Project (also described in this chapter). This platform, apart from being a useful database, also provides an easy to use software that allows gene differential expression analyses comparing the most significant types of cancer with their respective healthy tissues. Furthermore, in Oncomine, there is much information from a variety of cancer subtypes and clinical-based and pathology-based analyses[307].

In our first analysis, we assessed ACKR3 expression using the Oncomine platform. We found that ACKR3 expression was seen to be upregulated in two different lung cancer studies. More specifically, in the first study (Bhattacharjee Lung) [308], ACKR3 gene expression was about 6,4 fold upregulated when 21 human lung squamous cell carcinoma specimens were compared to 17 healthy lung specimens as shown by the log2 difference of the median of the two groups (Figure 5.1A). In another study[309], ACKR3 was also upregulated in lung squamous carcinoma 4-fold when 5 human lung squamous cell carcinoma specimens were compared with 5 healthy lung specimens (Figure 5.1B).

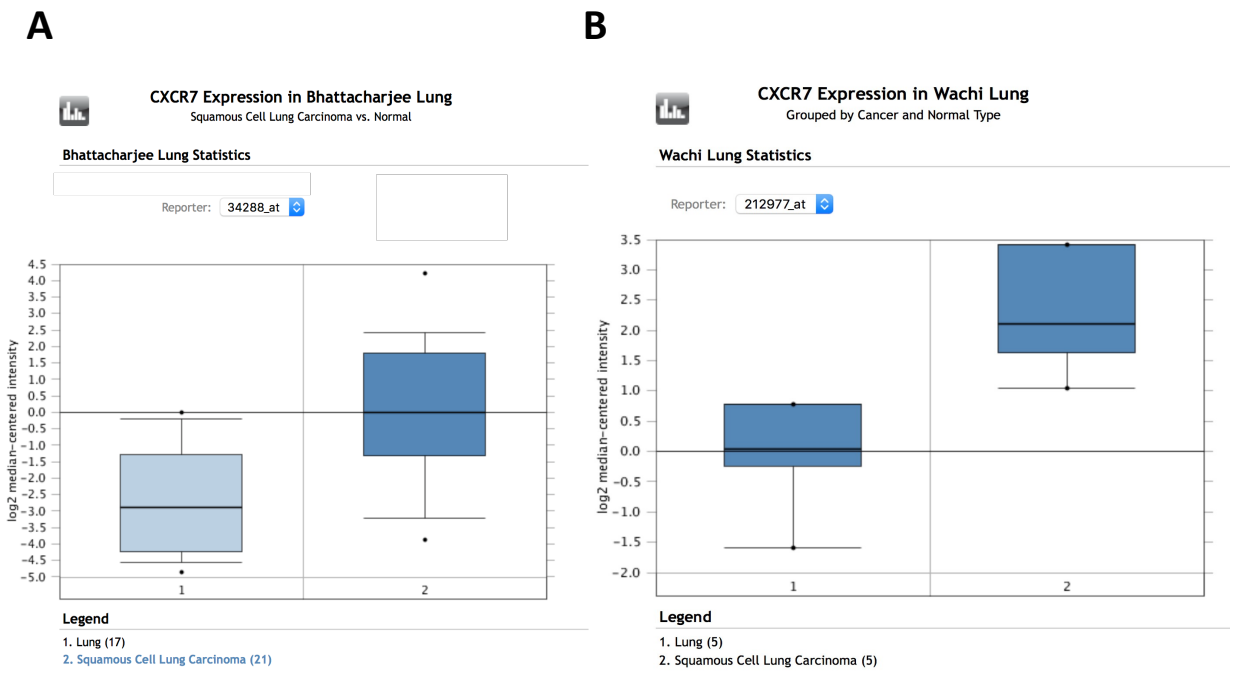

Figure 5.1 ACKR3 gene expression in lung cancer based on two different studies obtained from the Oncomine platform. *A) ACKR3 is upregulated 6.4 fold in 21 human lung squamous carcinoma specimens compared to 17 human healthy lung specimens in the Bhattacharjee lung study and B) ACKR3 is 4 fold upregulated in the Wachi lung study that compared 5 human lung squamous carcinoma specimens compared to 5 healthy lung specimens. Box-and-whisker plot: Whiskers indicate the 10th and the 90th percentile, boxes indicate the 25th to 75th percentile, and horizontal solid lines indicate the median. Circles indicate the minimum and maximum values.*

5.2.2 The Cancer Genome Atlas (TCGA)

Nowadays, technological advances have led to an explosion of oncogenic analyses and generation of a significant amount of data that uncover the complexity involved in gene expression patterns in cancer. The Cancer Genome Atlas (TCGA) is a project/ initiative that started in 2005, was funded by US government, and had as a goal to identify and catalogue genomic and gene expression data from major different human cancers. The project was overviewed by the National Cancer Institute (NCI) and the National Human Genome Research Institute (NHGRI). The project started with a pilot period study in three types of cancer: glioblastoma, lung and ovarian. The information collected in the TCGA includes gene expression profile, Single Nucleotide Polymorphisms (SNPs), DNA methylation, miRNA profiling and exon sequencing of more than 1000 genomes[310].

In cancer, often mutations in genes can lead to loss of function of the gene or lead to altered function of the gene protein product. These alterations in genes may cause the aberrant growth of cancer cells. Mutations in genes that become oncogenes can be inherited or caused by exposure to substances and other environmental conditions. For the purposes of this study, we exploited the data deposited in the TCGA database to assess if ACKR3 is frequently mutated in different types of human cancers. Our analysis of exome sequencing data deposited in TCGA revealed that there is no positive correlation between mutations in the ACKR3 gene and tumourigenesis.

Subsequently, we interrogated the ACKR3 gene expression in different types of human cancers using data from the TCGA database (Figures 5.2- 5.8). The RNA Seq counts were deposited in the form of RSEM log2 (RNA-Seq by Expectation Maximisation). We downloaded and analysed these data using Graph Pad Prism software. More specifically, unpaired two-tailed t-test was applied to the groups of control vs tumours samples. When we compared the gene expression data expression from cancer patients (tumour versus healthy tissue) we observed that ACKR3 gene is significantly upregulated in several types of human cancers.

More specifically, ACKR3 was upregulated in glioblastoma (GBM), glioma (GBMLGG), lung squamous carcinoma (LUSC), Head-Neck Squamous Cell Carcinoma (HNSC) and Pan-Kidney cohort (KIPAN) among others. For the purposes of the present study, we decided to focus our analysis on lung cancer subsets. In lung squamous carcinoma (LUSC), gene expression of ACKR3 is upregulated 3.62 fold in tumour versus control samples (Figure 5.4 B).

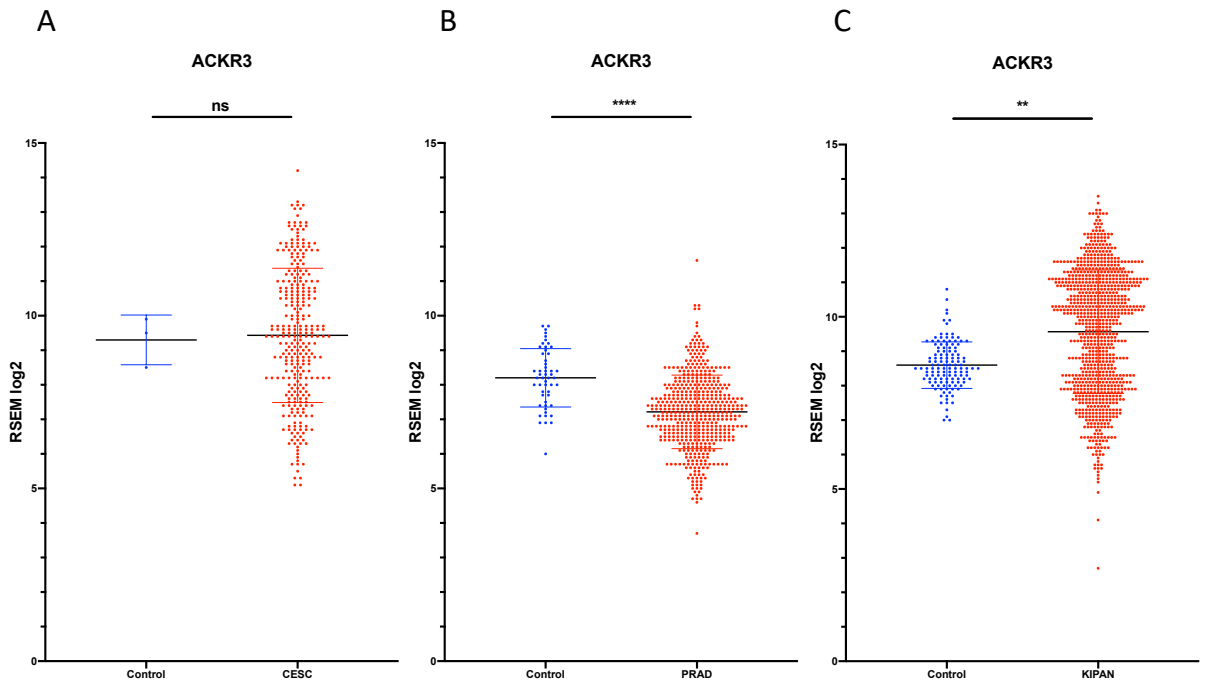

Figure 5.2 ACKR3 expression in different human cancers as obtained from the TCGA database. *Tumour samples are depicted with red colour and healthy control samples with blue. ACKR3 is A) upregulated 0.99 fold in 306 Cervical squamous cell carcinoma and endocervical adenocarcinoma (CESC) patients versus 3 healthy control samples, B) downregulated 0.501 fold in 498 Prostate Adenocarcinoma (PRAD) patients versus 52 healthy control samples C) upregulated 2.67 fold in 891 Pan-Kidney cohort (KIPAN) patients versus 129 healthy control samples. An unpaired two-tailed t-test was applied to the groups of control vs tumour samples. The expression is depicted in the form of RSEM (log2). Statistical significance is indicated as *P≤0.05, **P≤0.01, ***P≤0.001, ****P≤0.0001, ns = P>0.05. All error bars represent the SD of the mean.*

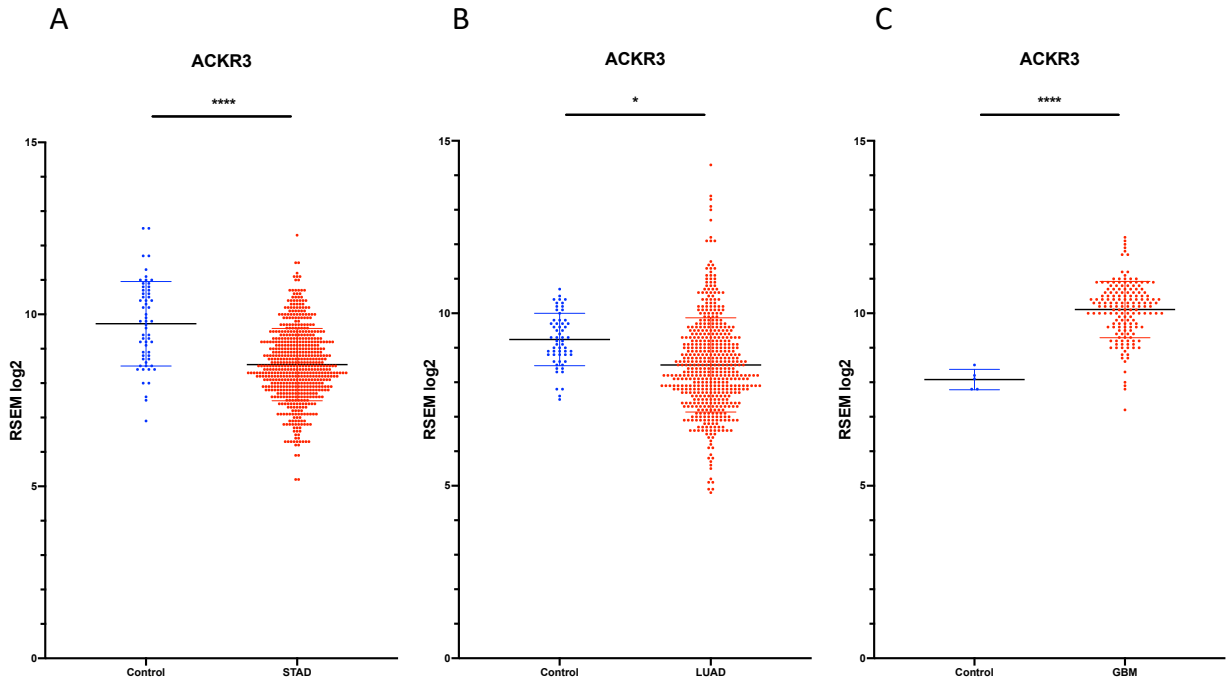

Figure 5.3 ACKR3 expression in different human cancers as obtained from the TCGA database. *Tumour samples are depicted with red colour and healthy control samples with blue. ACKR3 is A) downregulated 0.601 fold in 415 Stomach Adenocarcinoma (STAD) patients versus 35 healthy control samples, B) downregulated 0.553 fold in 517 Lung Adenocarcinoma (LUAD) patients versus 59 healthy control samples, C) upregulated 4.27 fold in 166 Glioblastoma Multiforme (GBM) patients versus 5 healthy control samples. An unpaired two-tailed t-test was applied to the groups of control vs tumour samples. The expression is depicted in the form of RSEM (log2). Statistical significance is indicated as: *P≤0.05, **P≤0.01,***P≤0.001, ****P≤0.0001, ns = P>0.05. All error bars represent the SD of the mean.*

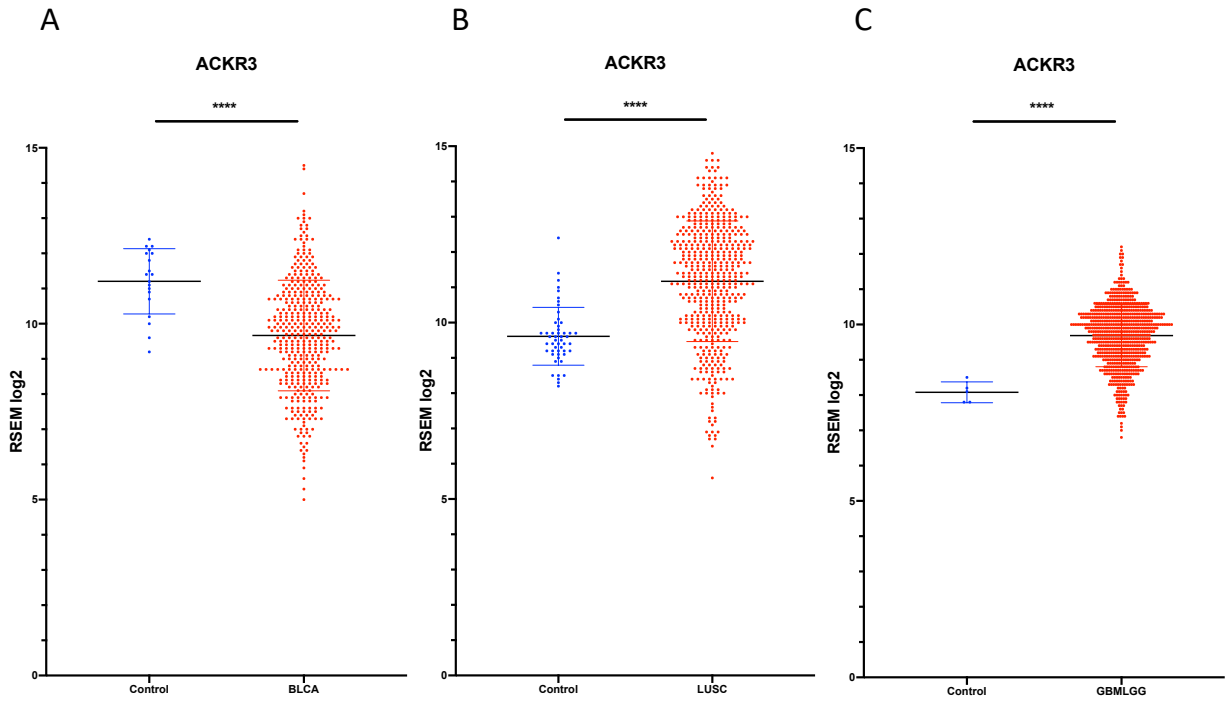

Figure 5.4 ACKR3 expression in different human cancers as obtained from the TCGA database. *Tumour samples are depicted with red colour and healthy control samples with blue. ACKR3 is A) downregulated 0.324 fold in 408 Urothelial Bladder Carcinoma (BLCA) patients versus 19 healthy control samples, B) upregulated 3.62 fold in 501 Lung Squamous Carcinoma (LUSC) patients versus 51 healthy control samples, C) upregulated 3.21 fold in 696 Glioma (GBMLGG) patients versus 5 healthy control samples. An unpaired two-tailed t-test was applied to the groups of control vs tumour samples. The expression is depicted in the form of RSEM (log2). Statistical significance is indicated as: *P≤0.05, **P≤0.01,***P≤0.001, ****P≤0.0001, ns = P>0.05.All error bars represent the SD of the mean.*

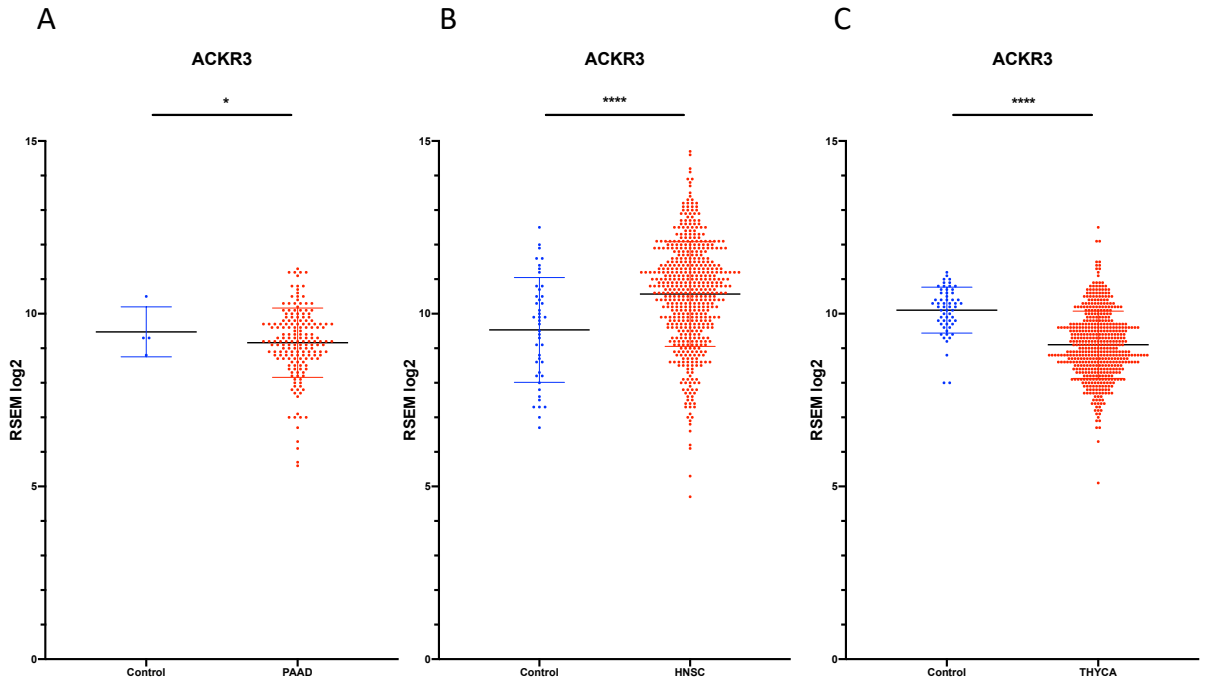

Figure 5.5 ACKR3 expression in different human cancers as obtained from the TCGA database. *Tumour samples are depicted with red colour and healthy control samples with blue. ACKR3 is A) downregulated 0.933 fold in 179 Pancreatic adenocarcinoma (PAAD) patients versus 4 healthy control samples, B) upregulated 1.96 fold in 522 Head-Neck Squamous Cell Carcinoma (HNSC) patients versus 44 healthy control samples, C) downregulated 0.438 fold in 509 Thyroid Cancer (THYCA) patients versus 59 healthy control samples. An unpaired two-tailed t-test was applied to the groups of control vs tumour samples. The expression is depicted in the form of RSEM (log2). Statistical significance is indicated as: *P≤0.05, **P≤0.01, ***P≤0.001, ****P≤0.0001, ns = P>0.05.All error bars represent the SD of the mean.*

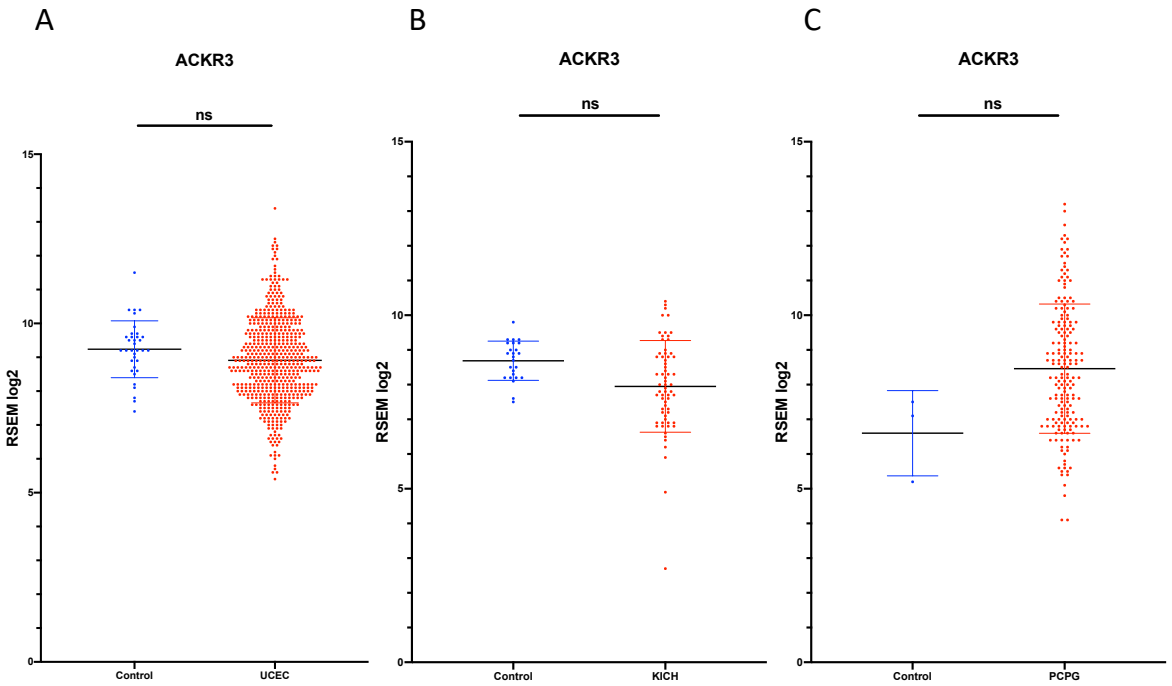

Figure 5.6 ACKR3 expression in different human cancers as obtained from the TCGA database. *Tumour samples are depicted with red colour and healthy control samples with blue. ACKR3 is A) downregulated 0.782 fold in 546 Uterine Corpus Endometrial Carcinoma (UCEC) patients versus 35 healthy control samples, B) downregulated 0.547 fold in 66 Kidney Chromophobe (KICH) patients versus 25 healthy control samples, C)upregulated 2.34 fold in 184 Pheochromocytoma and Paraganglioma (PCPG) patients versus 3 healthy control samples An unpaired two-tailed t-test was applied to the groups of control vs tumour samples. The expression is depicted in the form of RSEM (log2). Statistical significance is indicated as: *P≤0.05, **P≤0.01,***P≤0.001, ****P≤0.0001, ns = P>0.05.All error bars represent the SD of the mean.*

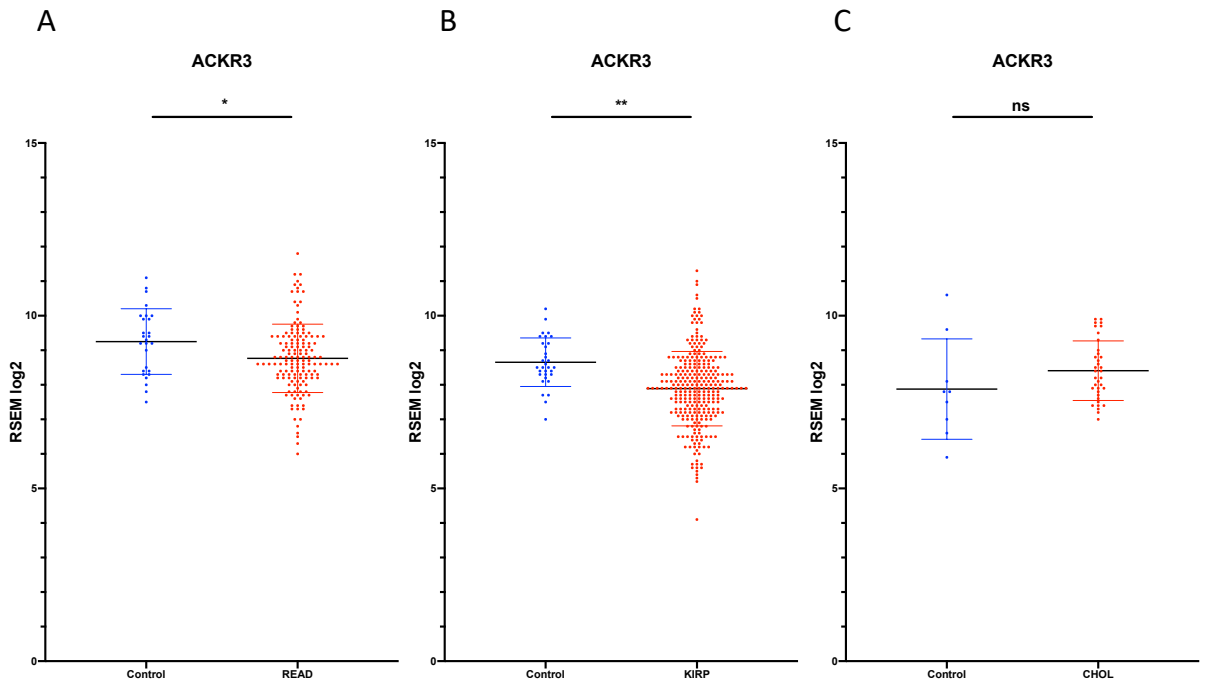

Figure 5.7 ACKR3 expression in different human cancers as obtained from the TCGA database. *Tumour samples are depicted with red colour and healthy control samples with blue. ACKR3 is A) downregulated 0.503 fold in 167 Rectum Adenocarcinoma (READ) patients versus 10 control samples, B) downregulated 0.656 fold in 291 Kidney renal papillary cell carcinoma (KIRP) patients versus 32 healthy control samples, C) upregulated 1.47 fold in 36 Cholangiocarcinoma (CHOL) patients versus 9 healthy control samples. An unpaired two-tailed t-test was applied to the groups of control vs tumour samples. The expression is depicted in the form of RSEM (log2). Statistical significance is indicated as *P≤0.05, **P≤0.01,***P≤0.001, ****P≤0.0001, ns = P>0.05.All error bars represent the SD of the mean.*

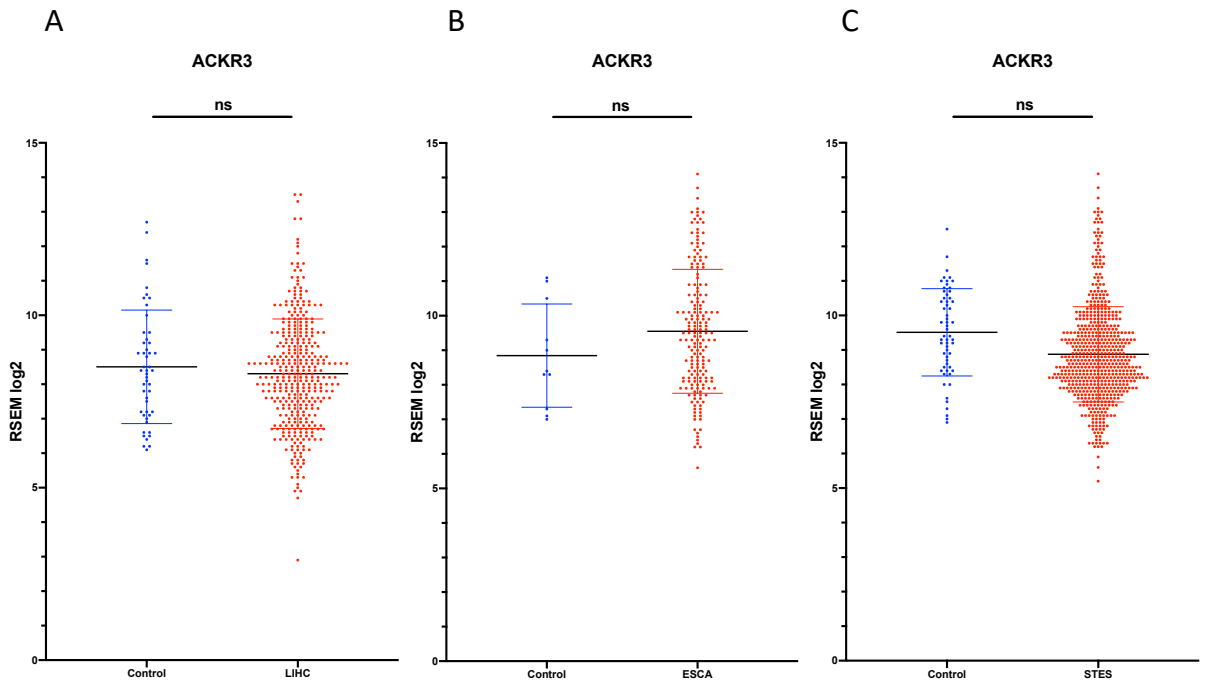

Figure 5.8 ACKR3 expression in different human cancers as obtained from the TCGA database. *Tumour samples are depicted with red colour and healthy control samples with blue. ACKR3 is A) downregulated 0.896 fold in 373 Liver Hepatocellular Carcinoma (LIHC) patients versus 50 control samples. B) upregulated 2.03 fold in 185 ACKR3 Esophageal Carcinoma (ESCA) patients versus 11 control samples. C) downregulated 0.694 fold in 600 Stomach and Esophageal carcinoma (STES) patients versus 46 control samples An unpaired two-tailed t-test was applied to the groups of control vs tumour samples. The expression is depicted in the form of RSEM (log2). Statistical significance is indicated as: *P≤0.05, **P≤0.01,***P≤0.001, ****P≤0.0001, ns = P>0.05.All error bars represent the SD of the mean.*

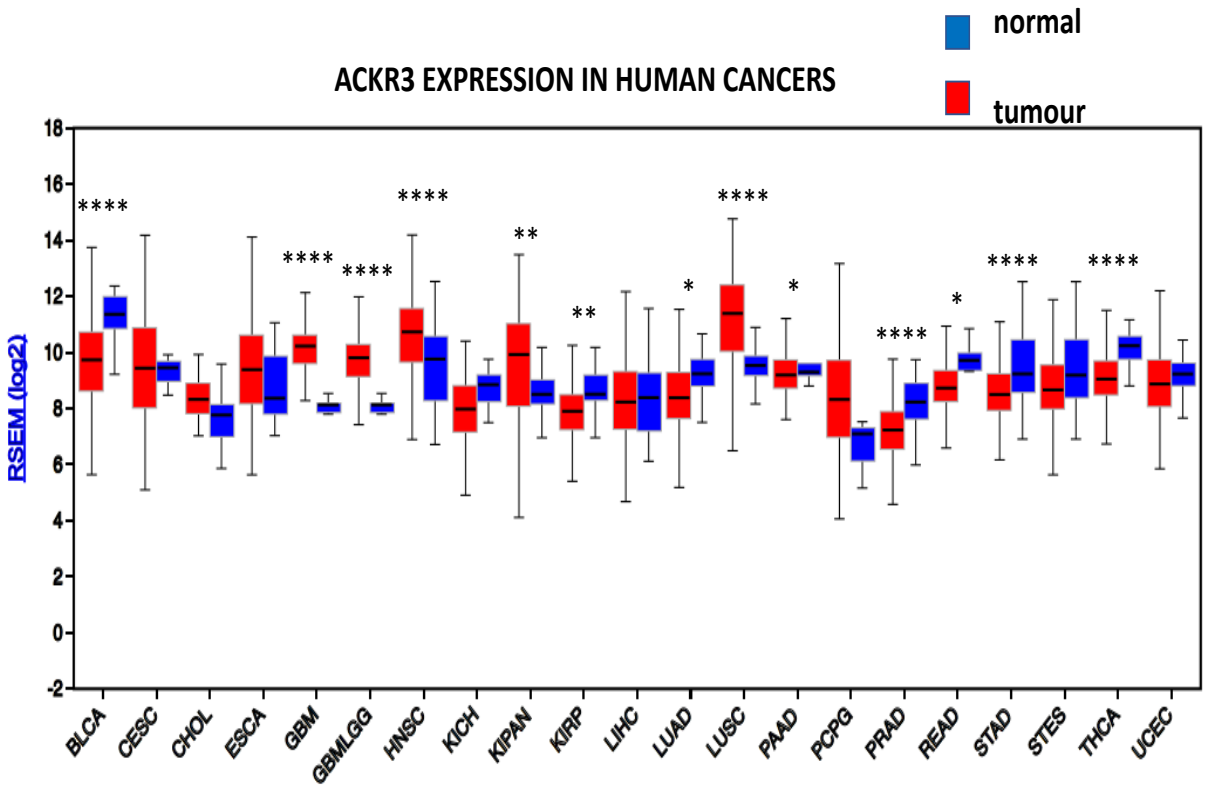

Figure 5.9 ACKR3 expression in different human cancers as obtained from the TCGA database. *Schematic summary of Figures 5.2 – 5.8. Tumour samples are depicted with red colour and healthy control samples with blue.*
*The expression is depicted in the form of RSEM (log2). An unpaired two-tailed t-test was applied to the groups of control vs tumour samples. Statistical significance is indicated as: *P≤0.05, **P≤0.01,***P≤0.001, ****P≤0.0001, ns = P>0.05.All error bars represent the SD of the mean.*

5.3 ACKR3 involvement at the early stages of metastasis in the lung

To investigate if ACKR3 is involved in the early stages of the metastatic process in the lung, we used the established pseudometastatic B16F10 melanoma mouse model.
The role of CXCR4 in cancer metastasis has been extensively investigated in the literature and its roles in secondary metastatic site colonization already established. In this model, we already know from the literature that CXCR4 silencing impairs the metastasis/ colonization of the tumour cells in the lung. We also know that this phenotype is CXCL12- dependent, as the use of CXCL12 antagonists phenocopied the CXCR4 knockdown[311,312].

To understand the role of ACKR3 in this model, we used the ACKR3 B16F10 KO clone 10 that we generated in chapter 4. We also included the CXCR4 KO B16F10 clone 32, that could serve as a control of a known phenotype in this model. We injected $2x10^5$ B16F10 cells into the tail vein of 7-8 week old female C57BL/6 mice. After two weeks, mice were sacrificed according to Schedule 1 procedures, lungs were removed and were examined macroscopically and microscopically. Every lung was assessed for tumour burden by counting all tumour nodules.

We observed a reduction in the number of pulmonary tumour nodules in the ACKR3 KO group compared to the wt ones. More specifically, in the ACKR3 KO group, we observed a reduction from the mean value of 230 nodules observed in the WT group, to around 100 nodules. The CXCR4 KO group exhibited less tumour burden than both the wt and the ACKR3 KO group. The mean number of nodules per lung in the CXCR4 KO group was around 50 (Figure 5.10). Our observation in the CXCR4 KO group is in agreement with what others observed in the model, using other techniques (siRNA/shRNA knockdown)[313].This ACKR3 phenotype has not been described before, but there is controversy in the literature about the ability of ACKR3 to drive chemotaxis thus metastasis. Further investigation is needed to clarify if this phenotype is CXCR4 driven or if other mechanisms contribute.

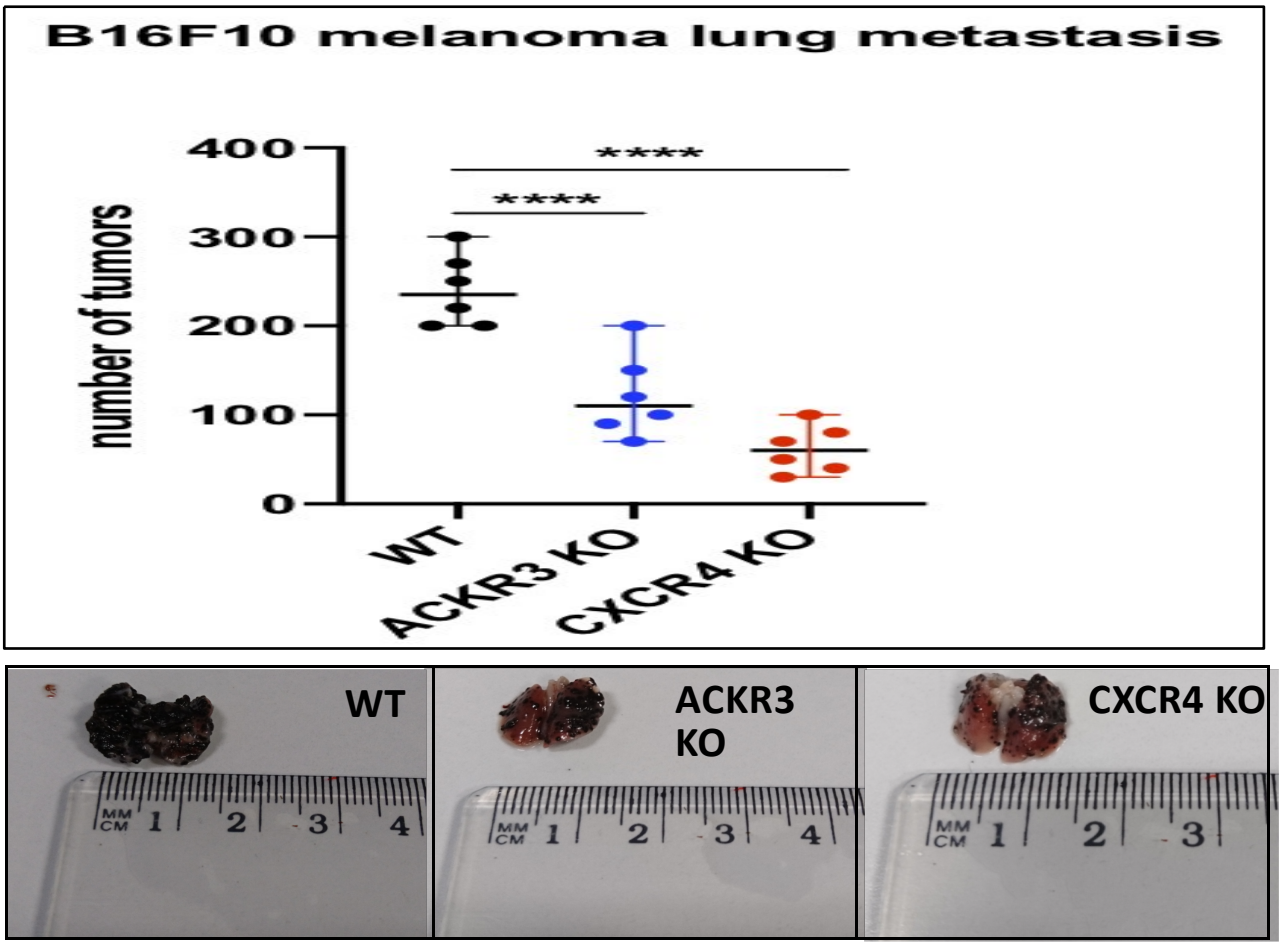

Figure 5.10 ACKR3 KO reduces the pulmonary metastatic nodules in the B16F10 melanoma metastatic model*. ACKR3 knockout B16F10 cells exhibit reduced metastasis, as assessed by the number of tumour nodules counted in the lung two weeks' post-injection. CXCR4 knockout B16F10 cells served as a control of a known phenotype in this model. Groups of mice were blinded and subsequently the tumours were counted by two individuals to ensure an unbiased counting. Non-parametric Kruskal Wallis test was applied for multiple comparisons. Both KO groups (ACKR3 KO and CXCR4 KO were compared against the control (wt) group. Statistical significance is indicated as: *P≤0.05, **P≤0.01,***P≤0.001, ****P≤0.0001, ns = P>0.05. All error bars represent the SD of the mean.*

5.4 ACKR3 role in tumour growth

Finally, to assess the role of ACKR3 in tumour growth, we used the LLC ACKR3 KO clone 31 that we generated in chapter 4 in a subcutaneous mouse model. Briefly, $2x10^5$ LLC cells were injected subcutaneously in the flank of 7-8 week old female C57BL/6 mice. On day nine after injection, tumours became palpable, and we could start the measurements. Tumours were measured every second day, and on day eighteen, when they reached the largest acceptable size, the protocol was terminated according to the Home Office Project Licence regulations (Figure 5.11). On day eighteen, tumours were resected, weighed and pictures taken.

In this model, we observed that ACKR3 null LLC cells have significantly impaired tumour growth. This phenotype has also been observed in a previous study, where ACKR3 was silenced using siRNAs. In the same study it was demonstrated that LLC cells do not express CXCR4 *in vitro*, but it needs to be determined if the expression of CXCR4 increases *in vivo* in these cells[253]. This will allow us to clarify if the ACKR3 null phenotype is CXCR4-driven or if there are other mechanisms involved that drive this phenotype.

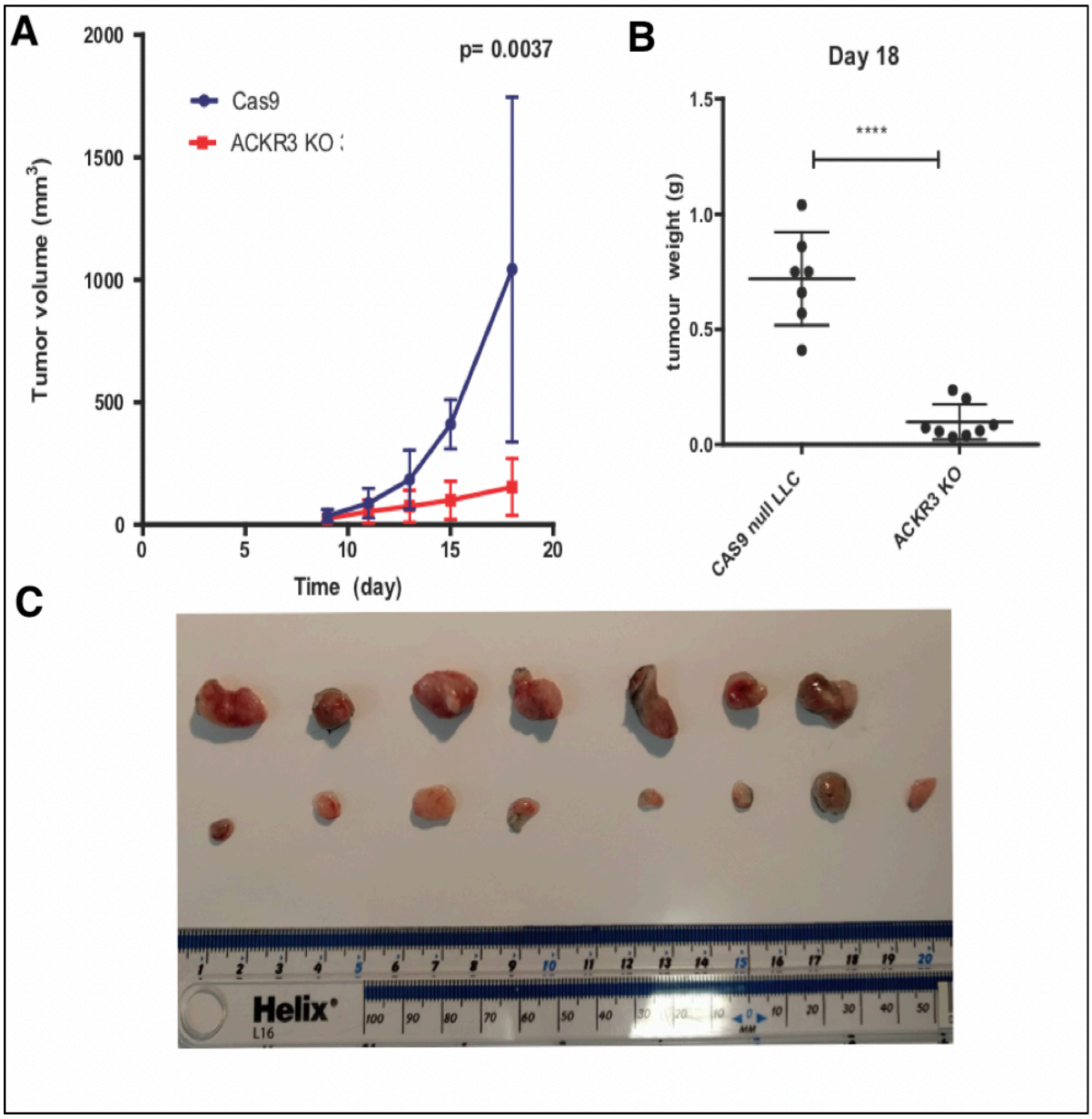

Figure 5.11 ACKR3 absence impairs the tumour growth in an LLC subcutaneous mouse model. *A) ACKR3 KO LLC exhibited a significant reduction in tumour growth after 18 days. One-way analysis of variance (ANOVA) was applied with Tukey's correction for multiple comparisons. B) Tumour weight on day 18, was also significantly reduced in the ACKR3 KO group. Paired t student's test was applied. C) Images of wt (upper row) tumours and ACKR3 KO (lower row) on day 18. Statistical significance is indicated as, *P≤0.05, **P≤0.01,***P≤0.001, ****P≤0.0001, ns = P>0.05.All error bars represent the SD of the mean.*

5.5 Summary and discussion of the chapter

In chapter 5, we exploited information from the publicly available cancer databases such as TCGA, but also from the Oncomine software, to interrogate the ACKR3 expression in different types of human cancers. In the analysis of the data obtained from the TCGA, we identified several types of human cancers in which ACKR3 is upregulated including glioblastoma (GBM), glioma (GBMLGG) and lung squamous carcinoma (LUSC) among others. Subsequently, we used the knockout cell lines that we generated in chapter four, to investigate the role of ACKR3 in tumour growth but also in the ‘’seeding step’’ during metastasis in the lung.

To this end, B16F10 ACKR3 and CXCR4 KO cells were injected into the tail vein of C57BL/6J mice, and after two weeks we assessed tumour burden in the lung. We observed that the CXCR4 KO cell group exhibited significantly reduced tumour burden in the lung – a phenotype that is previously described in the literature.
ACKR3 KO B16F10 cell group phenocopied the CXCR4 KO, but the tumour burden was higher than the one observed in the CXCR4 KO group. This phenotype indicates a role for ACKR3 in the ‘’seeding’’ initial step of metastasis in the lung. Furthermore, if this phenotype is CXCR4 dependent or there are other mechanisms involved needs to be further investigated.

Finally, we used the LLC subcutaneous tumour model to assess ACKR3 involvement in tumour growth. Indeed, we observed a significant reduction in tumour size and weight when we implanted LLC ACKR3 null cells in the flank of C57BL/6 mice. This phenotype was observed before in a study, where LLCs were knocked down using siRNAs. Our study verifies this phenotype, but the mechanism that ACKR3 uses to control tumour growth in this model requires further investigation. In our study, the lack of ACKR3 expression in the tumour cells possibly leads to an increase in the concentration of the ACKR3 ligands within the tumour microenvironment. Since all the *in vivo* experiments were performed on a C57BL/6J mouse strain background, this excludes the involvement of CXCL11 (C57BL/6J mice do not express CXCL11) [314]in the ACKR3 null phenotype.

This fact allows us to suggest a CXCL11-independent mechanism for the observed phenotypes in these murine models.

CHAPTER 6

Discussion

6.1 Main findings of the study

In the present study, we investigated the involvement of ACKR3 in cancer progression and metastatic potential. In the literature, there is a substantial body of evidence that indicates that ACKR3 is upregulated in several types of cancers but also the tumour-associated vasculature. To this end, at first, we tried to query cancer gene expression databases to understand in which types of human cancers ACKR3 expression is significantly altered. Our analyses revealed that ACKR3 is upregulated in several types of human cancer including squamous cell lung carcinoma, among others. Taking into consideration these initial findings from patient data, we decided to focus on ACKR3 role in lung cancer.

One significant obstacle we encountered in this study is the lack of specific ACKR3 antibodies. In the present study we validated, for the first time, two commercially available anti ACKR3 antibodies using an ACKR3 GFP reporter mouse. Our flow cytometry-based validation revealed that both antibodies were non-specific when tested in lung stromal cell populations of the ACKR3 reporter mouse. This observation led us to conclude that more complementary methods should be used for ACKR3 detection. The use of the ACKR3/ GFP reporter mouse allowed us to characterise the expression of ACKR3 in stromal cells in the resting lung and trachea. This approach helped identify ACKR3 positive cells in three stromal cell types: blood endothelial cells, lymphatic endothelial cells and fibroblasts. Although our finding is in accordance with several reports in the literature, further characterisation of the GFP/ACKR3 positive populations to ensure that the reporter mouse model accurately reflects biology would be useful. Probably a real-time PCR in GFP positive sorted populations could further verify ACKR3 expression in these cell types.

Finally, we employed CRISPR/Cas9 genome editing to generate ACKR3 null cancer cell lines to model cancer progression and metastatic potential of ACKR3 deficient tumours. We noticed a significant reduction in both tumour growth and tumour cell colonisation in the lung. Our observations are in broad agreement with other studies in the literature.

In the context of cancer, tumour endothelial cells support tumour growth by supplying the tumour with nutrients, but also by affecting the immune cell infiltration and stromal composition of the tumour. In the scientific literature, there are several studies that demonstrate that ACKR3 is upregulated in the tumour vasculature. Taking into consideration all the endothelial cell functions that ACKR3 regulates, there is the possibility that ACKR3 promotes tumour angiogenesis but also the recruitment of immune cells that promote tumour growth, such as tumour-associated macrophages (TAMs) and tumour associated neutrophils (TANs)[315].

Within the tumour microenvironment, hypoxic conditions induce NF kappa B- mediated CXCL8 expression in vascular endothelial cells, which results in angiogenesis in breast and colon cancer. It has been shown, that CXCL8 induces upregulation of ACKR3, which is likely involved in endothelial progenitor cell mediated angiogenesis[316].
Furthermore, tumour associated endothelial cells secrete CXCL12 that promotes ACKR3-mediated angiogenesis via ERK1/2 phosphorylation via an autocrine/paracrine loop. It is also reported that vascular endothelial growth factor (VEGF) stimulation upregulates ACKR3 expression in endothelial cells. VEGF is stimulated by hypoxia that is characteristic of tumours and ACKR3 is also stimulated by hypoxia-inducible factor (HIF1a). Regarding this, it is likely that once hypoxic conditions are established within the tumour, ACKR3 expression by tumour endothelial cells is induced by both HIF1a and VEGF. After this, ACKR3 plays a decisive role in tumour-associated angiogenesis and subsequent tumour growth[317] .

In the cancer literature, there are no studies that can give us information about the expression levels of ACKR3 in the lymphatic system or in cancer-associated fibroblasts (CAFs), but it would be interesting to assess if there is any alteration in the levels of expression in these cells. After our observations about the expression of ACKR3 in the resting lung we generated ACKR3 and CXCR4 null murine cancer cell lines using

CRISPR/Cas9 genome editing technology to model ACKR3 involvement in lung cancer progression but also in the initial seeding steps in cancer metastasis in the lung. We observed a role for ACKR3 in both mouse models we employed in chapter 5.

In lung cancer, ACKR3 has been reported to promote tumour development by increasing tumour cell proliferation and inhibiting apoptosis. More specifically, in lung cancer, TGF-β increased ACKR3 expression, and this was correlated with a poor prognosis. In breast and prostate cancer, ACKR3 was reported to form heterodimers with EGFR and promote tumour cell proliferation in a ligand-independent way[318]. Finally, in renal cancer, ACKR3 expression promoted tumour growth by activating the mTOR pathway and ACKR3 expression was correlated with a poor clinical outcome[319].

One of the ligands that ACKR3 scavenges, and which has been associated with tumour progression, is CXCL12. ACKR3 is mainly a scavenger receptor for CXCL12, and there is the possibility that, by regulating the levels of CXCL12 in the microenvironment, ACKR3 assists CXCR4-mediated signalling by preventing CXCR4 saturation. In our models, the lack of ACKR3 could cause an increase in the levels of CXCL12 in the extracellular milieu. The CXCL12-CXCR4 signalling has been associated with dendritic cell trafficking into tumours but also with tumour cell proliferation[320]. In ovarian cancer cells, CXCL12 and hypoxia-induced VEGF synergise to induce neoangiogenesis and endothelial cell survival[321].

CXCR4 has also been shown to induce proliferation in glioblastoma tumour cells. In another study, it was shown that a proliferative phenotype in glioma cells could be induced by CXCL12, and that it is mediated through ERK and AKT signalling cascades. CXCL12 can also increase proliferation in ovarian cancer cells and prostate cancer[322,323]. In small cell lung cancer (SCLC) cell lines, CXCR4 is almost ubiquitously expressed in different cell lines, and CXCL12 can induce proliferation, cell adhesion and morphological changes in these cells[324]. In preclinical models, pharmacological

inhibition of CXCR4-CXCL12 signalling using anti-CXCL12 antibodies abrogated tumour extravasation and metastasis and reduced tumour growth[325,326]. Some studies have shown that expression of ACKR3 is associated with increased proliferation and adhesion properties in the context of cancer[327,328,229].

In prostate cancer, CXCL8 leads to upregulation of ACKR3 that causes a more proliferative phenotype in these cells. More specifically transient siRNA silencing of ACKR3 in PC-3 and LNCaP human prostate cancer cell lines reduced by more than 50% the proliferation rate. The downregulation of ACKR3 blocked the cell cycle and caused cell cycle arrest in the G1 phase. Furthermore, exogenous administration of ACKR3 ligands CXCL11 and CXCL12 did not increase the proliferative ability of those cells. This indicates that the ACKR3 driven proliferative phenotype is independent of the ACKR3 ligands. Instead, the authors proposed that ACKR3 interacts with EGFR (estrogen growth factor receptor) and leads to ERK mediated proliferation[261].

In a recent clinical study, it has been proposed that ACKR3 is upregulated in prostate cancer patients that exhibit resistance after treatment with enzalutamide, a new androgen receptor antagonist. These groups of patients exhibited higher levels of MAPK/ERK activation. This enzalutamide-resistant phenotype was attributed to elevated levels of ACKR3, and is β arrestin/MAPK-dependent but ACKR3 ligand- independent. In this study, ACKR3 could serve as a clinical biomarker in this group of patients. Furthermore, treatment with MAPK/ ERK inhibitors improved the therapeutic outcome of enzalutamide in this resistant group of patients. This study is another example of ACKR3 providing a survival advantage to tumour cells[330].

In a breast cancer study, the authors took advantage of an in vivo bioluminescence imaging assay to monitor ACKR3 scavenging of its ligand CXCL12 that was secreted within the tumour microenvironment. Furthermore, they used orthotopic human breast cancer xenografts, and demonstrated that ACKR3 scavenges CXCL12 and reduces its bioavailability within the tumour. They also demonstrated through staining of primary

human breast cancers that CXCR4 and ACKR3 are frequently expressed on different cell populations within the same tumour[331].

Tumour xenografts of human mammary fibroblasts secreting CXCL12, exhibited increased proliferation and spontaneous metastasis of CXCR4 positive cancer cells when a separate population of cancer cells expressing ACKR3 was present. Finally, the use of a CXCL12 inhibitor in orthotopic tumours decreased the ACKR3+ cancer cells' effect on the growth of CXCR4+ cancer cells[332,333].

While the role of ACKR3 in promoting cancer growth is well established, the role of ACKR3 in the metastatic process is controversial. Cell migration and invasion that lead to metastasis require degradation of basement membrane extracellular matrix proteins by matrix metalloproteinases (MMPs). ACKR3 expression is associated with the secretion of MMP2, MMP3 and MMP9. ACKR3 overexpression is also linked with mesenchymal to epithelial transition, which is associated with metastasis. ACKR3 promotes metastasis in a breast cancer model as well as in hepatocellular carcinoma through upregulation of osteopontin[334]. In a lymphoma model, ACKR3 regulated CXCR4-mediated transendothelial migration of tumour cells[335].

In contrast, other studies propose a different role for ACKR3 in metastasis. More specifically, one study proposed that ACKR3 inhibits breast tumour metastasis by decreasing CXCR4-mediated production of metalloproteinase-12 and matrix degradation[268]. In rhabdomyosarcomas, ACKR3 expression was associated with a reduced metastatic phenotype[336].

Collectively, these paradigms highlight the pleiotropic mechanisms that ACKR3 uses to regulate the tumour growth and metastatic potential in different types of cancer. In the cancer setting, ACKR3 is working together with other receptors such as CXCR4 and

EGFR and can regulate the cell cycle, thus proliferation, metastasis of CXCR4+ cells, angiogenesis and cell adhesion[207,337].

Apart from the very well described CXCL12-depended mechanism that regulate tumour growth and metastasis the other less characterised ACKR3 ligands could play a role in the ACKR3 depended phenotypes observed in this study.
For example MIF ligand is a positive regulator for tumour growth in the Lewis Lung carcinoma subcutaneous model. More specifically, the authors reported a significant reduction in tumour growth after subcutaneous injection in MIF-1 KO mice or in a mutant mouse strain of MIF(Mif P1G mice) that abolishes the MIF topoisomerase enzymatic activity. This observation was phenocopied when using a MIF topoisomerase inhibitor in the same mouse model. This study could provide a mechanistic explanation in our ACKR3 KO observation in Lewis Lung carcinoma mouse model in chapter 5[338].

Furthermore, adrenomedullin, has also being implicated in tumour growth. More specifically *in vivo* administration of an anti- adrenomedullin antibody in a prostate tumour xenograft model abrogated tumour growth. Immunohistochemistry analyses of αAM-treated tumours revealed reduced tumour vascularisation, with included a reduction in both of blood and lymphatic endothelial cells[339].

6.2 Future directions

Based on some interesting initial observations in this study, there are several future experimental directions to shed more light on the mechanisms that ACKR3 uses to control cancer development.

Initially, one crucial limitation when working with C57BL/6 mice, is the fact that this mouse strain is lacking the expression of a functional CXCL11 protein. CXCL11 is one of the two main ligands of ACKR3. The absence of CXCL11 from our *in vivo* studies presents a major disadvantage that the experiments performed on the C57BL/6 genetic background, do not fully resemble the human microenvironment. One solution to this problem is the use of a different mouse strain that expressed CXCL11, such as the DBA/2 or BDF1 mouse strains.

Another important set of experiments will include the use of the ACKR3 LLC KO cell line in an orthotopic lung cancer mouse model. Several orthotropic lung cancer mouse models have been established in the literature that includes, the intrathoracic injection of lung cancer cell lines in the lung with the help of an ultrasound or non-invasive approaches with the use of a catheter. The orthotopic cancer mouse models are always preferable as they better resemble the microenvironment of the organ where the cancer develops[340,334].

To understand if the ACKR3 phenotype in our *in vivo* cancer models is immune system-driven, the use of immunodeficient mice would be a powerful tool. More specifically, the ACKR3 null cancer cells exhibit the same phenotype after being transplanted in immunodeficient mice, this would be a strong indication that the ACKR3 KO phenotype is immune system independent. On the other hand, if the phenotype resembles the wt phenotype, we can consider evaluating the different immune cell subsets that could possibly be involved in this process. It is also important to characterise the cytokine/chemokine differences between the wt and the ACKR3 null tumours, using ELISA or Luminex assays. The use of ACKR3 inhibitors targeting the tumours would also

be a useful tool to assess if this approach will generate similar phenotypes like the ones, we observed using the ACKR3 null cells.

Another important step would be the visualisation of ACKR3 in human biopsies from lung cancer patients. Although there are already several studies that evaluate the expression of ACKR3 in cancer biopsies using standard immunohistochemistry methods, the use of controversial ACKR3 antibodies in these studies should be taken into account when interpreting the results. One more expensive and laborious, but also more suitable, method in this case is the visualisation of the ACKR3 mRNA using RNA *in situ* hybridisation approaches (RNA ISH).

Finally, the use of spontaneous lung cancer models will allow us to evaluate the expression of ACKR3 in the tumour nodules. These mouse models could also be a useful tool to identify expression of ACKR3 in certain cell populations that are considered the ‘’cells of origin’’ in the lung cancer research field. Several studies have identified small stem cell populations residing in the lung but also in the trachea epithelium and that are considered to have cancer stem cell properties. These cancer stem cells can differentiate into all the cell types of the tumour. One obstacle in the use of spontaneous cancer mouse models in the lung cancer field is the lack of mouse models that accurately recapitulate patient histology for every lung cancer subtype. Also, we should consider that the existing murine cancer models usually have a long latency, that raises the cost related to animal care.

6.3 Concluding Remarks

ACKR3 acts both as a signalling receptor through β arrestin and as a scavenger receptor regulating the equilibrium of its ligands in the extracellular milieu.

Pharmacological targeting of ACKR3 seems a promising approach in several pathological conditions, including cancer. ACKR3 inhibitors have already attracted attention and exhibited some promising results in glioblastoma cancer mouse models[267].

Specific ACKR3 agonists or antagonists, depending on the pathophysiological context, need to be generated to improve the clinical outcome. One important challenge in these efforts is the lack of specificity since ACKR3 belongs to the GPCR family, and there are members with high homology with ACKR3. Another critical challenge is the fact that new ligands of ACKR3 are being discovered, so we need to fully understand and characterise the ACKR3 interactome to appreciate its contribution in different biological settings, including the pathophysiological conditions.

Appendices

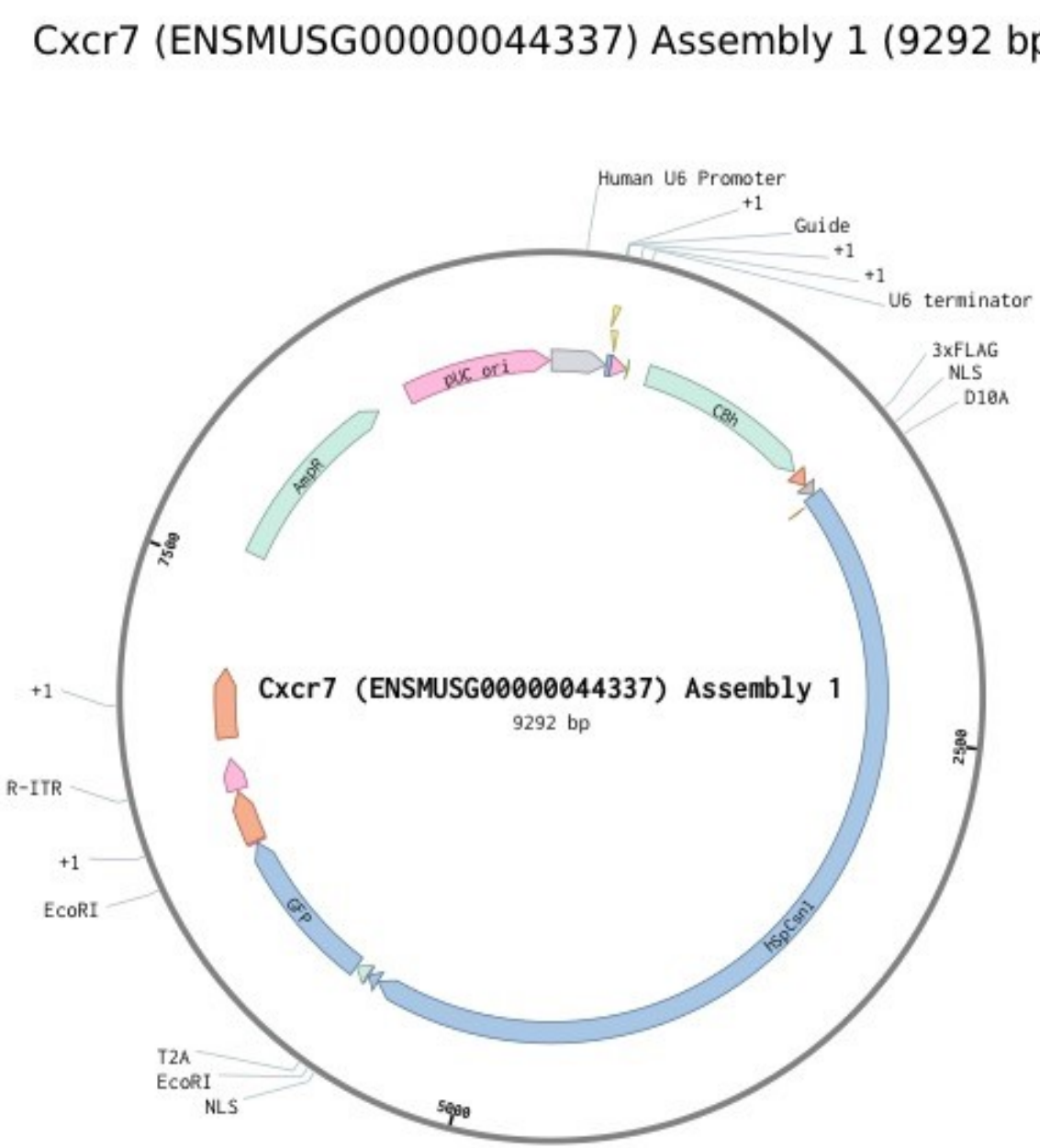

Schematic representation of the first CRISPR CAS 9 nickase plasmid (pX461 Addgene plasmid) targeting the mouse ACKR3(CXCR7) gene. Guide RNAs were cloned immediately after the U6 promoter.

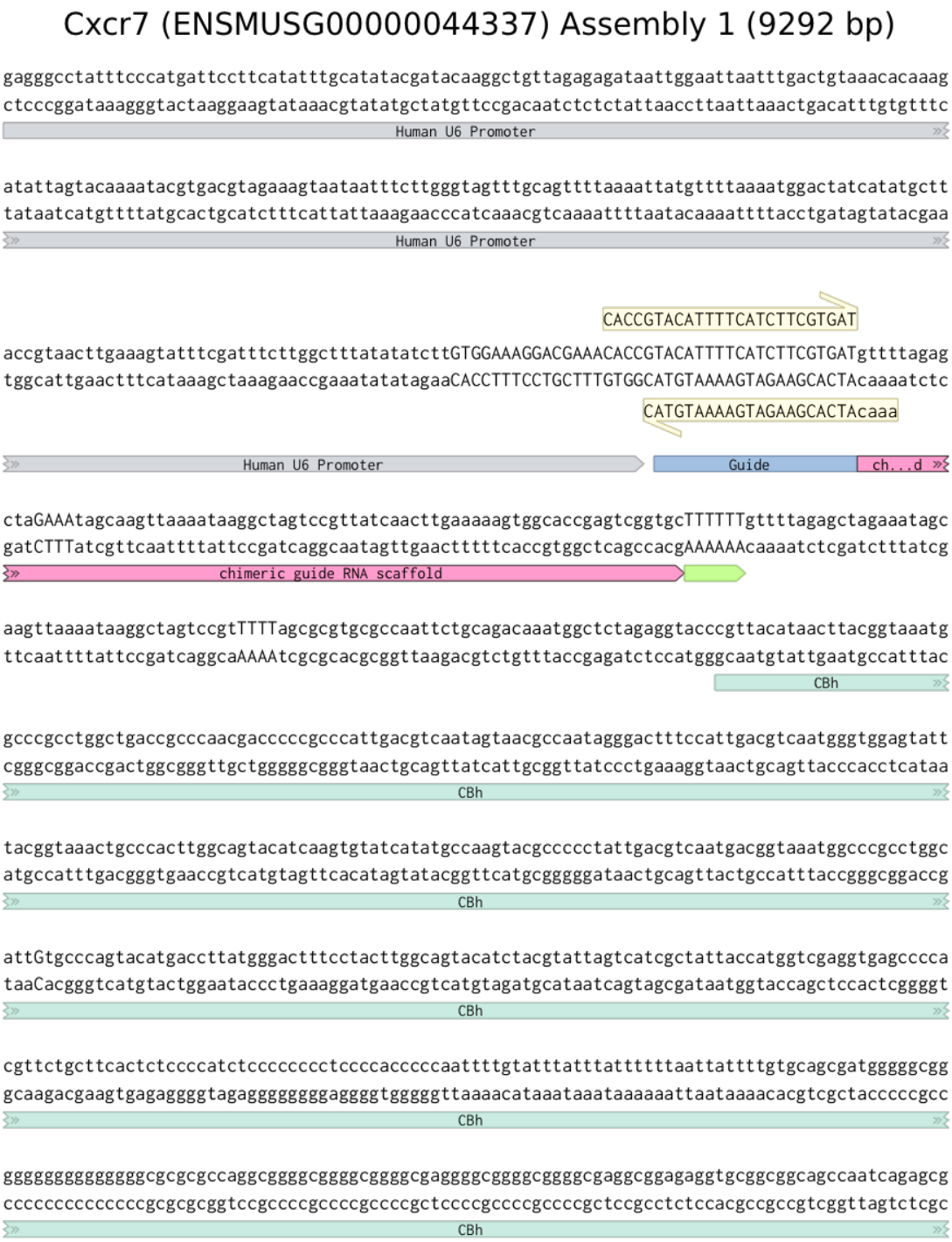

Sequence illustration that indicates where the first pair of guide RNAs (forward and reverse) were cloned in the (pX461 Addgene plasmid).

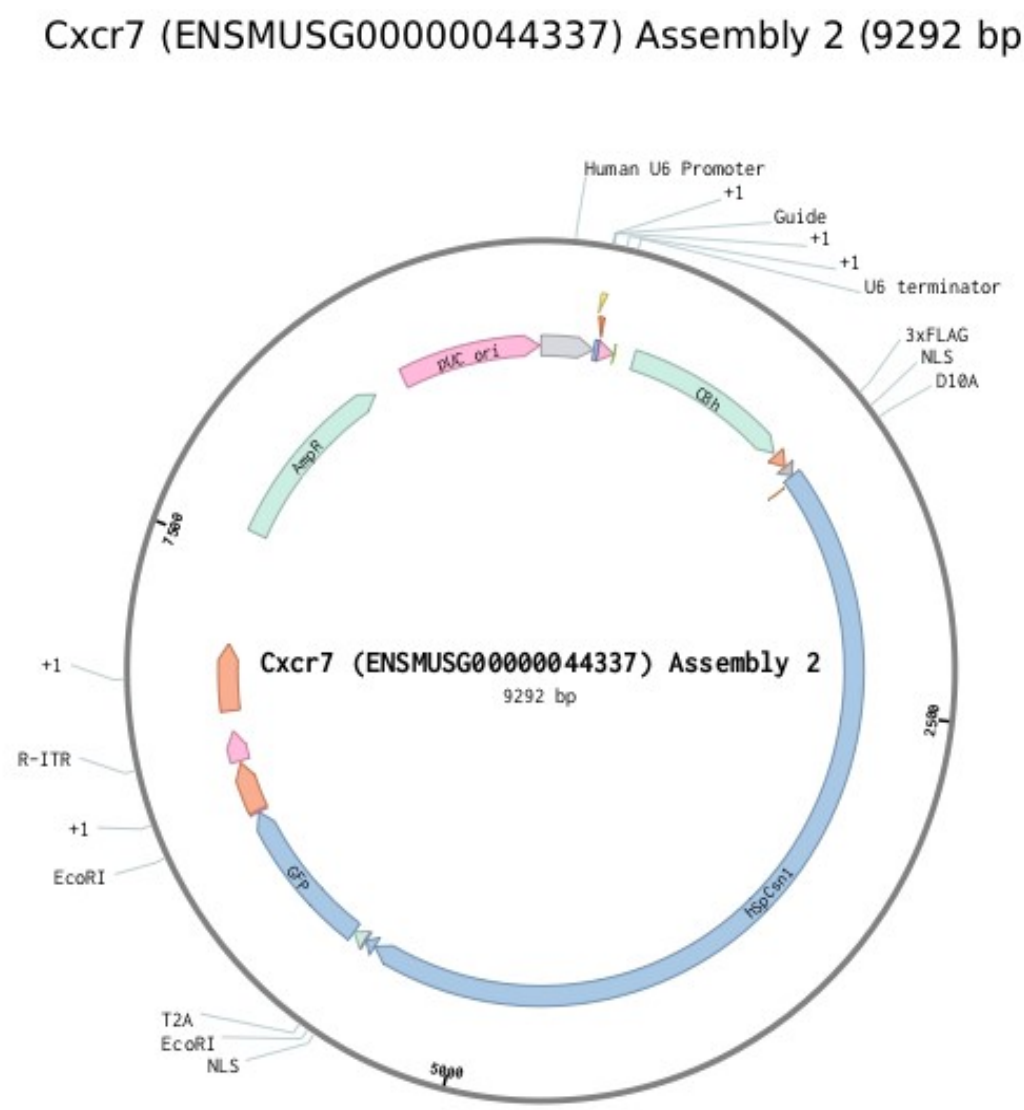

Schematic representation of the second CRISPR CAS 9 nickase plasmid (pX461 Addgene plasmid) targeting the mouse ACKR3(CXCR7) gene. Guide RNAs were cloned immediately after the U6 promoter.

Cxcr7 (ENSMUSG00000044337) Assembly 2 (9292 bp)

Sequence illustration that indicates where the second pair of ACKR3 guide RNAs (forward and reverse) were cloned in the (pX461 Addgene plasmid).

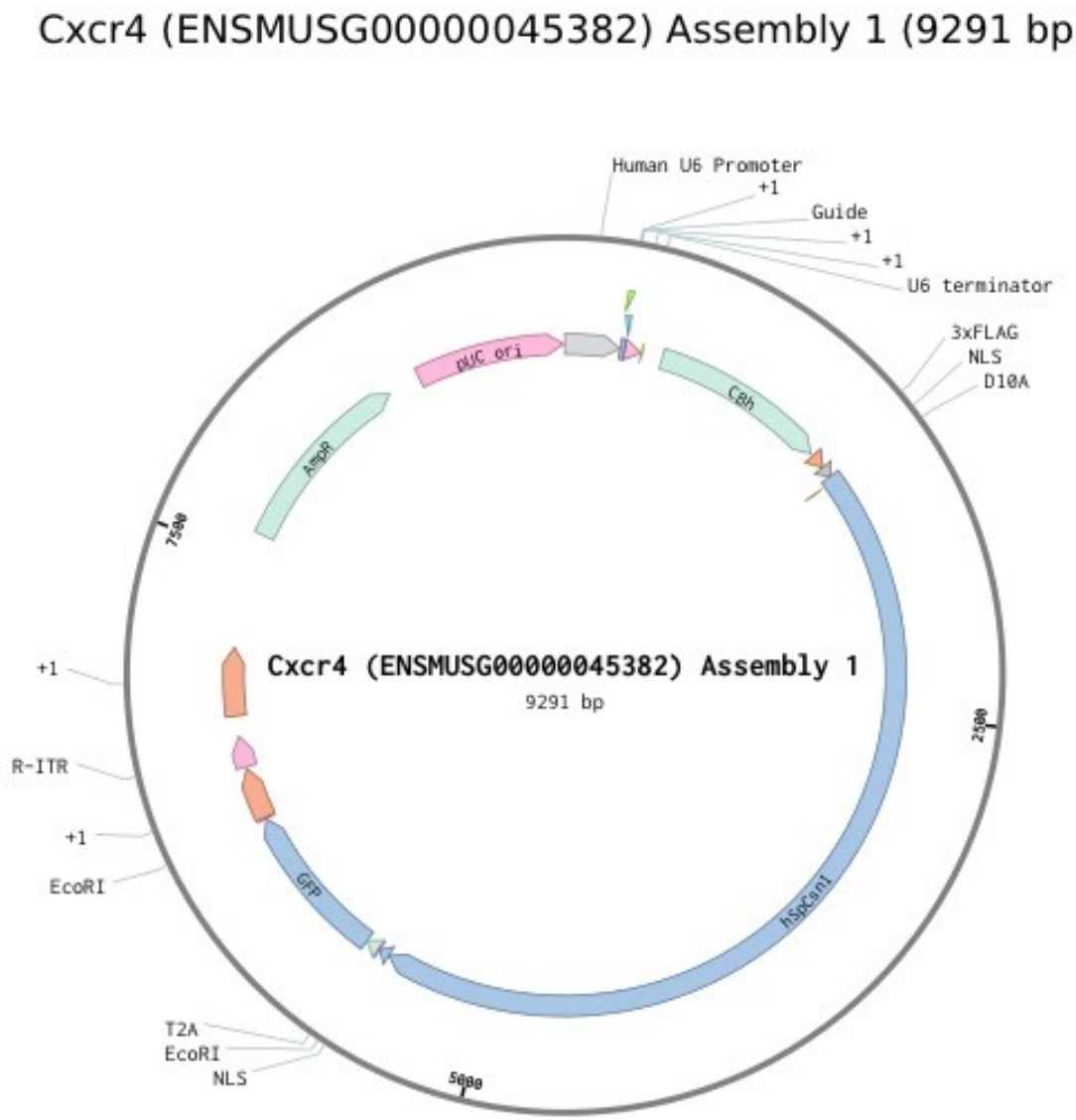

Schematic representation of the first CRISPR CAS 9 nickase plasmid (pX461 Addgene plasmid) targeting the mouse CXCR4 gene. The guide RNAs were cloned immediately after the U6 promoter.

Sequence illustration that indicates the location that the first pair of CXCR4 guide RNAs (forward and reverse) was cloned in the (pX461 Addgene plasmid).

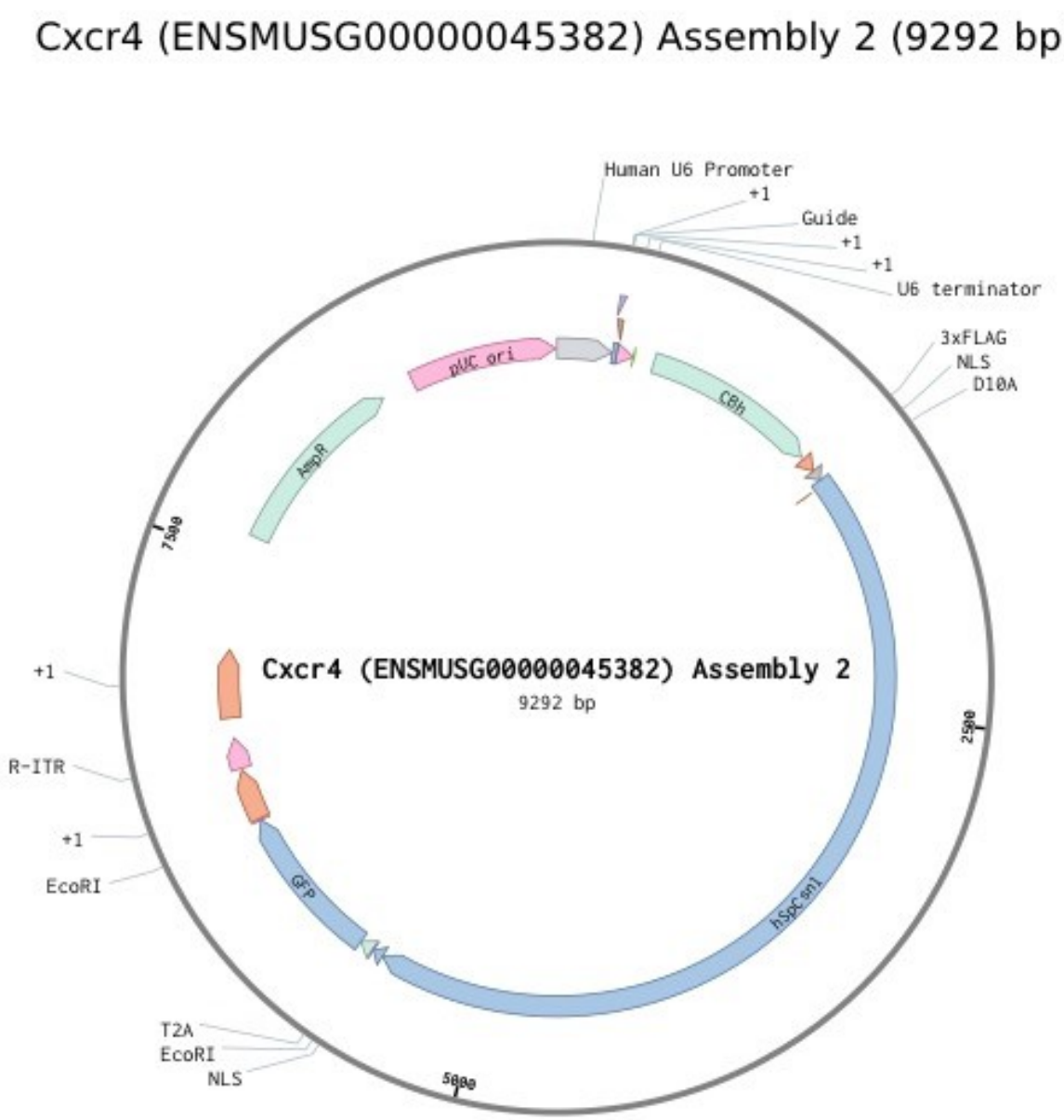

Schematic representation of the second CRISPR CAS 9 nickase plasmid (pX461 Addgene plasmid) targeting the mouse CXCR4 gene. The guide RNAs were cloned immediately after the U6 promoter.

Sequence illustration that indicates the location that the second pair of CXCR4 guide RNAs (forward and reverse) was cloned in the pX461 plasmid (Addgene).

Bibliography

1. Medzhitov R (2010) Inflammation 2010: new adventures of an old flame. Cell; 140(6):771-6

2. Abbas A.B.; Lichtman A.H. (2009) Ch.2 Innate Immunity In Saunders (Elsevier) (ed.). Basic Immunology. Functions and disorders of the immune system (3rd ed.). ISBN 978-1-4160-4688-2

3. Chen, L., Deng, H., Cui, H., Fang, J., Zuo, Z., Deng, J., … Zhao, L. (2017) Inflammatory responses and inflammation-associated diseases in organs. Oncotarget, 9(6), 7204–7218.]

4. Nathan C, Ding A (2010) Non resolving inflammation. Cell.; 140(6):871-82

5. Abdulkhaleq, L. A., Assi, M. A., Abdullah, R., Zamri-Saad, M., Taufiq-Yap, Y. H., & Hezmee, M. (2018) The crucial roles of inflammatory mediators in inflammation: A review. Veterinary world, 11(5), 627–635\

6. Balkwill F, Mantovani A (2001) Inflammation and cancer: back to Virchow? Lancet. Feb 17; 357(9255):539-45

7. Kawanishi, S., Ohnishi, S., Ma, N., Hiraku, Y., & Murata, M. (2017) Crosstalk between DNA Damage and Inflammation in the Multiple Steps of Carcinogenesis. International journal of molecular sciences, 18(8), 1808.

8. Gudkov, A. V., & Komarova, E. A. (2016) p53 and the Carcinogenicity of Chronic Inflammation. Cold Spring Harbor perspectives in medicine, 6(11), a026161.

9. Francescone, R., Hou, V., & Grivennikov, S. I. (2014) Microbiome, inflammation, and cancer. Cancer journal (Sudbury, Mass.), 20(3), 181–189.

10. Ng, L.G., Ostuni, R. & Hidalgo, A. Heterogeneity of neutrophils. (2019) Nat Rev Immunol 19, 255–265

11. Papayannopoulos, V. (2018) Neutrophil extracellular traps in immunity and disease. Nat Rev Immunol 18, 134–147

12. Lee, W. L., Harrison, R. E., & Grinstein, S. (2003) Phagocytosis by neutrophils. Microbes and Infection, 5(14), 1299–1306.

13. Diebold S.S. (2009) Activation of Dendritic Cells by Toll-Like Receptors and C-Type Lectins. In: Lombardi G., Riffo-Vasquez Y. (eds) Dendritic Cells. Handbook of Experimental Pharmacology, vol 188. Springer, Berlin, Heidelberg

14. Worbs, T., Hammerschmidt, S. & Förster, R. (2017) Dendritic cell migration in health and disease. Nat Rev Immunol 17, 30–48

15. Eisenbarth, S.C. (2019) Dendritic cell subsets in T cell programming: location dictates function Nat Rev Immunol 19, 89–103

16. Joffre OP, Segura E, Savina A, Amigorena S. (2012) Cross-presentation by dendritic cells. Nat Rev Immunol.;12(8):557-69.

17. Wynn, T. A., Chawla, A., & Pollard, J. W. (2013) Origins and Hallmarks of Macrophages: Development, Homeostasis, and Disease. Nature, 496(7446), 445–455.

18. Epelman, S., Lavine, K. J., & Randolph, G. J. (2014) Origin and Functions of Tissue Macrophages. Immunity, 41(1), 21–35.

19. Mosser, David M, and Justin P Edwards. (2008) Exploring the full spectrum of macrophage activation. Nature reviews. Immunology vol. 8,12 958-69.

20. Murray PJ, Wynn TA (2011) Protective and pathogenic functions of macrophage subsets. Nat Rev Immunol, 11(11):723-37.

21. Pennock, N. D., White, J. T., Cross, E. W., Cheney, E. E., Tamburini, B. A., & Kedl, R. M. (2013) T cell responses: naive to memory and everything in between. Advances in physiology education, 37(4), 273–283.

22. Fang, P., Li, X., Dai, J. et al. (2018) Immune cell subset differentiation and tissue inflammation. J Hematol Oncol 11, 97.

23. Lever, M., Maini, P., van der Merwe, P. et al. (2014) Phenotypic models of T cell activation. Nat Rev Immunol 14, 619–629 .

24. Smith-Garvin, J. E., Koretzky, G. A. et Jordan, M. S. (2009) T cell activation. Annual review of immunology, 27, 591–619.

25. Arundhati Mandal, Chandra Viswanathan (2015) Natural killer cells: In health and disease. Hematology/Oncology and Stem Cell Therapy, Volume 8, Issue 2,Pages 47-55

26. Crouse, J., Xu, H.C., Lang, P.A., Oxenius, A. (2015) NK cells regulating T cell responses: Mechanisms and outcome Trends in Immunology, 36 (1), pp. 49-58.

27. Lauffenburger, D.A. & Zigmond, S.H. (1981) Chemotactic factor concentration gradients in chemotaxis assay systems. J. Immunol. Methods 40, 45–60

28. Yoshie O, Imai T, Nomiyama H. (2001) Chemokines in immunity. Adv Immunol. 78:57–11

29. Furie MB, Randolph GJ. (1995) Chemokines and Tissue Injury. Am J Pathol 146:1287–301

30. Wang, Fei. (2009) The signaling mechanisms underlying cell polarity and chemotaxis. Cold Spring Harbor perspectives in biology vol. 1,4

31. Miller, A. F., & Falke, J. J. (2004) Chemotaxis Receptors and Signaling. Advances in Protein Chemistry, 393–444

32. Horuk R (1996) Chemoattractant Ligands and Their Receptors

33. Nomiyama H. et al. (2013) Systematic classification of vertebrate chemokines based on conserved synteny and evolutionary history. Genes Cells 18, 1–16 5

34. Zlotnik A, Yoshie O. (2000) Chemokines: a new classification system and their role in immunity. Immunity.; 12:121–127

35. Zlotnik, A., Yoshie, O. & Nomiyama, H. (2006) The chemokine and chemokine receptor superfamilies and their molecular evolution. Genome Biol 7, 243

36. Knaut, H., Werz, C., Geisler, R. et al. (2003) A zebrafish homologue of the chemokine receptor Cxcr4 is a germ-cell guidance receptor. Nature 421, 279–282

37. Le Y, Zhou Y, Iribarren P, Wang J (2004) Chemokines and chemokine receptors: their manifold roles in homeostasis and disease. Cellular & Molecular Immunology. 1 (2): 95–104. PMID 16212895

38. Moser, B. (2004) Chemokines: role in inflammation and immune surveillance. Annal of the Rheumatic Diseases, 63(suppl_2), ii84–ii89

39. Kufareva, I.; Salanga, C.L.; Handel, T.M (2015) Chemokine and chemokine receptor structure and interactions: Implications for therapeutic strategies. Immunol. Cell Biol., 93, 372–383

40. Rajagopalan, L.; Rajarathnam, K (2006) Structural basis of chemokine receptor function—A model for binding affinity and ligand selectivity. Biosci. Rep., 26, 325–339

41. Wang, X., Sharp, J. S., Handel, T. M., & Prestegard, J. H. (2013) Chemokine oligomerization in cell signaling and migration. Progress in molecular biology and translational science, 117, 531–578

42. Mihov, D.; Spiess, M. (2015) Glycosaminoglycans: Sorting determinants in intracellular protein traffic. Int. J. Biochem. Cell Biol., 68, 87–91

43. Handel, T. M., Johnson, Z., Crown, S. E., Lau, E. K., and Proudfoot, A. E. (2005) Regulation of protein function by glycosaminoglycans—as exemplified by chemokines. Annu. Rev. Biochem. 74, 385–410

44. Ali, S.; Hardy, L.A.; Kirby, J.A. (2003) Transplant immunobiology: A crucial role for heparan sulfate glycosaminoglycans? Transplantation, 75, 1773–1782

45. Bao, X.; Moseman, E.A.; Saito, H.; Petryanik, B.; Thiriot, A.; Hatakeyama, S.; Ito, Y.; Kawashima, H.; Yamaguchi, Y.; Lowe, J.B.; et al. (2010) Endothelial heparan sulfate controls chemokine presentation in recruitment of lymphocytes and dendritic cells to lymph nodes. Immunity, 33, 817–829

46. Laing KJ, Secombes CJ (2004) "Chemokines". Developmental and Comparative Immunology. 28 (5): 443–60

47. Proudfoot, A. E., Handel, T. M., Johnson, Z., Lau, E. K., Li Wang, P., Clark-Lewis, I., Borlat, F., Wells, T. N., & Kosco-Vilbois, M. H. (2003) Glycosaminoglycan binding and oligomerization are essential for the in vivo activity of certain chemokines. Proceedings of the National Academy of Sciences of the United States of America, 100(4), 1885–1890

48. Groves, D. T., & Jiang, Y. (1995) Chemokines, a Family of Chemotactic Cytokines. Critical Reviews in Oral Biology &Medicine,6(2),109– 118

49. Islam, S. A., Chang, D. S., Colvin, R. A., Byrne, M. H., McCully, M. L., Moser, B., Lira, S. Charo, I. F., & Luster, A. D. (2011) Mouse CCL8, a CCR8 agonist, promotes atopic dermatitis by recruiting IL-5+ T(H)2 cells. Nature immunology, 12(2), 167–17

50. Boring, L., Gosling, J., Chensue, S. W., Kunkel, S. L., Farese, R. V., Jr, Broxmeyer, H. E., & Charo, I. F. (1997) Impaired monocyte migration and reduced type 1 (Th1) cytokine responses in C-C chemokine receptor 2 knockout mice. The Journal of clinical investigation, 100(10), 2552–2561

51. Hirota, K., Yoshitomi, H., Hashimoto, M., Maeda, S., Teradaira, S., Sugimoto, N., Yamaguchi, T., Nomura, T., Ito, H., Nakamura, T., Sakaguchi, N., & Sakaguchi, S. (2007) Preferential recruitment of CCR6-expressing Th17 cells to inflamed joints via CCL20 in rheumatoid arthritis and its animal model. The Journal of experimental medicine, 204(12), 2803–2812

52. Tiberio, L., Del Prete, A., Schioppa, T., Sozio, F., Bosisio, D., & Sozzani, S. (2018). Chemokine and chemotactic signals in dendritic cell migration. Cellular & molecular immunology, 15(4), 346–352

53. Fong AM, Robinson LA, Steeber DA, et al. (1998) Fractalkine and CX3CR1 mediate a novel mechanism of leukocyte capture, firm adhesion, and activation under physiologic flow. J Exp Med.; 188(8):1413-1419.

54. M.B. Dorner, X. Zhou, C. Opitz, A. Mora, S. Güttler, A. Hutloff, H.W. Mages, K. R anke, M. Schaefer, et al.(2009) Selective expression of the chemokine receptor XCR1 on cross-presenting dendritic cells determines cooperation with CD8+ T cells. Immunity. 31:823–833.

55. Blaschke S., Middel P., Dorner B. G., Blaschke V., Hummel K. M., Kroczek R. A., Reich K., Benoehr P., Koziolek M., Muller G. A. (2003) Expression of activation induced, T cell-derived, and chemokine-related cytokine/lymphotactin and its functional role in rheumatoid arthritis. Arthritis Rheum. 48, 1858–187210.1002/art.11

56. Levashova, Z. B., Sharma, N., Timofeeva, O. A., Dome, J. S., & Perantoni, A. O. (2007) ELR+ CXC Chemokines and their Receptors in early metanephric development. Journal of the American Society of Nephrology, 18(8), 2359–2370.

57. Kiefer F Siekmann AF (2011) The role of chemokines and their receptors in angiogenesis. Cellular and Molecular Life Sciences682811–2830.

58. Rees PA, Greaves NS, Baguneid M, Bayat A. (2015) Chemokines in Wound Healing and as Potential Therapeutic Targets for Reducing Cutaneous Scarring. Advances in Wound Care. Nov;4(11):687-703.

59. Sugiyama, T., Kohara, H., Noda, M., & Nagasawa, T. (2006) Maintenance of the Hematopoietic Stem Cell Pool by CXCL12-CXCR4 Chemokine Signaling in Bone Marrow Stromal Cell Niches. Immunity, 25(6), 977–988.

60. Robert Fredriksson, Malin C. Lagerstrom, Lars-Gustav Lundin, and Helgi B. (2003) The G-Protein-Coupled Receptors in the Human Genome Form Five Main Families. Phylogenetic Analysis, Paralogon Groups, and Fingerprints. Molecular Pharmacology.63(6):1256–1272, .

61. Clapham DE, Neer EJ (1997) G protein beta gamma subunits. Annual Review of Pharmacology and Toxicology. 37: 167–203.

62. Hughes, C. E., & Nibbs, R. (2018) A guide to chemokines and their receptors. The FEBS journal, 285(16), 2944–2971.

63. Craig Murdoch, Adam Finn (2000) Chemokine receptors and their role in inflammation and infectious diseases. Blood ; 95 (10): 3032–3043.

64. Chatterjee, S., Behnam Azad, B., & Nimmagadda, S. (2014) The intricate role of CXCR4 in cancer. Advances in cancer research, 124, 31–82.

65. Takabatake, Y., Sugiyama, T., Kohara, H., Matsusaka, T., Kurihara, H., Koni, P. A., Nagasawa, Y., Hamano, T., Matsui, I., Kawada, N., Imai, E., Nagasawa, T., Rakugi, H., & Isaka, Y. (2009). The CXCL12 (SDF-1)/CXCR4 axis is essential for the development of renal vasculature. *Journal of the American Society of Nephrology : JASN*, *20*(8), 1714–1723.

66. Baekkevold, E. S., Yamanaka, T., Palframan, R. T., Carlsen, H. S., Reinholt, F. P., von Andrian, U. H., Brandtzaeg, P., & Haraldsen, G. (2001). The CCR7 ligand elc (CCL19) is transcytosed in high endothelial venules and mediates T cell recruitment. *The Journal of experimental medicine*, *193*(9), 1105–1112.

67. Forster R., Schubel A., Breitfeld D., Kremmer E., Renner-Muller I., Wolf E., Lipp M. (1999) CCR7 coordinates the primary immune response by establishing functional microenvironments in secondary lymphoid organs. Cell;99:23–33

68. Voigt, S.A. Camacho, B.A. de Boer, M. Lipp, R. Forster, C. Berek (2000) CXCR5-deficient mice develop functional germinal centers in the splenic T cell zone Eur. J. Immunol., 30 pp. 560-567

69. Tuteja, Narendra. (2009) Signalling through G protein coupled receptors. Plant signalling & behavior vol. 4,10 : 942-7.

70. Nelken NA, Coughlin SR, Gordon D, Wilcox JN. (1991) Monocyte chemoattractant protein-1 in human atheromatous plaques. J Clin Invest.;88: 1121.

71. Gu L, Okada Y, Clinton SK, et al. (1998) Absence of monocyte chemoattractant protein-1 reduces atherosclerosis in low density lipoprotein receptor-deficient mice. Molecular Cell, Volume 2, Issue 2, 275 - 281

72. Boring L, Gosling J, Cleary M, Charo IF. (1998) Decreased lesion formation in CCR2-/-mice reveals a role for chemokines in the initiation of atherosclerosis. Nature.; 394:894.

73. Han KH, Tangirala RK, Green SR, Quehenberger O. (1998) Chemokine receptor CCR2 expression and monocyte chemoattractant protein-1-mediated chemotaxis in human monocytes: a regulatory role for plasma LDL. Arterioscler Thromb Vasc Biol.; 18:1983

74. Weber C, Draude G, Weber KS, Wubert J, Lorenz RL, Weber PC. (1999) Downregulation by tumor necrosis factor-alpha of monocyte CCR2 expression and monocyte chemotactic protein-1-induced transendothelial migration is antagonized by oxidized low-density lipoprotein: a potential mechanism of monocyte retention in atherosclerotic lesions. Atherosclerosis.; 145:115

75. Teupser D, Pavlides S, Tan M, Gutierrez-Ramos JC, Kolbeck R, Breslow JL. (2004) Major reduction of atherosclerosis in fractalkine (CX3CL1)-deficient mice is at the

brachiocephalic artery, not the aortic root. Proc Natl Acad Sci U S A.; 101: 17795–17800

76. Moatti D, Faure S, Fumeron F, Amara Mel W, Seknadji P, McDermott DH, Debre P, Aumont MC, Murphy PM, de Prost D, Combadiere C. (2001) Polymorphism in the fractalkine receptor CX3CR1 as a genetic risk factor for coronary artery disease. Blood.; 97: 1925–1928.

77. McDermott DH, Halcox JP, Schenke WH, Waclawiw MA, Merrell MN, Epstein N, Quyyumi AA, Murphy PM. (2001) Association between polymorphism in the chemokine receptor CX3CR1 and coronary vascular endothelial dysfunction and atherosclerosis. Circ Res 2001;89:401–407

78. Feng Y, Broder CC, Kennedy PE, Berger EA. (1996) HIV-1 entry cofactor: functional cDNA cloning of a seven-transmembrane, G protein-coupled receptor .Science.; 272:872

79. Doranz BJ, Rucker J, Yi Y, et al. (1996) A dual-tropic primary HIV-1 isolate that uses fusin and the beta- chemokine receptors CKR-5, CKR-3, and CKR-2b as fusion cofactors. Cell.; 85:1149

80. Dragic T, Litwin V, Allaway GP, et al. (1996) HIV-1 entry into CD4 cells is mediated by the chemokine receptor CC-CKR-5. Nature.; 381:667.

81. Samson M., Libert F., Doranz B.J. 9 (1996) Resistance to HIV-1 infection in caucasian individuals bearing mutant alleles of the CCR-5 chemokine receptor gene. Nature. 1996;382:722–72

82. Hütter, G., Neumann, M., Nowak, D. et al. (2011) The effect of the CCR5-delta32 deletion on global gene expression considering immune response and inflammation. J Inflamm 8, 29

83. Glass, W. G., McDermott, D. H., Lim, J. K., Lekhong, S., Yu, S. F., Frank, W. A., Pape, J., Cheshier, R. C., & Murphy, P. M. (2006) CCR5 deficiency increases risk of symptomatic West Nile virus infection. The Journal of experimental medicine, 203(1), 35–40

84. Rodger D. MacArthur, Richard M. Novak (2008) Maraviroc: The First of a New Class of Antiretroviral Agents, Clinical Infectious Diseases, Volume 47, Issue 2, 15 July 2008, Pages 236–241

85. Lukacs NW, Kunkel SL (1998) Chemokines and their role in disease. Int J Clin Lab Res.; 28:91

86. Schroder JM, Noso N, Sticherling M, Christophers E. (1996) Role of eosinophil chemotactic C-C chemokines in cutaneous inflammation. J Leukoc Biol.; 59:1

87. Schulz BS, Michel G, Wagner S, et al. (1993) Increased expression of epidermal IL-8 receptor in psoriasis: down-regulation by FK-506 in vitro. J Immunol.; 151:4399.

88. Tuschil A, Lam C, Haslberger A, Lindley I. (1992) Interleukin-8 stimulates calcium transients and promotes epidermal cell proliferation. J Invest Dermatol.; 99:294.

89. Hedrick, M. N., Lonsdorf, A. S., Hwang, S. T., & Farber, J. M. (2010) CCR6 as a possible therapeutic target in psoriasis. Expert opinion on therapeutic targets, 14(9), 911–922

90. Homey, B., Alenius, H., Müller, A. et al. (2002) CCL27–CCR10 interactions regulate T cell–mediated skin inflammation. Nat Med 8, 157–165.

91. Kunkel SL, Lukacs N, Kasama T, Strieter RM. (1996) The role of chemokines in inflammatory joint dis- ease. J Leukoc Biol.; 59:6

92. Buckley, C. D., and McGettrick, H. M. (2018) Leukocyte trafficking between stromal compartments: lessons from rheumatoid arthritis. Nat. Rev. Rheumatol. 14, 476–48

93. Szekanecz, Z., Vegvari, A., Szabo, Z., & Koch, A. E. (2010) Chemokines and chemokine receptors in arthritis. Frontiers in bioscience (Scholar edition), 2, 153–167.

94. Rampersad, R. R., Tarrant, T. K., Vallanat, C. T., Quintero-Matthews, T., Weeks, M. F., Esserman, D. A., Clark, J., Di Padova, F., Patel, D. D., Fong, A. M., & Liu, P. (2011). Enhanced Th17-cell responses render CCR2-deficient mice more susceptible for autoimmune arthritis. PloS one, 6(10), e25833.

95. Szekanecz, Z., Koch, A. (2016) Successes and failures of chemokine-pathway targeting in rheumatoid arthritis. Nat Rev Rheumatol 12, 5–13

96. Nagarsheth, N., Wicha, M. S., & Zou, W. (2017) Chemokines in the cancer microenvironment and their relevance in cancer immunotherapy. Nature Reviews Immunology, 17(9), 559–572.

97. Hanahan, D., & Weinberg, R. A. (2011) Hallmarks of Cancer: The Next Generation. Cell, 144(5), 646–674.

98. Bonavita O, Massara M, Bonecchi R. (2016) Chemokine regulation of neutrophil function in tumours. Cytokine Growth Factor Rev.30:81–6.

99. Correale P, Rotundo MS, Botta C, Del Vecchio MT, Tassone P, Tagliaferri P. (2012) Tumor infiltration by chemokine receptor 7 (CCR7)(+) T-lymphocytes is a favorable prognostic factor in metastatic colorectal cancer. Oncoimmunology. 1:531–2.

100. Mburu YK, Wang J, Wood MA, Walker WH, Ferris RL. (2006) CCR7 mediates inflammation-associated tumor progression. Immunol Res. 36:61–72.

101. Gobert M, Treilleux I, Bendriss-Vermare N, Bachelot T, Goddard-Leon S, Arfi V, et al. (2009) Regulatory T cells recruited through CCL22/CCR4 are selectively activated in lymphoid infiltrates surrounding primary breast tumors and lead to an adverse clinical outcome. Cancer Res. 69:2000–9.

102. Wendel M, Galani IE, Suri-Payer E, Cerwenka A. (2008) Natural killer cell accumulation in tumors is dependent on IFN-gamma and CXCR3 ligands. Cancer Res. 68:8437–45.

103. Scarpino S, Stoppacciaro A, Ballerini F, Marchesi M, Prat M, Stella MC, et al. (2000) Papillary carcinoma of the thyroid, hepatocyte growth factor (HGF) stimulates tumor cells to release chemokines active in recruiting dendritic cells. Am J Pathol. 156:831–7.

104. Zlotnik A, Burkhardt AM, Homey B. (2011) Homeostatic chemokine receptors andorgan-specific metastasis. Nat Rev Immunol. 11:597–606.

105. Takanami I. (2003) Overexpression of CCR7 mRNA in non-small cell lung cancer, correlation with lymph node metastasis. Int J Cancer. 105:186–9.

106. Muller A, Homey B, Soto H, Ge N, Catron D, Buchanan ME, et al. (2001) Involvement of chemokine receptors in breast cancer metastasis. Nature.; 410:50–6.

107. Wiley HE, Gonzalez EB, Maki W, Wu MT, Hwang ST. (2001) Expression of CC chemokine receptor-7 and regional lymph node metastasis of B16 murine melanoma. J Natl Cancer Inst.; 93:1638–43.

108. Gunther K, Leier J, Henning G, Dimmler A, Weissbach R, Hohenberger W, et al. (2005) Prediction of lymph node metastasis in colorectal carcinoma by expression of chemokine receptor CCR7. Int J Cancer.; 116:726–33.

109. Phillips RJ, Burdick MD, Lutz M, Belperio JA, Keane MP, Strieter RM. (2003) The stromal derived factor-1/CXCL12-CXC chemokine receptor 4 biological axis in non-small cell lung cancer metastases. Am J Respir Crit Care Med.; 167:1676–86.

110. Koizumi K, Hojo S, Akashi T, Yasumoto K, Saikil (2007) Chemokine receptors in cancer metastasis and cancer cell-derived chemokines in host immune response. Cancer Sci.;98(11):1652–1658.

111. Owen JD, Strieter R, Burdick M, Haghnegahdar H, Nanney L, Shattuck-Brandt R, Richmond A (1997) Enhanced tumor-forming capacity for immortalized melanocytes expressing melanoma growth stimulatory activity/growth-regulated cytokine beta and gamma proteins. Int J Cancer. 73:94–103,

112. Keeley EC, Mehrad B, Strieter RM. (2010) CXC chemokines in cancer angiogenesis and metastases. Adv Cancer Res. 106:91–111.

113. Lin L, Chen YS, Yao YD, Chen JQ, Chen JN, Huang SY,et al. (2015) CCL18 from tumor-associated macrophages promotes angiogenesis in breast cancer. Oncotarget 6:34758–73.

114. Wente, M. N., Keane, M. P., Burdick, M. D., Friess, H., Büchler, M. W., Ceyhan, G. O., Hines, O. J. (2006) Blockade of the chemokine receptor CXCR2 inhibits pancreatic cancer cell-induced angiogenesis. Cancer Letters, 241(2), 221–227.

115. Lau TS, Chung TK, Cheung TH, Chan LK, Cheung LW, Yim SF, et al. (2014) Cancer cell-derived lymphotoxin mediates reciprocal tumor-stromal interactions in human ovarian cancer by inducing CXCL11 in fibroblasts. J Pathol. 232:43–56.

116. Mishra P, Banerjee D, Ben-Baruch A (2011) Chemokines at the crossroads of tumor-fibroblast interactions that promote malignancy. J Leukoc Biol. 89:31–9.

117. Yang XL, Liu KY, Lin FJ, Shi HM, Ou ZL (2017) CCL28 promotes breast cancer growth and metastasis through MAPK-mediated cellular anti-apoptosis and pro-metastasis. Oncol Rep. 38:1393–401.

118. Liang K, Liu Y, Eer D, Liu J, Yang F, Hu K (2018) High CXC chemokine ligand 16 (CXCL16) expression promotes proliferation and metastasis of lung cancer via regulating the NF-kappa B pathway. Med Sci Monit. 24:405–11.

119. Bingyan Liu, Yiping Jia, Jun Ma, Shaoqiu Wu, Haosheng Jiang, Yan Cao, Xianjun Sun, Xiang Yin, Shuo Yan, Mingyi Shang, Aiwu Mao (2016) Tumor-associated macrophage-derived CCL20 enhances the growth and metastasis of pancreatic cancer, Acta Biochimica et Biophysica Sinica, Volume 48, Issue 12, 1, Pages 1067–1074.

120. Dhawan, P., & Richmond, A. (2002) Role of CXCL1 in tumorigenesis of melanoma. Journal of leukocyte biology, 72(1), 9–18.

121. De Clercq E. (2019) Mozobil® (Plerixafor, AMD3100), 10 years after its approval by the US Food and Drug Administration. Antiviral chemistry & chemotherapy, 27,

122. Haringman, J. J., Kraan, M. C., Smeets, T. J., Zwinderman, K. H. & Tak, P. P. (2003) Chemokine blockade and chronic inflammatory disease: proof of concept in patients with rheumatoid arthritis. Ann. Rheum. Dis. 62, 715–721.

123. Horuk R. (2005) BX471: a CCR1 antagonist with anti-inflammatory activity in man. Mini Rev Med Chem.;5(9):791–804.

124. Chu, H. X., Arumugam, T. V., Gelderblom, M., Magnus, T., Drummond, G. R., & Sobey, C. G. (2014) Role of CCR2 in inflammatory conditions of the central nervous system. Journal of cerebral blood flow and metabolism : official journal of the International Society of Cerebral Blood Flow and Metabolism, 34(9), 1425–1429.

125. James E. Pease (2017) Designing small molecule CXCR3 antagonists, Expert Opinion on Drug Discovery, 12:2, 159-168.

126. Nibbs, R. J. B., & Graham, G. J. (2013) Immune regulation by atypical chemokine receptors. Nature Reviews Immunology, 13(11), 815–829.

127. Mantovani, A., Bonecchi, R. & Locati, M. (2006) Tuning inflammation and immunity by chemokine sequestration: decoys and more. Nature Rev. Immunol. 6, 907–918.

128. Bachelerie, F., Ben-Baruch, A., Burkhardt, A. M., Combadiere, C., Farber, J. M., Graham, G. J., Horuk, R., Sparre-Ulrich, A. H., Locati, M., Luster, A. D., Mantovani, A., Matsushima, K., Murphy, P. M., Nibbs, R., Nomiyama, H., Power, C. A., Proudfoot, A. E., Rosenkilde, M. M., Rot, A., Sozzani, S., … Zlotnik, A. (2013). International Union of Basic and Clinical Pharmacology. [corrected]. LXXXIX. Update on the extended family of chemokine receptors and introducing a new nomenclature for atypical chemokine receptors. Pharmacological reviews, 66(1), 1–79.

129. Graham, G. J., Locati, M., Mantovani, A., Rot, A. & Thelen, M. (2012) The biochemistry and biology of the atypical chemokine receptors. Immunol. Lett. 145,30– 38

130. Watts, A. O. et al. (2013) β-arrestin recruitment and G protein signaling by the atypical human chemokine decoy receptor CCX-CKR. J. Biol. Chem. 288, 7169–7181.

131. Rajagopal, S. et al. β-arrestin but not G protein mediated signaling by the 'decoy' receptor CXCR7. (2010) Proc. Natl Acad. Sci. USA 107, 628–632.

132. Horuk R., Wang Z.X., Peiper S.C., Hesselgesser J. (1994) Identification and characterization of a promiscuous chemokine-binding protein in a human erythroleukemic cell-line. J. Biol. Chem.; 269:17730–17733.

133. Gardner L., Patterson A.M., Ashton B.A., Stone M.A., Middleton J. (2004) The human Duffy antigen binds selected inflammatory but not homeostatic chemokines. Biochem. Biophys. Res. Commun.; 321:306–312.

134. Szabo M.C., Soo K.S., Zlotnik A., Schall T.J. (1995) Chemokine class-differences in binding to the Duffy antigen-erythrocyte chemokine receptor. J. Biol. Chem.; 270:25348–25351.

135. Sozzani S, Del Prete A, Bonecchi R, Locati M. (2015) Chemokines as effector and target molecules in vascular biology. Cardiovasc Res. 107:364–72.

136. Du J, Luan J, Liu H, Daniel TO, Peiper S, Chen TS, et al. (2002) Potential role for Duffy antigen chemokine-binding protein in angiogenesis and maintenance of homeostasis in response to stress. J Leukoc Biol. 71:141–53.

137. Pruenster M, Mudde L, Bombosi P, Dimitrova S, Zsak M, Middleton J, et al. (2009) The Duffy antigen receptor for chemokines transports chemokines and supports their promigratory activity. Nat Immunol. 10:101–8.

138. R. Horuk, C.E. Chitnis, W.C. Darbonne, T.J. Colby, A. Rybicki, T.J. Hadley, L.H. Miller et all (1993) A receptor for the malarial parasite Plasmodium vivax — the erythrocyte chemokine receptor, Science 261 1182–1184.

139. L.H. Miller, S.J. Mason, J.A. Dvorak, M.H. Mcginniss, I.K. Rothman (1975) Erythrocyte receptors for (*Plasmodium knowlesi*) malaria — Duffy blood-group determinants, Science 189 561–563.

140. Howes, Rosalind E et al. (2011) The global distribution of the Duffy blood group. Nature communications vol. 2: 266.

141. Nomiyama H, Osada N, Yoshie O (2011) A family tree of vertebrate chemokine receptors for a unified nomenclature. Dev Comp Immunol 35:705–15.10.1016/j.dci.2011.01.019

142. Wan W, Liu Q, Lionakis MS, Marino AP, Anderson SA, Swamydas M, et al. (2015) Atypical chemokine receptor 1 deficiency reduces atherogenesis in ApoE-knockout mice. Cardiovasc Res 106(3):478–87.10.1093/cvr/cvv124

143. Nibbs R.J.B., Wylie S.M., Yang J.Y., Landau N.R., Graham G.J. (1997) Cloning and characterization of a novel promiscuous human beta-chemokine receptor D6. J. Biol. Chem.; 272:32078–32083.

144. Nibbs R.J.B., Wylie S.M., Pragnell I.B., Graham G.J (1997) Cloning and characterization of a novel murine beta chemokine receptor, D6 — comparison to three other related macrophage inflammatory protein-1 alpha receptors, CCR-1, CCR3, and CCR-5. J. Biol. Chem.; 272:12495–12504.

145. Nibbs R.J.B., Kriehuber E., Ponath P.D., Parent D., Qin S.X., Campbell J.D.M., Henderson A., Kerjaschki D., Maurer D., Graham G.J., Rot A. (2001) The

betachemokine receptor D6 is expressed by lymphatic endothelium and a subset of vascular tumors. Am. J. Pathol.; 158:867–877.

146. McKimmie C.S., Fraser A.R., Hansell C., Gutierrez L., Philipsen S., Connell L., Rot A., Kurowska-Stolarska M., Carreno P., Pruenster M., Chu C.C., Lombardi G., Halsey C., McInnes I.B., Liew F.Y., Nibbs R.J., Graham G.J. (2008) Haemopoietic cell expression of the chemokine decoy receptor D6 is dynamic and regulated by GATA1 (vol 181, pg 3353, 2008) J. Immunol.; 181:8170–8181.

147. Graham G.J., McKimmie C.S. (2006) Chemokine scavenging by D6: a movable feast? Trends Immunol.; 27:381–386

148. Lee KM, Danuser R, Stein JV, Graham D, Nibbs RJ, Graham GJ (2014) The chemokine receptors ACKR2 and CCR2 reciprocally regulate lymphatic vessel density. EMBO J 33:2564–80.10.15252/embj.201488887

149. Madigan J, Freeman DJ, Menzies F, Forrow S, Nelson SM, Young A, et al (2010) Chemokine scavenger D6 is expressed by trophoblasts and aids the survival of mouse embryos transferred into allogeneic recipients. J Immunol 184:3202–12.10.4049/jimmunol.0902118

150. Martinez de la Torre Y, Buracchi C, Borroni EM, Dupor J, Bonecchi R, Nebuloni M, et al. (2007)Protection against inflammation- and autoantibody-caused fetal loss by the chemokine decoy receptor D6. Proc Natl Acad Sci U S A 104:2319 24.10.1073/pnas.0607514104

151. Graham GJ. (2009) D6 and the atypical chemokine receptor family: novel regulators of immune and inflammatory processes. Eur J Immunol 39:342–51.10.1002/eji.200838858

152. Bordon Y, Hansell CA, Sester DP, Clarke M, Mowat AM, Nibbs RJ. (2009) The atypical chemokine receptor D6 contributes to the development of experimental colitis. J Immunol 182:5032–40.10.4049/jimmunol.0802802

153. Vetrano S, Borroni EM, Sarukhan A, Savino B, Bonecchi R, Correale C, et al. (2010) The lymphatic system controls intestinal inflammation and inflammation associated colon cancer through the chemokine decoy receptor D6. Gut 59:197 206.10.1136/gut.2009.183772

154. Whitehead GS, Wang T, DeGraff LM, Card JW, Lira SA, Graham GJ, et al. (2007) The chemokine receptor D6 has opposing effects on allergic inflammation and airway reactivity. Am J Respir CritCareMed175:243–9.10.1164/rccm.200606-839OC

155. Di Liberto D, Locati M, Caccamo N, Vecchi A, Meraviglia S, Salerno A, et al. (2008) Role of the chemokine decoy receptor D6 in balancing inflammation, immune activation, and antimicrobial resistance in Mycobacterium tuberculosis infection. J Exp Med 205:2075–84.10.1084/jem.20070608

156. Hansell, Christopher A H et al. (2018) The Atypical Chemokine Receptor Ackr2 Constrains NK Cell Migratory Activity and Promotes Metastasis Journal of immunology (Baltimore, Md.: 1950) vol. 201,8 : 2510-2519.

157. Nibbs RJ, Gilchrist DS, King V, Ferra A, Forrow S, Hunter KD, et al. (2007) The atypical chemokine receptor D6 suppresses the development of chemically induced skin tumors. J Clin Invest 117:1884–92.10.1172/JCI30068

158. Vetrano S, Borroni EM, Sarukhan A, Savino B, Bonecchi R, Correale C, et al. (2010) The lymphatic system controls intestinal inflammation and inflammation associated colon cancer through the chemokine decoy receptor D6. Gut 59:197–206.10.1136/gut.2009.183772

159. Comerford I, Milasta S, Morrow V, Milligan G, Nibbs R. (2006) The chemokine receptor CCX-CKR mediates effective scavenging of CCL19 in vitro. Eur J Immunol 36:1904–16.10.1002/eji.200535716

160. Comerford I., Nibbs R.J., Litchfield W., Bunting M., Harata-Lee Y., Haylock Jacobs S., Forrow S., Korner H., McColl S.R. (2010) The atypical chemokine receptor CCX– CKR scavenges homeostatic chemokines in circulation and tissues and suppresses Th17 responses. Blood.; 116:4130–4140

161. Heinzel K., Benz C., Bleul C.C. (2007) A silent chemokine receptor regulates steady-state leukocyte homing in vivo. Proc. Nat. Acad. Sci. U.S.A.; 104:8421–8426.

162. Ulvmar MH, Werth K, Braun A, Kelay P, Hub E, Eller K, et al. (2014) The atypical chemokine receptor CCRL1 shapes functional CCL21 gradients in lymph nodes. Nat Immunol 15:623–30.10.1038/ni.2889

163. Hoffmann F, Müller W, Schütz D, Penfold ME, Wong YH, Schulz S, and Stumm R (2012) Rapid uptake and degradation of CXCL12 depend on CXCR7 carboxylterminal serine/threonine residues. J Biol Chem 287(34): 28362-28377.

164. Naumann U, Cameroni E, Pruenster M, Mahabaleshwar H, Raz E, Zerwes HG, Rot A, and Thelen M (2010) CXCR7 functions as a scavenger for CXCL12 and CXCL11. PLoS One 5(2): 1-11.

165. Ödemis V, Lipfert J, Kraft R, Hajek P, Abraham G, Hattermann K, Mentlein R, and Engele J (2012) The presumed atypical chemokine receptor CXCR7 signals through G(i/o) proteins in primary rodent astrocytes and human glioma cells. Glia 60(3): 372-381.

166. Hao M, Zheng J, Hou K, Wang J, Chen X, Lu X, Bo J, Xu C, Shen K, and Wang J (2012) Role of chemokine receptor CXCR7 in bladder cancer progression. Biochem Pharmacol 84(2): 204- 214.

167. Rajagopal S, Kim J, Ahn S, Craig S, Lam CM, Gerard NP, Gerard C, and Lefkowitz RJ (2010) Beta- arrestin- but not G protein-mediated signaling by the decoy receptor CXCR7. Proc Natl Acad Sci USA 107(2): 628-632.

168. Ray, P., Mihalko, L. A., Coggins, N. L., Moudgil, P., Ehrlich, A., Luker, K. E., & Luker, G. D. (2012) Carboxy-terminus of CXCR7 regulates receptor localization and function. The international journal of biochemistry & cell biology, 44(4), 669–678.

169. Valentin, G. et al. (2007) The chemokine SDF1a coordinates tissue migration through the spatially restricted activation of Cxcr7 and Cxcr4b. Curr. Biol. 17, 1026–103

170. Libert, F. et al. (1989) Selective amplification and cloning of four new members ofther G protein-coupled receptor family. Science 244, 569–572

171. Burns, J.M. et al. (2006) A novel chemokine receptor for SDF-1 and ITAC involved in cell survival, cell adhesion, and tumor development. J. Exp. Med. 203, 2201–2213

172. Tripathi, V. et al. (2009) Differential expression of RDC1/CXCR7 in the human placenta. J. Clin. Immunol. 29, 379–386

173. Tarnowski, M. et al. (2010) CXCR7: a new SDF-1-binding receptor in contrast to normal CD34+ progenitors is functional and is expressed at higher level in human malignant hematopoietic cells. Eur. J. Haematol. 85, 472–483

174. Wang, H. et al. (2012) The CXCR7 chemokine receptor promotes B cell retention in the splenic marginal zone and serves as a sink for CXCL12. Blood 119, 465–468

175. Sanchez-Martin, L. et al. (2011) The chemokine CXCL12 regulates monocyte macrophage differentiation and RUNX3 expression. Blood 117, 88–97

176. Berahovich, R.D. et al. (2010) CXCR7 protein is not expressed on human or mouse leukocytes. J. Immunol. 185, 5130–5139

177. Hartmann, T.N. et al. (2008) A crosstalk between intracellular CXCR7 and CXCR4 involved in rapid CXCL12-triggered integrin activation but not in chemokine-triggered motility of human T lymphocytes and CD34+ cells. J. Leukoc. Biol. 84, 1130– 1140

178. Luker, K.E. et al. (2010) Constitutive and chemokine-dependent internalization and recycling of CXCR7 in breast cancer cells to degrade chemokine ligands. Oncogene 29, 4599–4610

179. Infantino, S. et al. (2006) Expression and regulation of the orphan receptor RDC1 and its putative ligand in human dendritic and B cells. J. Immunol. 176, 2197–2207

180. H. Hao, S. Hu, H. Chen, D. Bu, L. Zhu, C. Xu, F. Chu, X. Huo, Y. Tang, X. Sun, B.S. Ding, D.P. Liu, S. Hu, M. Wang (2017) Loss of endothelial CXCR7 impairs vascular homeostasis and cardiac remodeling after myocardial infarction: implications for cardiovascular drug discovery Circulation, 135 (13, pp. 1253-1264

181. R.D. Berahovich, B.A. Zabel, S. Lewen, M.J. Walters, K. Ebsworth, Y. Wang, J.C. Jaen, T.J. Schall (2014) Endothelial expression of CXCR7 and the regulation of systemic CXCL12 levels Immunology, 141 (1), pp. 111-122

182. V. Tripathi, R. Verma, A. Dinda, N. Malhotra, J. Kaur, K. Luthra (2009) Differential expression of RDC1/CXCR7 in the human placenta J Clin Immunol, 29 pp. 379-386

183. Puchert, M., Pelkner, F., Stein, G., Angelov, D.N., Boltze, J., Wagner, D.-C., Odoardi, F., Flügel, A., Streit, W.J. and Engele, J. (2017). Astrocytic expression of the CXCL12 receptor, CXCR7/ACKR3 is a hallmark of the diseased, but not developing CNS. Molecular and Cellular Neuroscience, 85, pp.105–118.

184. P. Abe, W. Mueller, D. Schutz, F. MacKay, M. Thelen, P. Zhang, R. Stumm (2014) CXCR7 prevents excessive CXCL12-mediated downregulation of CXCR4 in migrating cortical interneurons Development, 141 (9) pp. 1857-1863

185. J.A. Sanchez-Alcaniz, S. Haege, W. Mueller, R. Pla, F. Mackay, S. Schulz, G. Lopez-Bendito, R. Stumm, O. Marin (2011) Cxcr7 controls neuronal migration by regulating chemokine responsiveness Neuron, 69 (1) (2011), pp. 77-90

186. V. Odemis, K. Boosmann, A. Heinen, P. Kury, J. Engele (2010) CXCR7 is an active component of SDF-1 signalling in astrocytes and Schwann cells J. Cell Sci., 123 (Pt 7) pp. 1081-1088

187. Wang Y, Li G, Stanco A, Long JE, Crawford D, Potter GB, Pleasure SJ, Behrens T, Rubenstein JL (2011) CXCR4 and CXCR7 have distinct functions in regulating interneuron migration. Neuron. Jan 13; 69(1):61-76.

188. J. Kato, T. Tsuruda, T. Kita, K. Kitamura, T. Eto, (2005) Adrenomedullin: a protective factor for blood vessels, Arterioscler. Thromb. Vasc. Biol. 25 (12) 2480–2487.

189. Y. Takabatake, T. Sugiyama, H. Kohara, T. Matsusaka, H. Kurihara, P.A. Koni, Y. Nagasawa, T. Hamano, I. Matsui, N. Kawada, E. Imai, T. Nagasawa, H.

Rakugi, Y. Isaka, (2009) The CXCL12 (SDF-1)/CXCR4 axis is essential for the development of renal vasculature, J. Am. Soc. Nephrol. 20 (8) 1714-1723.

190. Schanz A, Baston-Bust D, Krussel JS, Heiss C, Janni W, Hess AP (2011) CXCR7 and syndecan-4 are potential receptors for CXCL12 in human cytotrophoblasts. J Reprod Immunol, 89: 18–25.

191. K.E. Quinn, A.K. Ashley, L.P. Reynolds, A.T. Grazul-Bilska, R.L. Ashley (2014) Activation of the CXCL12/CXCR4 signaling axis may drive vascularization of the ovine placenta, Domest. Anim. Endocrinol. 47 11–21.

192. H.L. Piao, S.C. Wang, Y. Tao, Q. Fu, M.R. Du, D.J. Li (2015) CXCL12/CXCR4 signal involved in the regulation of trophoblasts on peripheral NK cells leading to Th2 bias at the maternal-fetal interface, Eur. Rev. Med. Pharmacol. Sci. 19 (12) 2153– 2161.

193. L. Ren, Y.Q. Liu, W.H. Zhou, Y.Z. Zhang (2012) Trophoblast-derived chemokine CXCL12 promotes CXCR4 expression and invasion of human first-trimester decidual stromal cells, Hum. Reprod. 27 (2) 366–374.

194. M.J. Bilinski, J.G. Thorne, M.J. Oh, S. Leonard, C. Murrant, C. Tayade, B.A. Croy (2008) Uterine NK cells in murine pregnancy, Reprod. Biomed. Online 16 (2) 218–22

195. Q.E. Yang, D. Kim, A. Kaucher, M.J. Oatley, J.M. Oatley (2013) CXCL12-CXCR4 signaling is required for the maintenance of mouse spermatogonial stem cells, J. Cell. Sci. 126 (Pt 4) 1009–1020.

196. Westernstroer, N. Terwort, J. Ehmcke, J. Wistuba, S. Schlatt, N. Neuhaus, (2014) Profiling of Cxcl12 receptors, Cxcr4 and Cxcr7 in murine testis development and a

spermatogenic depletion model indicates a role for Cxcr7 in controlling Cxcl12 activity, PLoS One 9 (12) e112598.

197. Lataillade J. J., Domenech J., Le Bousse-Kerdilès M. C. (2015) Stromal cell derived factor-1 (SDF-1)/CXCR4 couple plays multiple roles on haematopoietic progenitors at the border between the old cytokine and new chemokine worlds: survival, cell cycling and trafficking. Eur.Cytok.Netw. 15 177–188.

198. Juarez J., Bendall L., Bradstock K. (2004) Chemokines and their receptors as therapeutic targets: the role of the SDF-1/CXCR4 axis. Curr. Pharm. Des. 10 1245–1259. 10.2174/1381612043452640

199. Bleul CC, Fuhlbrigge RC, Casasnovas JM, Aiuti A, Springer TA (1996) A highly efficacious lymphocyte chemoattractant, stromal cell-derived factor 1 (SDF-1). The Journal of Experimental Medicine. 184 (3):1101– 9.

200. Ara T, Nakamura Y, Egawa T, Sugiyama T, Abe K, Kishimoto T, Matsui Y, Nagasawa T (2003) Impaired colonization of the gonads by primordial germ cells in mice lacking a chemokine, stromal cell-derived factor-1 (SDF-1). Proceedings of the National Academy of Sciences of the United States of America. 100 (9):531923.

201. Askari AT, Unzek S, Popovic ZB, Goldman CK, Forudi F, Kiedrowski M, Rovner A, Ellis SG, Thomas JD, Di Corleto PE, Topol EJ, Penn MS (2003) Effect of stromal cell-derived factor 1 on stem-cell homing and tissue regeneration in ischaemic cardiomyopathy. Lancet. 362 (9385): 697–703.

202. Ma Q, Jones D, Borghesani PR, Segal RA, Nagasawa T, Kishimoto T, Bronson RT, Springer TA (1998) Impaired B-lymphopoiesis, myelopoiesis, and derailed cerebellar neuron migration in CXCR4-and SDF-1-deficient mice . Proceedings of the National Academy of Sciences of the United States of America. 95 (16):9448 53.

203. Li M., Ransohoff R. M. (2009) The roles of chemokine CXCL12 in embryonic and brain tumor angiogenesis. Semin. Cancer Biol. 19 111–115. 10.1016/j.semcancer.2008.11.001

204. Sugiyama, T., Kohara, H., Noda, M. & Nagasawa, T. (2006) Maintenance of the hematopoietic stem cell pool by CXCL12-CXCR4 chemokine signaling in bone marrow stromal cell niches. Immunity 25, 977–988

205. Cole K. E., Strick C. A., Paradis T. J., Ogborne K. T., Loetscher M., Gladue R. P., et al. (1998) Interferon-inducible T Cell alpha chemoattractant (I-TAC): a novel non-ELR CXC chemokine with potent activity on activated t cells through selective high affinity binding to CXCR3.J. Exp. Med. 187 2009–2021. 10.1084/jem.187.12.2009

206. Levoye A., Balabanian K., Baleux F., Bachelerie F., Lagane B. (2009) CXCR7 heterodimerizes with CXCR4 and regulates CXCL12-mediated G protein signaling. Blood 1136085–6093. 10.1182/blood-2008-12-196618

207. Tan, X., Sanders, P., Bolado, J. and Whitney, M. (2003). Integration of G-Protein Coupled Receptor Signaling Pathways for Activation of a Transcription Factor (EGR-3). Genomics, Proteomics & Bioinformatics, [online] 1(3), pp.173–179.

208. Gravel S, Malouf C, Boulais PE, Berchiche YA, Oishi S, Fujii N, Leduc R, Sinnett D, Heveker N. (2010) The peptidomimetic CXCR4 antagonist TC14012 recruits beta arrestin to CXCR7: roles of receptor domains. J Biol Chem Dec 3; 285(49):37939-43.

209. Lasagni L., Francalanci M., Annunziato F., Lazzeri E., Giannini S., Cosmi L., et al. (2003) An alternatively spliced variant of CXCR3 mediates the inhibition of endothelial cell growth induced by IP-10, Mig, and I-TAC, and acts as functional receptor for platelet factor 4. J. Exp. Med. 1971537–1549. 10.1084/jem.20021897

210. Proost P., Mortier A., Loos T., Vandercappellen J., Gouwy M., Ronsse I., et al. (2007) Proteolytic processing of CXCL11by CD13/aminopeptidase N impairs CXCR3 and CXCR7 binding and signaling and reduces lymphocyte and endothelial cell migration. Blood 110 37–44

211. Tarnowski M., Liu R., Wysoczynski M., Ratajczak J., Kucia M., Ratajczak M. Z. (2010) CXCR7: a new SDF-1-binding receptor in contrast to normal CD34+ progenitors is functional and is expressed at higher level in human malignant hematopoietic cells. Eur. J. Haematol. 85 472–483. 10.1111/j.1600-0609.2010. 01531.x

212. Kitamura K., Kangawa K., Kawamoto M., Ichiki Y., Nakamura S., Matsuo H., et al. (1993). Adrenomedullin: a novel hypotensive peptide isolated from human pheochromocytoma. Biochem. Biophys. Res. Commun. 192553–560. 10.1006/bbrc.1993.1451

213. Dunworth W. P., Fritz-Six K. L., Caron K. M. (2008) Adrenomedullin stabilizes the lymphatic endothelial barrier in vitro and in vivo. Peptides 29 2243–2249. 10.1016/j.peptides.2008.09.009

214. Caron K. M., Smithies O. (2001) Extreme hydrops fetalis and cardiovascular abnormalities in mice lacking a functional adrenomedullin gene. Proc. Natl. Acad. Sci. U.S.A. 98 615–619. 10.2307/3054732

215. Fritz-Six K. L., Dunworth W. P., Li M., Caron K. M. (2008) Adrenomedullin signaling is necessary for murine lymphatic vascular development. J. Clin. Investig. 118 40–50. 10.1172/JCI33302

216. McLatchie LM, Fraser NJ, Main MJ, Wise A, Brown J, Thompson N, Solari R, Lee MG, Foord SM (May 1998) RAMPs regulate the transport and ligand specificity of the calcitonin-receptor-like receptor. Nature. 393 (6683): 333–9.

217. Hay DL, Poyner DR, Sexton PM (January 2006) GPCR modulation by RAMPs. Pharmacol. Ther. 109 (1–2): 173–97. doi: 10.1016/j.pharm thera. 2005.06.015. PMID 16111761

218. Mizuno, K., Minamino, N., Kangawa, K., and Matsuo, H. (1980) A new endogenous opioid peptide from bovine adrenal medulla: isolation and amino acid sequence of a dodecapeptide (BAM-12P). Biochem. Biophys. Res. Commun. 95, 1482–1488.

219. Dores, R. M., McDonald, L. K., Steveson, T. C., and Sei, C. A. (1990) The molecular evolution of neuropeptides: prospects for the ’90s. Brain Behav. Evol. 36, 80–99.

220. Boersma, C. J. C., Pool, C. W., Van Heerikhuize, J. J., and Van Leeuwen, F. W. (1994) Characterization of opioid binding sites in the neural and intermediate lobe of the rat pituitary gland by quantitative receptor autoradiography. J. Neuroendocrinol. 6, 47–56.

221. Khachaturian, H., and Lewis, M. E. (1983) Telencephalic enkephalinergic systems in the rat brain. J. Neurosci. 3, 844–855.

222. Garzon, J., Sanchez-Blazquez, P., Höllt, V., Lee, N. M., and Loh, H. H. (1983) Endogenous opioid peptides: comparative evaluation of their receptor affinities in the mouse brain. Life Sci. 33, 291–294

223. Quirion, R., and Weiss, A. S. (1983) Peptide E and other proenkephalin-derived peptides are potent kappa opiate receptor agonists. Peptides 4, 445–449.

224. Lembo, P. M., Grazzini, E., Groblewski, T., O'Donnell, D., Roy, M. O., Zhang, J., et al. (2002) Proenkephalin a gene product activate a new family of sensory neuron– specific GPCRs. Nat. Neurosci. 5, 201–209.

225. Ikeda, Y., Kumagai, H., Skach, A., Sato, M., and Yanagisawa, M. (2013) Modulation of circadian glucocorticoid oscillation via adrenal opioid-CXCR7 signaling alters emotional behavior. Cell 155, 1323–1336.

226. Rossi, A. G., Haslett, C., Hirani, N., Greening, A. P., Rahman, I., Metz, C. N., et al. (1998) Human circulating eosinophils secrete macrophage migration inhibitory factor (MIF): potential role in asthma. J. Clin. Investig. 101, 2869–2874.

227. Nishihira, J., Koyama, Y., and Mizue, Y. (1998) Identification of macrophage migration inhibitory factor (MIF) in human vascular endothelial cells and its induction by lipopolysaccharide. Cytokine 10, 199–205.

228. Imamura, K., Nishihira, J., Suzuki, M., Yasuda, K., Sasaki, S., Kusunoki, Y., et al. (1996) Identification and immunohistochemical localization of macrophage migration inhibitory factor in human kidney. IUBMB Life 40, 1233–1242.

229. David, J. R. (1966) Delayed hypersensitivity in vitro: its mediation by cell-free substances formed by lymphoid cell-antigen interaction. Proc. Natl. Acad. Sci. U.S.A. 56, 72–77.

230. Leng, L., Metz, C. N., Fang, Y., Xu, J., Donnelly, S., Baugh, J., et al. (2003) MIF signal transduction initiated by binding to CD74. J. Exp. Med. 197, 1467–1476.

231. Bernhagen, J., Krohn, R., Lue, H., Gregory, J. L., Zernecke, A., Koenen, R. R., et al. (2007) MIF is a noncognate ligand of CXC chemokine receptors in inflammatory and atherogenic cell recruitment. Nat. Med. 13, 587–596.

232. Tarnowski, M., Grymula, K., Liu, R., Tarnowska, J., Drukala, J., and Ratajczak, J. (2010) Macrophage migration inhibitory factor is secreted by rhabdomyosarcoma cells, modulates tumor metastasis by binding to CXCR4 and CXCR7 receptors and inhibits recruitment of cancer-associated fibroblasts. Mol. Cancer Res. 8, 1328–1343.

233. Chatterjee, M., Borst, O., Walker, B., Fotinos, A., Vogel, S., Seizer, P., et al. (2014) Macrophage migration inhibitory factor limits activation-induced apoptosis of platelets via CXCR7-dependent Akt signaling. Circ. Res. 115, 939–949.

234. Boldajipour, B., et al. (2008) Control of chemokine-guided cell migration by ligand sequestration. Cell 132(3): 463-473.

235. Sierro, F., et al. (2007) Disrupted cardiac development but normal hematopoiesis in mice deficient in the second CXCL12/SDF-1receptor,CXCR7. Proc Natl Acad Sci U S A 104(37): 14759-14764.

236. Klein, K. R., et al. (2014) Decoy receptor CXCR7 modulates adrenomedullin-mediated cardiac and lymphatic vascular development. Dev Cell 30(5): 528-540.

237. Wang, Y., et al. (2011) CXCR4 and CXCR7 have distinct functions in regulating interneuron migration. Neuron 69(1): 61-76.

238. Ding, B. S., et al. (2014) Divergent angiocrine signals from vascular niche balance liver regeneration and fibrosis. Nature 505(7481): 97-102.

239. Rafii, S., et al. (2015) Platelet-derived SDF-1 primes the pulmonary capillary vascular niche to drive lung alveolar regeneration. Nat Cell Biol 17(2): 123-136.

240. Cao, Z., et al. (2016) Targeting of the pulmonary capillary vascular niche promotes lung alveolar repair and ameliorates fibrosis. Nat Med 22(2): 154-162.

241. Hao, H.et al. (2017) Loss of Endothelial CXCR7 Impairs Vascular Homeostasis and Cardiac Remodeling After Myocardial Infarction: Implications for Cardiovascular Drug Discovery. Circulation 135(13): 1253-126

242. Dai, X., et al. (2017) Elevating CXCR7 Improves Angiogenic Function of EPCs via Akt/GSK-3beta/Fyn-Mediated Nrf2 Activation in Diabetic Limb Ischemia. Circ Res 120(5): e7-e23.

243. Chatterjee, M., et al. (2014) Macrophage migration inhibitory factor limits activation-induced apoptosis of platelets via CXCR7-dependent Akt signaling. Circ Res 115(11): 939-949.

244. Avraham, H. (2019) CXCL12 mediates the migration of metastatic breast cancer cells through the activation of PI-3 kinase/AKT and Focal adhesion kinase. [online] Cancer Research.

245. Ehtesham, M., Min, E., Issar, N. M., Kasl, R. A., Khan, I. S., & Thompson, R. C. (2013) The role of the CXCR4 cell surface chemokine receptor in glioma biology. Journal of Neuro-Oncology, 113(2), 153–162.

246. Domanska,U.M.,Kruizinga,R.C.,Nagengast,W.B.,Timmer-Bosscha,H.,Huls, G., de Vries, E. G. E., & Walenkamp, A. M. E. (2013) A review on CXCR4/CXCL12 axis in oncology: No place to hide. European Journal of Cancer, 49(1), 219–230.

247. Balabanian K, Lagane B, Infantino S, Chow KY, Harriague J, Moepps B,Arenzana-Seisdedos F, Thelen M, Bachelerie F (2005) The chemokine SDF1/CXCL12 binds to and signals through the orphan receptor RDC1 in T lymphocytes. The Journal of Biological Chemistry.

248. Hattermann K, Held-Feindt J, Lucius R, Muerkoster SS, Penfold ME, Schall TJ,et al. (2010) The chemokine receptor CXCR7 is highly expressed in human glioma cells and mediates antiapoptotic effects. Cancer Res; 70:3299–308.

249. Wang J, Shiozawa Y, Wang Y, Jung Y, Pienta KJ, Mehra R, et al. (2008) The role of CXCR7/RDC1 as a chemokine receptor for CXCL12/SDF-1 in prostate cancer. J Biol Chem; 283:4283–94

250. Singh, Rajendra Kumar, and Bal L Lokeshwar. (2011) The IL-8-regulated chemokine receptor CXCR7 stimulates EGFR signaling to promote prostate cancer growth. Cancer research vol. 71,9: 3268-77.

251. Burns JM, Summers BC, Wang Y, Melikian A, Berahovich R, Miao Z, et al. (2006) A novel chemokine receptor for SDF-1 and I-TAC involved in cell survival, cell adhesion, and tumor development. J Exp Med; 203:2201–13.

252. Maréchal R, Demetter P, Nagy N, Berton A, Decaestecker C, Polus M, Closset J, Devière J, Salmon I, Van Laethem JL. (2009) High expression of CXCR4 may predict poor survival in resected pancreatic adenocarcinoma. Br J Cancer.; 100(9): 1444-51

253. Miao Z, Luker KE, Summers BC, Berahovich R, Bhojani MS, Rehemtulla A et al. (2007) CXCR7 (RDC1) promotes breast and lung tumor growth in vivo and is expressed on tumor-associated vasculature. Proc Natl Acad Sci USA; 104: 15735–15740.

254. Iwakiri S, Mino N, Takahashi T, Sonobe M, Nagai S, Okubo K et al. (2009) Higher expression of chemokine receptor CXCR7 is linked to early and metastatic recurrence in pathological stage I non-small cell lung cancer. Cancer; 115:2580–2593.

255. Xu, Huanbai; Wu, Qiong; Dang, Shipeng; Jin, Min; Xu, Jingwei; Cheng, Yiji; Pan, Minglin; Wu, Yugang; Zhang, Chunhui; Zhang, Yanyun (2011) Alteration of CXCR7 Expression Mediated by TLR4 Promotes Tumor Cell Proliferation and Migration in Human Colorectal Carcinoma PLoS ONE, vol. 6, issue 12, p. e27399 12/2011

256. Hao M, Zheng J, Hou K, Wang J, Chen X, Lu X, et al. (2012) Role of chemokine receptor CXCR7 in bladder cancer progression. Biochem Pharmacol; 84:204–14.

257. Liu L, Zhao X, Zhu X, Zhong Z, Xu R, Wang Z, et al. (2013) Decreased expression of miR-430 promotes the development of bladder cancer via the upregulation of CXCR7. Mol Med Rep; 8:140–6.

258. Maishi N, Ohga N, Hida Y, Akiyama K, Kitayama K, Osawa T, et al. (2012) CXCR7: a novel tumor endothelial marker in renal cell carcinoma. Pathol Int; 62:309–17.

259. Gahan JC1, Gosalbez M, Yates T et al. (2012) Chemokine and chemokine receptor expression in kidney tumors: molecular profiling of histological subtypes and association with metastasis J Urol. Mar;187(3):827-33.

260. Salazar N, Muñoz D, Kallifatidis G, Singh RK, Jordà M, Lokeshwar BL. (2014) The chemokine receptor CXCR7 interacts with EGFR to promote breast cancer cell proliferation. Mol Cancer. 2014;13:198.

261. Singh RK, Lokeshwar BL. (2011) The IL-8-regulated chemokine receptor CXCR7 stimulates EGFR signaling to promote prostate cancer growth. Cancer Res; 71:3268– 77

262. Zheng K, Li HY, Su XL, Wang XY, Tian T, Li F, et al. (2010) Chemokine receptor CXCR7 regulates the invasion, angiogenesis and tumor growth of human hepatocellular carcinoma cells. J Exp Clin Cancer Res; 29:31.

263. Dai X, Tan Y ,Cai S, Xiong X, Wang L, Ye Q, et al. (2011) The role of CXCR7 on the adhesion, proliferation and angiogenesis of endothelial progenitor cells. J Cell Mol Med; 15:1299–309.

264. Roberto Würth, Federica Barbieri, Adriana Bajetto, Alessandra Pattarozzi, Monica Gatti, Carola Porcile, Gianluigi Zona, Jean-Louis Ravetti, Renato Spaziante, Tullio Florio (2011) Expression of CXCR7 chemokine receptor in human meningioma cells and in intratumoral microvasculature, Journal of Neuroimmunology, Volume 234, Issues 1–2

265. Zheng, K., Li, H. Y., Su, X. L., Wang, X. Y., Tian, T., Li, F., & Ren, G. S. (2010) Chemokine receptor CXCR7 regulates the invasion, angiogenesis and tumor growth of human hepatocellular carcinoma cells. Journal of experimental & clinical cancer research 29(1), 31.

266. Li, X., Wang, X., Li, Z., Zhang, Z., & Zhang, Y. (2019) Chemokine receptor 7 targets the vascular endothelial growth factor via the AKT/ERK pathway to regulate angiogenesis in colon cancer. Cancer medicine, 8(11), 5327–5340.

267. Salazar, N., Carlson, J. C., Huang, K., Zheng, Y., Oderup, C., Gross, J., Zabel, B. A. (2018) A Chimeric Antibody against ACKR3/CXCR7 in Combination with TMZ Activates Immune Responses and Extends Survival in Mouse GBM Models. Molecular therapy : the journal of the American Society of Gene Therapy, 26(5), 1354–1365.

268. Hernandez L, Magalhaes MA, Coniglio SJ, Condeelis JS, Segall JE. (2011) Opposing roles of CXCR4 and CXCR7 in breast cancer metastasis. Breast Cancer Res.;13(6):R128.

269. Miao Z, Luker KE, Summers BC, Berahovich R, Bhojani MS, Rehemtulla A, Kleer CG, Essner JJ, Nasevicius A, Luker GD, et al. (2007) CXCR7 (RDC1) promotes

breast and lung tumor growth in vivo and is expressed on tumor-associated vas culature. Proc Natl Acad Sci USA 104:15735–15740.

270. Wani N, Nasser MW, Ahirwar DK, Zhao H, Miao Z, Shilo K, and Ganju RK (2014) C-X-C motif chemokine 12/C-X-C chemokine receptor type 7 signaling regulates breast cancer growth and metastasis by modulating the tumor microenvironment. Breast Cancer Res 16:R54.

271. Sirkisoon, S. R., Carpenter, R. L., Rimkus, T., Doheny, D., Zhu, D., Aguayo, N. R., Xing, F., Chan, M., Ruiz, J., Metheny-Barlow, L. J., Strowd, R., Lin, J., Regua, A. T., Arrigo, A., Anguelov, M., Pasche, B., Debinski, W., Watabe, K., & Lo, H. W. (2020). TGLI1 transcription factor mediates breast cancer brain metastasis via activating metastasis-initiating cancer stem cells and astrocytes in the tumor microenvironment. Oncogene, 39(1), 64–78.

272. Zabel, B. A., Lewén, S., Berahovich, R. D., Jaén, J. C., & Schall, T. J. (2011) The novel chemokine receptor CXCR7 regulates trans-endothelial migration of cancer cells. Molecular cancer, 10, 73.

273. Grymula, K., Tarnowski, M., Wysoczynski, M., Drukala, J., Barr, F. G., Ratajczak, J. Ratajczak, M. Z. (2010) Overlapping and distinct role of CXCR7-SDF-1/ITAC and CXCR4-SDF-1 axes in regulating metastatic behavior of human rhabdomyosarcomas. International journal of cancer, 127(11), 2554–2568.

274. Calatozzolo C, Canazza A, Pollo B, Di Pierro E, Ciusani E, Maderna E, Salce E, Sponza V, Frigerio S, Di Meco F, et al. (2011) Expression of the new CXCL12 receptor, CXCR7, in gliomas. Cancer Biol Ther 11:242–253.

275. Hao M, Zheng J, Hou K, et al. (2012) Role of chemokine receptor CXCR7 in bladder cancer progression. Biochem Pharmacol.;84(2):204–214.

276. Long, P., Sun, F., Ma, Y. et al. (2016) Tumor Biol. 37: 7473.

277. Liu, T., Guo, J., & Xu, X. (2017) CXC chemokine-7 inhibits growth and migration of oral tongue squamous cell carcinoma cells, mediated by the epithelial-mesenchymal transition signaling pathway. Molecular Medicine Reports, 16, 6896-6903.

278. Jin Z, Nagakubo D, Shirakawa AK, Nakayama T, Shigeta A, Hieshima K, et al. (2009) CXCR7 is inducible by HTLV-1 Tax and promotes growth and survival of HTLV1-infected T cells. Int J Cancer; 125:2229–35.

279. Van Rechem C, Rood BR, Touka M, Pinte S, Jenal M, Guerardel C, et al. (2009) Scavenger chemokine (CXC motif) receptor 7 (CXCR7) is a direct target gene of HIC1 (hypermethylated in cancer 1). J Biol Chem; 284:20927–35.

280. Zheng J, Wang J, Sun X, Hao M, Ding T, Xiong D, et al. (2013) HIC1 modulates prostate cancer progression by epigenetic modification. Clin Cancer Res; 19:1400–10.

281. Staton AA, Knaut H, Giraldez AJ. (2011) miRNA regulation of Sdf1 chemokine signaling provides genetic robustness to germ cell migration. Nat Genet; 43:204–11.

282. Rashidi B, Yang M, Jiang P, Baranov E, An Z, Wang X, Moossa AR, Hoffman RM (2000) A highly metastatic Lewis lung carcinoma orthotopic green fluorescent protein model. Clinical & Experimental Metastasis. 18 (1): 57–6

283. Fidler I, Metastasis: Quantitative Analysis of Distribution and Fate of Tumor Emboli Labeled With 125I-5-Iodo-2′ -deoxyuridine, JNCI: Journal of the National Cancer Institute, Volume 45, Issue 4, October 1970, Pages 773–782

284. Perfetto, Stephen P et al. (2010) Amine-reactive dyes for dead cell discrimination in fixed samples. Current protocols in cytometry vol. Chapter 9: Unit 9.34.

285. Strong A, Thierry AC, et all . (2006) Synthetic chemokines directly labelled with a fluorescent dye as tools for studying chemokine and chemokine receptor interactions. European Cytokine Network.;17(1):49-59.

286. Engber, Daniel (2011) The Trouble With Black-6: A tiny alcoholic takes over the lab. Slate.com.

287. Cruz-Orengo, L., Holman, D. W., Dorsey, D., Zhou, L., Zhang, P., Wright, M., … Klein, R. S. (2011) CXCR7 influences leukocyte entry into the CNS parenchyma by controlling abluminal CXCL12 abundance during autoimmunity. The Journal of experimental medicine, 208(2), 327–339.

288. Source: JAX stock #008591. The Jackson Laboratories.

289. Holmes N (2006) CD45: all is not yet crystal clear. Immunology. 117 (2): 145–155. doi:10.1111/j.1365-2567.2005.02265. x. PMC 1782222.

290. Yamamoto H, Yun EJ, Gerber HP, Ferrara N, Whitsett JA, Vu TH. (2007) Epithelial–vascular cross talk mediated by VEGF-A and HGF signaling directs primary septae formation during distal lung morphogenesis. Dev Biol; 308:44–53

291. Astarita JL, Acton SE, Turley SJ (2012) Podoplanin: emerging functions in development, the immune system, and cancer. Frontiers in Immunology. 3: 283.

292. Zhang, Min et al. (2017) CXCL12 enhances angiogenesis through CXCR7 activation in human umbilical vein endothelial cells. Scientific reports vol. 7,1 8289.

293. Johnson, L. A., & Jackson, D. G. (2008) Cell Traffic and the Lymphatic Endothelium. Annals of the New York Academy of Sciences, 1131(1), 119– 133.

294. Neusser, M. A., Kraus, A. K., Regele, H., Cohen, C. D., Fehr, T., Kerjaschki, D.,Segerer, S. (2010) The chemokine receptor CXCR7 is expressed on lymphatic endothelial cells during renal allograft rejection. Kidney International, 77(9), 801–808.

295. Naumann U, Cameroni E, Pruenster M, Mahabaleshwar H, Raz E, et al. (2010) CXCR7 functions as a scavenger for CXCL12 and CXCL11. PLoS One 5: e9175.

296. Schutyser E, Su Y, Yu Y, Gouwy M, Zaja-Milatovic S, et al. (2007) Hypoxia enhances CXCR4 expression in human microvascular endothelial cells and human melanoma cells. Eur Cytokine Netw 18: 59–70.

297. Costello CM, McCullagh B, Howell K, Sands M, Belperio JA, et al. (2012) A role for the CXCL12 receptor, CXCR7, in the pathogenesis of human pulmonary vascular disease. Eur Respir J 39: 1415–1424.

298. Liu, Y., Carson-Walter, E., & Walter, K. A. (2014) Chemokine Receptor CXCR7 Is a Functional Receptor for CXCL12 in Brain Endothelial Cells. PLoS ONE, 9(8), e103938.

299. Cruz-Orengo L, Holman DW, Dorsey D, Zhou L, Zhang P, et al. (2011) CXCR7 influences leukocyte entry into the CNS parenchyma by controlling abluminal CXCL12 abundance during autoimmunity. J Exp Med 208: 327–339.

300. Ngamsri C, Anika Müller, Hans Bösmüller, Jutta Gamper-Tsigaras, Jörg Reutershan, Franziska M. Konrad (2017) The Pivotal Role of CXCR7 in Stabilization of the Pulmonary Epithelial Barrier in Acute Pulmonary Inflammation. The Journal of Immunology, 198 (6) 2403-2413

301. Berahovich R.D Mark E.T. Penfold Thomas J.Schall (2010) Nonspecific CXCR7 antibodies. Immunology Letters Volume 133, Issue 2, Pages 112-114

302. Pickar-Oliver, A., Gersbach, C.A. (2019) The next generation of CRISPR–Cas technologies and applications. Nat Rev Mol Cell Biol 20, 490–507

303. Van der Oost J, Matthijs M. Jore, Edze R. Westra, Magnus Lundgren, Stan J.J. Brouns (2019) CRISPR-based adaptive and heritable immunity in prokaryotes, Trends in Biochemical Sciences, Volume 34, Issue 8

304. Satomura, A., Nishioka, R., Mori, H. et al. (2017) Precise genome-wide base editing by the CRISPR nickase system in yeast. Sci Rep 7, 2095

305. Xu, S., Tang, J., Wang, C. et al. (2019) CXCR7 promotes melanoma tumorigenesis via Src kinase signaling. Cell Death Dis 10, 191.

306. André, N.D., Silva, V.A., Watanabe, M.A., & De Lucca, F.L. (2016) Knockdown of chemokine receptor CXCR4 gene by RNA interference: Effects on the B16-F10 melanoma growth. Oncology Reports, 35, 2419-2424.

307. Rhodes, Daniel R et al. (2004) ONCOMINE: a cancer microarray database and integrated data-mining platform. Neoplasia (New York, N.Y.) vol. 6,1: 1-6.

308. Bhattacharjee, A et al. (2001) Classification of human lung carcinomas by mRNA expression profiling reveals distinct adenocarcinoma subclasses.” Proceedings of the National Academy of Sciences of the United States of America vol. 98,24 13790-5.

309. Wachi, Shinichiro et al. (2005) Interactome-transcriptome analysis reveals the high centrality of genes differentially expressed in lung cancer tissues.” Bioinformatics (Oxford, England) vol. 21,23 (2005): 4205-8.

310. Daniela S. Gerhard (2008) TCGA Moving Molecular Oncology Forward. NCI cancer Bulletin, Director's Update. National Cancer Institute.

311. Takekoshi, Tomonori et al. (2012) A locked, dimeric CXCL12 variant effectively inhibits pulmonary metastasis of CXCR4-expressing melanoma cells due to enhanced serum stability Molecular cancer therapeutics vol. 11,11 2516-25.

312. André, N. D., Silva, V. A., Watanabe, M. A., De Lucca, F. L. (2016) Knockdown of chemokine receptor CXCR4 gene by RNA interference: Effects on the B16-F10 melanoma growth. Oncology Reports 35.4: 2419-2424.

313. Castro-Lopez, N et all (2018) Requirement of CXCL11 chemokine production for induction of protection against pulmonary cryptococcosis. The Journal of Immunology May 1, 2018, 200 (1 Supplement) 52.31;

314. Winkler, A. E., Brotman, J. J., Pittman, M. E., Judd, N. P., Lewis, J. S., Jr, Schreiber, R. D., & Uppaluri, R. (2011). CXCR3 enhances a T-cell-dependent epidermal proliferative response and promotes skin tumorigenesis. Cancer research, 71(17), 5707–5716.

315. Salazar, N., & Zabel, B. A. (2019) Support of Tumor Endothelial Cells by Chemokine Receptors. Frontiers in immunology, 10, 147.

316. Yamada K, Maishi N, Akiyama K, Alam MT, Ohga N, Kawamoto T, et al. (2015) CXCL12-CXCR7 axis is important for tumor endothelial cell angiogenic property. Int J Cancer 137:2825–36. 10.1002/ijc.2965

317. Liu H, Xue W, Ge G, Luo X, Li Y, Xiang H, et al. (2010) Hypoxic preconditioning advances CXCR4 and CXCR7 expression by activating HIF-1 alpha in MSCs. Biochem Biophys Res Commun. 401:509–15. 10.1016/j.bbrc.2010.09.076

318. Wu, Y., Tang, S., Sun, G. et al. (2016) CXCR7 mediates TGFβ1-promoted EMT and tumor-initiating features in lung cancer. Oncogene 35, 2123–2132

319. Ieranò, C., Santagata, S., Napolitano, M., Guardia, F., Grimaldi, A., Antignani, E., ..Scala, S. (2014) CXCR4 and CXCR7 transduce through mTOR in human renal cancer cells. Cell death & disease, 5(7), e1310.

320. Mistarz, A., Komorowski, M. P., Graczyk, M. A., Gil, M., Jiang, A., Opyrchal, M., … Kozbor, D. (2019) Recruitment of Intratumoral CD103+ Dendritic Cells by a CXCR4 Antagonist-Armed Virotherapy Enhances Antitumor Immunity. Molecular therapy oncolytics, 14, 233–245.

321. Kryczek I, Lange A, Mottram P, Alvarez X, Cheng P, Hogan M, et al. (2005) CXCL12 and vascular endothelial growth factor synergistically induce neoangiogenesis in human ovarian cancers. Cancer Res.;65(2):465–72.

322. Barbero S, Bonavia R, Bajetto A, Porcile C, Pirani P, Ravetti JL, Zona GL, Spaziante R, Florio T, Schettini G. (2003) Stromal cell-derived factor 1α stimulates human glioblastoma cell growth through the activation of both extracellular signal regulated kinases 1/2 and Akt. Cancer Res 63: 1969–1974

323. Sonoda Y, Ozawa T, Aldape KD, Deen DF, Berger MS, Pieper RO. (2001) Akt pathway activation converts anaplastic astrocytoma to glioblastoma multiforme in a human astrocyte model of glioma. Cancer Res 61: 6674–6678

324. Phillips RJ, Burdick MD, Lutz M, Belperio JA, Keane MP, Strieter RM. (2003) The stromal derived factor-1/CXCL12-CXC chemokine receptor 4 biological axis in nonsmall cell lung cancer metastases. Am J Respir Crit Care Med 167: 1676–1686,

325. Bertolini F, et al. (2002) CXCR4 neutralization, a novel therapeutic approach for non-Hodgkin's lymphoma. Cancer Res.; 62:3106–3112.

326. Rubin JB, et al. (2003) A small-molecule antagonist of CXCR4 inhibits intracranial growth of primary brain tumors. Proc Natl Acad Sci USA.; 100:13513– 13518

327. Liang Z, et al. (2005) Silencing of CXCR4 blocks breast cancer metastasis. Cancer Res.; 65:967–971.

328. Lapteva, N., Yang, A.-G., Sanders, D.E., Strube, R.W. and Chen, S.-Y. (2005). CXCR4 knockdown by small interfering RNA abrogates breast tumor growth in vivo. Cancer Gene Therapy, 12(1), pp.84–89.

329. Li, S., Fong, K., Gritsina, G., Zhang, A., Zhao, J. C., Kim, J., … Yu, J. (2019) Activation of MAPK signaling by CXCR7 leads to enzalutamide resistance in prostate cancer. Cancer Research, canres.2812.2018.

330. Luker, K E et al. (2012) Scavenging of CXCL12 by CXCR7 promotes tumor growth and metastasis of CXCR4-positive breast cancer cells. Oncogene vol. 31,45 4750-8.

331. Ray, P., Stacer, A. C., Fenner, J., Cavnar, S. P., Meguiar, K., Brown, M., … Luker, G. D. (2015) CXCL12-γ in primary tumors drives breast cancer metastasis. Oncogene, 34(16), 2043–2051.

332. Sun, Y., Mao, X., Fan, C., Liu, C., Guo, A., Guan, S., … Jin, F. (2014) CXCL12/CXCR4 axis promotes the natural selection of breast cancer cell metastasis. Tumour biology : the journal of the International Society for Oncodevelopmental Biology and Medicine, 35(8), 7765–7773.

333. Xue TC, Chen RX, Ren ZG, Zou JH, Tang ZY, Ye SL. (2013) Transmembrane receptor CXCR7 increases the risk of extrahepatic metastasis of relatively well differentiated hepatocellular carcinoma through upregulation of osteopontin. Oncol Rep; 30:105

334. Puddinu, V., Casella, S., Radice, E., Thelen, S., Dirnhofer, S., Bertoni, F., & Thelen, M. (2017) ACKR3 expression on diffuse large B cell lymphoma is required for tumor spreading and tissue infiltration. Oncotarget, 8(49), 85068–85084.

335. Grymula, K., Tarnowski, M., Wysoczynski, M., Drukala, J., Barr, F. G., Ratajczak, J., Kucia, M., Ratajczak, M. Z. (2010) Overlapping and distinct role of CXCR7-SDF1/ITAC and CXCR4-SDF-1 axes in regulating metastatic behavior of human rhabdomyosarcomas. Int. J. Cancer 127, 2554-2568.

336. Thelen, M., Thelen, S. (2008) CXCR7, CXCR4 and CXCL12: an eccentric trio? J. Neuroimmunol.198,9–13.68.

337. Liu, Xiang et al. (2012) Establishment of an orthotopic lung cancer model in nude mice and its evaluation by spiral CT. Journal of thoracic disease vol. 4,2 141-5

338. Mawhinney, L., Armstrong, M. E., O' Reilly, C., Bucala, R., Leng, L., Fingerle-Rowson, G., Fayne, D., Keane, M. P., Tynan, A., Maher, L., Cooke, G., Lloyd, D., Conroy, H., & Donnelly, S. C. (2015). Macrophage migration inhibitory factor (MIF) enzymatic activity and lung cancer. Molecular medicine (Cambridge, Mass.), 20(1), 729–735.

339. Berenguer-Daize, C., Boudouresque, F., Bastide, C., Tounsi, A., Benyahia, Z., Acunzo, J., Dussault, N., Delfino, C., Baeza, N., Daniel, L., Cayol, M., Rossi, D., El Battari, A., Bertin, D., Mabrouk, K., Martin, P.-M. and Ouafik, L. (2013). Adrenomedullin Blockade Suppresses Growth of Human Hormone-Independent Prostate Tumor Xenograft in Mice. Clinical Cancer Research, 19(22), pp.6138–6150.

340. Orthotopic Lung Cancer Murine Model by Nonoperative Transbronchial Approach Nakajima, Takahiro et al. The Annals of Thoracic Surgery, Volume 97 , Issue 5 1771 – 1775